UNIVERSITÉ DU QUÉBEC À MONTRÉAL

APPLICATION OF GLYCODENDRIMERS AS ANTI-ADHERENCE INHIBITORS AGAINST PSEUDOMONAS AERUGINOSA IN CYSTIC FIBROSIS

THESIS

PRESENTED

AS PARTIAL REQUIREMENT OF

THE MASTER IN CHEMISTRY

BY

SHADY (ASAL) SHOJAEEASL

JULY 2019

UNIVERSITÉ DU QUÉBEC À MONTRÉAL

APPLICATION DE GLYCODENDRIMÈRES COMME INHIBITEURS ANTI-ADHÉRENTS CONTRE LE *PSEUDOMONAS AERUGINOSA* POUR LA FIBROSE KYSTIQUE

MÉMOIRE

PRÉSENTÉ

COMME EXIGENCE PARTIELLE

DE LA MAITRISE EN CHIMIE

PAR

SHADY (ASAL) SHOJAEEASL

JUILLET 2019

REMERCIEMENTS

Je suis reconnaissante à Dieu pour toutes ses bénédictions, le pouvoir qu'il m'a donné afin de surmonter des épreuves et pour toutes les qualifications qu'il m'a contribuées afin de réaliser mes projets. En particulier, dans un pays étranger qui est devenu ma deuxième patrie.

Maintenant, à ce stade crucial de ma vie, j'ai encore une fois besoin de l'assistance de Dieu, ainsi que celle de quelques autres personnes remarquables qui n'ont jamais refusé de m'aider tout au long de ma vie. Il est inutile de dire à quel point la vie d'une fille dépendante de la famille peut être difficile à l'étranger. Cependant, j'ai réussi à surmonter et à tolérer les difficultés pour réussir dans mes études. En partie, grâce au Pr René Roy dont les conseils et assistance ont contribué à mon succès dans ce programme de recherche.

Je tiens également à exprimer mes remerciements aux docteurs Rabi Rej et Rahul Bagul pour leurs conseils et leur aide au cours de toutes ces années passées à l'université.

Les mots n'expriment pas mes émotions et mes sentiments profonds pour ma famille pour leur amour et leur soutien tout au long de ma vie. Je remercie, tout particulièrement mon père qui m'a toujours motivée pour poursuivre mes études; ma sœur aînée, Shilla, dont l'affection a toujours réchauffé mon cœur, ainsi que ma sœur cadette, Dr Pouneh Shojaee Asl, et son mari, Dr Amir Alaie, qui m'ont toujours inspirée. C'est le soutien émotionnel et financier de ma famille qui m'a permis de surmonter les problèmes et d'atteindre mes objectifs.

Enfin, je remercie ma mère, la personne la plus chère et la plus belle de ma vie. Diplômée en chimie de l'Université de Téhéran en 1963, elle était sans aucun doute ma meilleure professeure et conseillère qui m'a aidée à ouvrir la voie à un avenir brillant. Depuis toujours, je rêvais d'aller très loin dans mes études comme ma chère sœur. Je dédie ma thèse à ma mère pour exprimer ma sincère gratitude et mon affection pour son amour maternel inestimable.

Je suis également reconnaissante à mon professeur respectueux, le directeur de Pharmaqam, Dr. Steve Bourgault, et également Dr. Sylvain Canesi, ainsi qu'à tous les membres du personnel de Pharmaqam pour leurs soutiens exceptionnels.

Je souhaite bonne santé, bonheur, paix et prospérité à mes chers professeurs et à ma très chère famille.

Mes reconnaissances les plus sincères,

Shady Asal Shojaee Asl

ACKNOWLEDGMENT

In the name of God

I am grateful to God for all the blessings and kindness, for all the power given to me to endure hardships in a foreign country which has now become my second homeland, and for all the qualifications which have contributed to my achievements. Now at this crucial stage of life, I once again need special support and concern from God and also some other conspicuous people who have never failed to assist me through my life. It is needless to say how difficult life could be for a family-dependent girl abroad; however, I have managed to overcome, endure these difficulties and succeed. I want to thank Pr René Roy for his assistance contributed to my success in this research program.

I shall also express my gratitude to Dr. Rabi Rej and Dr. Rahul Bagul for their kind concern, advice, and assistance through all these years at university.

To appreciate my beloved family, words fail to express my deep emotions and feelings for them and their life-long love and support. I, hereby, thank my father who has always motivated me to continue my education; my older sister, Shilla, whose sisterly affections has always warmed my heart. My other sister, Dr. Pouneh Shojaee Asl, and her husband, Dr. Amir Alaie, have always inspired me in my life. It was my family's emotional and financial support that enabled me to overcome problems and to reach my goals.

Finally, I thank my mother, the dearest, loveliest person in my life. She was a Chemistry graduate from Tehran University in 1963. She undoubtedly was my best teacher and advisor to recognize my talents and paved my way to a bright future. It has always been her life-long dream for me to reach high levels of education like my dear sister. I dedicate my thesis to my mother to show my sincere gratitude and affection for her inestimable maternal love.

I am also grateful to my highly-respected professor and Director of Pharmaqam, Dr. Steve Bourgault and to my other respected professor, Dr. Sylvain Canesi, and to all the staff members in Pharmaqam for their kind concerns and high sense of cooperation. I do wish good health, happiness, peace, and prosperity for my dear professors and beloved family.

My sincere regards to all,
Shady Asal Shojaee Asl

TABLE DES MATIÈRES

FIGURE LIST

Figure Page

SCHEME LIST

Scheme Page

TABLE LIST

Table Page

ABBREVIATION AND ACRONYMS LIST

Ac	Acetyl
Boc	Tert-butoxycarbonyl
DBU	1,8-Diazabicyclo[5.4.0]undec-7-ene
DCM	Dichloromethane
DMAP	4-(Dimethylamino) pyridine
DMF	*N,N*-dimethylformamide
DMSO	Dimethylsulfoxide
FCC	Flash Column Chromathography
HPLC	High performance liquid chromatography
NHS	*N*-Hydroxysuccinimide
NMR	Nuclear Magnetic Resonance
Phth	Phthalimide
SPE	Solid Phase Extraction
SPR	Surface Plasmon Resonace
TBDMSCl	*tert*-Butyldimethylsilyl chloride
TFA	Trifluoroacetic Acid
THF	Tetrahydrofurane
TLC	Thin Layer Chromatography
$CDCl_3$	Deuterated chloroform
CM	Centimeter

COSY	Correlation Spectroscopy
CuAAc	Copper(I)-catalyzed alkyne-azide cycloaddition
Cu	Copper
Da	Dalton
Equiv.	Equivalent
Et_2O	Diethyl ether
EtOAc	Ethyl acetate
EtOH	Ethanol
FT-IR	Fourier-transform Infrared Spectroscopy
HSQC	Heteronuclear Single Quantum Coherence Spectroscopy
Hz	Hertz
IC_{50}	Isothermal Calorimetry
L	Litre
M	Molar
MALDI-TOF	Matrix Assistated Laser DesorptionéIonisation Time Of Flight Spectroscopy
MeOH	Methanol
MeONa	Sodium methoxide
Mg	Miligram
MS	Mass spectrometry
Nm	Nanometer
P-	*Para*
PA-IL	*Pseudomonas aeruginosa* Lectin
PAMAM	Polyamidoamine
Rf	Retention factor

α	Alpha
β	Beta
Ac	Acetyl
Ac_2O	Anhydride acetic
AcOEt	Ethly Acetate
Asp	Ac.Aspartic
Asn	Asparagine
Arg	Arginine
Phe	Phenylalanine
Trp	Tryptophan
Gln	Glutamine
Thr	Threonine
Val	Valine
Tyr	Tyrosine
His	Histidine
Pro	Proline
° C	Centigrade degree
D_2O	Deuterium oxide
DMSO-d6	Deuterated Dimethylsulfoxide
MeOD	Deuterated methanol

RÉSUMÉ

De nombreuses infections débutent par adhésion de l'agent pathogène sur la paroi cellulaire de l'hôte. Les agents pathogènes, bactériens ou viraux, ciblent les cellules hôtes au moyen d'interactions complémentaires entre les sucres présents à la surface de la membrane cellulaire. Ces sucres liés de manière covalentes sont appelés des glyconjugués. Notamment, le *Pseudomonas aeruginosa,* le responsable de la fibrose kystique, cible les cellules pulmonaires par l'entremise de ses lectines (PA-IL et PA-IIL) qui interagissent avec les galactosides et fucosides présents a la surface de la cellule hôte. À cet effet, il a été démontré que la présence de récepteurs complémentaires aux lectines pathogéniques était capable d'interférer avec le mécanisme de reconnaissance par effet de compétition. Ainsi, les infections pathogéniques peuvent être traitées en inhibant le mécanisme de reconnaissance.

Ma thèse porte sur le développement d'un traitement contre la fibrose kystique en agissant sur le mécanisme de reconnaissance du *Pseudomonas aeruginosa.* Plus spécifiquement, par le design de dendrimères avec des unités de galactosides capable d'interagir avec la lectine PA-IL du *Pseudomonas aeruginosa.* Pour ce faire, des dendrimères multivalents avec 3,5 et 12 unités de galactosides furent synthétisés. La synthèse des dendrimères furent effectuées par le couplage d'oxime entre des galactopyranoside qui ont été amino oxylé et un squelette de polyaldéhyde. Les galactopyranoside ont été préparés en utilisant la chimie "Click" pour coupler le *2-azidoéthyle β-D-galactopyranoside avec des dérivés de* O*-propargyle hydroxylamino.*

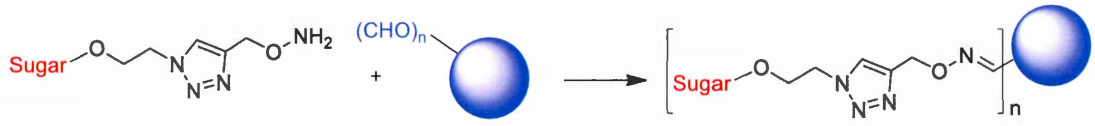

Mots-clés: Dendrimère, Glycodendrimère, PA-IL, Chimie "Click", Couplage d'oxime, Ligand amino oxylé, Squelette de polyaldéhyde.

ABSTRACT

Infections by pathogenic agents are frequently triggered by their adhesion on host surfaces. The early step in adhesion strategy involves initial recognition of host cell glycoconjugates by sugar-binding proteins (lectins) on, or released by the viruses or the bacteria that are specific for the targeted tissues. *Pseudomonas aeruginosa* is an opportunistic pathogen implicated in the development of lung infections in cystic fibrosis (CF) patients through these sugar–protein complementary interactions. *P. aeruginosa*'s mechanism of action is governed by the adhesion of their virulence lectins (PA-IL and PA-IIL) that bind to galactoside and fucoside subunits of glycoconjugates, respectively. Our project is to design potent anti-adhesion inhibitors against the galactoside-dependent PA-IL. To enhance the binding affinities of galactoside residues, nanometer size glycodendrimers have been synthesized.

The synthesis of three multivalent glycodendrimers with 3, 6, and 12 galactoside moieties were prepared using oxime ligation between aminooxylated galactosides and three different synthesized poly-aldehyde scaffolds. The necessary aminooxylated galactopyranoside has been prepared using efficient and versatile "click chemistry" between the known 2-azidoethyl-β-D-galactopyranoside and a suitably *O*-propargylated hydroxylamino derivative (Figure below as model study).

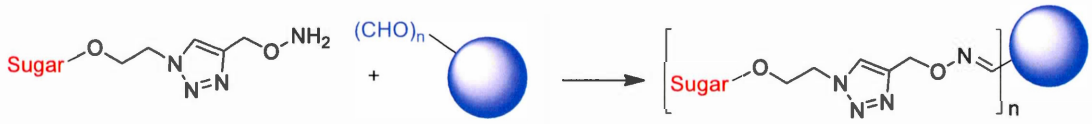

Keywords : dendrimers, Glycodendrimers, PA-IL, click chemistry, oxime ligation, aminooxylated ligand, poly-aldehyde cores

CHAPTER I

INTRODUCTION TO DENDRIMERS

1.1 Introduction to dendrimers

1.1.1 Dendrimers

Dendrimers are known as a hyper-branched, monodispersed and three-dimensional macromolecules; it is composed of a well-defined core, backbone and multivalent periphery.[1,2] As a result of their distinctive architectural morphology and structural properties, it has been the subject of studies for decade in various field of research that spans catalysis, pharmaceutical, biological and many more field of applications. [3–7]

The concept of dendrimer as three-dimensional hyper branched architecture was first proposed on theoretical evidence by Flory in 1940's.[8–10] A German scientist, Fritz Vögtle synthesized these molecules successfully at University of Bonn in 1978 based on cascade molecules referring to the polyamines synthesis cascade.[11,12] In other words, the synthetic methodology to generate dendrimers was presented by Vögtle and his coworkers.[3] In 1981, R. G. Denkewalter designed new polylysine dendrimers up to 10^{th} generation.[5] The first series of dendrimers were designed and synthesized in 1985 based on the well-established method by presenting the poly(amidoamine) (PAMAM) by Tomalia.[13]

Significant efforts were made to overcome the synthetic complexity of these macro-entities by building molecules with diverse and well-designed architectures for different applications. Moreover, the extreme interest of scientists in exploring the dendrimers potential as therapeutic agents has been due to their versatility in architecture and multivalency.[14–16]

A dendrimer consists of two words "dendron" which means "tree like" and "meras" which means "part of" in Greek language. Dendrimers are designed in a sequential pattern around the central core in layer by layer style where each layer is considered as a new generation. Also, they are star-shaped macromolecules in which each layer could vary in chemical identity.[17]

The size of the dendrimers is related to the number of their generations; that is, the dendrimers in lower generations are more asymmetric, while higher generations tends to form the spherical style. However, as the size of the dendrimer increases, the steric encombrance between the chemical moieties at the periphery becomes more important and restrict the dendrimer growth. This phenomenon is named "starburst limit effect" and vary from dendrimer to dendrimer depending on the chemical entities used to produce the dendrimer.

1.1.2 Dendrimer anatomy

A typical dendrimer anatomy can be divided in four constituents as shown in **Figure 1-1:** 1) central core, 2) repetitive branching units called generations, 3) peripheral terminal groups, 4) internal cavities.

Thus, all the above-mentioned components have principal roles in the chemical and physical properties of dendrimers which makes them different from linear polymers. The core provides the total shape and direction of the dendrimers; in addition, it determines the number of surface group. In addition, the multiplicity of polymeric

branches is related to the type of central core used to. Dendrimers platform possess multivalent and multifunctional nanoconjugates. The peripheral terminal groups also control the solubility of dendrimers. Moreover, dendrimer activity is not restricted to chemical interactions of peripheral moieties but they can also trap compounds of interest in their internal cavities. Hence, the interest in dendrimers as a drug delivery vessel.

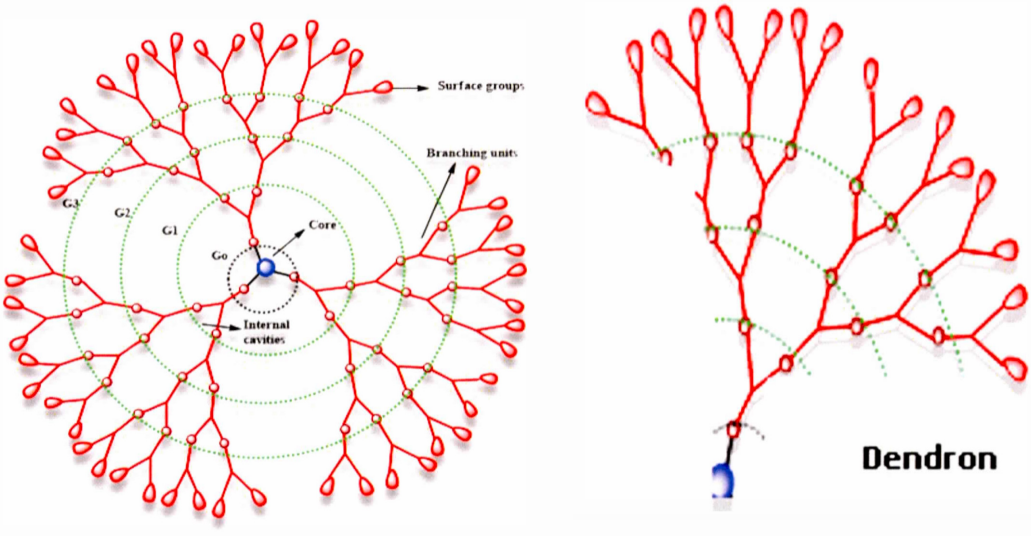

Figure 1-1. Dendron and dendrimer architecture.

1.1.3 Applications

Dendrimers have been explored in a wide range of applications such as drug and gene delivery,[18–21] sensing,[22,23] electronics,[24,25] diagnostics,[26] and nanoengineering[27] which is shown in **Figure 1-2**. In addition, dendrimers are majorly used for other principal applications such as bacterial biofilm inhibitors[28] which is the main subject of this study [29] as therapeutic agents[30] due to their versatility, multivalency and their low polydispersity. Briefly, dendrimers are presented as convenient candidates for all different applications mentioned in the scheme below. Their surfaces and their interior part (as their core) can be utilized to attach different functional moieties.

Dendrimers have been largely used in drug delivery due to their monodisperse nature and because they are small enough to travel across biological barriers. Among them, PAMAM and triazine based dendrimers have been investigated for drug delivery.[31] As shown **Figure 1-3** (a) and (b), drug delivery by dendrimers can occur mainly from three different mechanisms :

- Covalent conjugation: The existence of large functional groups on the surface of dendrimers make them appropriate for covalent conjugation of numerous drugs with relevant functional groups in which the targeting agents and drug molecules are covalently attached to the multivalent surface of the dendrimers.

- Electrostatic interaction: The high density of functional groups like amine or carboxyl on the surface of dendrimers have potential applications in enhancing the solubility of hydrophobic drugs by electrostatic attractions.

- Encapsulation: Hydrophobic drugs can be solubilized by physical incorporation in their interior part and inserted into internal layers of dendrimers in higher generations.[32]

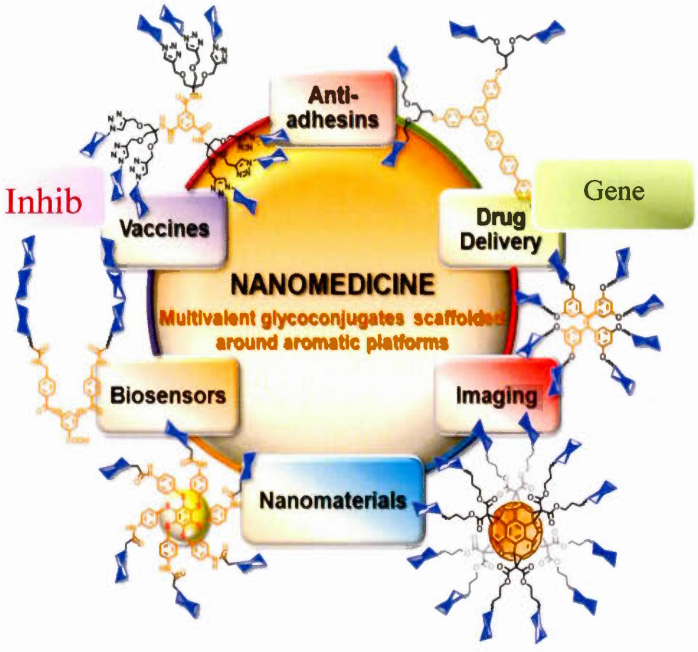

Figure 1-2. Dendrimers applications.[1,33]

In other words, the internal cavities of the dendrimers can serve as a pocket that can encapsulate a molecule of interest through self-assembly. It is kept inside the dendrimer through intermolecular interaction (hydrophobic or hydrogen bonding) or electrostatic interaction until they reach their intended target. In this way, dendrimer can deliver drugs locally with high efficiency, which allows to reduces drug cytotoxicity and is known as theranostics (combining therapy and diagnostics).[34,35]

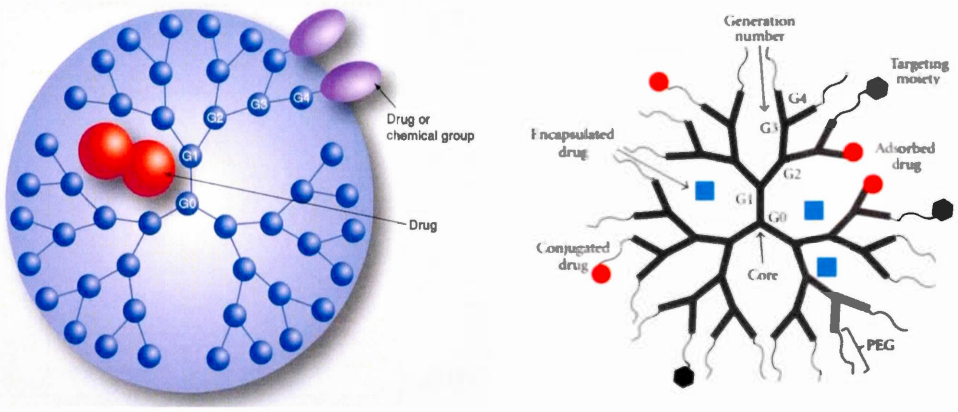

Figure 1-3. (a) Encapsulation & covalent conjugation for drug delivery on dendrimers (b) Combination drug delivery system on dendrimers: concurrent delivery of water-soluble and -insoluble drugs by adsorption to the surface (ionic interaction), encapsulation within hydrophobic micro cavities inside branching clefts or direct covalent conjugation to the surface functional groups.[36]

Additionaly, dendrimer can serve as a scaffold to increase the drug loading capacity and improve bio availability due to the multivalent interaction of peripheral moieties and internal cavities.

For example, dendrimers are highly advantageous for cancer treatment where the tumor can be targeted with high precision. Another application of dendrimers is connected to gene delivery. DNA and siRNA can be attached to terminal groups of dendrimers through electrostatic interactions to form a complex named dendriplex which leads to a better transfection efficiency.

1.1.4 Dendrimers as multivalent ligands and inhibitors against bacterial biofilm formation

Pathogenic bacteries produces biofilm through interaction of surface proteins with oligosaccharides on epithelial of host cells and is known as glycoprotein interaction. Dendrimers with oligosaccharides as peripheral terminal moieties can be used to mimic

the glycoprotein interaction. In this way, they can as a competitive pathway inhibit interaction with bacterial protein and inhibit biofilm formation.

1.2 Strategies for dendrimer synthesis

Historically, dendrimers has been synthesized following three different strategies: divergent, convergent and "onion peel". Where each method possesses its own advantages and disadvantages as shown in **Figure 1.4**.

1.2.1 The divergent method

Dendrimers were first synthesized by the divergent method which was developed by Tomalia [37,38] and Newkome. The divergent method involves an inside-outward and stepwise approach, where a monomer, a molecule which possess one reactive site and multiple dormant groups, is added iteratively to a core molecule.

The dendrimer growth starts with the addition of the monomer reactive site to the core, resulting in the 1st generation dendrimer where the dormant groups of the monomer stands at the periphery and the core at the center of the macromolecule. Then the dormant sites can be activated for subsequent monomer addition, to produce the next generation of dendrimer. The dendrimer growth then proceeds iteratively by addition of monomer until it reaches the desired size. At this point, the dendrimer can be capped off with the terminal moieties of interest.[39]

The divergent approach offers great control over the size and terminal functionalities of the dendrimers which is impossible when using the convergent approach. However, at each monomer addition step there is a chance of incomplete reactions, resulting in dendrimers with structural defects. And because it is difficult to purify dendrimers,

monodispersity is an issue for the divergent approach especially at higher dendrimer generation. Thus, the divergent approach requires high yield monomer reactions, excess amount of monomers and lengthy purification steps to produce monodisperse dendrimers.

1.2.2 The convergent method

As oppose to the divergent approach, the convergent method presented by Hawker and Fréchet is an outside-inward approach.[40] In this method, the branches of the dendrimer called "dendrons" are synthesized separately in earlier steps; where the dendrons can serve as large building blocks that can be attached to a central core to obtain a dendrimer. Using this approach enables the attachment of different dendrons on the same core to design multifunctional dendrimers. Moreover, there is a greater control over the synthesis of dendrons resulting in reduced reagents consumption and simplified purification procedure. Nonetheless, due to steric hindrance, there is a limit to the size of the dendrons that can be attached to a single core. Consequently, the convergent method produces smaller dendrimers compared to the divergent method and is not suitable for biological applications.[41]

1.2.3 Onion-peel method

The onion-peel method is a novel strategy which was developed by R. Roy and co-workers.[42–44] This method was mostly used for divergent construction of dendrimers and glycodendrimers in which, the various species of building blocks are used at each layer of the dendritic growth. The synthesized dendrimers through this strategy are essentially different from the conventional dendrimers due to their different chemical composition of branches at each generation. Dendrimers provided by this method have heterogeneous layers meanwhile the conventional dendrimers follow the repetitive manner to form the different generations. In addition, they include similar and monotonous chemical units at their scaffold. [42–44] In other words, the novel "onion peel"

approach provides the opportunity to accelerate the collection of surface groups together with different chemical entities considering the biophysical versatility between the dendrimer generations. Recently the construction of dendrimers through onion peel methodology via convergent and divergent has been recently reported by R. Roy and his group.[45] According to this prominent strategy, heterogeneous layers were chemically assembled at each generation by utilization of extremely effective chemical reactions, namely "click chemistry" including the copper-catalyzed azide-alkyne cycloaddition (CuAAC), thiol-ene (TEC), thiol-yne (TIC).[46,47] It also includes coupling and esterification via diverse orthogonal building blocks. Notably, it enables the use ot building block to tailor the dendrimer properties such as the presence of UV-vis transitions.

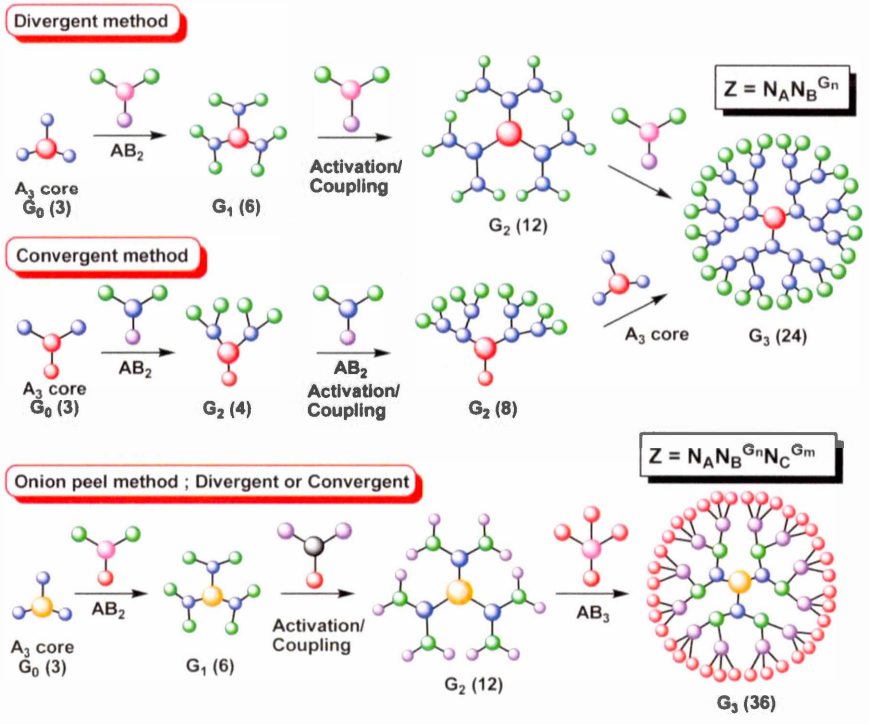

Figure 1-4. Dendrimers synthesis strategies: divergent, concergent and onion peel method.[42]

1.3 "Click chemistry"

"Click chemistry" designate a group of reactions that fulfill a set of criterias, namely reactions that are stereospecific, that can be performed under mild conditions, that gives high yield and are easy to purify.[48–50] "Click reactions" are well adapted for the synthesis of dendrimers and are critical to the development of new dendrimers. Among the existing click reaction, thiol-ene (TEC), thiol-yne (TYC)[47] and copper-catalyzed azide-alkyne cycloaddition (CuAAC) are the most widely used.[46]

"CuAAC"is a copper-catalyzed reaction of an azide with an alkyne functional group in order to form stereospecific 1,4 heterocycles of triazole. The first synthesized triazole was reported by Arthur Michael in 1893, but the study of 1,3 dipolar cycloaddition to form 1,2,3-triazole has been introduced by Huisgen in 1963 based on the reaction kinetics and the conditions. According to Huisgen's studies, the cycloaddition through this process leads to two regioisomers: 1,4 and 1,5-isomers, which basically requires energy such as heat as the essential factor.[51] Later in 2002, the discovery of the copper (I)-catalysis of 1,3 dipolar cycloaddition by K. Barry Sharpless[52] and Morten Meldal groups[53] solved the problem of Huisgen regiochemistry and kinetic. Significantly, Sharpless and coworkers specified the concept of "click chemistry" as the fast, versatile, regioselective method that thermodynamically is the favored reaction which leads to regiospecific 1,2,4-triazole ring. Hawker and coworkers illustrated the synthesis of dendrimers via two types of click methodology:

1. Azide-alkyne reaction followed by halogenation and azido substitution using the convergent method.[54]

2. Thiol-ene reaction divergent synthesis of dendrimer up to the 4th generation 4.[54]

Thus, Cu (I) catalyzed alkyne-azide "click reaction" is known as an effective method to synthesize diverse kind of dendrimers as the fast regioselective reactions in high yield with minimum purification. The major drawback of "click" reaction is due to the copper cytotoxicity in biological, biomedical and pharmaceutical applications. To address this issue, incubation with EDTA (ethylenediaminetetraacetic acid) is applied as one of the practical technique, (the lower limit of detection in quantifying methods), to remove the majority of residual copper.

By means of "click chemistry" reaction via "onion peel" approach, various dendrimers with different building blocks at their periphery can be constructed. Referred to as "multivalent ligands", these synthetic dendrimers offer multiple functionalities on their scaffold with more productivity and efficiency. Thus, they are significantly useful as therapeutic agent in anti-adhesion therapy.

In 2005, Sharpless and co-worker published the article[55] in which the "click" mechanism via Copper (I)-catalysis has been clarified in 5 stages which is shown in **Figure 1-5**,[51] including stage (A): copper acetylenide formation, stage (B): azide-copper acetylenide coordination, stage (C): cyclization to form an uncommon six-member metallocycle, stage (D): rearrangement 1,2, stage (E): proteolysis which leads to form the final favored product (1,4-isomer).

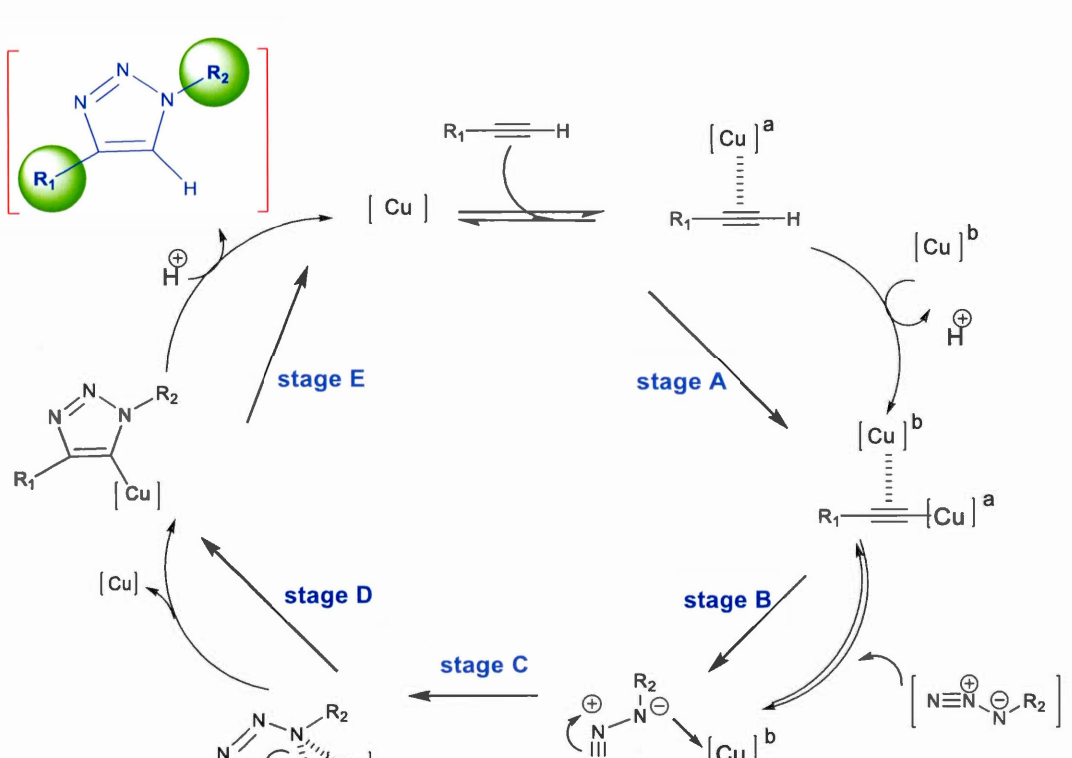

Figure 1-5. CuAAC five stages mechanism proposed by Sharpless.[56]

1.4 Glycodendrimers and their role aas inhibitor

Glycodendrimers are dendrimers with sugar moieties as terminal groups and most often serve as a biomimetic macromolecules, **(Figure 1-6)**. The exposed sugar moieties on the periphery are responsible for binding-recognition process with their cognate protein receptors.[42,57–62] Typical glycodendrimers are composed of dendrons capped with glycans e.g. mannose, fucose, galactose, etc. that are attached to various multivalent cores such as cyclotriphosphazene (N_3P_3) or cyanuric chloride ($C_3Cl_3N_3$). Their specific potencies to provide the carbohydrate-protein interaction make them notable for biomedical studies as agents in anti-adhesion therapy. Several reports including the very first example of Janus glycodendrimer[8] (Gal-Fuc) have been published.[9-10]

Besides, they afford other diverse applications as dendrimers. For instance, they are employed as drug delivery mediators or carrier agents in gene therapy.[37]

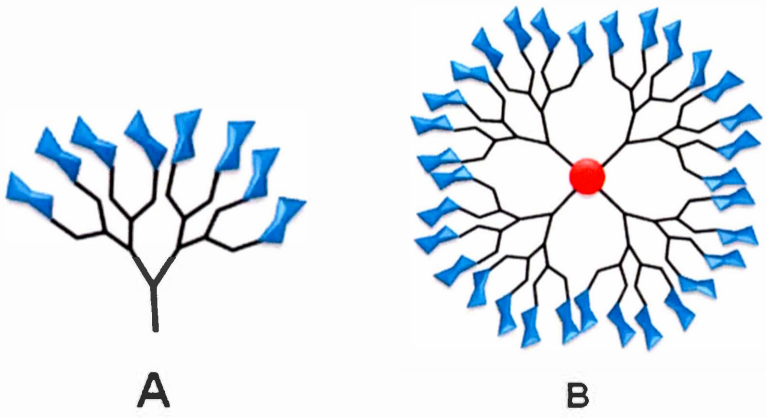

Figure 1-6. Structure of a glycodendrimer where glycans (mannose, fucose, galactose, etc.) are shown in blue, branching units in black and the core in red (A) Glycan dendron. (B) Glycodendrimer[42]

1.5 Aromatic scaffold for glycodendrimers

The mimetic glycoconjugate provided by glycodendrimer shows superior affinities in comparison to monovalent glycan-protein interaction. This artificial glycan-protein interaction is afforded through the "glycoside cluster effect" known as "multivalent glycoside effect"[45,63–66] Accordingly, the synthesis of multivalent glycosylated structures has been vastly developed.[67,60,61,68–74] Various synthetic strategies have been displayed for glycoclusters and glycodendrimers where using multivalent scaffolds plays the principal role that contributes to the formation of the arranged architectures.

Using different multivalent scaffolds in glycoclusters structures allow them to have better structural diversity with various building blocks which differs in valency and peripheral functionalities. Their utilization can promote the glycan-protein interaction due to the appropriate spatial orientation of sugar residues as suitable recognition units

on their periphery for proper binding. Correspondingly, fitting the topology of this kind of glycoclusters with geometry of proteins of the pathogen such as lectins, enhances their role of inhibitors in anti-adhesion therapy.

The first "aromatic scaffold" has been provided by Yariv and co-workers in the early 1960.[61,75] Despite the presence of an hydrophobic aromatic core, the dendrimer is still soluble in aqueous solution due to the presence of hydrophilic sugar moieties at the periphery. Consequently, dendrimer based on aromatic core can still be characterized in aqueous media by biological surveys and biophysical measurements. The molecules synthesized by using different rigid frameworks such as aromatic rings, heteroaromatics and complex polycyclic derivatives have various fascinating biological applications as well as anti-adhesion, vaccines, drug delivery agents, gene transfer functionary, imaging agents, biosensors, etc as shown in **Figure 1-7**.[61]

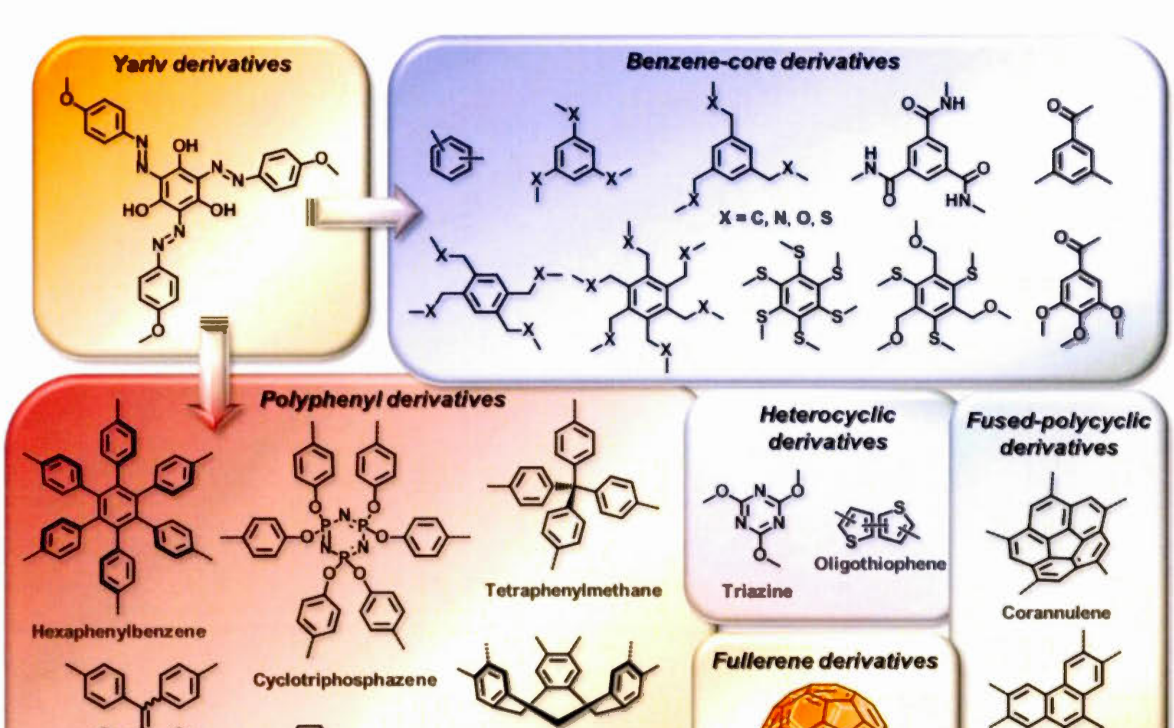

Figure 1-7. "Aromatic scaffold" used in designed glycodendritic architectures.[61]

Cyclotriphosphazene and triazine cores as aromatic scaffolds

Cyclotriphosphazene is a well known building block used in in organic, inorganic and high-polymer chemistry that can serves as a scaffold for the synthesis of a new class of glycodendrimers.[76] It has the advantage of being non-toxic and its aromatic π-π* transitions can be followed by UV-vis spectroscopy.

Allcock and his coworkers[77] synthesized the polyphosphazene compounds as a usage of carriers in drug delivery systems due to their biodegradability and biocompatibility which was followed by their thermal and chemical properties. Also, the star-shaped amino acids using N_3P_3 have been achieved by Inoue and his coworkers.[78,79] The

primary phosphonium cascade molecule was reported by Rengan and Engel[80] in the year 1991. Then many dendrimers were made by using the cyclotriphosphazene as the core by Majoral group since 1994. Above all advantages of the cyclotriphosphazene family, the antimicrobial and biological effects on bacterial cells is considered as an efficient eye-catching characteristic.[81–83] They highly possess potential to accommodate a higher number of functional units (such as dendrons) on their scaffold which leads to the higher generation in dendrimer synthesis. Triazine and cyclotriphosphazene core possess hydrophobic properties; however, upon functionalization with hydrophilic sugar moieties, they become water soluble which is important factor for glycoconjugate interaction in *vivo*. Thus, they offer better hydrophilic interaction between sugar residues and protein receptors. Therefore, we have projected our synthetic strategy using cyclotriphosphazene and triazine due to the mentioned significant properties.

1.6 Multivalency role in anti-adhesion therapy

Biologically, the carbohydrates of cell surface are derived from glycolipids, glycoproteins, and proteoglycans. Mostly, they exist on the cell surface as short units of oligosaccharides generally between one to six carbohydrate residues responsible for carbohydrate-protein interaction process, via sugar recognition site on protein of the pathogens.[84–86] The first carbohydrate-protein interaction between the bacteria and the host cell leads to the first pathological event. Subsequently the cascade of aggregation of such interaction results in a serious occurrence as infection. Although, the biological carbohydrate-dependent event highly depends on the short oligosaccharide sequences on host cells, it is not dispersed in a wide range. Moreover, according to the reported studies, the binding affinity of individual oligosaccharide groups with pathogen is low, with a dissociation constant (K_D) in the range of μM to mM.[87,88,89] Therefore, the nature of low affinities of carbohydrate-protein interaction, as well as the nature of insufficient quantity of carbohydrate residues on glycolipids prompts the important concept of

multivalency of glycodendrimers. In other words, the organized multivalent architectures offers enhanced binding interactions compared to host cells. Consequently, due to mimetic glycoconjugate interactions with their complementary protein receptors of the pathogen with higher affinities, they can be considered as inhibitors to block the biological carbohydrate-protein interactions. Briefly, multivalent glycodendrimers can enhance the glycoconjugate binding force which is the worthful target of this study.[87,89] Furthermore, the multivalency concept provided by glycodendrimers is essential to accomplish the effective recognition and binding, as well as the improvement of their antimicrobial activity[90–93] The multivalent binding of a bacterium or a bacterial toxin to a glycodendrimer is shown in **Figure 1-8** where the inhibitory role of glycodendrimer to block the biological carbohydrate-protein interaction is demonstrated.[90] **Figure 1-8A** is the depiction of a host cell with two dissimilar carbohydrates interacting with bacterium and bacterial toxin, in the absence of glycodendrimer. **Figure 1-8B** shows two different glycodendrimers containing the sugar moieties similar to host cells, the binding of the bacterium and the toxin to glycodendrimers will be achieved through the multivalent interaction to prevent the infection of host cells in a competitive manner.[90]

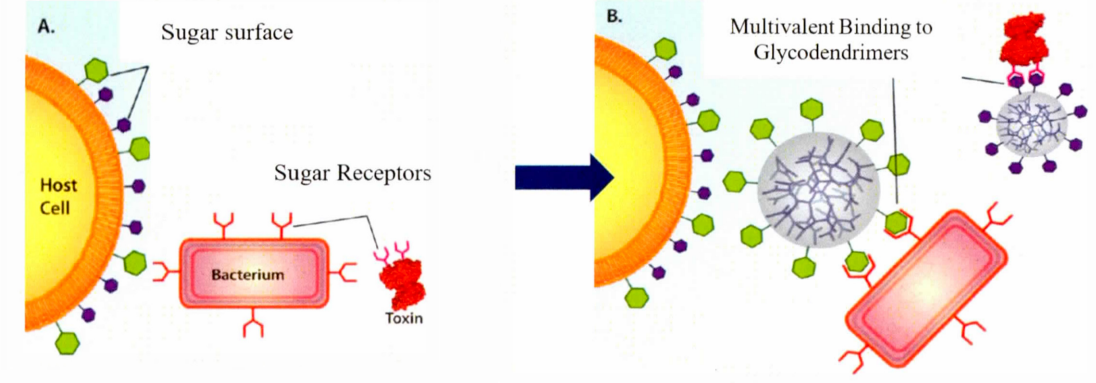

Figure 1-8. The multivalent binding of a bacterium or a bacterial toxin to a glycodendrimer.[90]

CHAPTER II

GLYCOBIOLOGY AND CYSTIC FIBROSIS

2.1 Carbohydrate-protein interactions

2.1.1 Introduction

Both physiologically and pathologically, carbohydrate-protein interactions are considered as the source of several biological processes.[94] Additionally, the mentioned interaction has a principle role in cell adhesion in which, the bacteria, virus, fungi, etc attach to the host cells resulting in the initial step of infection. That pathological phenomenon such as bacterial infection is due to the formation of the glyco-protein interaction. As explained earlier, the complex carbohydrates which are commonly situated at the cell surface, can interact with their complementary and appropriate proteinaceous receptors. This formation of carbohydrate-protein interaction is due to the contribution of a specific amino acid of a protein such as Lectin PA-IL with specific group of carbohydrate ligands like D-Galactose via two dissimilar methods namely hydrogen bond and hydrophobic interaction. X-ray crystallography study provides us with the major data about the combining sites of lectins with their specific ligands; in addition, it can offer the detailed information at the atomic level for interaction between the two molecules.[94] In this chapter the interaction between Lectin PA-IL as a galactophilic protein and its specific ligand D-Galactose will be discussed.

2.2 Lectin-Carbohydrate bonding

Lectins as well as other protein receptors can bind to their specific ligands through three major hydrogen bonds, hydrophobic interactions and electrostatic through salt bridges. There are other secondary interactions for the formation of such event like ion pairing; correspondingly, the coordination with metal ions.[94–97] Moreover, water molecules facilitate the bonding which would be described in the following pages.[97]

2.2.1 Hydrogen-bond as noncovalent interactions

Hydrogen-bonds are profoundly involved in granting specificity to the protein-carbohydrate interaction and their efficiency in protein-carbohydrate affinity.[94,98] The foundation of hydrogen-bonds is fundamental for proteins such as lectins to recognize selectively their appropriate carbohydrate ligands shown in **Figure 2-1**.[74,99,100] The presence of multiple hydroxyls on the carbohydrate architectures as the functional groups allow them to form the hydrogen-bonds between the OH groups of sugars and OH, C = O and NH functional groups of the amino acid side chains of the protein, mostly Asp, Asn, Glu, Gln, Arg, Ser, His, Tyr.[101] Moreover, the probability of multiple hydrogen-bonds on the same atom, enhances the interaction with more rigidity and specificity. This interaction is directional and the energy of such an interaction is estimated at intermediate level between van der Waals interactions and covalent interactions.[74,102,103] Hydrogen-bonds are considered as vital phenomena for biochemical events due to their contribution to the dynamic and rapid association/dissociation at room temperature in physiological milieu.

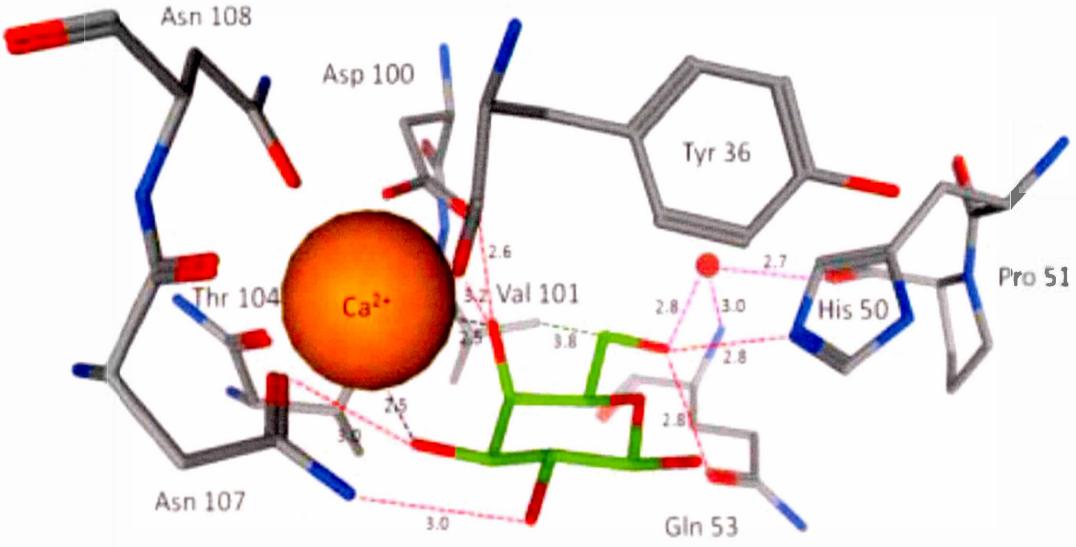

Figure 2-1. Amino acids involved in monomer of PA-IL bonding site in interaction with D-galactose (PDB code 1OKO). The interactions include direct hydrogen bonds, hydrogen bonds with water, interactions with calcium ion and hydrophobic interactions. Water molecule is shown as a red ball.[38,44]

2.2.2 Hydrophobic interaction

Carbohydrates are highly polar molecules; however, the steric disposition of hydroxyl groups of the pyranose ring generate additional hydrophobic C-H bond on their surface. This provides them with the ability to interact with their complementary amino acids of proteins via α and β sides (30 glycomimic).[32,94,104,105] The creation of the apolar face leads them to form a type of interaction with hydrophobic side chains of the lectin proteins frequently under "C-H π stacking" of the carbohydrate ring with aromatic amino acids of the binding sites of the lectin proteins such as Phenylalanine (Phe), Tryptophan (Trp), Tyrosine (Tyr). Hydrophobic stacking is presumed as the foundation of the hydrophobic interaction.[74,94,105] Stacking a carbohydrate ring on a side chain of an aromatic amino acid is related to the partially positive charges on the aliphatic protons of pyranoside ring and partially negative charges from the π electrons of the aromatic amino acids which can be summarized to "multiple weak C-H…π

interactions".[103,106,107] In addition, the methyl groups correlated to the 6-deoxy carbohydrates normally provide the hydrophobic interaction with aromatic amino acid residue as well as stacking event. Hydrophobic interactions can also occur with the aliphatic amino acids such as valine or leucine. According to the reports and surveys, the hydrophobic interactions play an undeniably principal role in stereospecific binding lectin A to the β-galactoside ligands with various chemical entities which is shown in **Figure 2-1**.[107–110]

2.2.3 Ionic interactions

Carbohydrates are frequently neutral; although, there is vast category of charged sugars which participate in ionic interactions such as sialic, iduronic acids, glucuronic, aminosugars and sulfated sugars. There are also modified-sugars such as sulfated sugars and phosphorylated sugars that are negatively charged or other types of sugars positively charged.[32] Basically, there is a strong affinity between the charged sugars and amino acids of lectin proteins due to the electrostatic forces (Coulomb`s law and Pauli`s repulsion) resulting in ionic interaction as an additional interaction with lectins. **Figure 2-2** presents ionic interactions between the anomeric sulfated functional group of sulfo-sialic acid with arginine 371, arginine 292 and arginine 118 "red dashed lines" with strong electrostatic forces also ionic interactions between glycerol moiety of sulfo-sialic acid analogue with glutamic acid "yellow dashed lines".[40]

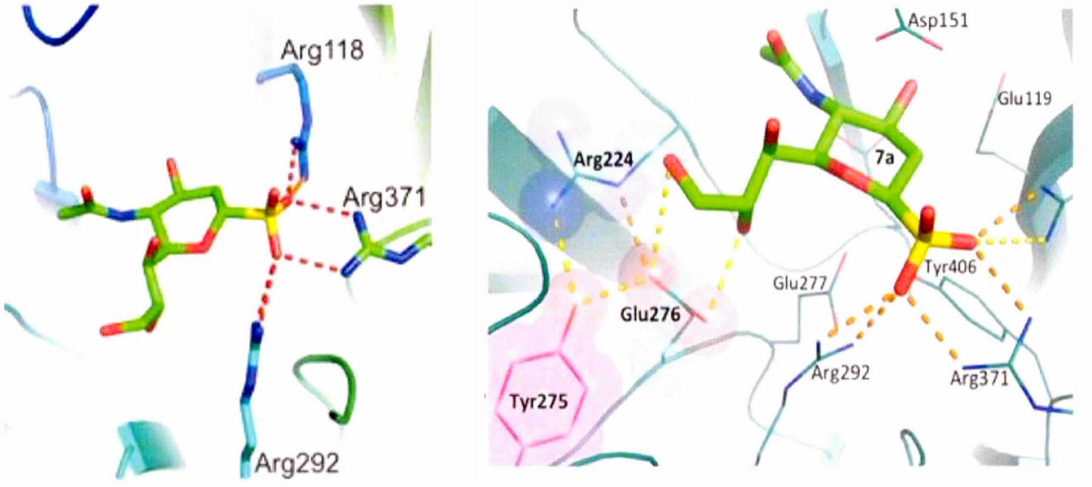

Figure 2-2. (Left) Ionic interactions between sulfated functional group of sulfo-sialic acid with Arg 371, Arg 292 and Arg 118 in red dashed lines. (Right) Ionic interactions of sulfo and glycerol moiety in sulfo-sialic acid analogue respectively with Arg 371, Arg 292, Arg 118 and Glu 276 in dashed lines, with stronger electrostatic interaction colored orange. Sulfur atom colored yellow (ref sialic acid).[111]

2.2.4 Metal interaction

Metal ions such as Ca^{2+} are situated in the vicinity of the binding sites of bacterial lectins and they are able to be bound indirectly to certain sugars. [74,112] The calcium cations as the complex with lectins, are often coordinated with negatively charged amino acids of lectins and the oxygen atoms of hydroxyl groups on carbohydrates. Ca^{2+} ion has a principal role to enhance the sugar-protein interaction through the relative stereochemistry and to maintain structural integrity of the lectin.[74,112] Tetrameric Lectin A and B of the opportunistic *Pseudomonas aeruginosa* bacteria are examples of calcium-dependent lectins, in which each monomer binding site is associated respectively with one and two Ca^{2+} atom. The complex of lectin-calcium atom is followed by the network of hydrogen bonds which provide them with the adequate binding sites considering the selective specificity that creates the remarkable medium affinity to the D-galactoside moiety and very higher affinity in micromolar range to fucose and mannose sugars. [113,114] The galactose -binding site of PA-IL includes one

calcium atom as shown in **Figure 2-3**.[114] According to **Figure 2-3**, each monomer of the tetrameric lectin is in direct interaction with one calcium ion in the specific binding zone planned for galactoside residue to be locating there. In the PA-IL/galactose complex, the oxygen atoms on the position 3 and 4 of galactose residue are directly involved in the spherical coordination with calcium ion, **Figure 2-3**.[114,115]

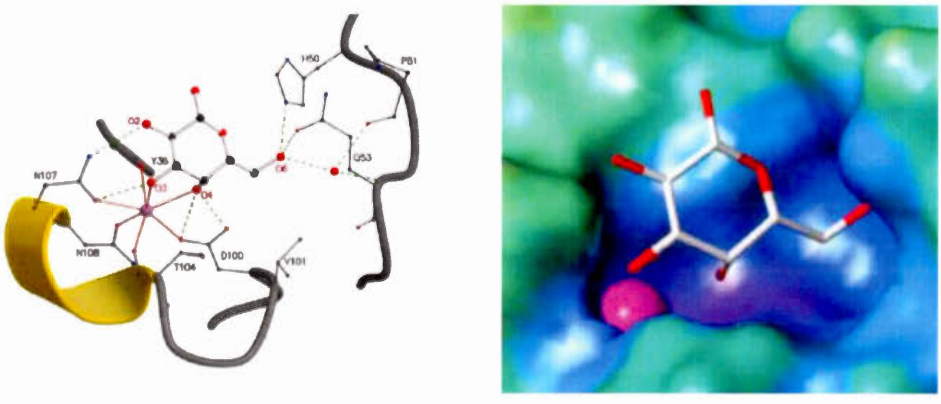

Figure 2-3. Binding site in the crystal structure of the PA-IL/galactose complex (PDB 1OKO). (Left) Stick model of the amino acids PA-IL coordinated with Ca^{+2} and in binding with galactose residue. Ca^{+2} coordination bond is shown in solid orange line, hydrogen bonds by dashed green line. Color coding: red for oxygen, blue for nitrogen, black for carbon, pink for calcium. (Right) Electrostatic surface of the protein-binding site related to PA-IL with Ca^{+2} and galactose. Color coding: from violet for negative to orange for positive of the protein-binding site, large pink sphere for Ca^{+2} and stick model for galactose residue. [114,115]

2.2.5 Role of water

As shown earlier in **Figure 2-1**, the extra hydrogen bonds between the ligand and PA-IL are related to the water bridges. The ligand-protein interactions are mostly mediated by water bridges.[116] In aqueous milieu, there are ligand-water and protein-water connections. The overall process of these bindings is replaced by the ligand-protein connections that is followed by water release turning to the aqueous system as the

solvent. The establishment of the hydrogen bond network in carbohydrate-protein complex where water act as hydrogen bond donor or acceptor is essential for ligand recognition.[31]

2.3 Galactose-PA-IL complex interaction

The interactions between a galactose ligand and a monomer lectin A of *P. aeruginosa,* as an example of the carbohydrate-protein interaction, are shown in **Figure 2-1**.[38] These interactions involve direct and indirect hydrogen bonds, hydrophobic interactions, and other interactions which are bridged to calcium ion and water molecules. Coordination of calcium ion with various type of *lec A* amino acids include Tyr36, Asp100, Thr104, Asn107, Asn108, and with Gal.O3 and Gal.O4 related to hydroxyl groups. Hydrogen-bonds include Gal.O2 with Asn107, Gal.O3 with Asn107, Gal.O4 with Asp100, Gal.O4 with Asp100, Gal.O6 with His50 and Gal.O6 with Gln53. Hydrophobic interactions include Gal.C1 with Tyr36, Gal.C2 with Tyr36, Gal.C4 with Thr104 and Gal.C6 with Val101. Moreover, there are several hydrogen bonds of 4 water molecules with Gal.O1, Gal.O2, Gal.O3 and Gal.O6. Additionally, there are bridging water molecules with Pro51 and Gln53 which help to establish and enhance the hydrogen bond network of the system.[44]

In conclusion, the lectin-galactoside interactions possess six direct hydrogen bonds between hydroxyl groups of the galactose and lectin A, and one additional water molecule bridge. Moreover, few hydrophobic interactions which can establish the carbohydrate-protein interaction via the contact between the apolar face of galactose residue and specific hydrophobic amino acids which has been explained earlier in **Figure 2-1**.[38,44]

2.4 Cystic fibrosis and the role of *Pseudomonas aeruginosa* lectin A

Cystic fibrosis is the most lethal genetic disease amongst the middle-aged Canadian population. The chronic lung infection resulting in the respiratory failure, is considered as the major cause of the mortality in cystic fibrosis and hospitalized patients. The chronic lung infection is due to the colonization and adhesion of the opportunistic bacteria *Pseudomonas aeruginosa* on the surface of lung epithelium which leads to the formation of a thick layer of bacterial aggregation in a term of a biofilm. *Pseudomonas aeruginosa* is a ubiquitous gram-negative bacteria which is found in various environment such as soil, water and vegetation. Moreover, it is responsible for numerous nosocomial infection that can affect people not only with the genetic disorder cystic fibrosis but also with human immunodeficiency such as HIV/AIDS. [117,38] The first adhesion to the host tissues is the initial concerned step toward infection achieved via oligosaccharide-mediated recognition by binding the sites of *P. aeruginosa* protein as shown in **Figure 2-4**.[28,118] Referred to this event, the initial carbohydrate-protein connection is fairly sufficient as a key role to provide the opening for pathogen for next phase of interactions that ends up with the severe cohesive attachments and eventually severe tissue damage. Correspondingly, galactose plays a fundamental role in carbohydrate recognition by the *P. aeruginosa* to initiate the adhesion process as shown in **Figure 2-4**. [114]

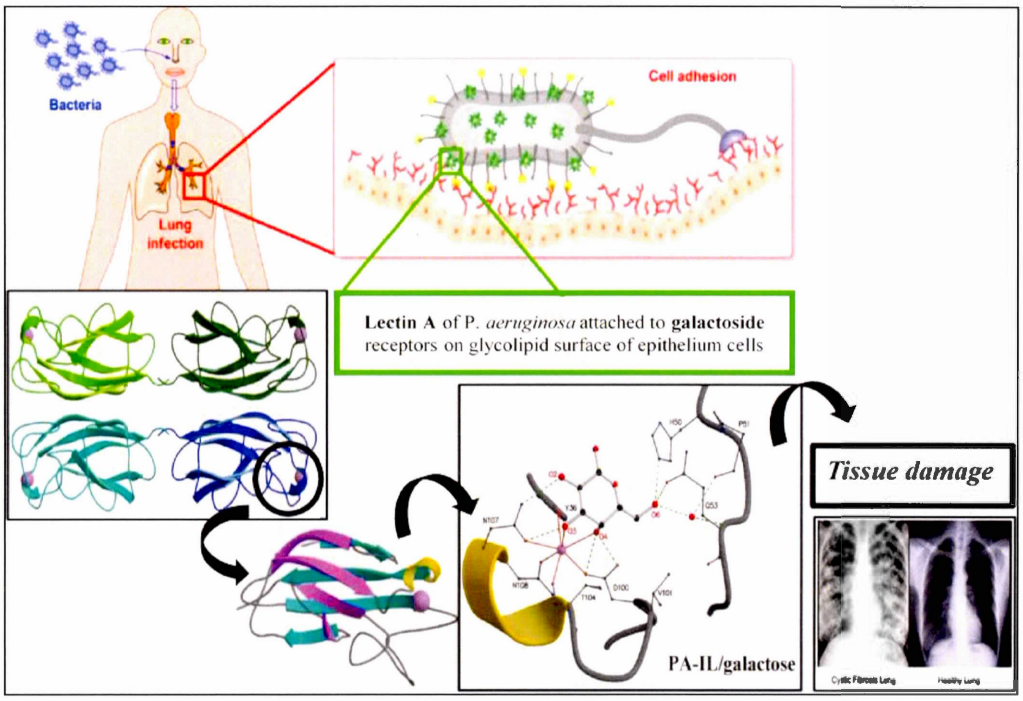

Figure 2-4. The initial process of the adhesion schematic description by *P. aeruginosa* on epithelium cells via galactose/PA-IL complex which leads to tissue damage.[44,46]

2.5 Biofilm formation

The colonies of microbial genotypes drive to the respiratory system and after their aggregation, their growth and division lead them to form the mature bacterial biofilm in the airway. Consequently, by dispersing a part of the biofilm, the free-floating bacteria would be released for future colonization which enters the cycle and forms the biofilm as a long-lasting infection, resistant to antibiotic-based treatments.[28] **Figure 2-5** illustrates the mechanism of biofilm formation.[119] The utilization of antibiotics such as ciprofloxacin for cystic fibrosis treatment has been correspondingly reported as a temporary treatment due to its short-term effect on the outer layer of microbial genotypes. However, the depth of the layer still includes a vast quantity of alive bacteria with reproductive functionality while discontinuing the treatment stimulates them to

recolonize and expand the biofilm layer. Accordingly, seeking for an alternative strategy is essentially crucial in order to avoid taking the antibiotic as the inefficient temporary solution. In fact, the biofilm formation is followed by the growth in the number of the galactose / PA-IL complexes; which is directly related to the tendency of galactophilic *LecA* to the galactose moieties exist on the cell surface.

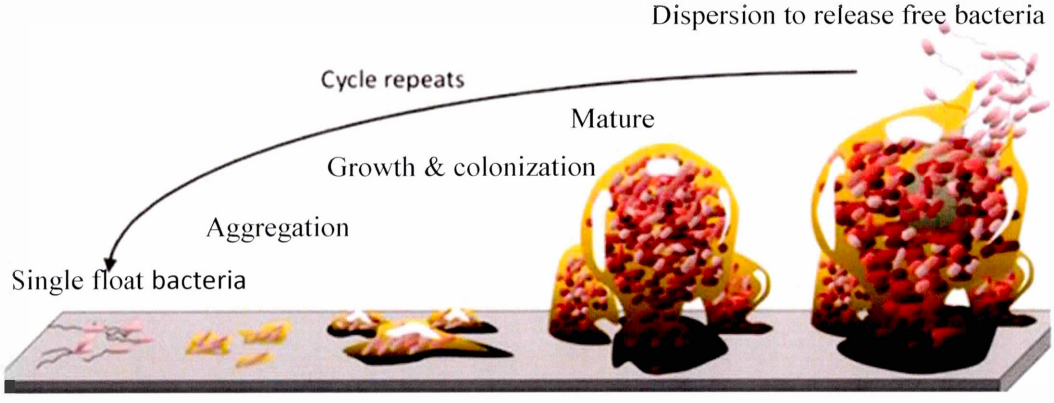

Figure 2-5. Mechanism of biofilm formation[120]

2.6 Structures and roles of *Pseudomonas aeruginosa* lectins

There are two types of carbohydrate-binding proteins of *P. aeruginosa* causing cystic fibrosis in which both proteins have been found on the outer membrane of the pathogen, named *LecA* or PA-IL and *LecB* or PA-IIL with their specificity for D-galactose and L-fucose, respectively.[120–122] Through this study we are mainly interested in PA-IL, a calcium dependent lectin that particularly recognizes D-galactose. PA-IL is considered as the first lectin of *P. aeruginosa* which is isolated by affinity chromatography, it is also the first bacterial protein which described galactose specificity.[123,124] PA-IL is a tetrameric protein with total molecular weight of 51KDa which consists of four identical monomers with 121 amino acids per subunit. Each monomer of the tetrameric

PA-IL is furnished with one calcium ion and water molecules which provides them with the adequate binding sites for galactose moieties as displayed in the crystal structure in **Figure 2-6. (left and right)**.[95] Carbohydrate-binding proteins of *Pseudomonas Aeruginosa* has a organized geometry. The topology of PA-IL based on conformational analysis was assessed to be as a tetrameric protein with rectangular architecture with the distance binding site (Ca^{+2}) ~71 A° for the long side and ~32 A° for the short side according to their ribbon structure shown in **Figure 2-6. (right)**.[125]

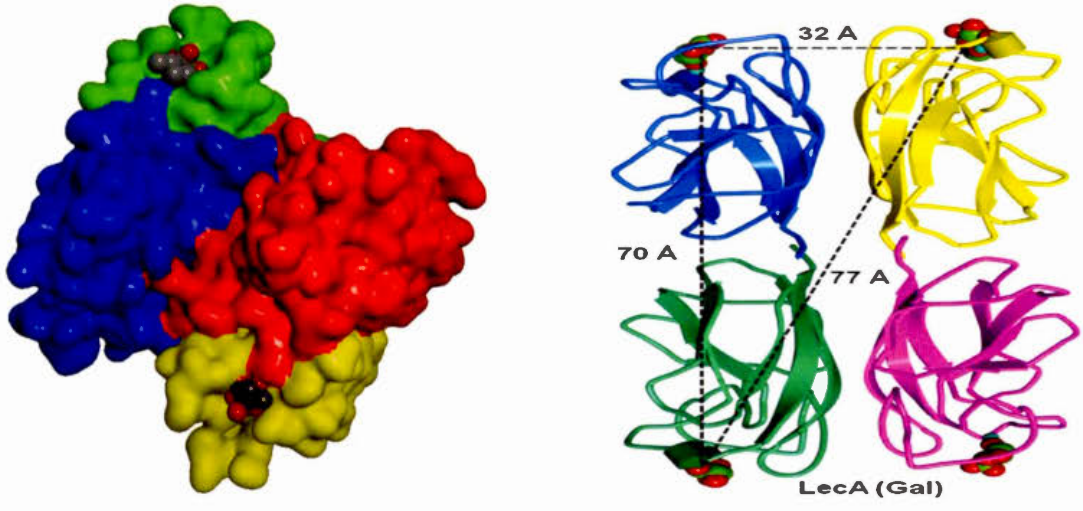

Figure 2-6. (Left) Crystal three-dimensional view of tetrameric PA-IL followed by calcium ion on the binding sites of each monomer, Roy. R scheme (Right) The distance measurement between calcium ions in tetrameric PA-IL binding sites showing their geometrically well- organized structure. (PBD code 1OKO)[42,48,49,110]

2.7 Multivalent interactions via multivalent mechanisms, non-aggregative mechanisms

Mono carbohydrate-protein interaction is a connection between a monovalent ligand and monovalent receptor considered as a reference for the noncovalent multivalent glyco-protein interactions through the biological or biomimicry process (glycosylated cell surface). Such multivalent interactions are followed by the complexity of binding as an issue due to the competition between the different biological mechanisms that can yield the various biological response which some of them are desirable and vice versa. Tetrameric PA-IL proteins possess 4 binding sites on a single face. This potency makes them able to interact with multiglycosylated ligands simultaneously such as glycosylated cell surface. Accordingly, these multivalent interactions occur through the known Chelate Association Mechanism (multivalency-driven increase of affinity) as shown Figure **2-8. (a)**.[74]Atomic force microscopy (AFM) has confirmed the chelate aggregative model in various cases, particularly for the interaction of tetravalent PA-IL, a galactose specific lectin, and a tetragalactosylated calixarene-based as its adequately well-matched ligand according to **Figure 2-7**.[126–114]

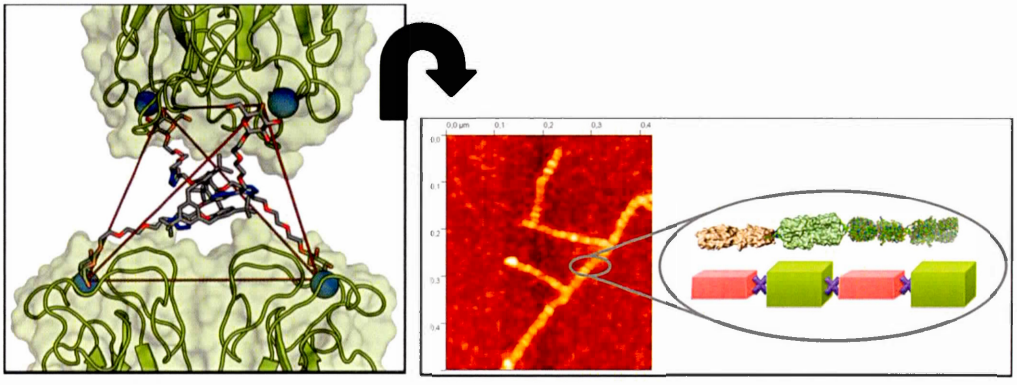

Figure 2-7. (left) Chelate aggregative model of tetravalent Calixarene-based in binding PA-IL from *Pseudomonas aeruginosa*. (Right) AFM observation of PA-IL filaments in interaction with the same glycocluster and model of the 1D-network.[74,126–130]

The other mechanism is named Receptor Clustering in which the monomer receptors such as lectins are provoked to interact with multivalent ligands; therefore, the monovalent receptors are diffused through the dynamic lipid bilayer to provide the maximum interactions with their multivalent partners. Thus, they form a clustered figure by the ligands according to Figure **2-8** (b). Receptor clustering is considered as an intra cellular mechanism.[74.131–137] The Subsite Association as the other mechanism is known when a heterobivalent ligand is connected simultaneously with two various binding sites correspondingly with two various affinities according to Figure **2-8** (c).[74.136,137] Additionally, the interaction between multivalent glycosylated ligands and monovalent receptors such as lectins can enhance the affinity by the intense density of ligands adjacent to the binding site region which leads to the higher number of reassociation according to **Figure 2-8** (d).[74.138]

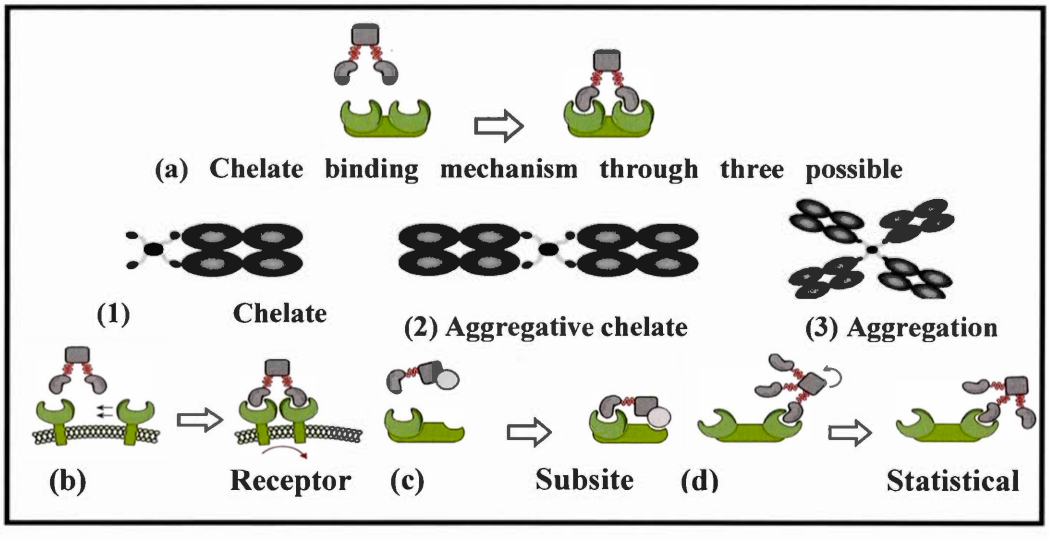

Figure 2-8. Nonaggregative mechanisms of noncovalent interactions between multivalent ligands and multivalent receptors.[69] Chelate binding model is exceptionally considered as both nonaggregative and aggregative which depends on the binding mode.[115-122]

2.8 Intra- vs Inter- Molecular cross- linking, aggregative mechanism

The various range of multivalent glyco-protein interactions are achieved through an intramolecular or intermolecular approach. Intermolecular approach is accomplished due to the aggregative non-covalent interactions between a high number of small ligands and receptors which lead them to the formation of a massive polymer chain or commonly two or three-dimensional network. The linear architecture of this type of approach between lectin and a divalent ligand related to Galectin-1, shown in **Figure 2-9** (a)[74], has been confirmed *in vitro* by X-ray diffraction data.[139] Accordingly, the increase glycoclusters valency can raise the formation of the massive three-dimensional network due to the marvellous affinity enhancement according to **Figure 2-9** (b).[74] As a result, the formed massive network via cross-linking precipitates.[65,74,140] The overall diminution of microscopic dissociation kinetics is a satisfactory approve for tremendous affinity enhancement in such a cross-linked network. The architecture of such networks using soybean agglutinin has been confirmed by X-ray diffraction. [141] The vast study of cross-linked networks has been done by Dam and co-workers. They have also illustrated the remarkable affinity enrichment between SBA and mucin of porcin origin.[142]

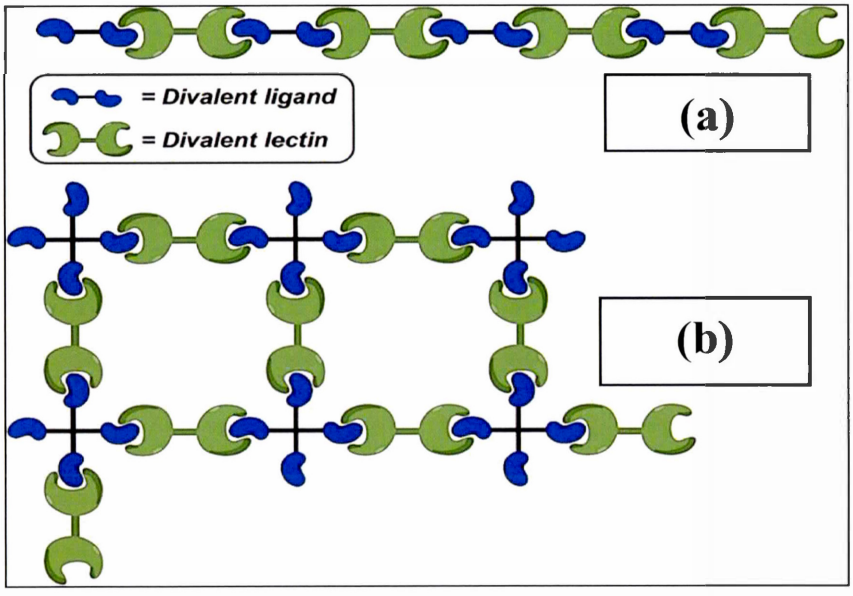

Figure 2-9. Multivalency generated cross-linking network of multivalent lectins by multivalent ligands. (a) The long chain polymer due to the interaction of divalent ligand and divalent lectin. (b) The Cross-linked network due to the interaction of tetravalent ligand and divalent lectin. [74]

In order to show the efficiency of galactoside residues and their inhibitory potentials as anti-adhesive agents considering their specificity for binding PA-IL, vast studies were done on the family of tetra propargylated calixarene. The effect of multivalencies on the various derivatives of this cluster has been also studied. The varieties were due to the different numbers of galactose moieties on their periphery (maximum 4 galactose residues). Isothermal titration microcalorimetry (ITC) as reproducible and reliable technique, provided the precise estimation on their inhibitory potencies and their binding affinities to tetrameric PA-IL with competitive efficiency.[143] ITC is a bioanalytical technique in which the measure of the released or absorbed heat is provided via association process between the ligand and protein entities based on the affinity concept. Correspondingly, it presents the thermodynamic data of such multivalent interactions as i) stoichiometry of binding, ii) variation of enthalpy and iii) dissociation constant which is achieved through the titration of a glycocluster ligand

solution with a solution involving the well-matched proteins such as lectins. According to ITC results, all the family of galactosylated calixarene cluster included monovalent, bivalent, trivalent and tetravalent have provided the low dissociation constant in a sub micromolar range. Among all, the two tetravalent ligands with 4 galactose residues possessed the highest affinities and the lowest value of dissociation constant (K_d), around 200 nM and 176 nM. However, both mentioned tetravalent glycoclusters with similar binding affinities, presented the dissimilar behaviour thermodynamically due to their topology and stoichiometry aspect. Therefore, ITC experiment indicated that the interaction of ligands with PA-IL was not only dependent on the valency but also was strongly dependent on the topology. Among the derivatives, the mentioned tetravalent clusters with K_d ~176 nM and ~200 nM had the topology 2:2 with binding stoichiometry (n=0.24) and the topology 3:1 with binding stoichiometry (n=0.26) respectively. Binding stoichiometry (n) is the number of a galactoside moieties which bind per monomer of PA-IL. Binding stoichiometry (n=0.24 and n=0.26) in both above clusters indicates that all four galactose residues in both derivatives were bound to PA-IL. However, in equal situation, the determining factor to proceed the binding is the effect of thermodynamic parameters such as enthalpy contribution as a favourable factor is observed in tetravalent with the topology 2:2. According to the binding stoichiometry and the topology, a single tetravalent galactosylated cluster should potentially interact with four different PA-IL tetramers simultaneously as an alternative shown in **Figure 2-8.** This approach as an intermolecular interaction leads to the vast aggregates. Chelation of the binding sites of two PA-IL tetramer is noted as another option for binding according to the **Figure 2-8** and **Figure 2-10**.[126] This approach is considered as an intramolecular interaction in which the two galactose residues of the intended tetravalent cluster, interact with two binding sites of a *lecA* in close vicinity on the same face. Therefore, the two other galactose residues of the same cluster are available to interact with another two binding sites of the other lecA which are situated diametrically in the opposite position in neighbouring site shown in **Figure 2-10**.[126] The resulted complex through this method is named "chelate". The interaction of a

single tetravalent cluster with all four binding sites of the same PA-IL is not possible due to the geometry of the protein. According to this survey, it is concluded that both tetravalent ligands have tremendous affinity enhancement for binding PA-IL. Moreover, they possessed the higher efficiency as an inhibitor compare to the other derivatives. In order to assess the most appropriate tetravalent glycoclusters with the higher capability as an effective ligand, the molecular modelling study was utilized. The achieved result was well-matched with chelate binding model. According to the chelate binding model, the tetravalent Calixarene with 2:2 topology can proficiently chelate two of the binding sites of a tetrameric PA-IL. In terms of geometry and energy, the best results were achieved when two of the galactoside residues of a single tetravalent cluster interacted with both binding sites on the small face of a one PA-IL monomer and the other two galactoside residues in interaction with both binding sites of another PA-IL on the opposite position. The chelates bonding is the best binding model according to the molecular studies and docking calculations considering the energy and geometry followed by highly enthalpy contribution as favourable factor which is not entirely opposed by the entropic cost.[144] Moreover, there was no steric conflict between the two lectin dimers facing each other. Hence, according to the above explained results and cross-linked network, the tetravalent Calixarene cluster, as a reference, was situated in the position to take the optimal topology to offer the intra-tetramer and inter-tetramer binding, shown in **Figure 2-10**. Correspondingly, a similar behaviour is expected for other designed ligands with terminal galactose moieties on their scaffold in which they are prompted to follow the same sequences to provide the cross-linked network for better efficiency.

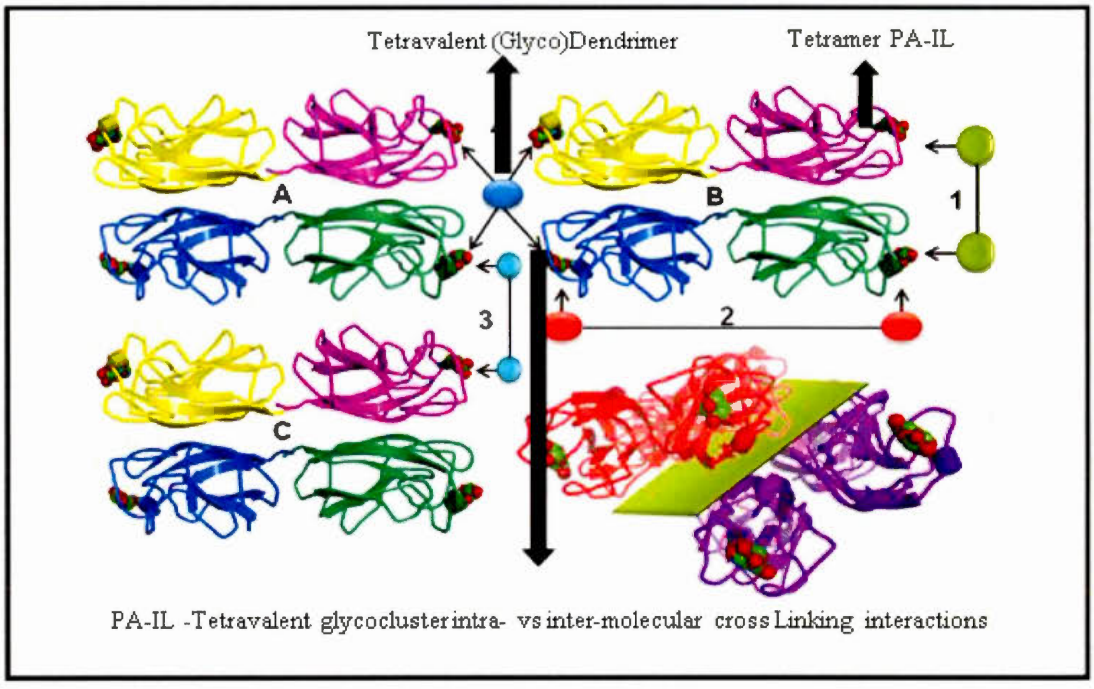

Figure 2-10. Glycoclusters are perfectly suited to inhibit bacterial lectins, Roy. R scheme.[126]

Additionally, there is another productive bioanalytical technique termed "surface plasmon resonance" (SPR), which is the study of receptor-ligand interaction. Through this method, measuring the affinity of the ligands to their well-matched receptor considering the kinetic parameters is achievable. SPR provides the real-time monitoring of adhesion on to a modified surface and can assess the inhibitory potencies of glycoclusters as anti-adhesive molecules and their potential applications as antimicrobial agents. Furthermore, this technique indicates whether the synthesized multivalent ligands have the competitive behaviour compare to the glycosylated surface.[31] SPR is the complementary method for ITC in which the mimics of biological process of binding the lectin to glycosylated cell surface is attainable by the synthetized glycoclusters. Such mimic glycoconjugates are evaluated to be confirmed as effective candidates to act as an inhibitor for binding of PA-IL to galactosylated surface. Through this technique, the interaction between lectin and glycosylated surface is

monitored in the presence and absence of a competitive ligand with more affinity compare to the glycosylated surface. The monitoring purpose is to assess the potency of the added ligand for formation the new glycoconjugate with more efficiency in order to inhibit the further adhesion of the lectin to the surface. SPR data, on the family of tetravalent Calixarene prooved that such multivalent galactosylated clusters are extremely efficient and highly impressive to behave as inhibitors to inhibit the *Pseudomonas aeruginosa* bacterial binding to the galactose ligands which exist on the surface of the host cells. Besides, according to ITC results, it is concluded that tetravalent Calixarene family has tremendous affinity enhancement for binding PA-IL. Such chelate-based interactions through the three-dimensional network, provide the appropriate and competitive glycoconjugates from both sides with more efficiency as explained earlier. **Table 2-1** indicates inhibition of the adhesion of PA-IL to the surface containing galactoside in presence of Calixarene family determined by SPR. This table also displays the ITC results consist of dissociation constants (K_d), thermodynamic parameters and binding stoichiometry (n) related to the glycoconjugates of Calixarene family bonded to PA-IL.[126] K_d is the dissociation constant obtained from IC_{50} with K_d = 150 mM for monovalent as the reference. IC_{50} is considered as a minimum concentration of the inhibitor needed to prevent %50 of the adhesion of PA-IL on galactosylated surface. β is relative potency of the multivalent inhibitor compares to the monovalent compound with β=1 as reference.[110]

Table 2-1. Microcalorimetry and SPR result related to glycoconjugates of Calixarene family binding to PA-IL. Monovalent is considered as the reference.[126]

Valency	Topology	n	-ΔH° [KJ mol $^{-1}$]	-TΔS° [KJ mol $^{-1}$]	-ΔG° [KJ mol $^{-1}$]	K_d [nM]	IC_{50} [nM]	β
1 Gal (ref)	-	~1	~36	~14	~22	150 000	71900	1
3 Gal	3:0	~0.79	~28.1	~-4.4	~32.5	2050	6400	73
4 Gal	3:1	~0.26	~98	~60	~38	200	1700	750
4 Gal	2:2	~0.24	~104	~65	~39	176	500	852
4 Man	4:0	-	No binding observed					

2.9 Carbohydrate specificity and affinity of the *P. aeruginosa* lectin A, PA-IL

The high level of affinity of PA-IL among the monosaccharides belongs to galactose with the remarkable specificity for N-acetyl-D-galactosamine as an exception considering its lower affinity compare to galactose; However, the notable grade of binding can be referred to the compensatory hydrogen bond provided by the O atom of the acetamido group as a one reason as well as the hydrophobic interaction offered by the methyl moiety of the same group as the other reason.[113,114,145] According to the reports, PA-IL displays the moderate affinity toward D-galactose with an association constant in the range of 3.4×10^{-4} M^{-1}.[113] However, prior to that, the existence of

hydrophobic groups on the anomeric position of galactose sugar regardless to the α or β configuration, can boost the affinity with the highest inhibitory potential and that belongs to phenyl-β-thiogalactoside due to the stacking phenomenon.[113] Moreover, α anomer of galactose with methyl moiety on anomeric carbon enhance the affinity compare to β anomer due to the participation of methyl group in hydrophobic interaction.[145] Among disaccharides, those with terminal α-D-galactose moiety can be recognized by lectin A with quantitative inhibitory potential such as αGal1-6Glc with affinity more than D-galactose and αGal1-3Gal less than D-galactose. The inhibitory ability of such ligands is shown in **table 2-2** according to the reported studies.[114,146–150]

Table 2-2. Carbohydrate specificity of PA-IL. D-Galactose is a reference value of 1.0 for a IC_{50} of 40 nM for inhibition binding of PA-IL to cyst hydatid glycoprotein.[114,146–150]

PA-IL inhibitor	Potency
phenyl-β-Gal	57.1
αGal1-6Glc	13.3
αGal1-3αGal-O-Me	4.7
αGal-O-Me	2.7
βGal-O-Me	2.2
αGal1-4Gal	1.8
D-Galactose	1.0*
αGal1-3Gal	0.8
D-GalNAc	0.5
βGal1-4Glc	0.5
D-Fucose	0.02

2.10 Conclusion

According to all the information above, PA-IL has a considerable affinity to α-galactosyl residues which exist on glycosphingolipid in lung epithelial cell membranes.[151,152] Such mentioned affinity causes to the formation of galactoside-binding lectins as adhesion to lung tissues which leads to the first step of bacterial infection. Therefore, various species of monosaccharide with glycomimetic ability have been evaluated through competition for their binding to PA-IL (i.e., galactose, fucose and mannose) in order to block the *Pseudomonas aeruginosa* bacterial infection. Among the mentioned monosaccharides, galactose showed the satisfactory behavior as an active ligand against the spread of infection in a murine pneumonia model.[153] Moreover, the treatment of infected lung cells by PA-IL, (the galactoside-binding lectins), with galactose or *N*-acetylgalactosamine (GalNAc) in mice model showed the inhibitory role and the protective effect of such compounds, preventing the infection from progression according to the reported literatures.[108,126,154–160] Given that, the biological carbohydrate-protein interactions in living cells are of low affinity.[161] Thus, in order to compensate the weak-binding interactions and to overcome the low-affinity of such interactions, the necessity of multiple copies of glycomimetic is required with inhibitory potency in higher level than biological glyco-protein complex; thus, it is reasonably desired to generate synthetic inhibitors with multivalent structures. Moreover, due to the affinity of PA-IL specifically to galactose residue; therefore, the presence of multivalent carbohydrate ligands is required with galactose terminal functionalities wherein they can offer higher-affinity glycomimetic as therapeutic agents in anti-adhesion therapy. This event is achievable through the design and synthesis of multivalent galactose-based glycodendrimers with their role of inhibitory for LecA as an attractive strategy for new anti-infection compounds. Glycodendrimers prepared through this strategy are well-known as one of the most potent multivalent ligands against infectious factor from a bacterial lectin of *Pseudomonas aeruginosa*.

The numerous synthetized *LecA* inhibitors have been reported according to the reports.[126,162–170]

Therefore, according to the all information above, it is concluded; infections by pathogenic agents are frequently triggered by their adhesion on host surfaces. The early step in adhesion strategy involves initial recognition of host cell glycoconjugates by sugar-binding proteins (lectins) on, or released by the viruses or the bacteria that are specific for the targeted tissues. *Pseudomonas aeruginosa* is an opportunistic pathogen implicated in the development of lung infections in cystic fibrosis (CF) patients through these sugar–protein complementary interactions. *P. aeruginosa*'s mechanism of action is governed by the adhesion of their virulence lectins (PA-IL and PA-IIL) that bind to galactoside and fucoside subunits of glycoconjugates, respectively. Our project is to design potent anti-adhesion inhibitors against the galactoside-dependent PA-IL. To enhance the binding affinities of galactoside residues, nanometer size glycodendrimers have been designed and carried out.

Therefore, the synthesis of three multivalent glycocluster in zero generation with 3, 6 and 12 galactoside moieties were achieved by efficient and versatile "click chemistry" involving oxime ligation between aminooxylated galactosides and three suitably prepared different poly-aldehyde scaffolds. Also, glycodendrimers with 9, 18, and 36 galactoside moieties were designed to prepare using recently developed "onion peel" strategy by our group. The necessary aminooxylated galactopyranoside has been synthesized from the known 2-azidoethyl-β-D-galactopyranoside that was condensed with a suitably *O*-propargylated hydroxylamino derivative. The model study of this strategy is shown in the figure below.

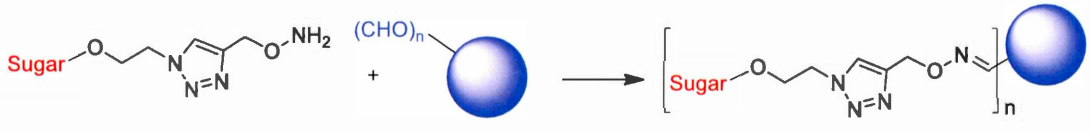

CHAPTER III

AMINOOXY ROLE AND OXIME-LIGATION

3.1.1 Aminooxy and Oxime ligation study

As explained earlier, carbohydrates have the crucial roles in biological events such as cellular adhesion, disease progression, and many other biological events.[171–175,176] Together the carbohydrates with aminooxy entities, represent their key role as major building blocks which in term, offer the glycoconjugate mimetics enhancement. Aminooxylated carbohydrates have been employed in various research fields in past few decades.[175] Their utilization as major building blocks for biomedical applications and biopharmaceutical research has been reported for their role in synthesis of antibiotics and anti-adhesive agents. They can mimic the glycoprotein interaction with significant potencies via their conjugation to various entities such as peptides or compounds bearing aldehyde or ketone terminal groups like the prepared poly-aldehyde precursor in this study through oxime ligation.[177–181] There are various synthetic approaches which lead to the formation of aminooxylated sugar derivatives as shown in **Figure 3.1**.[175,176]

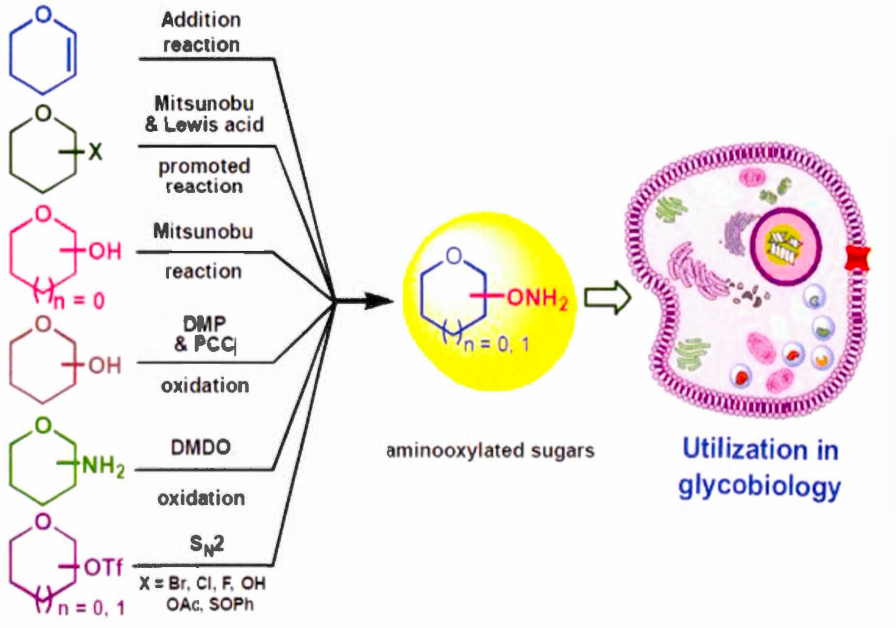

Figure 3-1. Aminooxylated carbohydrates as key building blocks toward therapeutic agents and the various synthetic approach toward sugar-ONH_2 derivatives.[175,176]

Oxime ligation as an efficient reaction offers several advantages such as mild reaction condition, short reaction times, free coupling reagent. It ensures excellent reproducibility, high yield and purity. The resulted compounds prepared through this strategy can be employed as inhibitors such as antitumoral, in vaccines, as anti-adhesive agents, and so on in various biological phenomena.

3.1.2 Formation of oxime bonds and their stability

Generally, the condensation of amines, hydrazides, and oxyamines with carbonyl functional group leads to the formation of imines, hydrazones, and oxime linkages respectively as is shown in **Figure 3-2.**[175] These simple ligations display a productive methodology in which, it can offer the vast diversity of bioconjugates under physiological conditions. Oxime compounds compared to imines, are more stable and

these are more widely utilized in biological applications due to their stability in aqueous media.[182–185] Their stability is due to the electron delocalization of the two lone pair electrons of the oxygen adjoining to nitrogen which causes more stability via α-effect which is shown in **Figure 3-3**.[175] Moreover, the participation of both the atoms involving nitrogen and oxygen in resonance, leads to the reduction of the electrophilicity of the sp2 carbon. For this reason, the nucleophilic attack by water is controlled. Moreover, due to the presence of inductive effect in such compounds resulting from the decrease of basicity of sp^2 nitrogen, the rate of acid-catalyzed hydrolysis is noticeably decreased. Accordingly, harsh acidic condition is needed for the hydrolysis of oxime bond. This shows the stability of oxime bonds which make these molecules appropriate for different biological applications.[186–191]

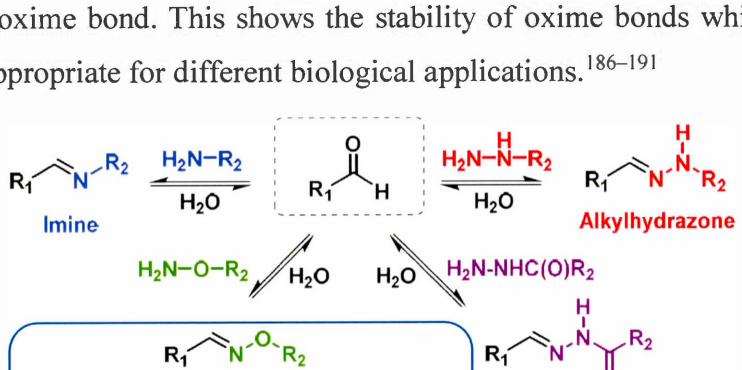

Figure 3-2. The chemistry of C=N double bonds, including aminooxylated spacer.[175,176]

Oxime bond formation reaction is fast and quantitative. The main drawback of the Oxime-based compounds come from the formation of a mixture of *E*/*Z*-stereoisomers through the oxime-ligation from the aminooxylated ligand and aldehyde precursors.[176,192] The formation of *E*/*Z*-stereoisomers leads to complicate the purification procedures and NMR studies in macromolecules such as glycoclusters as we observed through this research.

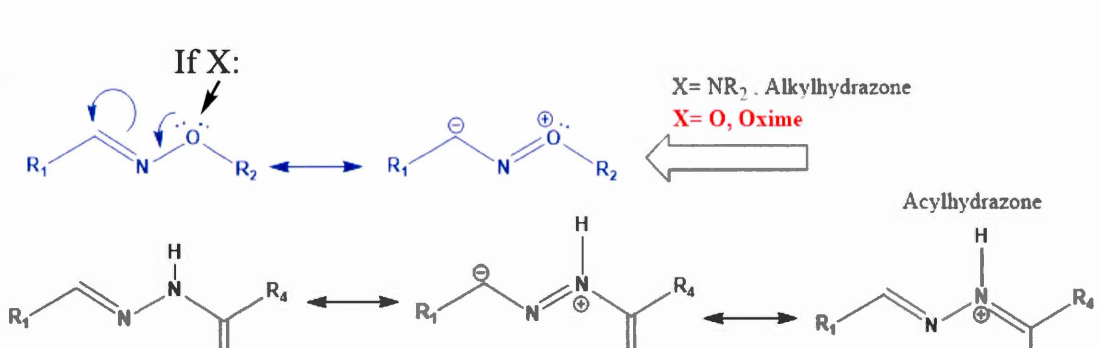

Figure 3-3. Relative stabilities of C = N double bonds and the α-effect.[175,176]

Oxime-ligation is an orthogonal chemoselective reaction that can yield the biomacromolecules in a controlled manner with reproducibility. Because of the stability of oxime-based conjugates and of their synthetic versatility, aminooxylated sugars play chemically the key role for their abilities to couple with various multivalent precursors leading to the formation of compounds with biological functionalities. The reasons, explained above, were satisfactory enough for choosing the aminooxylated galactopyranoside for this study. The oxime-based approach founded on oxime-ligation was considered as a method for synthesizing a large variety of glycoconjugates with predefined stereoisomeric glycosidic linkage.

3.2 Synthetic strategy

3.2.1 Synthesis of three different multivalent glycoclusters in zero generation, Strategy 1

The design and synthesis of three multivalent glycoclusters of zero generation with 3, 6 and 12 galactoside moieties was carried out. The goal was to achieve the mentioned glycoclusters according to the **Figure 3.4** by efficient and versatile "click chemistry"

involving oxime-ligation between aminooxylated galactosides and three suitably prepared different poly-aldehyde scaffolds, thus providing the zero generation dendrimers. The synthesis of aminooxylated β-D-galactopyranoside was anticipated from 2- phthalimidoethyl-β-D-galactopyranoside.

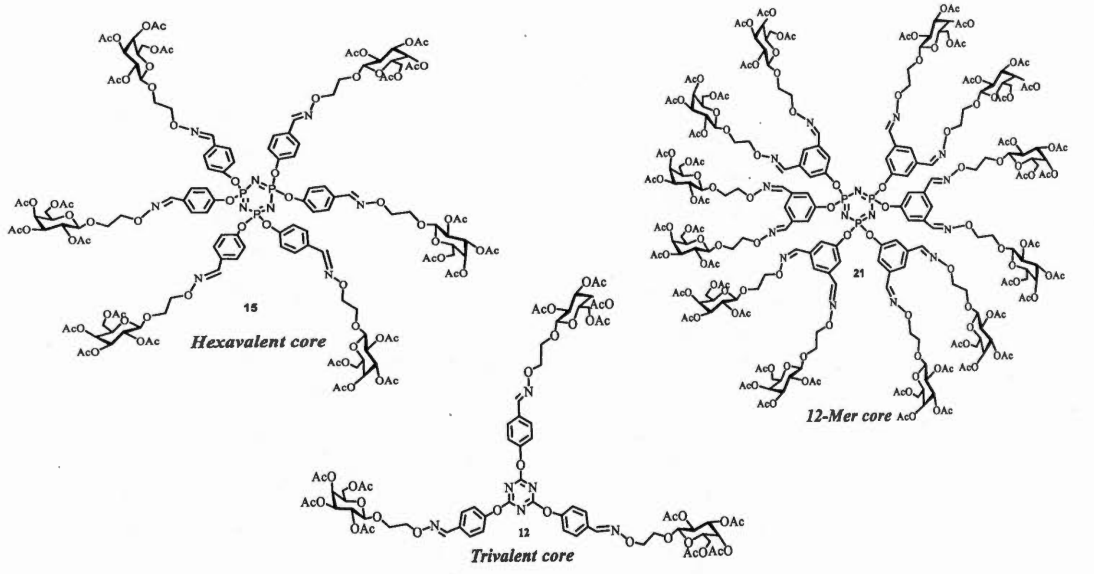

Figure 3-4. 3-mer, 6-mer and 12-mer glycoclusters in zero generation

3.2.2 Synthesis of multivalent poly-aldehyde core

The synthetic strategy was initiated based on the construction of series of symmetric polyaldehyde cores. These types of cores were designed and synthesized with varying (3, 6 and 12-mer) number of reactive aldehyde termini. These polyaldehyde scaffolds could be used as a starting material for oxime-ligation via the reagent free coupling between the aldehyde functional groups on the periphery of cores and aminooxylated β-D-galactose as the monomer in a convergent way. Oxime-ligation is eye-catching because of the speed of reaction as well as the reagent free nature. Synthesis of these building-blocks (cores) have been achieved by using trimeric cyanuric chloride

(trichloro triazine) and hexachlorocyclotriphosphazene ($N_3P_3Cl_6$) which were commercially available. In all three poly-aldehyde building-blocks, the strategy was based on the displacement of a chlorine by 4-hydroxybenzaldehyde **10**, which resulted the 3-mer **11**, and 6-mer **14**, cores. On the other hand, 12-mer **20** was prepared by reaction of pre-synthesized 3-hydroxyisophthalaldehyde **19** consist of two aldehyde functionalities, and hexachlorotriphosphazene using the same strategy as explained for cores **11** and **14**. Due to an additional aldehyde group on the periphery of each aromatic groups in compound **20** compare to compound **14**, it would provide higher number of aldehydic termini which can enhance the multivalent effect upon final ligation with sugar. Cyclotriphosphazene is a UV visible aromatic scaffold which offers the multivalency due to the branched architecture and can provide various pharmaceutical applications as explained earlier. Utilizing such aromatic clusters with many aldehyde groups would provide the easy control and better modulation of the peripheral ligands`s density. These molecules with various aldehyde groups will facilitate the ligation with sugar. In this study we followed Prof. Majoral`s typical models to build up the polyaldehyde scaffold which is explained below.

3.2.2.1 Synthesis of the Tri-(4-formacylphenoxy)-1,3,5-triazine (Trif), trivalent core

The synthesis of the symmetrically substituted cyanuric acid derivative **11** was achieved using the commercially available cyanuric chloride **9** as an initial building block. Cyanuric chloride **9** was treated with 4-hydroxybenzaldehyde **10** in presence of mild basic condition to afford the desired tri-substituted aldehyde **11** in a good yield (74%) **(Scheme 3.1)**. The ^{1}H NMR spectrum of compound **11** showed the aldehyde protons at δ 9.99 as well as the disappearance of phenolic group signal at δ 6.29 compared to the starting material, **Figure 3-5**. FT-IR spectrum of compound **11** (compared to compound **10**) showed the disappearance of the phenolic hydroxyl broad peak at 3209.24 cm^{-1}. Also peaks related to compound **11** were observed in the IR spectrum at 1732.97 cm^{-1} (C=O), 1697.97 cm^{-1} (CHO), 1563.34 cm^{-1} and 1591.66 cm^{-}

[1] (C_3N_3), 1360.30 cm^{-1} (C-N), 1208.22 cm^{-1} and 1159.79 cm^{-1} (C-O-ph) (**Figure 3-7**). Besides, ^{13}C NMR of the compound **11** showed the formation of a new signal at δ 173 which is related to the carbon of cyanuric chloride after linkage to the compound **10**, **Figure 3-6**. All the spectral data confirmed the structural integrity of the final product which is totally identical to the reference protocol.[193]

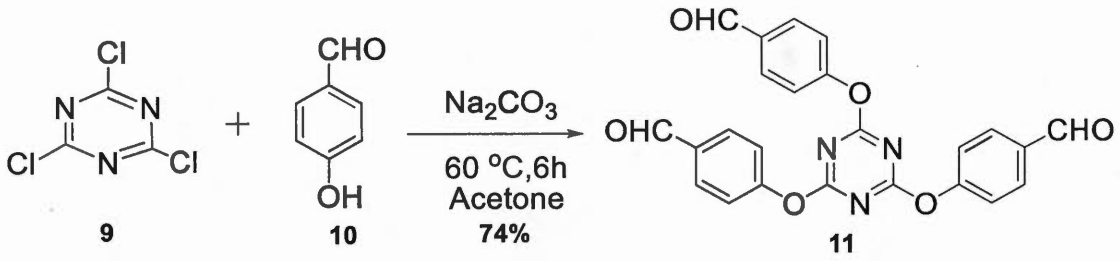

Scheme 3-1. Synthesis of 3-mer aldehyde cluster (Triazine) using cyanuric acid chloride (trichloro triazine) **11**

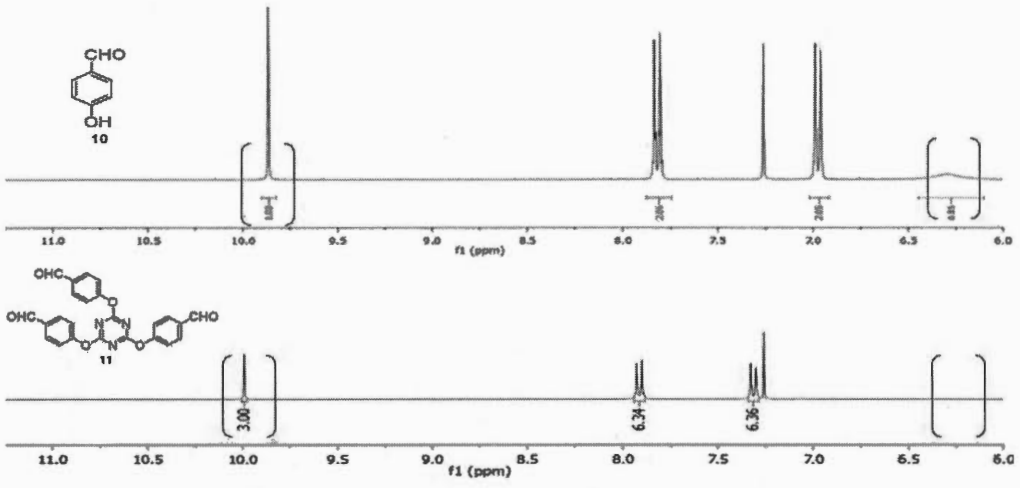

Figure 3-5. ^{1}H NMR spectrum (300 MHz, $CDCl_3$) of compound 10 and 11

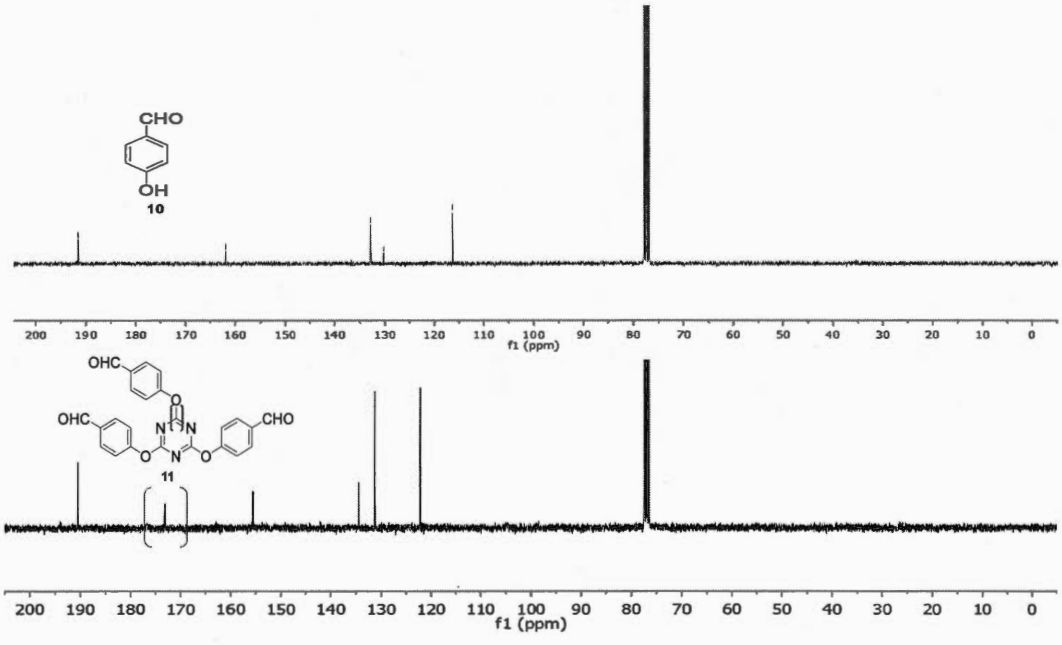

Figure 3-6. ^{13}C NMR spectrum (300 MHz, $CDCl_3$) of compound 10 and 11

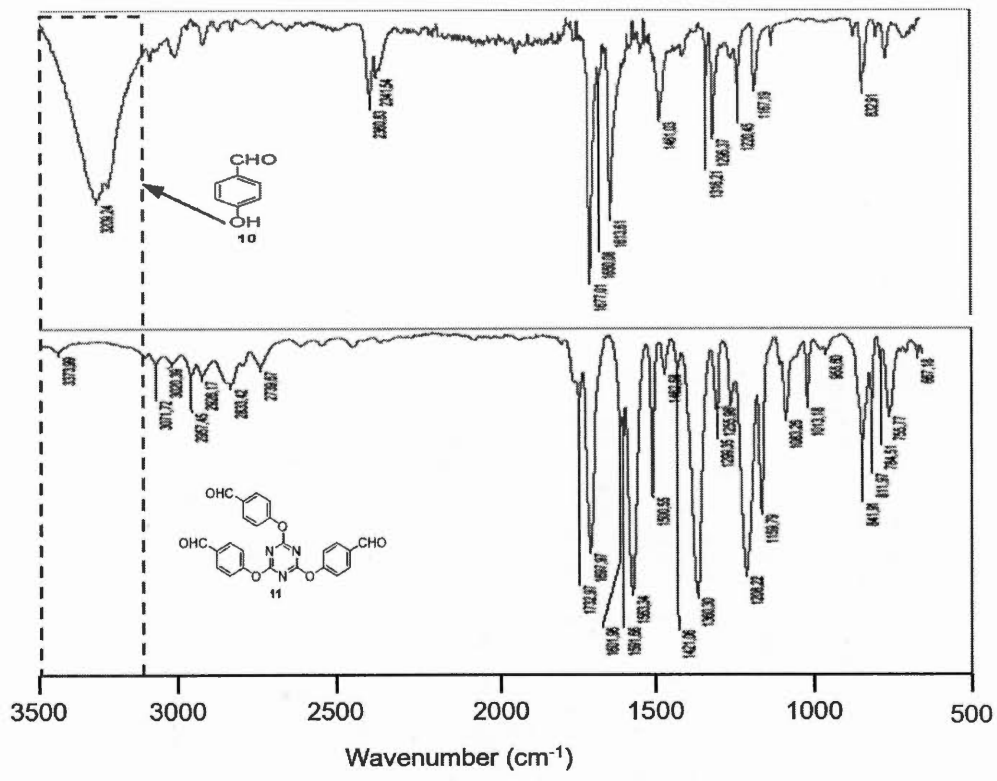

Figure 3-7. FT-IR spectrum of compound 11 compared to compound 10

3.2.2.2 Synthesis the hexavalent core of hexa-(4-formylphenoxy)-cyclotriphosphazene

Cyclotriphosphazene (N_3P_3) is non-toxic, UV visible and possess a symmetrical core, nicely equipped with 6 branches (A_6 monomer). The three situated upward and the rest three situated in downward forms a symmetric architecture. The family of such aromatic scaffold offer antimicrobial and biological effects on bacterial cells.[81–83] Their potential to accommodate a higher number of functional units such as dendrons on their scaffold leads to the formation of higher generation of dendrimers, as explained earlier, which are considered as significant properties for us through this study. The commercially available hexachlorocyclotriphosphazene scaffold was treated with 6.2

equiv. of 4-hydroxybenzaldehyde **10** in presence of mild basic condition by using K_2CO_3 with optimized stoichiometry. The complete hexa-substitution of hexachlorotriphosphazene **13** upon treatment with 4-formylphenoxy **10** resulted in formation of hexaformylphenoxy core **14** in a good yield (81%) **(Scheme 3.2)**.[194] The presence of the aldehyde protons signal (C*H*O) at δ 9.95 in the ^{1}H NMR confirmed the formation of the compound **14**. Also, the disappearance of phenolic hydroxyl group signal at δ 6.29 in the ^{1}H NMR spectrum of compound **14**, compared to the starting material provided additional evidence **(Figure 3-9)**. FT-IR spectrum of compound **14** compared to compound **10** showed the disappearance of the phenolic hydroxyl broad peak at 3209.24 cm^{-1} **(Figure 3-11)**. In addition, the final confirmation of compound **14** came from ^{31}P NMR which showed singlet at δ 7.08 which is different from chemical shift of the initial N_3P_3 at δ 19.99 as shown in **Figure 3.8** (a) and (b). It is known that the ^{31}P NMR of completely substituted cyclotriphosphazene, shows a singlet peak as compare to partially substituted cyclotriphosphazene where in ^{31}P-NMR display multiple peaks. ^{13}C NMR did not provide any new indication due to the equal number of carbons in both compounds **14** and **10** except of a slight chemical shifts in compound **14**, **(Figure 3-10)**. All the spectral data obtained are identical to the literature data and the data agrees with the reported literature values.[195]

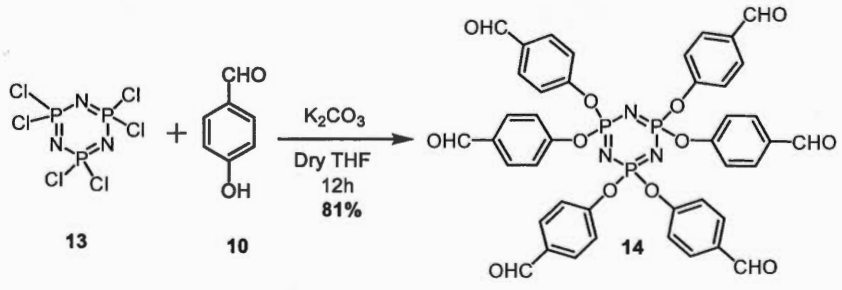

Scheme 3-2. Synthesis of 6-mer aldehyde cluster using hexachlorocyclotriphosphazene ($N_3P_3Cl_6$) 14.

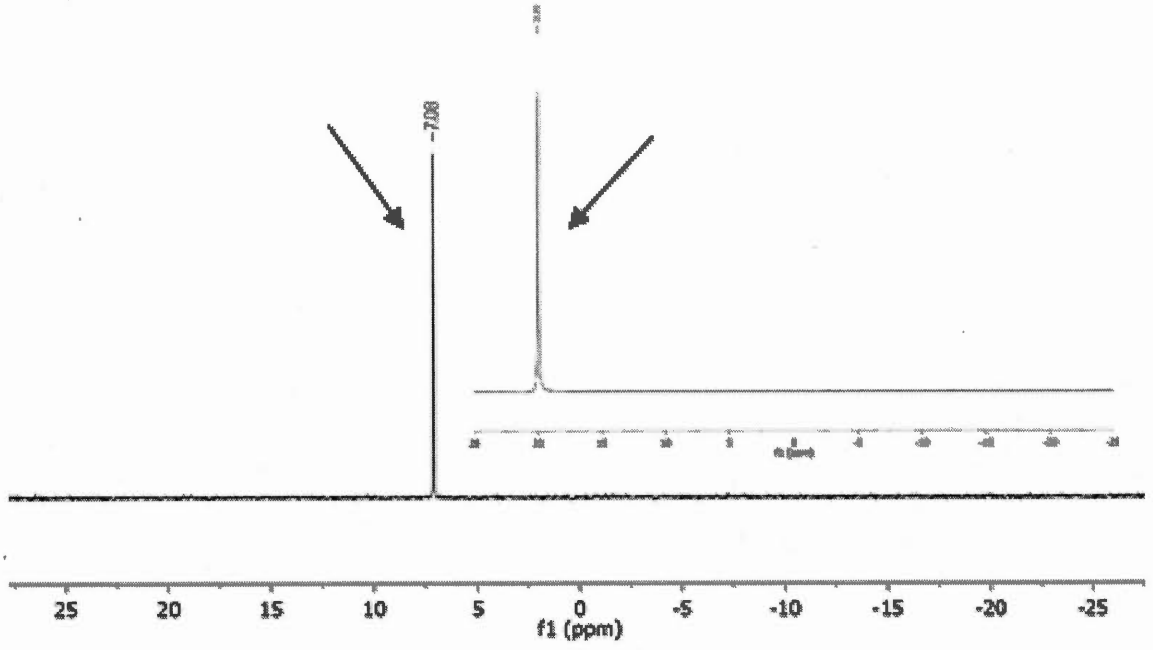

Figure 3-8. (a) ^{31}P NMR spectra (122 MHz) of 6-mer core **14. (b)** ^{31}P-NMR spectra (122 MHz) of the initial $N_3P_3Cl_6$ **13.**

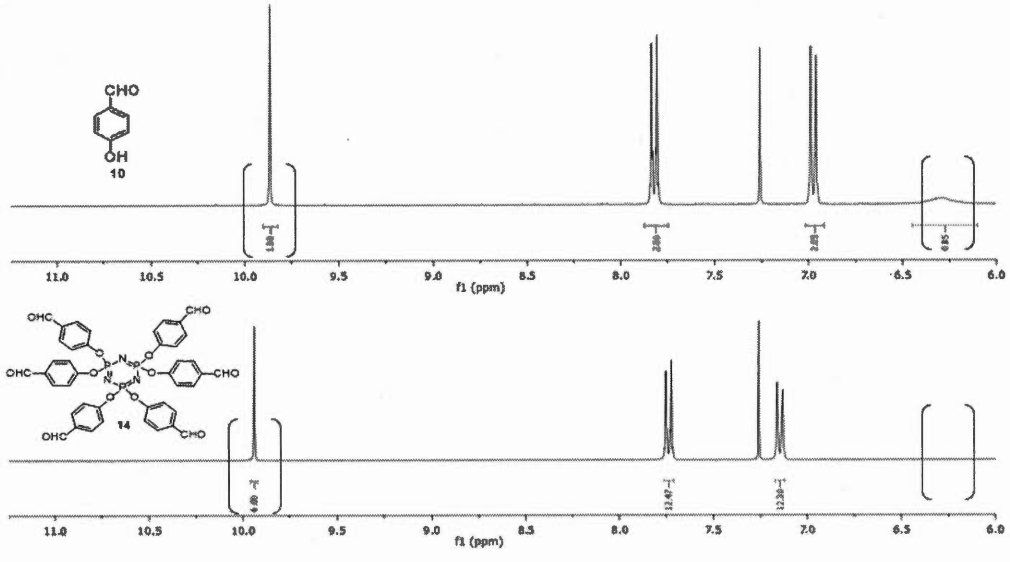

Figure 3-9. ^1H NMR spectrum (300 MHz, $CDCl_3$) of compound 10 and 14

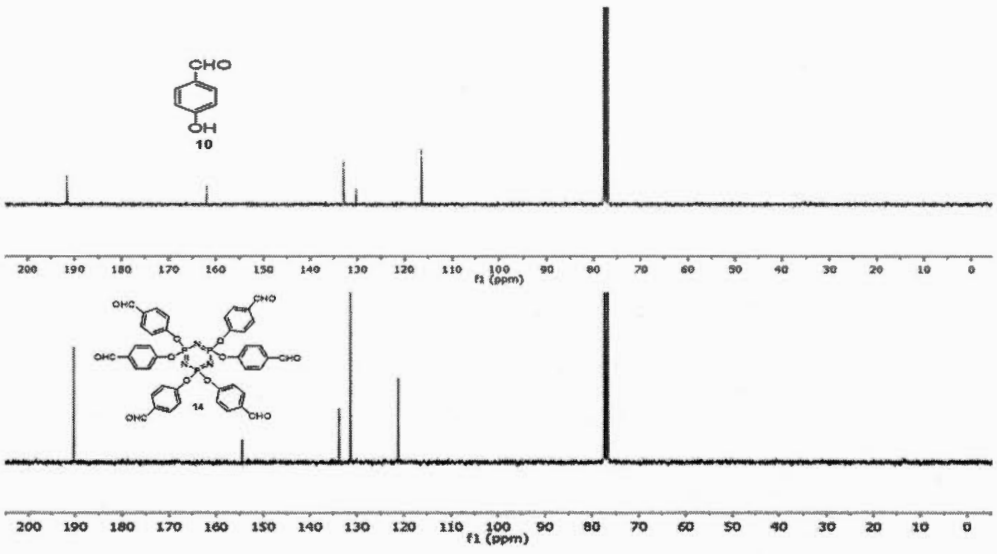

Figure 3-10. ^{13}C NMR spectrum (300 MHz, $CDCl_3$) of compound 14 and 10

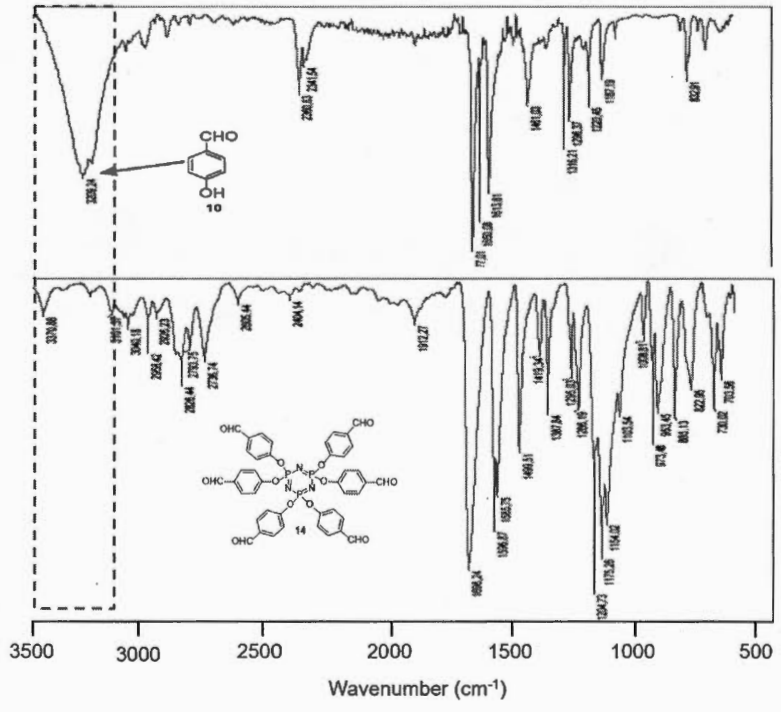

Figure 3-11. FT-IR spectrum of compound 10 compare to compound **14**

3.2.2.3 Synthesis the 12-mer aldehyde core using hexachlorocyclotriphosphazene ($N_3P_3Cl_6$)

The main goal of synthesis of such a 12-mer core was to achieve a higher level of functional termini which can provide us with higher number of functional groups which eventually enhance the efficiency of these type of glycoclusters. The required 12-mer was synthesized using the similar protocol of Jean Pierre Majoral`s procedure with 3-hydroxyisophthalaldehyde **19** as a starting precursor.[196] The synthesis was initiated with preparation of **19** using 3-hydroxyphthalic acid **16** as commercially available starting material **(Scheme 3.3)**.

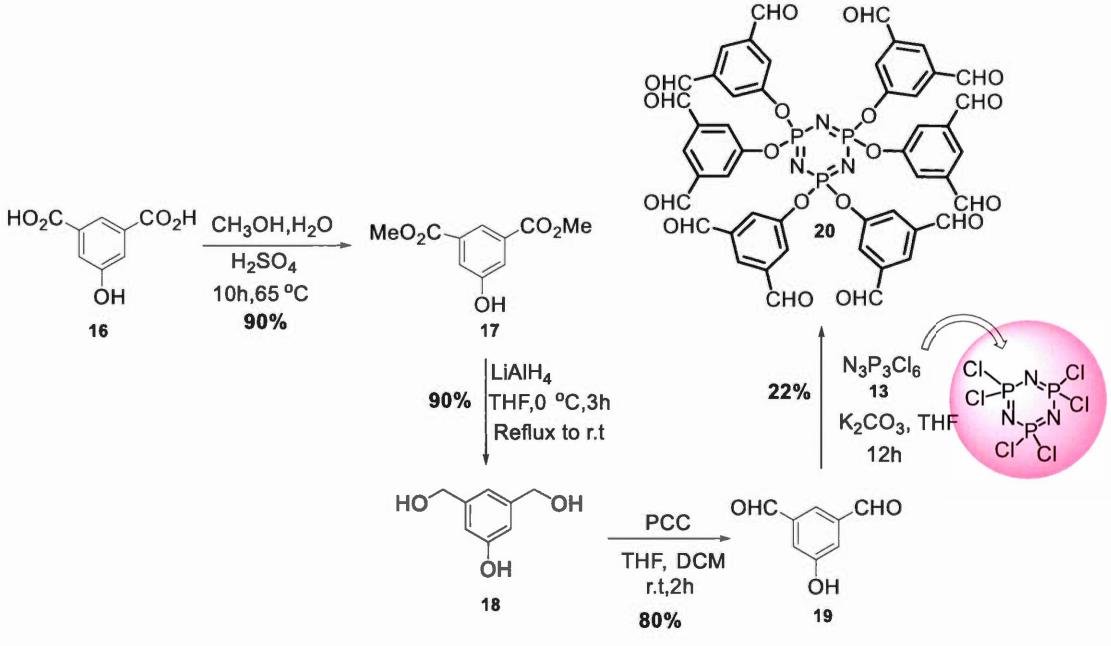

Scheme 3-3. Synthesis of 12-mer aldehyde cluster using ($N_3P_3Cl_6$) 20.

Indeed, synthesis was initiated by the esterification of 3-hydroxyphthalic acid **16** in acidic condition which led to the formation of the 3-(hydroxyldimethyl) isophthalate **17** having di-ester groups in good yield (90%) **(Scheme 3.3)**. In the next step, the di-

ester **17** was transformed to the di-alcohol 3-hydroxy-isophthalylalchohol **18** through the reduction reaction in the presence of 3 equiv. $LiAlH_4$ as a reducing agent. Optimized condition led to increase the yield (90%) compare to the reported protocol.[196] Subsequently the di-alcohol **18** was oxidized to the di-aldehyde functional groups by oxidation with pyridinium chlorochromate (PCC) which led to the formation of 3-hydroxyisophthalaldehyde **19** in good yield (80%) **(Scheme 3.3)**. The completion of the reaction was confirmed by monitoring a singlet at 10.05 ppm in ^1H NMR which corresponds to the di-aldehyde protons as shown in **Figure 3.12**. Moreover, the characteristic frequency of the carbonyl and phenolic hydroxyl stretching were observed respectively in the IR spectrum at 1697 cm^{-1} and 3343 cm^{-1} which confirmed compound **19** as shown in **Figure 3.13**. However, the grafting of dialdehyde **19** in $N_3P_3Cl_6$, **13**, in order to form the desired precursor **20** showed the slow progression with non-satisfactory yield (22%); however, it was relatively comparable to the reported protocol **(Scheme 3.3)**. The completion of the reaction was confirmed by ^{31}P NMR spectrum (122 MHz) with the singlet signal at 7.80 which suggested the formation of the expected compound as is shown in **Figure 3.15**. Also the disappearance of phenolic hydroxyl signal at δ 5.79 in the ^1H NMR spectrum of compound **20**, compared to the precursor **19** (**Figure 3-14**) and slight chemical shift of aromatic protons provided additional evidence for the formation of the compound **20** which is identical to the compound reported by Majoral *et al.*[196] The data agrees with the reported literature values.

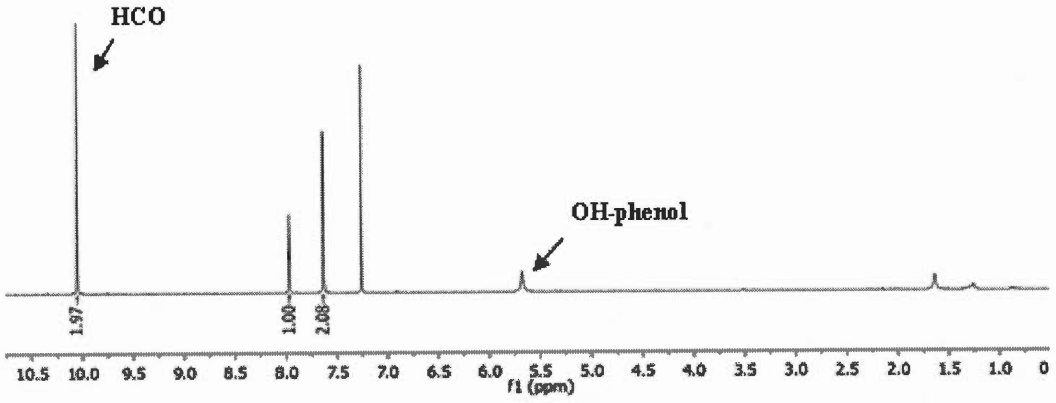

Figure 3-12.^{1}H NMR spectrum (300 MHz, $CDCl_3$) of compound 19

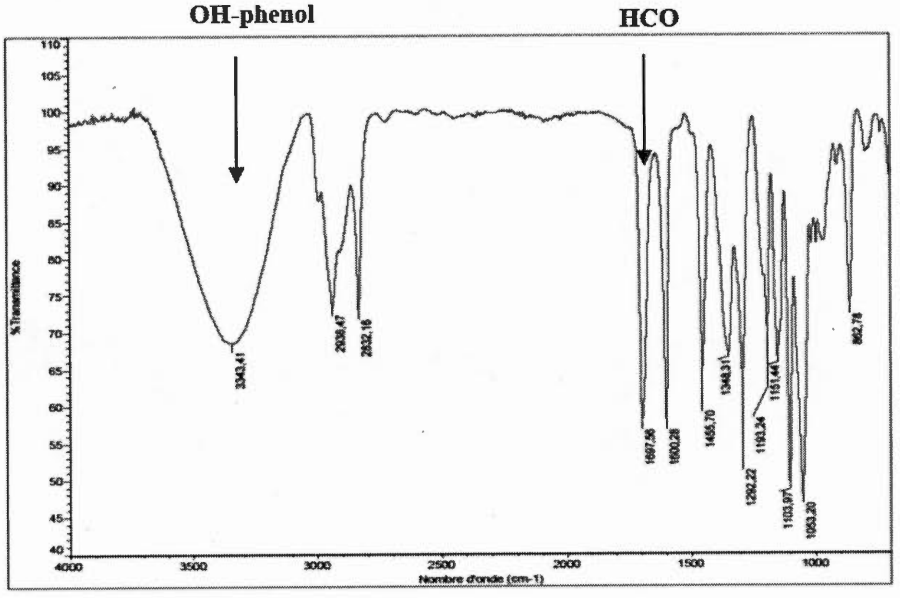

Figure 3-13. FT-IR spectrum of compound 19

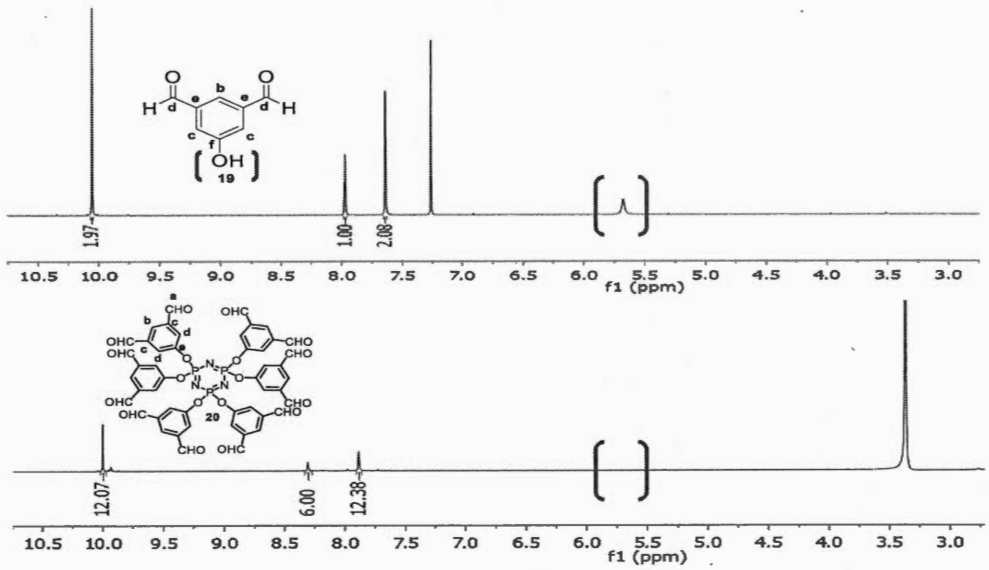

Figure 3-14. ^{1}H NMR spectrum (300 MHz, DMSO, d_6) of compound 20 compare to ^{1}H NMR spectrum (300 MHz, $CDCl_3$) of compound 19

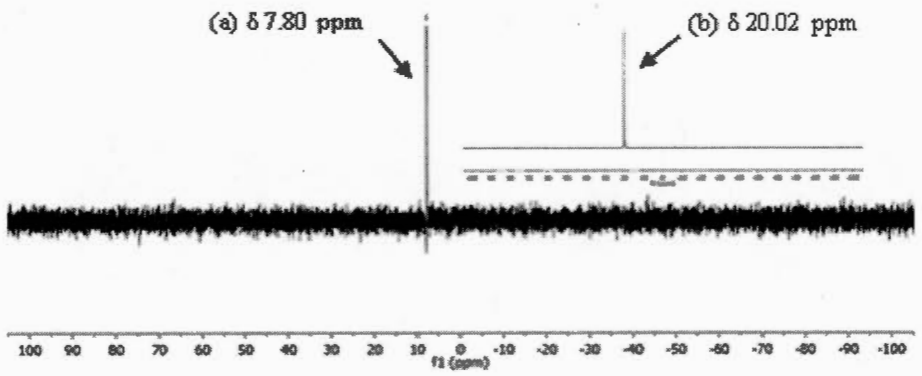

Figure 3-15. (a) ^{31}P NMR spectra (122 MHz) of 12-mer core 20. (b) ^{31}P NMR spectra (122 MHz) of the initial $N_3P_3Cl_6$ 13.

3.2.3 Synthesis of the 2-(aminooxy)ethyl β-D-galactopyranoside as the monomer ligand **8**

In order to achieve the syntheses of final glycoclusters **12**, **15**, and **21**, convergent synthetic strategy was anticipated wherein, the preparation of the aminooxy building blocks with galactose termini were essential. Importance of aminooxy building block lies in their simplicity of coupling with poly-aldehyde cores, which is reagent free and spontaneous. Therefore, the synthesis of aminooxy ligand **8** containing galactose was chosen as a peripheral functionality which was synthesized using commercially available D-galactopyranose **1** as starting precursor (mixture of alpha, beta isomers). In the first step D-galactopyranose **1** was protected using anhydrous sodium acetate in acetic anhydride to afford the compound **2** in a good yield (60%). In order to achieve exclusively β-isomer, the reaction mixture was extracted, separated and crystalized twice. The ^{1}H NMR and ^{13}C NMR signals at 5.69 (doublet, H_1) and 92.0 (C_1) indicated the completion, whereas the anomeric β-D-configuration was unequivocally confirmed by the presence of clear $J_{1,2}$ *trans* coupling constant of 8.3 Hz. In addition, ^{13}C NMR signal at δ 92.0 corresponds to the anomeric C_1 indicated the formation of the β-isomer of **2**.

According to the earlier studies, the flexibility enforcement can offer the mimic glycoconjugates with more efficiency through the hydrophilic-hydrophobic interactions with PA-IL. Thus, in order to provide the sugar ligand with a flexibility enhancement, the compound **2** was treated with 2-bromoethanol **3** in presence of $BF_3.Et_2O$ Lewis acid which led to the formation of β-isomer of 2,3,4,6-tetra-*O*-acetyl-2-bromoethyl-β-D-galactoside **5** with ethyl spacer **(Scheme 3.4)**. Dropwise and slow addition of ($BF_3.Et_2O$) was essential to afford desired glycosylated product **5** in good yield (67%) without undergoing the decomposition of the sugar ring. Moreover, there is exclusive formation of β-isomer due to the neighboring group effect as shown in **Figure 3.16**

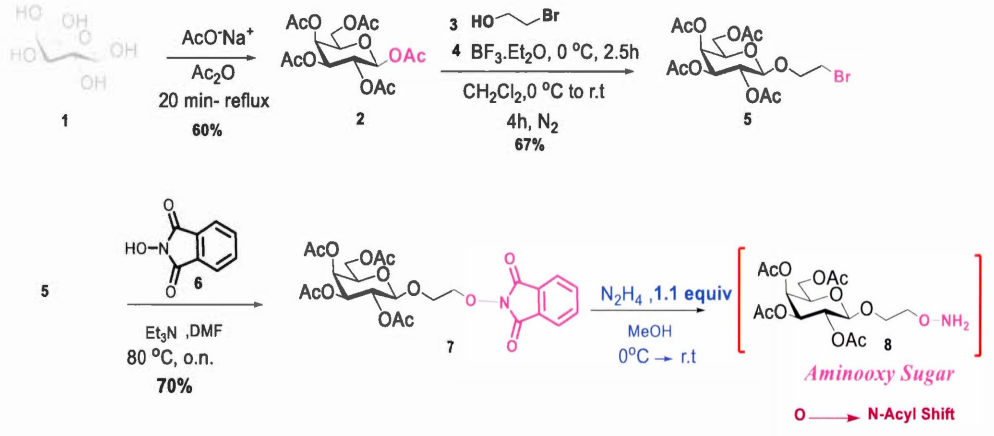

Scheme 3-4. Synthesis of aminooxy building block 8

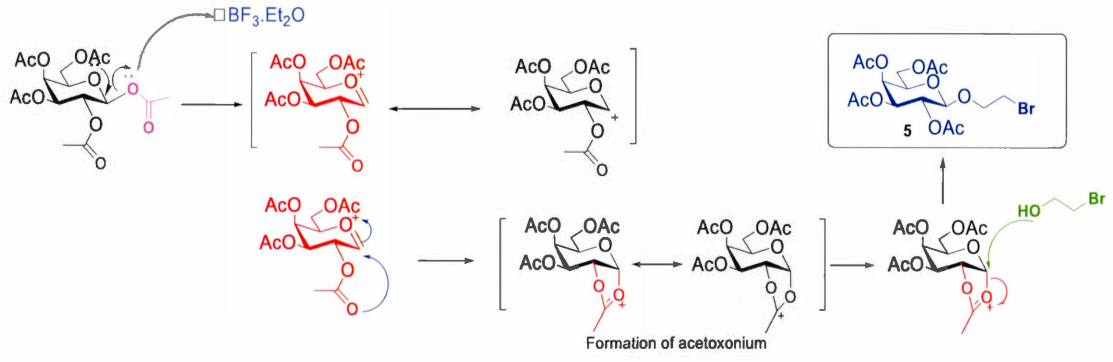

Figure 3-16. Glycosidation mechanism in presence of neighboring group participation

According to the mechanism of glycosidation reaction which is shown in **Figure 3.16**, the Lewis acid BF_3. Et_2O is intended to activate the acetate functional group of the anomeric position in order to facilitate it`s expulsion in to the reaction medium and to lead in to the formation of a glycosyl cation. The presence of the acetate function on the adjacent carbon in the equatorial position as a participating group, makes it possible to stabilize the positive charge by the intramolecular creation of an acetoxonium in the

form of the five-membered ring blocked by the critical anchimeric effect that controls the stereoselectivity to make the β-side more accessible for the nucleophilic attack of reagent **3** toward the anomeric carbon of acetoxonium to form compound **5**. In the ^{1}H NMR of compound **5** multiplet at δ 3.50 corresponds to C*H*$_2$Br and presence a signal at δ 29.82 in ^{13}C NMR corresponds to *C*H$_2$Br indicated the completion of the glycosidation. The anomeric β-D-configuration was unequivocally confirmed by the presence of anomeric proton at δ 4.53 with a $J_{1,2}$ *trans* coupling constant of 7.9 Hz and by the signal at δ 101.3 in ^{13}C NMR spectrum which indicated the formation of β-isomer. Subsequently, the bromide group of the compound **5** was replaced with phthalimide functionality through the substitution reaction using deprotonated *N*-hydroxyphthalimide spacer **6** in a mild basic condition provided by triethylamine to afford 2-phthalimidoethyl β-D-galactopyranoside **7** as a stable crystalline compound in a good yield (70%) **(Scheme 3.4)**. Once again, the formation of the compound **7** was showed by standard characterization techniques of the ^{1}H NMR wherein, the presence of aromatic protons (C*H*O) at δ 7.89-7.72, and changing in the chemical shift of the anomeric proton (H-1) in compound **5** from δ 4.53 to δ 4.73, indicates the formation of compound **7** as shown in **(Figure 3-17)**. Moreover, the (H$_Y$) in compound **7** in ^{1}H NMR shows two signals, one multiplet at δ 4.09-3.99 and another at δ 3.95 corresponding to C*H*$_2$ONPhthalimido group compared to the chemical shift of C*H*$_2$Br at δ 3.50 in compound **5 (Figure 3-17)**. The signal of *C*$_Y$ of compound **7** in ^{13}C NMR appeared at δ 61.2 while *C*$_Y$ in compound **5** showed the signal at δ 29.82. Also the presence of a signal at δ 163.4 in ^{13}C NMR corresponding to carbonyl carbon of phthalimido group (*C*O) confirmed the formation of compound **7** (see Annex). FT-IR spectrum of compound **7** is shown in **Figure 3-18**.

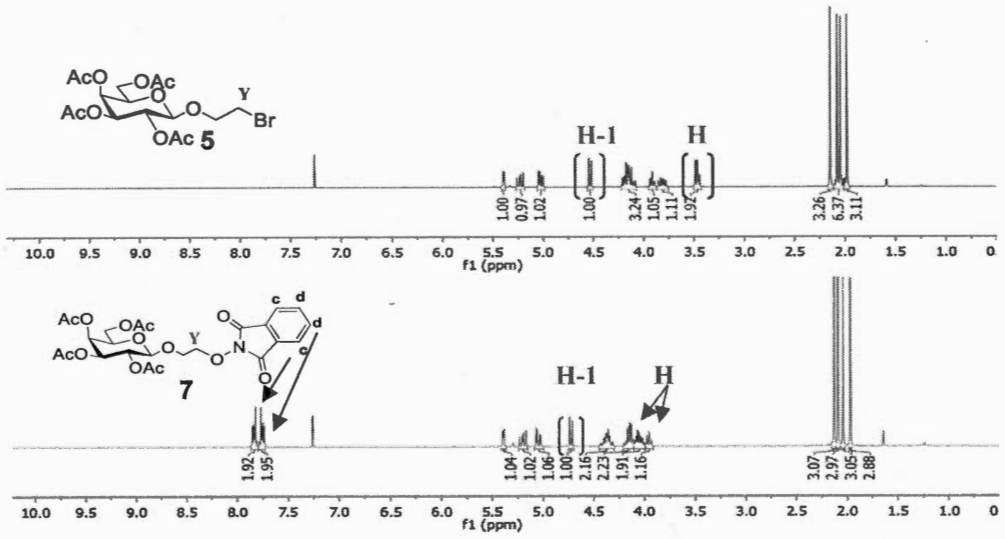

Figure 3-17. Comparison the ^{1}H NMR spectra ($CDCl_3$, 300 MHz) of 5 and 7 with appearance of the characteristic signals for aromatic protons in compound 7

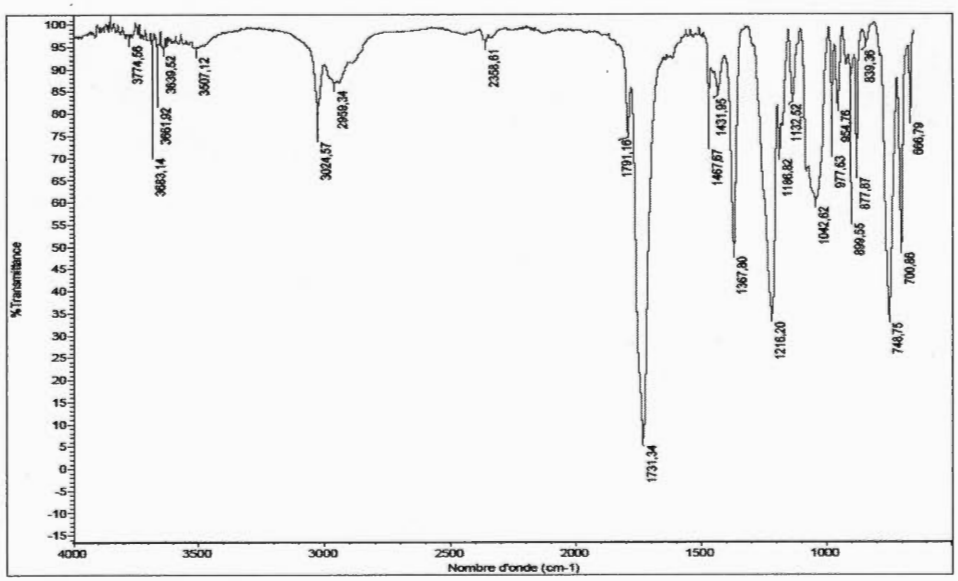

Figure 3-18. FT-IR spectrum of compound **7**

3.2.3.1 Synthesis of aminooxylated sugar in this study and oxime ligation

The synthesis of aminooxylated glycopyranosyl moieties and their conjugation with 3-mer, 6-mer and 12-mer poly-aldehyde precursors lead to the formation of different glycocluster compounds **12**, **15**, and **21** **(Figure 3.4).** After successful synthesis of 2-phthalimidoethyl β-D-galactopyranoside **7**, the desired aminooxy derivative **8** had to be synthesized by treating compound **7** with hydrazine hydrate ($N_2H_4.H_2O$) in methanol at room temperature for 20 minutes. However, to our disappointment, this synthetic protocol did not furnish the desired ligand. Therefore, we revised the synthetic protocol by conducting the reaction at lower temperature (-20 °C).

In order to hydrolyze the phthalimido functionality without affecting the protected acetate groups, the selective deprotection of phthalimido group of compound **7** (using 1.1 equivalent of the reagent) was accomplished to obtain the compound **8a (Scheme 3.4)**. Freezing of the reaction mixture at -20 °C was carried out in anticipation of restricted motion which in turn would reduce acyl migration rate based on our hypothesis. Indeed, the present methodology afforded desired product **8a** in moderate yield. It is important to note that the pH of the reaction mixture was maintained neutral to avoid the possible acyl migration or O-N bond cleavge. The compound **8a** was characterized using ^{1}H NMR and ^{13}C NMR spectroscopy wherein disappearance of aromatic C*H* corresponding phthalimide functionalities and appearance of amine proton (N*H*$_2$), at δ 5.5 confirmed the formation of ligand **8a** as shown in **Figure 3.19**. The ninhydrin test on TLC analysis showed positive response indicating the presence of free amino group. However, the resulted compound found to be unstable as coupling reaction with compound **29** did not lead to the corresponding oxime product. It could be due to less energetic O-N (~200 kJ/mol) bond cleavage or undergoing acyl migration or the presence of hydrazine acetatmide (as indicated by a sharp singlet at δ 1.85 in ^{1}H NMR spectrum shown in **Figure 3-19**). Having learned about the instability of the compound **8a**, we contemplated two strategies: i) Complete deprotection of sugar (in

order to avoid acyl migration as our hypothesis) as well as the deprotection of phthalimido group using excess of $N_2H_4.H_2O$ (8 equiv.). Indeed, treatment compound **7** with excess of hydrazine hydrate led to form the product, **8b**, with impurities as shown in **Figure 3.19**. To our disappointment, we did not observe the desired product **8b**. The ninhydrin test on TLC analysis showed negative response for compound **8b** indicating the absence of free amino group which proves aforementioned the O-N bond cleavage hypothesis or acyl migration which needs the further research.

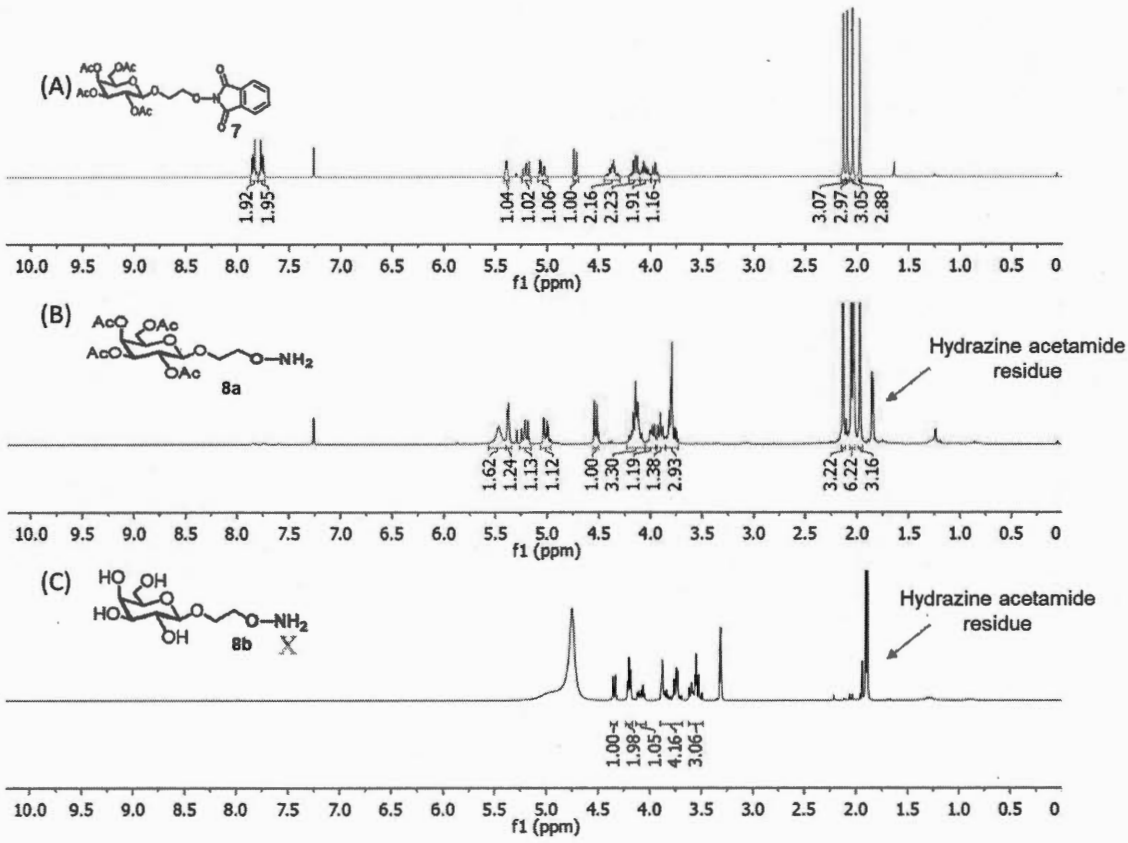

Figure 3-19. Comparison of ^{1}H NMR of aminooxylated ligands

ii) To deprotect the sugar acetate selectively using potassium carbonate (K_2CO_3) in methanol. Treatment of K_2CO_3 in methanol afforded selective deprotection of sugar acetates but it would need an additional step to deprotect phthalimido functionality. Eventually, we discarded both protocols and revised the synthetic rout using completely different strategy.

The new synthetic strategy includes incorporation of longer linker using triazole moiety **36** as shown in **Scheme 3-5**. The aim of introducing a longer spacer was contemplated to forbid an intra molecular acyl migration. Having this in mind, we began synthesis of a new aminooxylated ligand with longer linker **37** using propargylated phthalimide **35** and 2,3,4,6-tetra-*O*-acetyl-2-Azidoethyl-β-D-galactoside **22** as starting material **(Scheme 3-5)**.

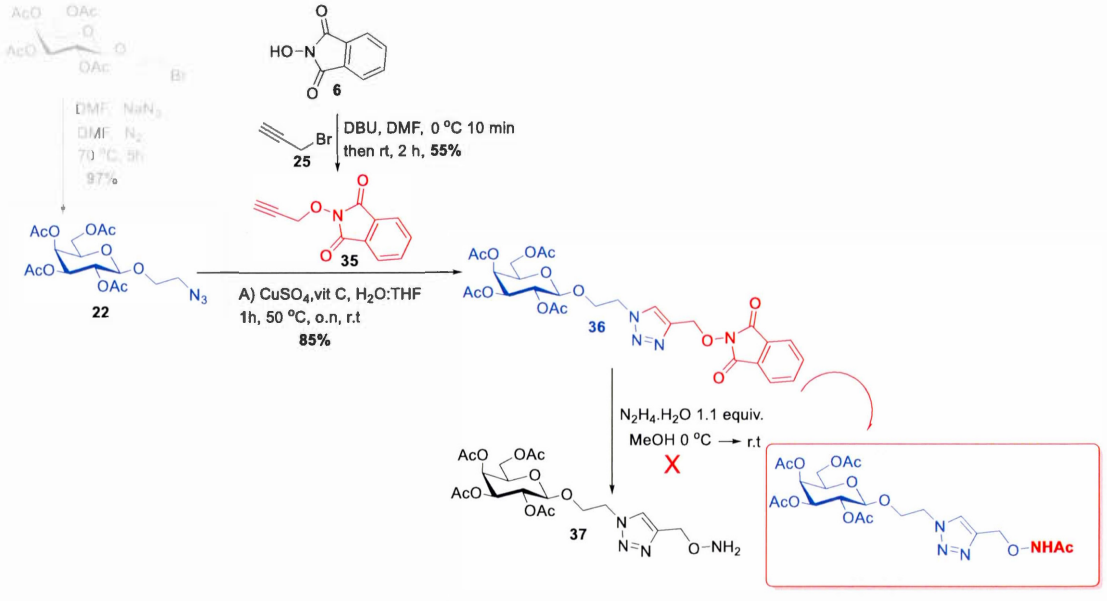

Scheme 3-5. Synthesis of new aminooxylated ligand with longer spacer 37

Compound **35** was synthesized in a single step from *N*-hydroxyphthalimide **6** upon treatment with propargyl bromide **25** in presence of DBU in DMF in a 55% yield. Completion of the reaction was characterized using ^{1}H NMR, HSQC ^{13}C NMR and FT-IR. From ^{1}H NMR, propargylic proton (C*H*) was identified by the appearance of a new triplet at δ 2.59 and the aromatic moiety was identified by the presence of two doublets at δ 7.89- δ 7.73 which confirms the formation of compound **35 (Figure 3-20)**. ^{13}C NMR presented the new signals related to the propargylic carbon at δ 76.3 (C_mH) and δ 64.9 (C_nH) **(Figure 3-21)**. Finally, FT-IR spectrum showed the peaks related to the (C=O amide), alkynyl C-H and alkynyl carbon of compound **35** respectively at 1732.30, 3289.31 and 2131.18 cm^{-1} **(Figure 3-22)**.

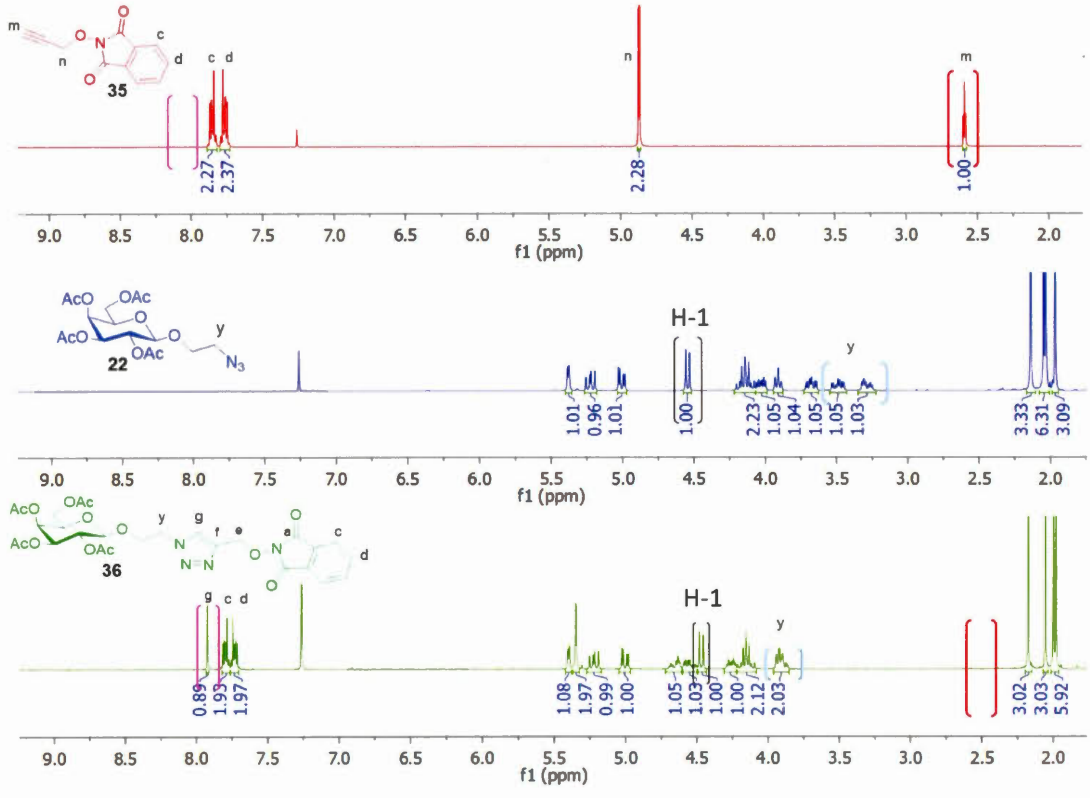

Figure 3-20. ^{1}H NMR (300 MHz, $CDCl_3$) between compound 35, 22, and 36

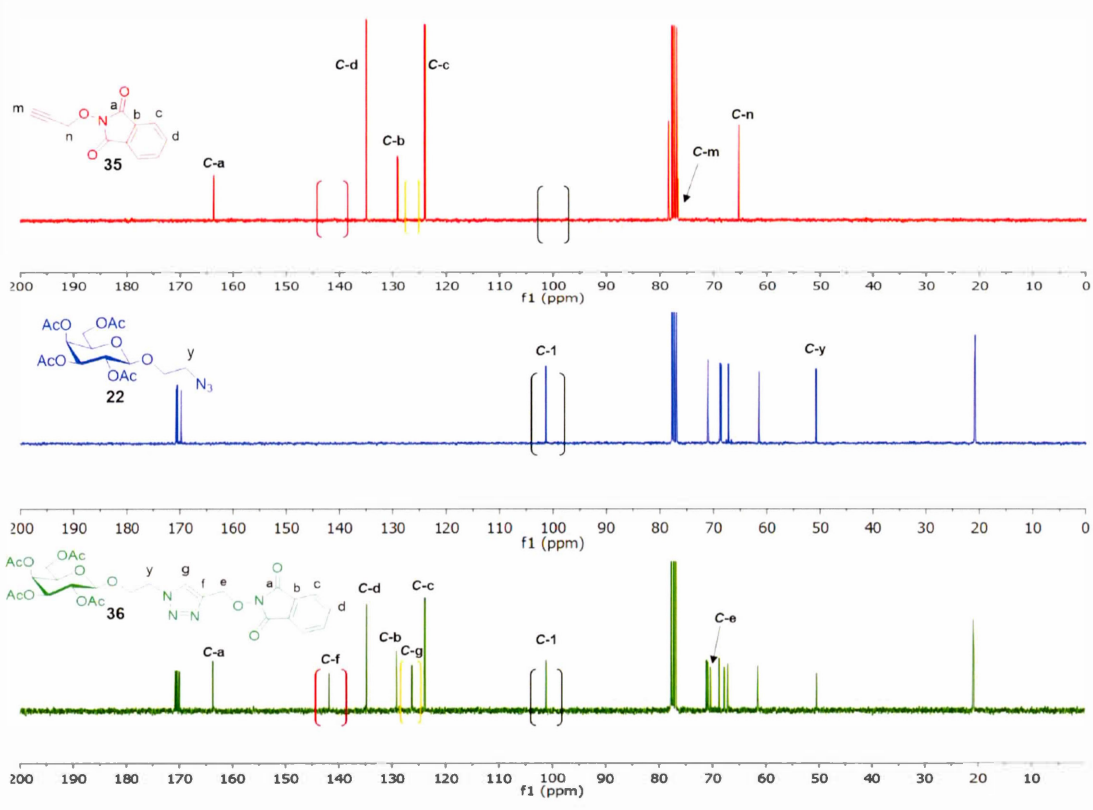

Figure 3-21. ^{13}C NMR (300 MHz, $CDCl_3$) between compound 35, 22, and 36

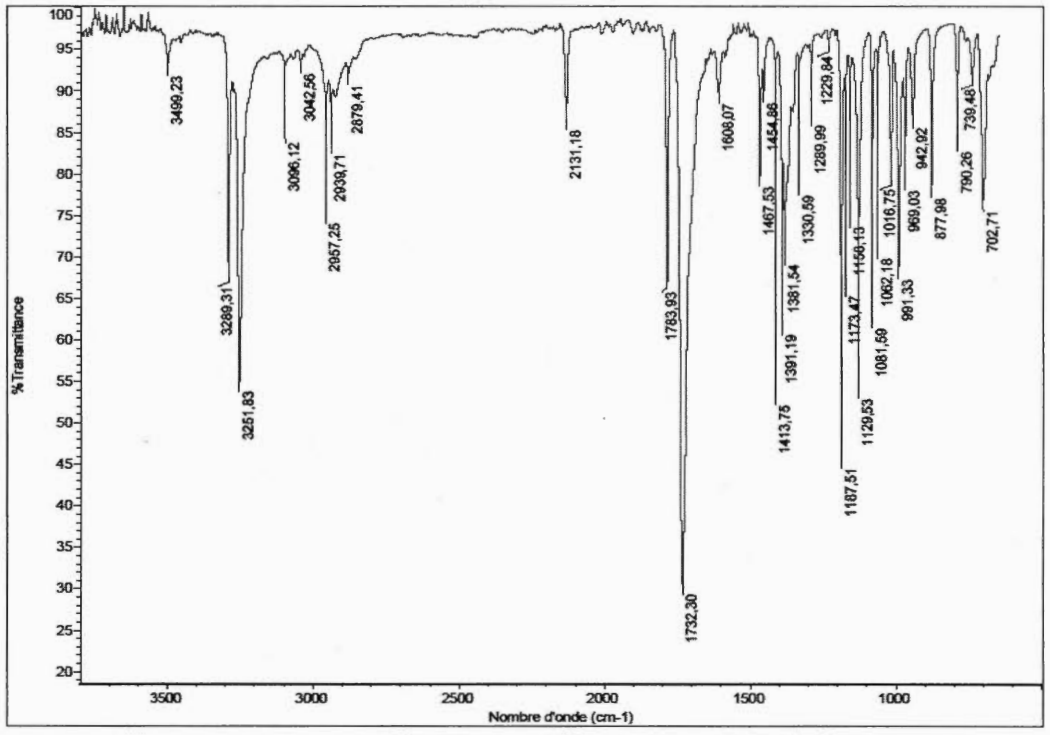

Figure 3-22. FT-IR spectrum of compound 35

On the other hand, compound **22** was achieved from the previously synthesized compound **5** which was then treated with sodium azide in presence of DMF at 70 °C through a substitution reaction in excellent yield (97%). ^{1}H NMR of compound **22** showed multiplet at δ 3.5 and another diastereotopic proton at δ 3.29 correspond to CH_2N compared to the resonance of CH_2Br in compound **5** at δ 3.50 as shown in **Figure 3-23** (a). Also, the presence of δ 50.4 corresponds to *C*H$_2$N and absence of δ 29.8 which corresponds to CH_2Br in ^{13}C NMR confirmed the completion of the substitution. Anomeric β-D-configuration was unequivocally confirmed by the presence of anomeric proton at δ 4.55 with a $J_{1,2}$ *trans* coupling constant of δ 7.9 Hz and δ 101.3 in ^{13}C NMR indicated the formation of β-isomer (see annex). Moreover, the characteristic frequency

of the azide stretching was observed in the IR spectrum at 2104 cm^{-1} as shown in **Figure 3.24**.

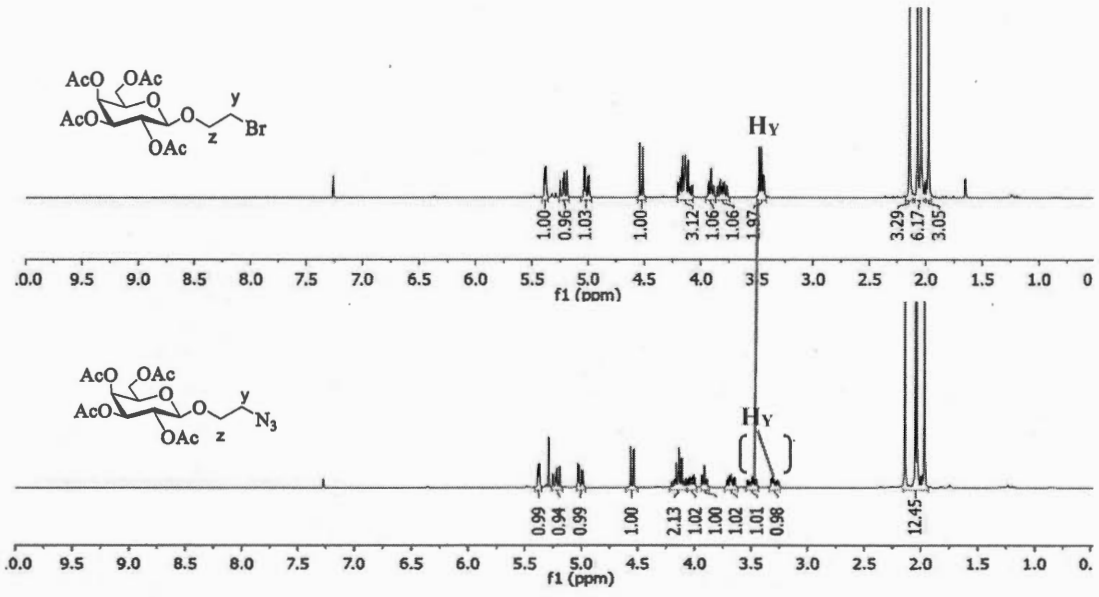

Figure 3-23. ^{1}H NMR (300 MHz, $CDCl_3$) proton magnetic environment of H_Y between compound 5 and 22

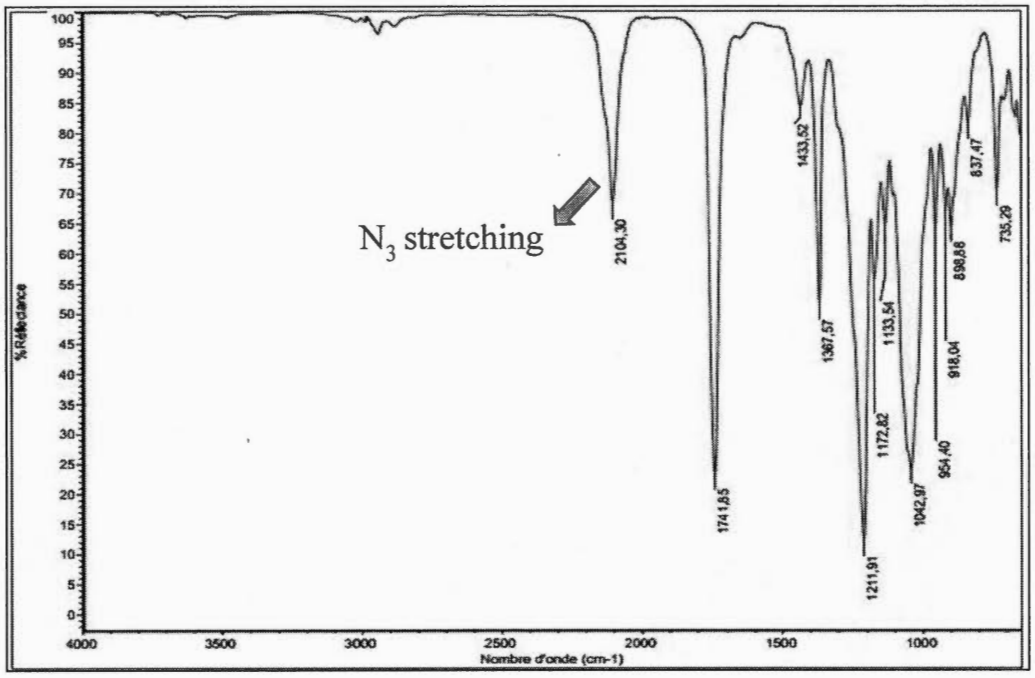

Figure 3-24. FT-IR spectroscopy of compound 22

Subsequently, the desired compound **36** was synthesized by coupling two mentioned compounds **22** and **35** in H_2O: THF in the presence of aqueous solution of $CuSO_4.5H_2O$ and sodium ascorbate as a catalyst at 50 °C. The pure compound **36** was obtained after column chromatography in excellent yield (89%). Completion of the reaction was evident using ^1H NMR, HSQC, COSY, ^{13}C NMR and FT.IR. Complete disappearance of the propargylic C*H* signal at δ 2.59 in ^1H NMR and the appearance of the newly formed characteristic singlet of the triazole moiety at δ 7.92 confirmed the formation of the compound **36 (Figure 3.20)**. Moreover, the signal at δ 125.8 corresponding triazole in ^{13}C NMR confirmed the structural integrity of desired compound **36** as shown in **Figure 3.21**. FT-IR spectrum of compound **36** showed the disappearance of the peaks relatet to the alkynyl C-H and alkynyl carbon of compound **35** respectively

at 3289.31 and 2131.18 cm^{-1} and the presence of the (C=O amide) at 1738.83 cm^{-1} which confirmed the formation of compound **36 (Figure 3-25)**.

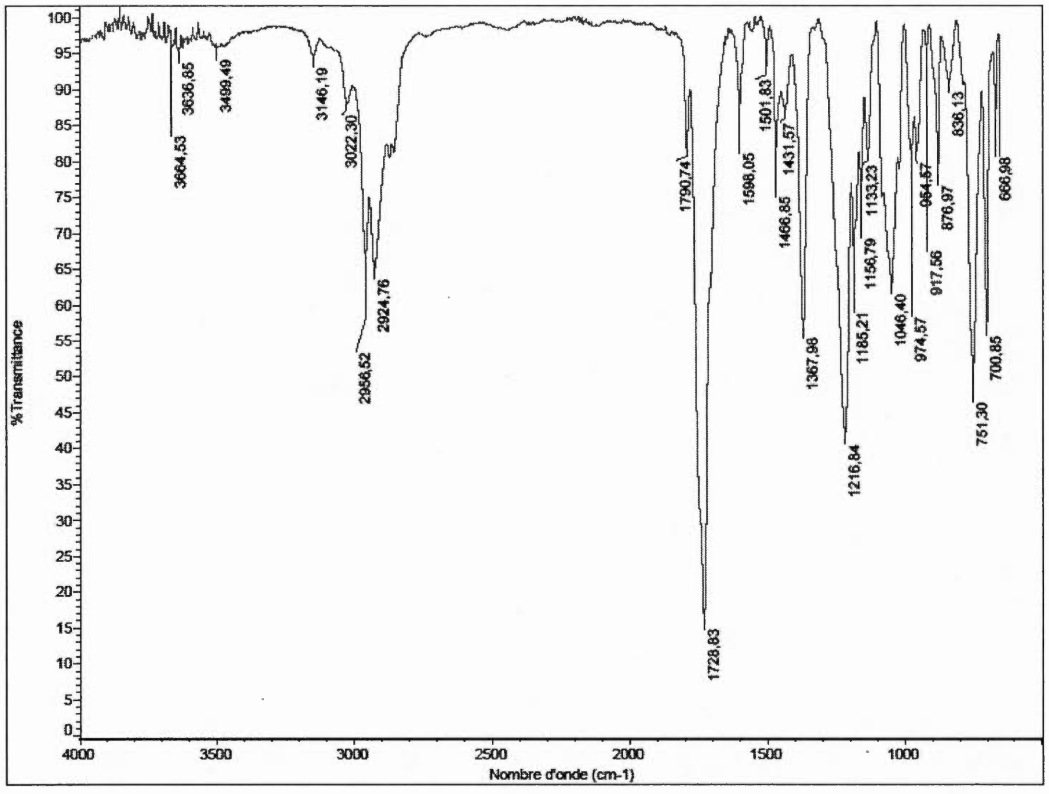

Figure 3-25. FT-IR spectroscopy of compound 36

Having achieved successful synthesis of compound **36**, we were in the position to deprotect phthalimido functionality in compound **36** which is now suitable for oxime-ligation with three different poly-aldehyde cores. However, as observed in the case of compound **7 (Scheme 3-4)**, we faced the similar impediment of acyl migration. Therefore, we did not proceed further with this protocol.

3.3 Synthesis of higher generation of glycoclusters via "onion peel" strategy & oxime-ligation

Higher generation dendrimers were anticipated by introducing a multivalent dendron having longer spacer such as compound **41 (Scheme 3-6)**. Installation of this new dendron was envisaged via recently developed "onion peel" strategy from our lab wherein use of two coupling reactions namely CuAAc and oxime-ligation where implemented to stich sugar peripheries and conjugate to the poly-aldehyde cores **11**, **14** and **20**. Concomitantly, tri-propargylated dendron **41** was selected for further modification and the synthetic scheme was initiated using commercially available pentaerythritol **38** as starting material shown in **Scheme 3-6**.

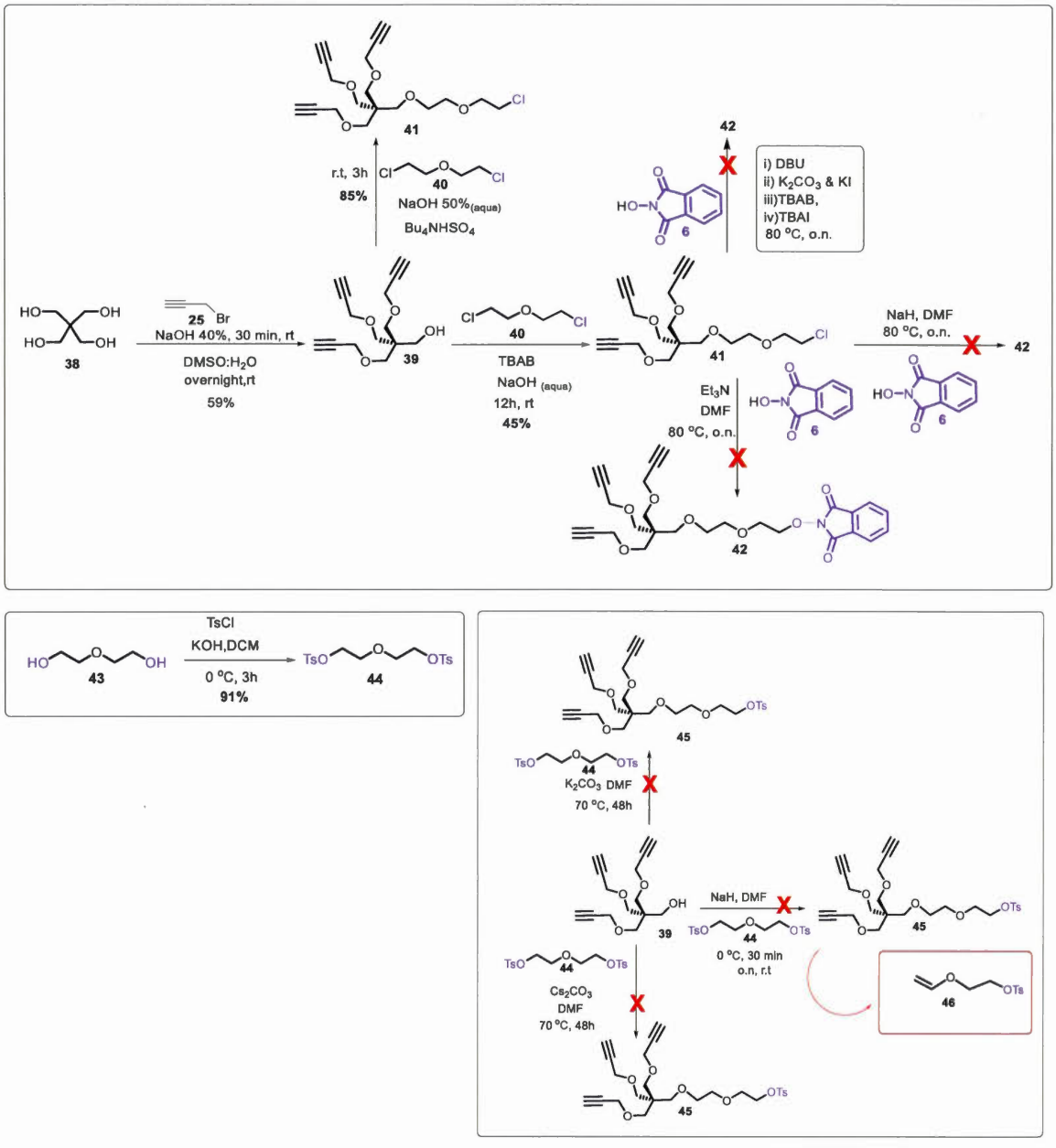

Scheme 3-6. Synthesis of higher generation of glycoclusters via "onion peel" strategy and oxime-ligation using aminooxylated dendron

Subsequently, the compound **38** was treated with propargyl bromide **25** in presence of NaOH 40% for overnight in DMSO:H_2O to achieve the compound **39** in good yield (59%). Completion of the reaction was characterized using ^{1}H NMR wherein the appearance of newly expected triplet at δ 2.42 corresponding propargylic proton (C*H*) confirmed the formation of the compound **39.** Next, the compound **41** having long spacer was achieved through an additional reaction by treating **39** with 2-chloroethyl ether **40** in presence of Bu_4NHSO_4 (phase transfer catalyst) at room temperature for 48 hours in excellent yield (85%). Reaction yield was optimized up to 85% using Bu_4NHSO_4 which was noticeably higher than reported protocols wherein TBAB was used. Chloride functionality was subjected to substitution reaction upon treatment with *N*-hydroxyphthalimide **6** in DMF at 80 °C to afford compound **42**; However, several attempts using conditions showed in **(Scheme 3-6)** such as i) Et_3N ii) DBU iii) K_2CO_3, KI iv) TBAB v) TBAI and vi) NaH failed to produce the desired product. Therefore, we revised the protocol using similar scaffold with tosylate functionality at focal point. In order to synthesis desired tosylated derivative, compound **39** was treated with diethylene glycol bis(*p*-toluenesulfonate) **44** which was prepared from commercially available diol **43** using literature procedure in excellent yield (91%) as shown in **Scheme 3-6**. In contrast to our expectation, the reaction did not furnish the compound **45**. Instead, eliminated product **46** was observed wherein tosylate undergo elimination even in a mild basic condition as shown in **Figure 3-26**. Formation of compound **46** was characterized using ^{1}H NMR wherein the appearance of two newly unexpected signals at δ 6.4 and δ 4.10 corresponding alkene protons (CC*H*) compared to the linker **44** seems to confirm the formation of the compound **46** as shown in Figure **3-26.** However, due to the absence of COSY spectrum of compound **46,** the formation of this compound is considered based on our hypothesis which requires supplementary researches .

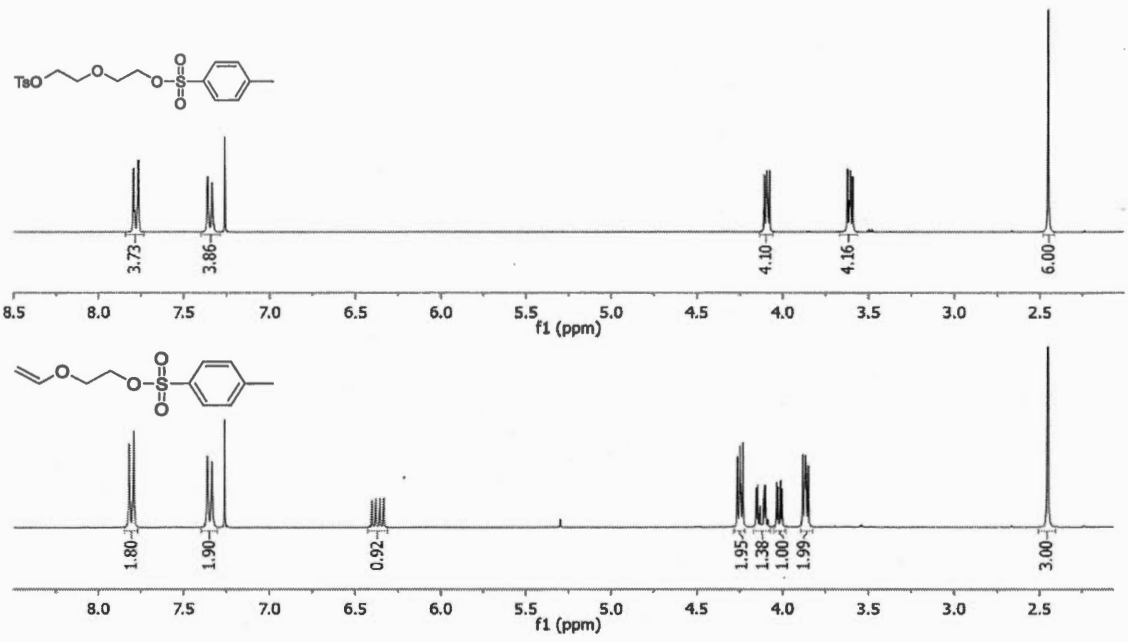

Figure 3-26. ^{1}H NMR (300 MHz, $CDCl_3$) of the eliminated product 46 compare to the linker 44

Due to the failures of our previous strategies wherein the synthesis of aminooxy ligands **8, 36 and 42** where acyl migration (based on our hypothesis) was bottle-neck, we revised the synthetic strategy based on a completely different substrate (starting precursors) which contains a triazole as a linker and terminal boc functionality. Based on our previous experiences wherein acyl migration was facilitated in the basic reaction environment, we purposefully chose Boc protected hydroxyl amine which could be deprotected in acidic condition. Synthesis of the compound **27** was projected by efficient click chemistry reaction which would be further coupled with poly-aldehyde cores **11**, **14**, and **20** using oxime ligation methodology to obtain desired glycoclusters **31**, **32**, and **33**. The precursor **27** was synthesized via coupling of the compounds **22** and **26**. Required synthons **22** and **26** were prepared using commercially available D-galactose **1** and hydroxlyamine hydrochloride **47** as starting materials respectively **(Scheme 3-7)**.

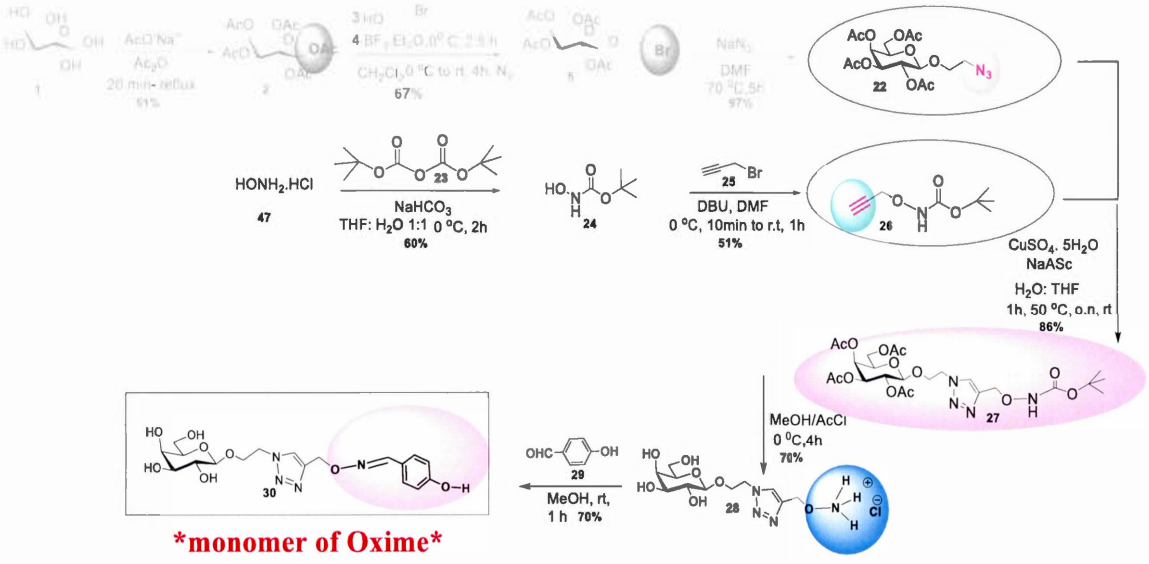

Scheme 3-7. Synthesis of the new monomer of oxime via oxime ligation from aminooxy salt ligand

The compound **22** was a suitable building block for the ligation to a propargylated derivative consisting of a Boc protective group **26,** through the click chemistry. Also, compound **26** was synthesized in two steps. Commercially available hydroxyl-amine hydrochloride **47** which was treated with di-*tert*-butyl dicarbonate or bis (tert-butoxycarbonyl)oxide (Boc_2O) **23** in presence of sodium bicarbonate in THF:H_2O at 0 °C to achieve compound **24** in good yield (60%) **(Scheme 3-7)**. The compound **24** was characterized using ^1H NMR and ^{13}C NMR spectroscopy wherein a singlet at δ 1.48 corresponding t-butyl C*H* and appearance of carbamide proton (N*H*) at δ 6.13 and hydroxyl proton (O*H*) at δ 6.96 confirmed the formation of the compound **24** as shown in **Figure 3-27**. Subsequently tert-butylhydroxycarbamate **24** was treated with propargyl bromide **25** in the presence of DBU in DMF at 0 °C temperature to afford compound **26** in satisfactory yield (51%). *Tert*-butyl(prop-2-yn-1-yloxy) carbamate **26** was characterized using ^1H NMR and ^{13}C NMR spectroscopy. The appearance of (CC*H)* in ^1H NMR at δ 2.49 corresponds to the proton of propargyl functionality and a singlet

at 1.48 corresponds to Boc protons (CH_3)$_3$ confirmed the formation of compound **26**, **(Figure 3.16)**. Moreover, the presence of a signal at δ 63.6 corresponding propargylic carbon (*C*CH) and a signal at δ 28.1 corresponding (CH_3)$_3$ of Boc in ^{13}C NMR confirmed the formation of compound **26** (see annex).

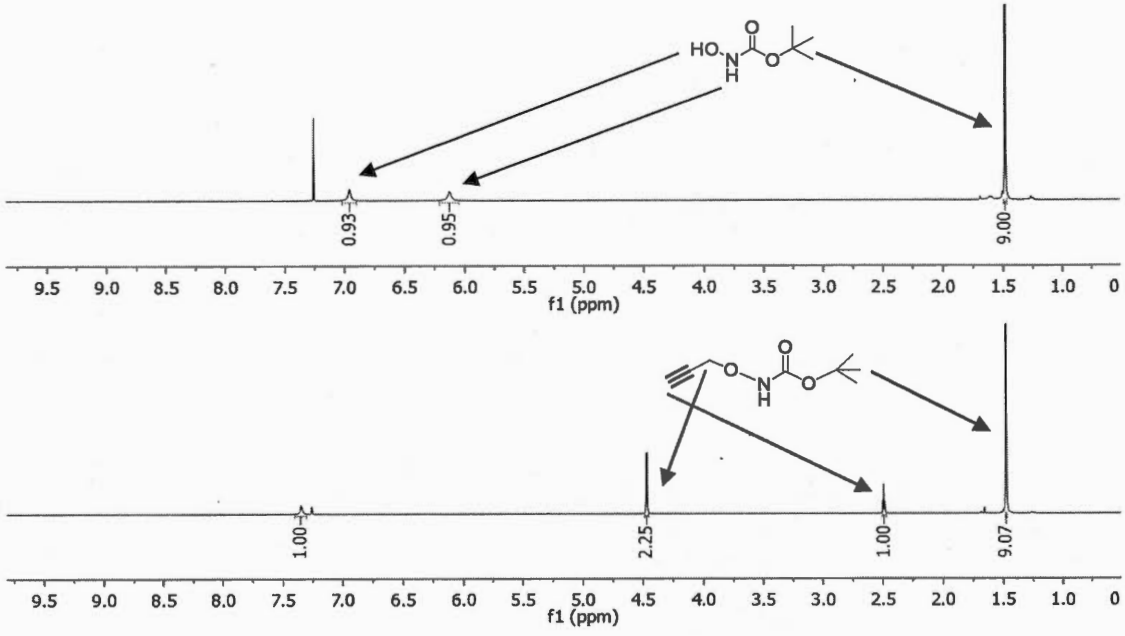

Figure 3-27. ^{1}H NMR (300 MHz, $CDCl_3$) between compound 24 and 26.

Having compound **22** which has azide functionality and **26** having suitably placed propargyl functionality in hand, we were in a position to couple using CuAAC click reaction to afford compound **27** with an excellent yield (86%). The desired compound **27** was synthesized by coupling two mentioned compounds **22** and **26** in H_2O:THF in the presence of aqueous solution of $CuSO_4.5H_2O$ and sodium ascorbate as catalyst at 50 °C and then at room temperature. The pure compound **27** was obtained after using column chromatography. Completion of the reaction was evidenced using ^{1}H NMR, HSQC, COSY, ^{13}C NMR and mass spectrometry wherein the ^{1}H NMR indicated the

complete disappearance of the propargylic C*H* signal at δ 2.49 and the appearance of the newly formed characteristic singlet of the triazole moiety at δ 7.70 which confirmed the formation of the compound **27** shown in **Figure 3.28**. Moreover, the signal at δ 125.2 corresponds to triazole in ^{13}C NMR (see annex). Mass spectral analysis further confirmed the structural integrity of the desired compound **27** (ESI-MS: *m/z* calcd. for $C_{24}H_{36}N_4O_{13}$ ($M+ H^+$): 589.2279, Found: 589.7) (see annex). Having achieved successful synthesis of compound **27**, we were in the position to hydrolyze Boc and deprotection of acetate groups in one step to afford required compound **28**. Concomitantly, the compound **27** in methanol was treated with 10% of Acetyl chloride (98%) at -10 °C up to 0 °C for four hours to furnish ammonium salt **28** in good yield (70%). Formation of the desired compound **28** as an ammonium salt was observed using ^1H NMR in comparison with the compound **27** consisting of Boc protective group, where the decrease in signal of the Boc (CH_3)$_3$ at δ 1.49 and four acetate groups at δ 2.16-1.94 confirmed the formation of the compound **28** as shown in **Figure 3-28**. Moreover, the mass spectral analysis further confirmed the structural integrity of the desired compound **28** (ESI-MS : *m/z* calcd. for $C_{11}H_{20}N_4O_7$ ($M+ H^+$): 320.1332, Found: 321.9 ($M+H^+$), 343.8 ($M+Na^+$), 363.8 ($M+K^+$)) (annex).

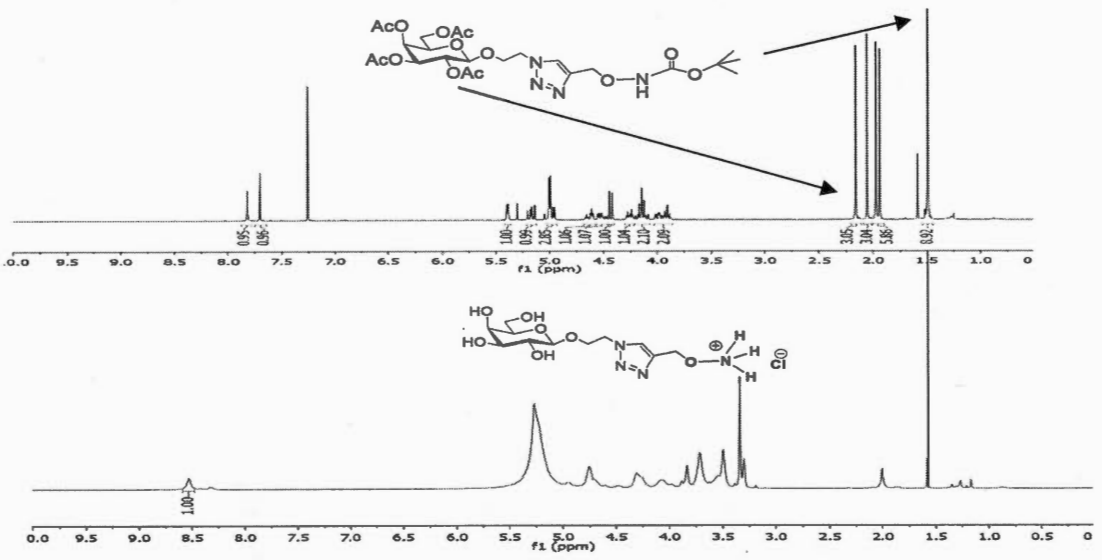

Figure 3-28.^{1}H NMR (300 MHz, $CDCl_3$) of compound 27 and ^{1}HNMR (300 MHz, MeOD) of compound 28 (solubilized better in MeOD than in D_2O)

Using AcCl in MeOH led to generate the sufficient amount of HCl in situ which could hydrolyzed the Boc and acetyl groups on the sugar periphery simultaneously. However, this strategy leads to significantly less migration of acetyl groups, O-N bond cleavage or hydrazine acetamide impurities, (based on achieved data), compared to previous strategy which was confirmed by the presence of a signal at δ 1.85 ppm using ^{1}H NMR. In order to prevent migration and drive the reaction to completion, an additional amount of AcCl is needed for the simultaneous deprotection of acetate and BOC. In addition, the migration of an acetate group from the glycoside to the aminooxy result in no mass change, hence mass spectrometry cannot be used to characterize the fully deprotected ligand. Instead, the ninhydrine test was used to determine the presence a free amine.

In order to check the feasibility of the oxime ligation, we carried out the condensation of the afforded salt **28** with a monomer aldehyde which would be beneficial in order

to evaluate the productivity of this reaction for the larger glycoclusters. Therefore, the reaction performed on commercially available *para*-hydroxybenzaldehyde **29**. The resultant reaction led to the formation of oxime ligated compound **30**. The synthesis of the 2-azidoethyl-carbaldoxime-β-D-galactopyranoside **30** was achieved through condensation process in good yield, (oxime coupling of compound **27** which was formed in situ as explained above and compound **29** in MeOH for 1 hour at room temperature **(Scheme 3-7)**. Renaudet and co-workers have recently mentioned that the oxime ligation reaction afford the mixture of *E*/*Z*-stereoisomers when the conjugation occurs by a unsymmetrical aldehyde.[176] According to the literature, more stable *E*-isomer is prefered with respect to the C=N bond.[192] Surprisingly, herein after using symmetrical aldehyde, compound **30** was obtained in a ratio of 9,7/1 *E*/*Z* mixture **(Figure 3.29)**. Moreover, the high polarity of the deprotected sugar led to the difficulties in purification which could be the bigger obstacle for the synthesis of multivalent glycoclusters in further steps. Completion of the reaction and structural integrity of the product was characterized using ^{1}H NMR, HSQC, COSY, ^{13}C NMR and mass spectrometry wherein the ^{1}H NMR identified the appearance of newly expected oxime singlet (*NCH*) at δ 8.20 and the newly formed characteristic doublets of the aromatic (C*H*) moiety at δ 7.47 and δ 6.81 which confirmed the formation of compound **30.** Together with the existence of the formed characteristic singlet of the triazole moiety at δ 8.05. Moreover, the signal at δ 125.6 corresponds to the oxime (N*C*H) and signal at δ 151.5 corresponds to the triazole in ^{13}C NMR (see annex). The mass spectral analysis clearly established the nature of the compound **30** (ESI-MS-TOF: *m/z* calcd. for $C_{18}H_{24}N_4O_8$: 424.16 found: 425.1673 [M+ H^+] and 447.1493 [M+ Na^+] as shown in **Figure 3.30**.

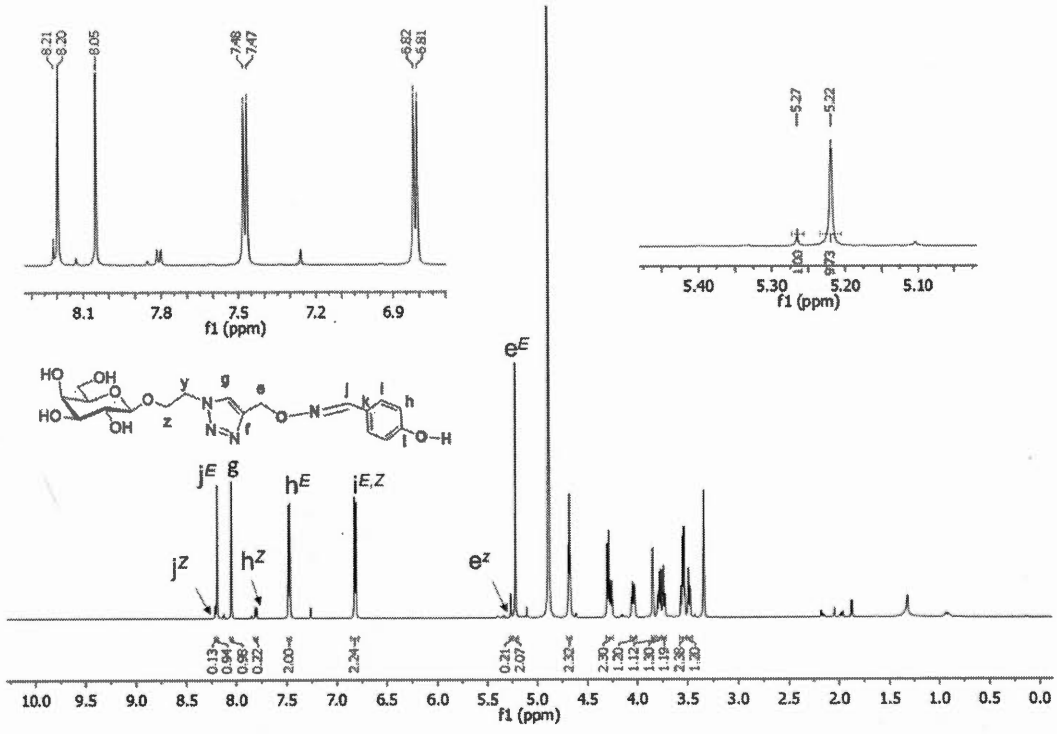

Figure 3-29. ^{1}H NMR (600 MHz, MeOD) of compound 30

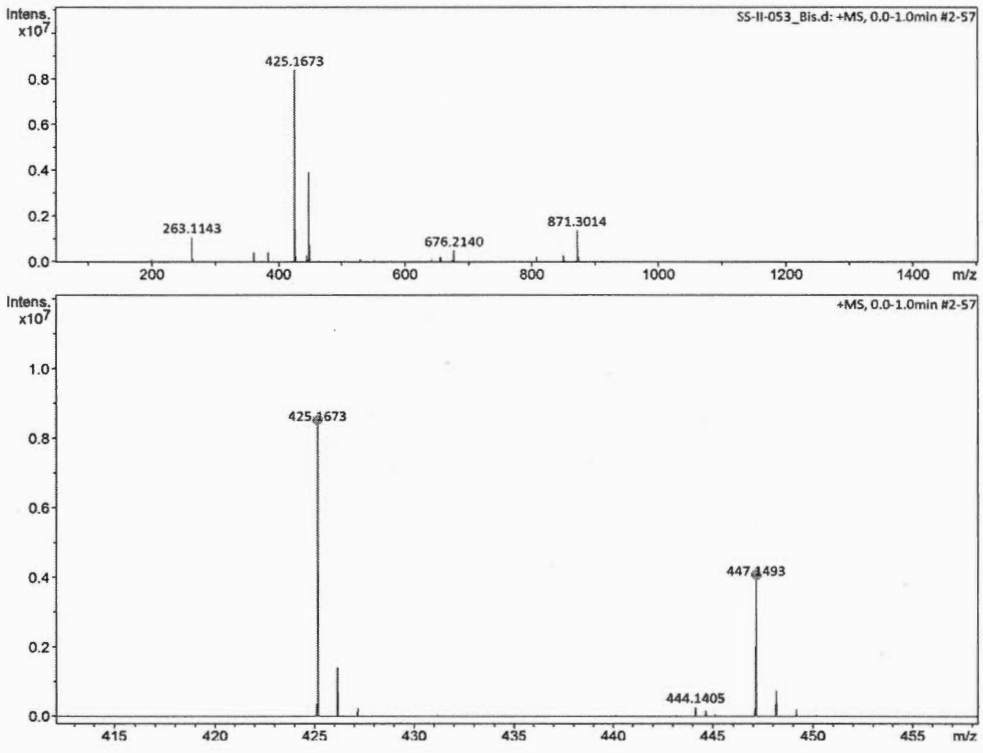

Figure 3-30. HRMS (ESI^+) spectrum of compound 30

3.4 Synthesis of three different multivalent glycoclusters based on the second strategy (G_0)

Having successfully accomplish the condensation of aminooxy **28** with the monomer aldehyde **29**, we were eager to extend the same methodology for the preparation of final glycoclusters **31**, **32**, and **33** having 3, 6, and 12 sugar moieties, respectively. By following similar oxime-ligation strategy, ammonium salt **28** which was the basic building block, was treated with three different poly-aldehyde cores **11**, **14**, and **20** having 3, 6, and 12 aldehyde functionalities to afford final dendrimers. The model study of this strategy is shown in the **Figure 3.31**.

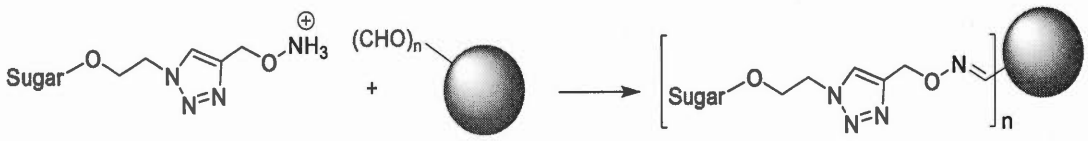

Figure 3-31. Oxime ligation strategy to achieve 3-mer, 6-mer, and 12-mer glycoclusters

Coupling of compounds **28** and poly-aldehyde cores **11**, **14** and **20** provided dendrimers with 3, 6 and 12 galactoside moieties according to **Scheme 3.8** Therefore, compound **28** in MeOH: H_2O (4:1) was treated with poly-aldehyde cores for overnight at room temperature respectively with the same procedure. In order to ensure complete conjugation (oxime-ligation), excess aminooxy salt **28** (1.5 to 2 equivalent) was used per aldehyde group.

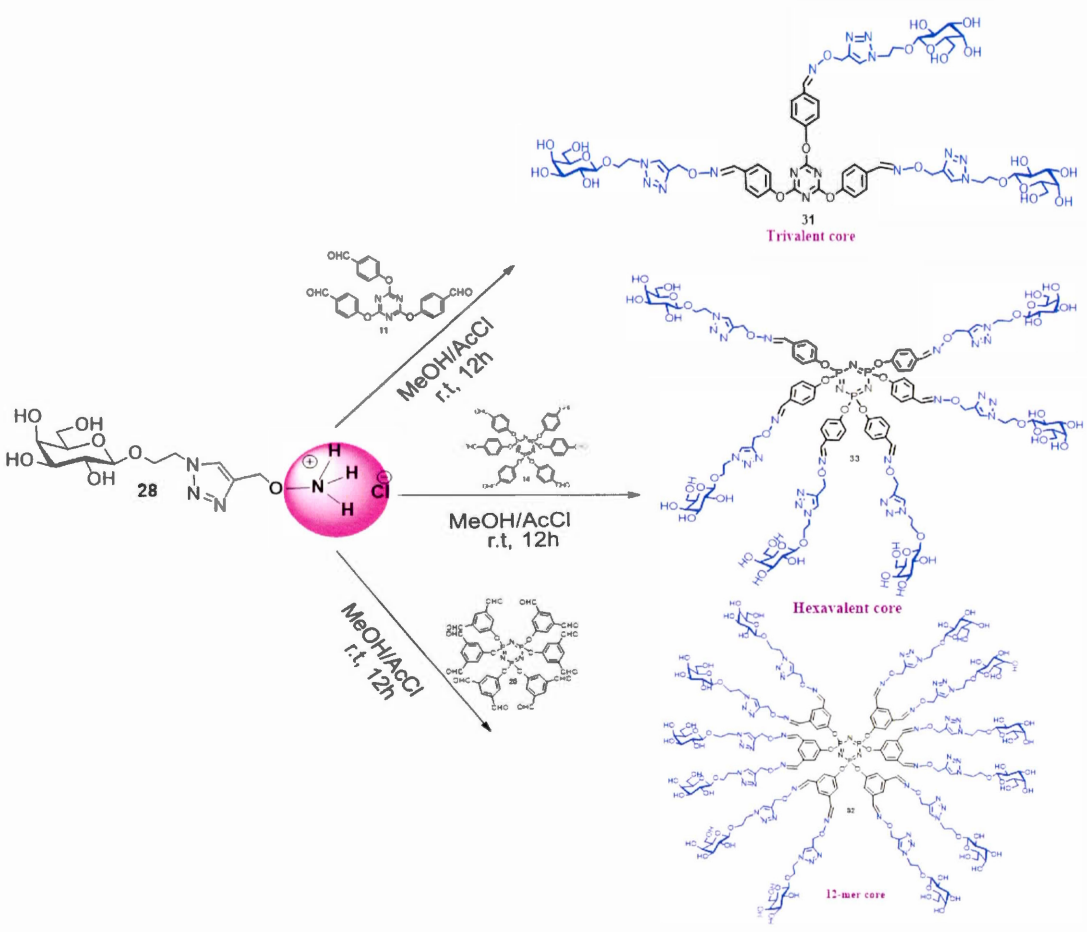

Scheme 3-8. Synthesis of 3-mer, 6-mer and 12-mer glycoclusters in zero generation

Completion of the reaction was monitored by TLC however, due to the polar nature of final glycoclusters, we could not distinguish the formation of mono, bis and tris substitution in the case of **31** and the similar pattern in the case of **33**. Therefore, we assumed the completion of the reaction based on the literature procedure and consumption of starting material. In addition, the highly polar nature of glycocluster

due to the numerous of hydroxyl functionalities, were the biggest impediment for the conventional column chromatography purification; thus, we have chosen the dialysis technique and size exclusion chromatography. Nevertheless, both methods were found to be not useful due to the narrow window of the sizes of differentially (partially reacted) substituted products. On the other hand, due to the small size of 3-mer glycocluster, compound **31**, the separation of three substitution was not possible by dialysis. Therefore, it was purified using semi-preparative high-performance liquid chromatography (HPLC) by choosing appropriate eluent system (H_2O/ACN (4:1); R_f = 0.54). Although HPLC purification was useful to separate the monomer from few partially substituted derivatives, we could not achieve 100% purified compound through this method. The ^{1}H NMR of the resulting fraction is shown in **Figure 3-32.** Also, mass spectrum of this fraction indicated the formation of the oxime-based glycocluster **31**. The mass spectral analysis clearly established the nature of the compound **31** (ESI-MS-TOF: *m/z* calcd. For $C_{57}H_{69}N_{15}O_{24}$: 1347.46 found: 1348.8 [M+ H^+] and 1370.8 [M+ Na^+] (see annex).

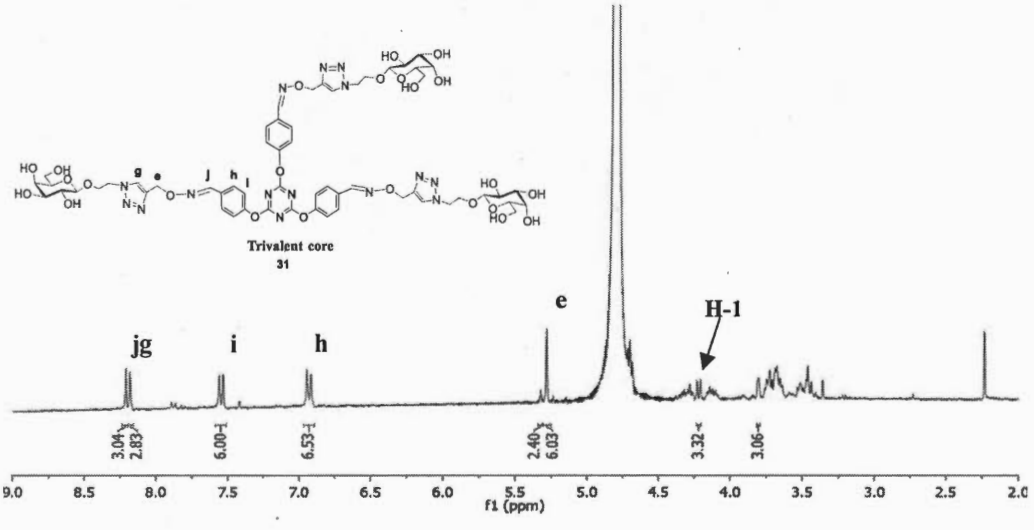

Figure 3-32. ^{1}H NMR (600 MHz, D_2O) of fraction collected from HPLC for compound 31.

Purification of 6-mer glycocluster, **33**, could not be accomplished using HPLC due to the exclusively soluble nature of 6-mer **33** in DMSO which is not a compatible solvent for HPLC. However, we could remove excess of ligand **28** which had been used as starting material by dialysis in 1000 molecular weight cut off bags. The partially purified 6-mer from dialysis was dried under reduced pressure. The remaining residue was triturated using MeOH and allowed it to settle the insoluble portion which we assumed could be our compound. After 5 minutes solvent was decanted, and the insoluble residue were dried under vacuum. This compound was characterized using ^{1}H NMR according the **Figure 3-33** and ^{31}P NMR according to the **Figure 3-34.** According to the literature procedure, the mixture of *Z*/*E*-isomers though the oxime-ligation provided us with difficulties to obtain the pure compound. The mass spectral analysis clearly established the nature of the compound **33** (ESI-MS-TOF: *m/z* calcd. For $C_{108}H_{138}N_{27}O_{48}P_3$: 2673.84 found: 2699.523 [M+ D^++ Na^+]. (Annex)

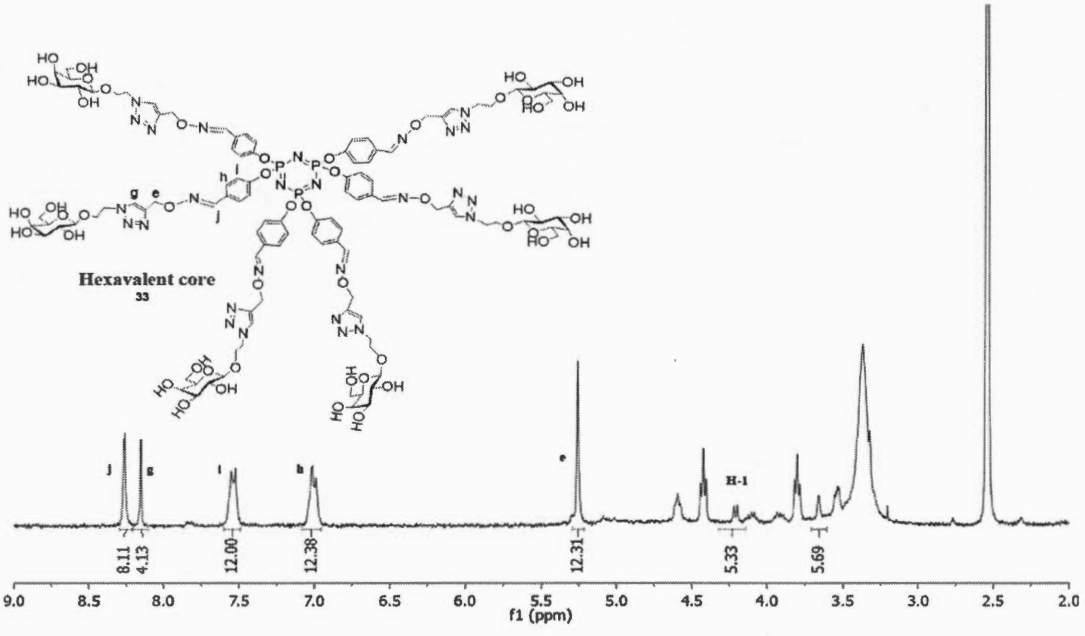

Figure 3-33. ^{1}H NMR (300 MHz, DMSO) of remaining residue of compound 33 after dialysis.

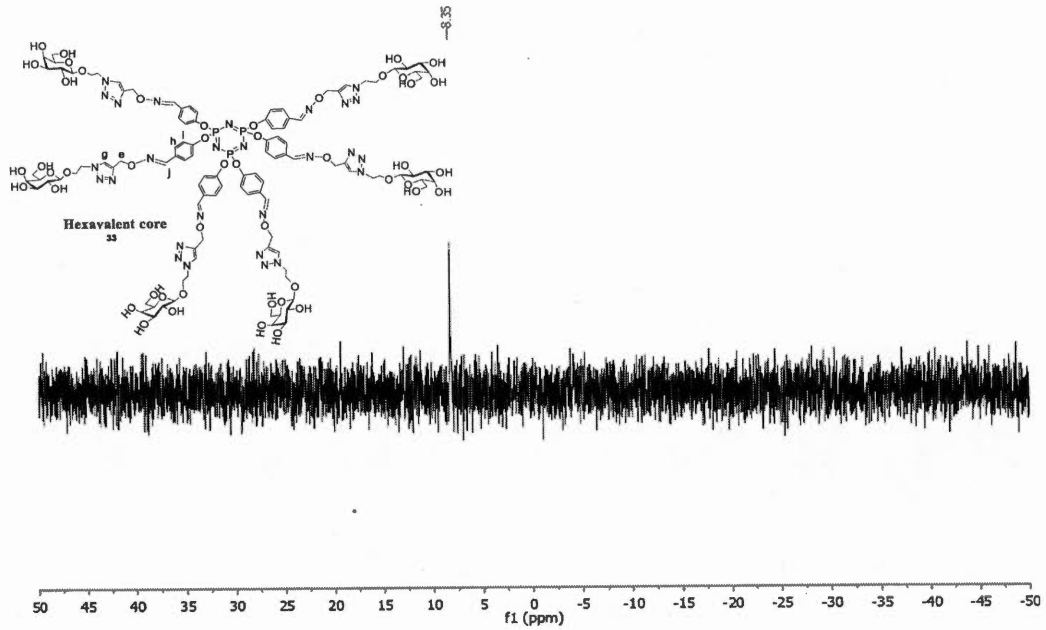

Figure 3-34. ^{13}P NMR (300 MHz, DMSO) of remaining residue of compound 33 after dialysis.

CHAPTER IV

EXPERIMENTAL

4.1 MATERIALS AND METHODS

DMF was tested with ninhydrin to insure that there is no amine impurities and kept over molecular sieve. The DCM, DMF, toluene and THF were obtained from a solvent purifier, MBRAUN. MeOH was dried with activated molecular sieve. The solvents used for the chromatography are of HPLC quality. Solvents and reagents were deoxygenated when necessary by purging whit nitrogen. Nanopure water, purified through Barnstead NANO Pure II filter with Barnstead Megühm-CM Sybron meter, was used for lyophilization. All reagents were used as supplied without prior purification unless otherwise stated, and obtained from Sigma-Aldrich Chemical Co. Ltd. The progress of the reactions is followed by thin layer chromatography (TLC) on aluminum silica gel plate (Merk 60 F254) using appropriate eluent systems. The revelation is carried out by irradiation under light UV (λ =254 nm), and on the other hand, by soaking in specific developers, an acid mixture (sulfuric acid /methanol / water: 5/45/45; v/v/v) for protected compounds. Purification was performed by flash column chromatography using silica gel from Silicycle (60 Å, 40-63 µm) with the indicated eluent. ^{1}H NMR and ^{13}C NMR nuclear magnetic resonance spectra were recorded with Varian-Gemini 2000 or Varian-Innova AS600 instruments. The ^{1}H NMR spectra are recorded at a frequency of 300 MHz or 600 MHz, and ^{13}C NMR are recorded at 75 or 150 MHz, respectively. All NMR spectra were measured at 25 °C in indicated deuterated solvents. Proton and carbon chemical shifts are reported in ppm

and coupling constants (J) are reported in Hertz (HZ). The chemical shifts (δ) are expressed in parts per million (ppm) relative to tetramethylsilane (TMS) used as an internal reference for the other solvents. The resonance multiplicities in the ^{1}H NMR spectra are described as "s" (singlet), "d" (doublet), "t" (triplet), "quint" (quintuplet) and "m" (multiplet). The reference solvents which were used to make these measurements consist of deuterated chloroform ($CDCl_3$), deuterium oxide (D_2O), deuterated methanol (CD_3OD) and deuterated dimethyl sulfoxide (CD_3) 2SO. The reference values for ^{1}H NMR, are δ 7.27, δ 4.79, and δ 3.31, respectively. For ^{13}C NMR, the following values are δ 77.0 ($CDCl_3$), δ 49.0 (CD_3OD) and δ 39.5 (DMSO-d6). 2D Homonuclear correlation ^{1}H-^{1}H COSY and Heteronuclear correlation ^{1}H-^{13}C HETCOR experiments were used to confirm NMR peak assignments. *Characteristic signals of deprotected of the glycodendrimers' periphery was assigned in comparison with corresponding the prepared monomer of oxime as reference.* Fourier transform infrared (FT-IR) spectra were obtained with Thermo-scientic, Nicolet model 6700 equipped with ATR. The absorptions are given in wave numbers (cm^{-1}). The intensity of the bands is described as s (strong), m (medium) or w (weak).

Penta-*O*-acetyl-β-D-galactopyranose (2)

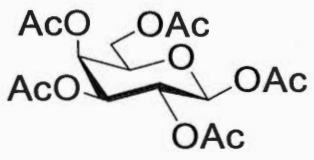

The compounds **2** was prepared according to the literature procedure. [17] A suspension of anhydrous sodium acetate (5.00 g, 61.05 mmol, 1.10 equiv.) in acetic anhydride (70 mL) was stirred at reflux. D-galactose (10.0 g, 55.51 mmol, 1.00 equiv.) was added in small portions to the mixture and was stirred at reflux for a further 10 minutes. The solution was poured in to ice-water (400 mL), followed by addition of dichloromethane (120 mL), the organic layer was separated. The organic phase was washed with ice cold water (2 x 200 mL), saturated aqueous solution of sodium bicarbonate (2 x 200 mL) and brine (2 x 200 mL). The organic solution was dried over Na_2SO_4, filtered and concentrated under reduced pressure to give a crude yellow oil. The yellow oil was dissolved in the minimum amount of Et_2O (~25 mL), subsequently petroleum ether (~50 mL) and EtOH (~200 mL) were added which resulted in to the precipitation. The suspension was then kept first at 24 °C for 2-3 hours then at -14 °C for 16 hours. The residue was filtered and washed with petroleum ether to give a product containing the α, β mixture. In order to ensure exclusive formation of β product, the remaining solid residue was recrystallized again in minimum amount of hot ethanol to afford penta-*O*-acetyl-β-D-galactopyranose **2** as white solid (10.86 g, 60%); (EtOAc /Hexane (3:2)); mp 142-143 °C; [Ref. mp 142-144 °C; Ref. mp 142 °C; Ref. mp 137-139 °C (EtOH)]; $[\alpha]_D$ +23.00 (*c* 1.0, $CHCl_3$) [Ref.[18a] $[\alpha]_D$ +23.4 (*c* 1.0, $CHCl_3$)]; ^{1}H NMR (300 MHz, $CDCl_3$): δ 5.69 (d, 1H, $J_{1,2}$ = 8.3 Hz, h-1), 5.42 (dd, 1H, $J_{3,4}$ = 3.4 Hz, $J_{4,5}$= 0.9 Hz, H-4), 5.33 (dd, 1H, $J_{2,3}$ = 10.4 Hz, $J_{1,2}$ 8.3 Hz, H- 2), 5.07 (dd, 1H, $J_{2,3}$= 10.4 Hz, $J_{3,4}$ = 3.4 Hz, H-3), 4.2 – 4.1 (m, 2H, H-6a,a'), 4.1 – 4.0 (m, 1H, H-5), 2.16, 2.11, 2.03, 1.99 ppm (5 x s, 15H, 5 x $COCH_3$) . ^{13}C NMR (300 MHz, $CDCl_3$): δ 170.2, 170.0, 169.8,

169.2, 168.9 (5 x *C*OCH$_3$), 92.0 (*C*-1), 71.6 (*C*-5), 70.7 (*C*-3), 67.7 (*C*-2), 66.7(*C*-4), 60.9 (*C*-6), 20.8, 20.7, 20.5, 20.5, 20.4 ppm (5 x CO*C*H$_3$). The data agrees with the reported literature values.

Tert-Butyl _N_-Hydroxycarbamate (24)

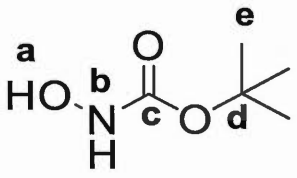

The compounds **24** was prepared according to the literature procedure.[197] A solution of di-*tert*-butyl dicarbonate or bis(*tert*-butoxycarbonyl) oxide; (BocO)$_2$CO **47** (5g, 0.023 mol, 1.0 equiv.) in 1:1 THF: H_2O (60 mL) and hydroxyl-aminehydrochloride (2.39 g, 0.034 mol, 1.5 eq.) was treated at 0 ^{0} C with $NaHCO_3$ (2.85g, 0.034mol, 1.5 eq.).The solution was stirred at 0 ^{0} C for 2h. After completion of reaction, the solution was diluted with EtOAC. Subsequently, the extracted organic layer, was washed with saturated aqueous sodium bicarbonate (3 x 30 mL $NaHCO_3$, H_2O) and saturated aqueous NaCl (3 x 30 mL) then dried over Na_2SO_4. The solvent was removed under reduced pressure. The residue was dissolved in minimum amount of diethyl ether and crystalized with ether petroleum to afford **24** as a white solid compound (1.843 g, 0.0139 mol, 60%). ^{1}H NMR (300 MHz, $CDCl_3$): δ 6.96 (s, 1H, H-a), 6.13 (s, 1H, H-b), 1.48 ppm (s, 9H, H-e). ^{13}C NMR (300 MHz, $CDCl_3$): δ 158.8 (*C*-c), 82.0 (*C*-d), 28.1 ppm (*C*-e). The data agrees with the reported literature values.[197]

***Tert*-butyl *N*-(2-propynyloxy)-carbamate (26)**

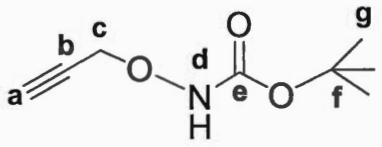

The compound **26** was synthesized according to a modified literature procedure.[198] To a cooled solution (5-10 °C) of *tert*-butylhydroxycarbamate (3.00 g, 22.53 mmol, 1.0 equiv.) stirring in DMF (25 mL) was added DBU (6 mL, 40.55 mmol, 1.8 equiv.) in one portion. After 10 minutes, Propargyl bromide (3.61 mL, 40.55 mmol, 1.8 equiv.) was added dropwise in cooled temperature. When the addition was completed, the ice bath was removed and the reaction mixture was stirred at room temperature for 2 hours. Once starting material (limiting reagent) was consumed as an approve of completion of the reaction, EtOAc (50 mL) and water (25 mL) were added, then aqueous phase was separated and were back- extracted with EtOAc (3 x 30 mL). The combined organic phase was washed with water (4 x 30 mL) and respectively with satd. $NaHCO_3$ (4 x 30 mL) and brine (3 x 30 mL). The extract was dried over Na_2SO_4, filtered and evaporated under reduced pressure. Reaction mixture was purified through silica gel column chromatography using the appropriate eluent system (Toluene/ EtOAc (4:1); $R_f = 0.5$) to afford compound **26** as a beige-gray oil (1.95 g, 11.39 mmol, 51%); ^{1}H NMR (300 MHz, $CDCl_3$): δ 7.35 (s, 1H, H-d), 4.47 (s, 2H, H-c), 2.49 (s, 1H, H-a), 1.48 ppm (s, 9H, H-g). ^{13}C NMR (300 MHZ, $CDCl_3$): δ 156.3 (*C*-e), 82.0 (*C*-f), 78.1 (*C*-b), 75.5 (*C*-a), 63.6 (*C*-c), 28.1 ppm (*C*-g). The data agrees with the reported literature values.[198]

2-bromoethyl 2, 3, 4, 6-tetra-*O*-acetyl-β-D-galactopyranoside (5)

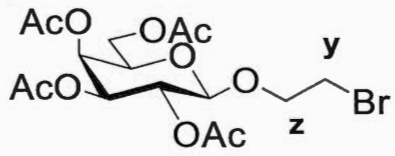

To the mixture of penta-*O*-acetyl-β-D-galactopyranose, **2** (2.00 g, 5.12 mmol, 1.0 equiv.) and 2-bromoethanol, (0.55 mL, 7.7 mmol, 1.5 equiv.) which dissolved in dichloromethane, (20 mL), BF_3. Et_2O, (0.94 mL, 7.7 mmol, 1.5 equiv.) was added at 0 °C dropwise during 30 minutes and then left the mixture in ice bath for 2 hours and then at room temperature around 4 hours. Progression of the reaction was followed by TLC. Upon completion of the reaction, the reaction mixture was quenched by drop wise addition of $NaHCO_3$ since no bubble seen and then worked up by adding dichloromethane (20 mL). The organic phase was washed with water (2 x 30 ml), sodium bicarbonate (2 x 30 ml) and brine (2 x 30 ml). The extract was dried on Na_2SO_4, filtered and evaporated under reduced pressure. Reaction mixture was purified through silica gel column chromatography (EtOAc/ Hexane (1:1); R_f = 0.41) to afford compound **5** (1.56 g, 0.0034 mol 67 %) as a white soft solid. ^1H NMR (300 MHz, $CDCl_3$): δ 5.38 (dd, 1H, *J*= 3.4 0.8 Hz, H-4), 5.22 (dd, 1H, *J*= 10.5, 7.9 Hz, H-2), 5.01 (dd, 1H, *J* = 10.5, 3.4 Hz, H-3), 4.53 (d, 1H, *J* = 7.9 Hz, H-1), 4.21 – 4.07 (m, 3H, H-6a,a', H-Za), 3.91 (td, 1H, *J* = 6.6, 0.9 Hz, H-5), 3.81 (ddd, 1H, *J* = 11.3, 7.3, 6.4 Hz, H-Za'), 3.50 – 3.42 (m, 2H, H_y), 2.14, 2.05, 1.98 ppm (4 x s, 12H, 4 x $COCH_3$). ^{13}C NMR (300 MHz, $CDCl_3$) δ 170.2, 170.1, 170.0, 169.0 (4 x *C*OCH_3), 101.3 (*C*-1), 70.7 (*C*-5), 70.6 (*C*-3), 69.6 (*C*-z), 68.4 (*C*-2), 66.8 (*C*-4), 61.1 (*C*-6), 29.82 (*C*-y), 20.73, 20.54, 20.52, 20.44 ppm (4 x CO*C*H_3).

2-Azidoethyl 2, 3, 4, 6-tetra-*O*-acetyl-β-D-galactopyranoside (22)

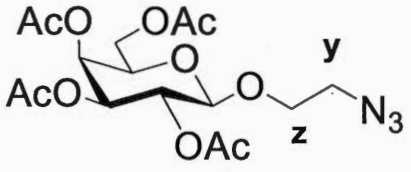

To the solution of 2-bromoethyl-2,3,4,6-tetra-*O*-acetyl-α-D-galactopyranoside (0.900 g, 1.98 mmol, 1.0 equiv.) in DMF (8 mL) was added sodium azide, NaN_3, (0.194 g, 2.97 mmol, 1.5 equiv.) and the mixture of the reaction stirred at 65 °C for 5 hours. Progression of the reaction was followed by TLC. Upon completion of the reaction, the reaction mixture was diluted with EtOAc (20 mL) and the two organic and aqueous phase were separated. The aqueous phase again extracted with EtOAc (3 x 20 mL) and the separated organic phase was washed with water (5 x 20 mL) and brine (3 x 20 mL). The extract was dried over Na_2SO_4, filtered and evaporated under reduced pressure. Reaction mixture was purified through crystallization with DCM/Hexane or through silica gel column chromatography (EtOAc/ Hexane (1:1); R_f = 0.44) to afford compound **22** as a colorless waxy oil to the white semi solid in low temperature (0.805 g, 1.93 mmol, 97 %). ^{1}H NMR (300 MHz, $CDCl_3$): δ 5.38 (dd, 1H, *J* = 3.4 Hz, 0.9 Hz, H-4), 5.23 (dd, 1H, *J* = 10.5, 7.9 Hz, H-2), 5.01 (dd, 1H, *J*= 10.5, 3.4 Hz, H-3), 4.55 (d, 1H, *J* = 7.9 Hz, H-1), 4.15 (tt, 2H, *J* = 11.3, 5.7 Hz, H-6a,a'), 4.03 (ddd, 1H, *J* = 10.6, 4.7, 3.5 Hz, H-Zb), 3.91 (td, 1H, *J* = 6.6, 1.0 Hz, H-5), 3.72 – 3.64 (m, 1H, H-Zb'), 3.54 – 3.45 (m, 1H, H-Yc), 3.29 (ddd, 1H, *J* = 13.4, 4.6, 3.4 Hz, H-Yc'), 2.14, 2.04, 1.92 ppm(4 x s, 12H, 4 x $COCH_3$). ^{13}C NMR (300 MHz, $CDCl_3$): δ 170.2, 170.1, 170.0, 169.3 (4 x *C*OCH_3) , 101.0 (*C*-1), 70.7 (*C*-5), 70.7 (*C*-3), 68.4 (*C*-2), 68.2 (*C*-4), 66.9 (*C*-z), 61.1 (*C*-6), 50.4 (*C*-y), 20.6, 20.5, 20.5, 20.4 ppm (4 x CO*C*H_3).

4-Azidoethoxy-2-(2,3,4,6-tetra-*O*-acetyl-β-D-galactopyranosyloxy)*tert*-butyl(4-methyloxy) carbamate (27)

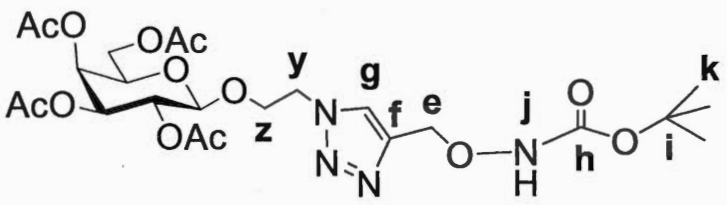

The compound **27** was synthesized according to a modified literature procedure.[199,200] A solution of 2-azidoethyl-2, 3, 4, 6-tetra-*O*-acetyl-β-D-galactopyranoside **22** (650 mg, 1.56 mmol, 1 equiv.) and *tert*-butyl (prop-2-yn-1-yloxy)carbamate **(26)** (399 mg, 2.34 mmol, 1.5 equiv.) in minimum amount of THF (3mL), were treated with an aqueous solution of $CuSO_4.5H_2O$, (78 mg, 0.0312 mmol, 0.02 equiv.) and sodium ascorbate (93 mg, 0.047 mmol, 0.03 equiv.) in 1 mL of H_2O. Biphasic mixture was then stirred at 50 °C for 1h and then at room temperature overnight. The completion of the reaction judged by the complete conversion of the limiting reagent. After completion of the reaction, EtOAc was added to the mixture (12 mL) and stirred for 30 minutes then was dried over Na_2SO_4, filtered and evaporated under reduced pressure. The main product **27** was afforded through silica gel column chromatography using the appropriate eluent system (DCM/ MeOH (9.9:0.1); $R_f = 0.3$) as a white solid (790 mg, 1.34 mmol, 86%). ^{1}H NMR (300 MHz, $CDCl_3$): δ 7.82 (s, 1H, H-j), 7.70 (s, 1H, H-g), 5.39 (d, 1H, $J = 2.5$ Hz, H-4), 5.17 (dd, 1H, $J = 10.5$, 7.9 Hz, H-2), 5.01 – 4.94 (m, 3H, H-3 & H-e), 4.68-4.49 (m, 2H, H-6), 4.43 (d, 1H, $J = 7.9$ Hz, H-1), 4.26 (d, 1H, $J = 10.3$ Hz, H-5), 4.21 – 4.08 (m, 2H, H-z,z'), 4.03 – 3.87 (m, 2H, H-y), 2.16, 2.05, 1.97, 1.94 (4 x s, 12H, 4 x $COCH_3$), 1.49 ppm (s, 9H, H-k).^{13}C NMR (75 MHZ, $CDCl_3$): δ 170.5, 170.3, 170.2, 170.1, (4×*C*OCH_3), 156.9 (*C*-h), 143.2 (*C*-f), 125.2 (*C*-g), 101.1 (*C*-1), 81.8 (*C*-i), 71.0 (*C*-y), 70.6 (*C*-3), 69.3 (*C*-e), 68.6 (*C*-2), 67.7 (*C*-5), 66.9 (*C*-4), 61.3 (*C*-z), 50.1 (*C*-6), 28.4 (*C*-k, (3×*C*H_3)), 20.8, 20.8, 20.7, 20.7 ppm (4× CO*C*H_3). The data agrees with the reported literature values.[200]

2-Azidoethyl-carbaldoxime-β-D-galactopyranoside (30)

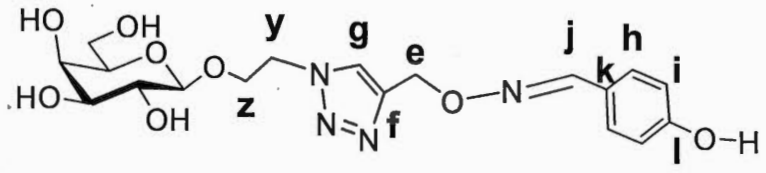

The compound **30** was synthesized according to a modified literature procedure.[201,202] A solution of 2-azidoethyl -β-D-galactopyranoside carbamate **(27)** (50 mg, 0.085 mmol) in methanol (2 mL), was treated with drop wised Acetyl chloride, AcCl 98% (200 µL, 2.8 mmol, 33.0 equiv.) in 0 °C for 4h. After completion of the reaction include Boc and acetyl deprotection, compound **9** the solvent was removed under reduced pressure. The dissolved residue in methanol (2 mL) was treated with 4-Hydroxybenzeldehyde (11.4mg, 0.093 mmol, 1.1 equiv.) for 2h at room temperature. Subsequently the solvent was removed under reduced pressure and the main product **30** was afforded through silica gel column chromatography using the appropriate eluent system (DCM/ MeOH (4:1); R_f = 0.54) as a white foam (25 mg, 0.059 mmol, 70%). ^{1}H NMR (600 MHz, MeOH) δ 8.20 (s, 1H, H-j), 8.05 (s, 1H, H-g), 7.47 (d, *J* = 8.5 Hz, 2H, H-h), 6.81 (d, *J* = 8.5 Hz, 2H, H-i), 5.22 (s, 2H, H-e), 4.68 (t, *J* = 5.0 Hz, 2H, H-y), 4.29 (d, *J* = 7.7 Hz, 1H, H-1), 4.26 (dd, *J* = 11.0, 5.4 Hz, 1H, H-z'),4.07 – 4.01 (m, 1H, H-z), 3.84 (d, *J* = 3.1 Hz, 1H, H-4), 3.78 (dd, *J* = 11.3, 7.1 Hz, 1H, H-3), 3.73 (dd, *J* = 11.4, 5.0 Hz, 1H, H-6a'), 3.38-3.52 (m, 2H, H-6a & H-2), 3.48 ppm (dd, *J* = 9.7, 3.2 Hz, 1H, H-5). ^{13}C NMR (151 MHz, MeOD): δ 161.5 (C-l), 151.5 (C-g), 146.3 (C-f), 130.7 (C-k), 127.5 (C-h), 125.6 (C-j), 117.4 (C-i), 106.1 (C-1), 77.7 (C-2), 75.5 (C-5), 73.2 (C-6), 71.1 (C-4), 70.0 (C-z,z'), 68.6 (C-e), 63.4 (C-3), 52.6 ppm (C-y). ESI-MS calcd for $C_{18}H_{24}N_4O_8$ $[M+H]^+$: 425.1594. Found: 425.1673. $[M+Na]^+$: 447.1491. Found: 447.1493

Tri-(4-formacylphenoxy)-1, 3, 3-triazine (11)

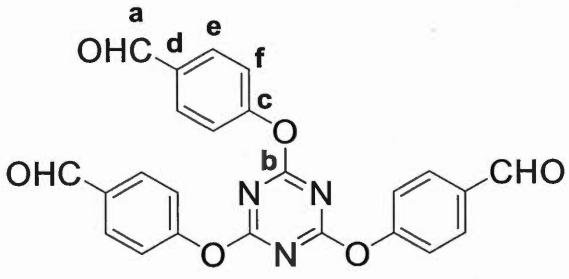

The compounds **24** was prepared according to the literature procedure.[193] Anhydrous sodium carbonate (2.3 g, 21.7 mmol, 4 equiv.) and 4-Hydroxybenzaldehyde (2.65 g, 21.7 mmol, 4 equiv.) were dissolved in acetone 4.8 mL and stirred at room temperature for 1 hour. In next step cyanuric chloride (1 g, 5.42 mmol, 1 equiv.) was added and the mixture was stirred at 60 °C for 6 hours then cooled to room temperature and the precipitate was filtered and washed three times by water 80 °C during 30 minutes to remove impurities. The white powder of tri-(4-formacylphenoxy)-1,3,3-triazine compound **11** was collected as a main product (1.769 g, 4 mmol, 74%) after dried in oven at 105 °C for 4 hours. Mp: 183-184 °C. ^{1}H NMR (300 MHz, $CDCl_3$): δ 9.99 (s, 3H, H-a), 7.91 (d, 6H, J = 8.7 Hz, H-e), 7.31 ppm (d, 6H, J = 8.6 Hz, H-f). ^{13}C NMR (300 MHz, $CDCl_3$): δ 190.5 (*C*-a), 173.0 (*C*-b), 155.6 (*C*-c), 134.4 (*C*-e), 131.2 (*C*-d), 122.1 ppm (*C*-f). All the data above is identical to the reference protocol.[193]

12-Mer aldehyde core (14)

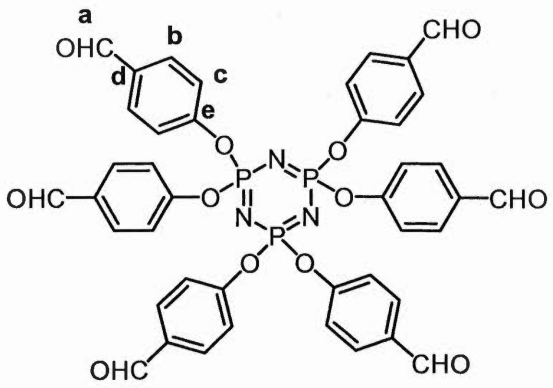

The compounds **14** was prepared according to the literature procedure.[195] Hexachlocyclotriphosphazene, $N_3P_3Cl_6$ (200 mg, 575 mmol, 1 equiv.), 4-Hydroxybenzaldehyde (440mg, 3.60 mmol, 6.2 equiv.) and K_2CO_3 (1000 mg, 7.23 mmol, 12.5 equiv.) were dissolved in THF (6 mL) and stirred for 12 hours. After the solvent was removed in vacuum and the residue was extracted with dichloromethane, DCM (3 x 25 mL) and the separated organic phase was washed with water (2 x 15 mL) and brine (2 x 15 ml) then dried over Na_2SO_4 and evaporated under reduced pressure. The obtained residue was purified through recrystallization with DCM/Hexane or through silica gel column chromatography (EtOAc/Hexane (1:1); R_f : 0.44) to afford compound **14** (442.1 mg, 464 mmol, 81 %) as a white solid. Mp: 92-94 °C. ^{1}H NMR (300 MHz, $CDCl_3$): δ 9.94 (s, 6H, H-a), 7.73 (d, 12H, J = 8.6 Hz, H-b), 7.14 ppm (d, 12H, J = 8.5 Hz, H-c). ^{13}C NMR (300 MHz, $CDCl_3$) δ 190.3 (*C*-a), 154.6 (*C*-e), 134.0 (*C*-b), 131.3 (*C*-d), 121.1 ppm (*C*-c). ^{31}P NMR (300 MHz, $CDCl_3$): δ 7.08 ppm (s). HRMS *m/z*: calcd for $C_{42}H_{30}N_3O_{12}P_3$ + (H^+), 862.1115. Found *m/z*: 862.1105. All the data above is identical to the reference protocol.[195]

Dimethyl 5-hydroxyisophthalate (17)

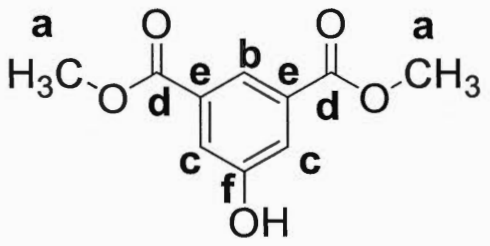

The compounds **17** was prepared according to the literature procedure.[196,203] 5-Hydroxyisophthalic acid (800 mg, 44 mmol, 1 equiv.) was dissolved in MeOH (70 mL) and stirred at room temperature. In the next step mixture was cooled down to 0 °C through ice bath while H_2SO_4 was added slowly and the reaction mixture was stirred up to room temperature. Subsequently the mixture was heated under reflux overnight. Progression of the reaction was followed by TLC. After completion of the reaction, the reaction mixture was cooled down to room temperature and solvent evaporated off. The residue was dissolved in EtOAc (300 mL) and the organic phase was washed with saturated aqueous sodium bicarbonate, $NaHCO_3$ (2 x 200 mL), water (2 x 200 mL), brine (2 x 200 mL) and dried over Na_2SO_4 and finally evaporated under reduced pressure. The obtained residue also was recrystallization in DCM/Hexane to afford compound **17** (8316 mg, 39.5 mmol, 90 %) as a white solid. ^{1}H NMR (300 MHz, $CDCl_3$): δ 8.25 (t, 1H, J = 1.4 Hz, H-b), 7.77 (d, 2H, J = 1.4 Hz, H-c), 3.94 ppm (s, 6H, H-a). ^{13}C NMR (300 MHz, MeOD): δ 167.6 (*C*-d), 159.2 (*C*-f), 133.0 (*C*-e), 122.4 (*C*-b), 121.4 (*C*-c), 52.6 ppm (*C*-a). The data agrees with the reported literature values.[203]

3,5-Bis(hydroxymethyl)phenol (18)

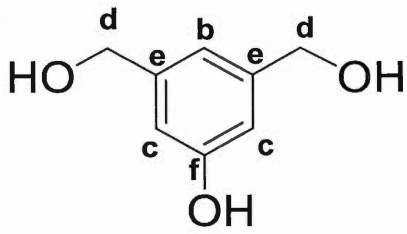

The compounds **18** was prepared according to the literature procedure.[196,203] A solution of dimethyl 5-hydroxyisophthalate **17** (1.50 g, 7.1 mmol, 1 equiv.) in dry THF (25 mL) was added dropwise to a stirred mixture of $LiAlH_4$ (800 mg, 21.3 mmol, 3 equiv.) in dry THF (40 mL). The mixture was heated under reflux for 2 hours and then stirred at room temperature overnight. EtOAc (1.5 mL), EtOH (0.7 mL), and brine (7 mL) were added dropwise to quench the reaction and the resulting suspension was filtered and washed with EtOH (2 x 50 mL). The filtrate was evaporated under vacuum to give compound **18** (1.112 g, 7.2 mmol, 90%) as a pale-grey, hydroscopic glass; (DCM/ MeOH (8.5:1.5); R_f = 0.43). ^{1}H NMR (300 MHz, MeOH): δ 6.83 (s, 1H, H-b), 6.74 (s, 2H, H-c), 4.56 ppm (s, 4H, H-d). ^{13}C NMR (75 MHz, MeOD): δ 158.6 (C-f), 144.3 (C-e), 117.6 (C-b), 113.7 (C-c), 65.1 ppm (C-d). EI-MS, *m/e* (relative intensity): 154 (100). HR EI-MS: calcd for $C_8H_{10}O_3$ (M^+): 154.0630, Found: 154.0632. The data agrees with the reported literature values.[203]

5-Hydroxybenzene-1, 3-dicarbaldehyde (19)

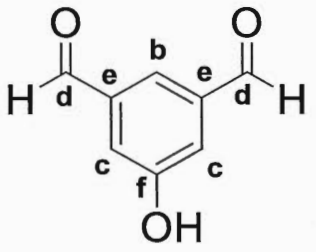

The compound **19** was synthesized according to a modified literature procedure.[196,203] 3,5-Bis(hydroxymethyl)phenol **18** (1.112 g, 7.2 mmol, 1.0 equiv.) was dissolved in dry THF (2 mL) and dry DCM (8 mL) and stirred at room temperature under nitrogen then pyridinium chlorochromate, PCC (3730 mg, 17.3 mmol, 2.4 equiv.) was added to the mixture and stirred at room temperature around 3 hours. TLC was used to monitor the reaction. Upon completion of the reaction, the mixture was diluted with dichloromethane (20 mL) and the mixture was filtered through celite and washed with DCM three times (3 x 15 mL). The organic phase was concentrated under reduced pressure and the main product **(19)** was afforded through silica gel column chromatography using the appropriate eluent system (EtOAc/Hexane (1:1); $R_f = 0.37$) as a rose-white solid (870 mg, 5.79 mmol, 80%). ^{1}H NMR (300 MHz, $CDCl_3$): δ 10.05 (s, 2H, H-d), 7.97 (t, 1H, $J = 1.3$ Hz, H-b), 7.64 (d, 2H, $J = 1.3$ Hz, H-c), 5.67 ppm (s, 1H, H-f (phenol)). FT-IR (cm^{-1}) 3343, 2938, 2832, 1697, 1600, 1456, 1348, 1292, 1193, 1151, 1104, 1053, 863. EI-MS, *m/e* (relative intensity): 150 (100), 121.0 (75). The data agrees with the reported literature values.[203]

12-Mer aldehyde core (20)

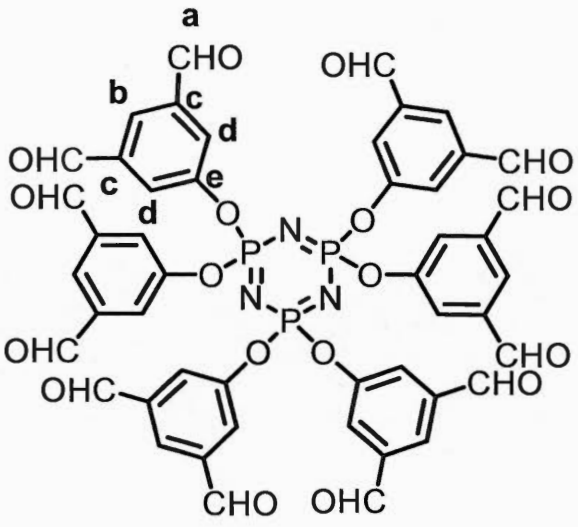

The compounds **20** was prepared according to the literature procedure.[196] 5-Hydroxybenzene-1,3-dicarbaldehyde **19** (130 mg, 0.860 mmol, 12 equiv.), Cesium carbonate (280 mg, 0.860 mmol, 12 equiv.) and hexachlocyclotriphosphazene, (25 mg, 0.072 mmol, 1 equiv.) were dissolved in THF (3 mL) and stirred for 12 hours. TLC was used to monitor the reaction. Upon completion of the reaction, the solvent was removed in vacuum and the residue was dissolved in minimum amount of dichloromethane and the obtained residue was purified through silica gel column chromatography using the appropriate eluent system (EtOAc/Hexane (1:1); R_f = 0.45) to afford compound **20** as a poorly soluble white powder (16 mg, 0.015 mmol, 22 %). HR EI-MS: calcd for $C_{48}H_{30}N_3O_{18}P_3$ (M^+): 1030, Found: 1030. ^{31}P NMR (122 MHz, DMSO, d_6): δ 7.91 ppm (s). ^1H NMR (300 MHz, DMSO, d_6): δ 10.00 (s, 12H, H-a), 8.31 (s, 6H, H-b), 7.89 ppm (s, 12H, H-d). The data agrees with the reported literature values.[196]

***O*-(2,3,4,6-tetra-*O*-acetyl-β-D-galactopyranosyl)-*N*-Hydroxyphthalimide (7)**

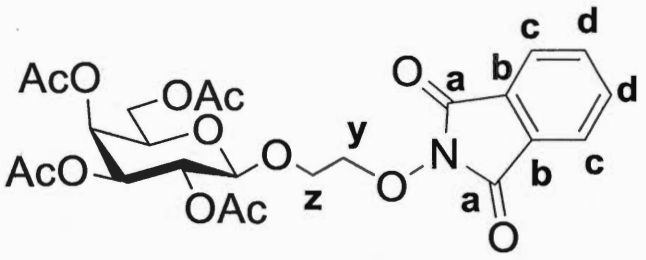

The compounds **7** was prepared according to the literature procedure. 2-Bromoethyl-2,3,4,6-tetra-*O*-acetyl-β-D-galactopyranoside **(5)** (2.00 g, 4.39 mmol, 1.0 equiv.) dissolved in 18 mL DMF, was added to the mixture of N-hydroxyphthalimide **6** (932 mg, 5.71 mmol, 1.3 equiv.) and Et_3N (0.79 mL, 5.71 mmol, 1.3 equiv.) in DMF (2mL) at 80 °C for overnight. Progression of the reaction was followed by TLC. Upon completion of the reaction, the reaction mixture was diluted with EtOAc and the organic phase washed with HCl 0.1M respectively with sodium bicarbonate, water and brine. The extract was dried over Na_2SO_4, filtered and evaporated under reduced pressure. Reaction mixture was purified through silica gel column chromatography using the appropriate eluent system (EtOAc/Hexane (1:1); R_f = 0.19) to afford compound **7** as a pale beige to white solid (1790 mg, 3.33mmol, 76 %); ^{1}H NMR (300 MHz, $CDCl_3$): δ 7.89 – 7.80 (m, 2H, H-c), 7.79 – 7.72 (m, 2H, H-d), 5.39 (dd, 1H, *J* = 3.4, 1.0 Hz, H-4), 5.20 (dd, 1H, *J* = 10.5, 7.9 Hz, H-2), 5.05 (dd, 1H, *J* = 10.4, 3.4 Hz, H-3), 4.73 (d,1H, *J* = 7.9 Hz, H-1), 4.45 – 4.29 (m, 2H, H-6,6'), 4.21 – 4.10 (m, 2H, H-z', H-5), 4.09 – 3.99 (m, 2H, H-z, H-y), 3.95 (td, 1H, *J* = 6.7, 1.0 Hz, H-y), 2.14, 2.10, 2.05, 1.98 ppm (4 x s, 12H, 4x $COCH_3$). ^{13}C NMR (75 MHz, $CDCl_3$): δ 170.3, 170.2, 170.0, 169.7 (4 x $COCH_3$), 163.4 (*C*-a), 134.5 (*C*-b), 128.8 (*C*-d), 123.5 (*C*-c), 101.2 (*C*-1), 77.5 (*C*-6), 70.9 (*C*-3), 70.6 (*C*-z), 68.5 (*C*-2), 67.0 (*C*-4), 66.9 (*C*-5), 61.2 (*C*-y), 20.7, 20.6, 20.6, 20.5 ppm (4 x $COCH_3$). The data agrees with the reported literature values.

_N_- Propargyloxyphthalimide, (Allyloxyamine) (35)

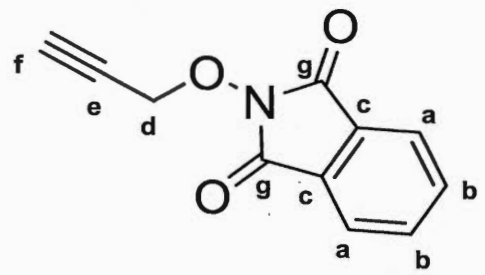

The compounds **35** was prepared according to the literature procedure.[198] DBU (1.27 mL, 13.21 mmol, 1.1 equiv.) was added in one portion to a cooled solution (5-10 °C) of *N*-hydroxyphthalimide **6** (2.00 g, 12.26 mmol, 1.0 equiv.) stirring in DMF (15 mL). After 10 min, Propargyl bromide **25** (1.175 mL, 1.32 mmol, 1.1 equiv.) was added dropwise in cooled temperature and then reaction mixture was stirred at room temperature around two hours, until the color turned from dark burgundy to yellow. Ethyl acetate and water were added respectively to the mixture of reaction and the aqueous phase separated. The combined organic phase was washed respectively with water, satd. $NaHCO_3$ until the aqueous phase was pale yellow, brine and dried over anhydr. Na_2SO_4. The solvent was evaporated to afford *N*- propargyloxyphthalimide **35** (1320 mg, 55%) as a white solid; (EtOAc/Hexane (1:1); R_f= 0.19). Mp 58 to 62 °C. ^{1}H NMR (300 MHz, $CDCl_3$): δ 7.89 – 7.82 (m, 2H, H-a), 7.80 – 7.73 (m, 2H, H-b), 4.87 (d, 2H, J = 2.4 Hz, H-d), 2.59 ppm (t, 1H, J = 2.4 Hz, H-f). ^{13}C NMR (75 MHz, $CDCl_3$): δ 163.2 (*C*-g), 134.5 (*C*-c), 128.7 (*C*-b), 123.6 (*C*-a), 78.0 (*C*-e), 76.3 (*C*-f), 64.9 ppm (*C*-d). The data agrees with the reported literature values.[198]

Azidoethoxy-2-(2,3,4,6-tetra-O-acetyl-*D*-galactopyranosyloxy) phthalimide (36)

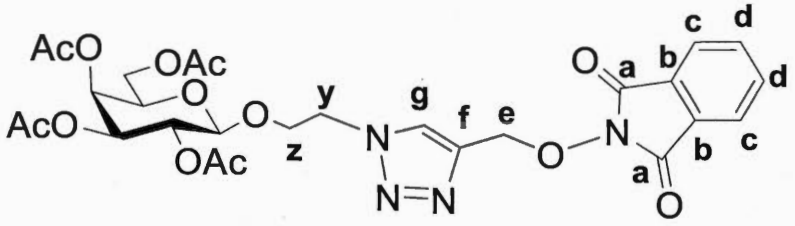

The compound **36** was synthesized according to a modified literature procedure.[199,200] A solution of 2-azidoethyl-2,3,4,6-tetra-*O*-acetyl-β-D-galactopyranoside **22** (200 mg, 0.48 mmol, 1.0 equiv.) and *N*-propargyloxyphthalimide **35** (145 mg, 0.72 mmol, 1.5 equiv.) were dissolved in minimum amount of THF (3mL), then were treated with an aqueous solution of $CuSO_4.5H_2O$, (24 mg, 0.0096 mmol, 0.02 equiv.) and sodium ascorbate (28 mg, 0.0144 mmol, 0.03 equiv.) in 1 mL of H_2O. Biphasic mixture was stirred at 50 °C for 1hour and then at room temperature overnight. The completion of the reaction judged by the complete conversion of the limiting reagent. After completion of the reaction, EtOAc was added to the mixture (12 mL) and the mixture was stirred for 30 minutes then was dried over Na_2SO_4, filtered and evaporated under reduced pressure. The main product **36** was afforded through silica gel column chromatography using the appropriate eluent system (EtOAc/ Hexen (3:2); $R_f = 0.25$) as a white solid (253 mg, 0.409 mmol, 85%) with; ^{1}H NMR (300 MHz, $CDCl_3$): δ 7.92 (s, 1H, H-g), 7.82 – 7.76 (m, 2H, H-c), 7.76 – 7.70 (m, 2H, H-d), 5.40 (dd, 1H, J = 3.5, 0.9 Hz, H-4), 5.35 (d, 2H, J = 1.4 Hz, H-e), 5.22 (dd, 1H, J = 10.5, 7.9 Hz, H-2), 5.00 (dd, 1H, J = 10.5, 3.4 Hz, H-3), 4.71 – 4.61 (m, 1H, H-6), 4.61 – 4.49 (m, 1H, H-6'), 4.47 (d, 1H, J = 7.9 Hz, H-1), 4.30 – 4.22 (m, 1H, H-z'), 4.22 – 4.08 (m, 2H, H-z & H-5), 3.91 (ddd, 2H, J = 13.9, 8.5, 2.2 Hz, H-y), 2.17, 2.05, 2.00, 1.98 ppm (4 x s, 12H, 4x $COCH_3$). ^{13}C NMR (75 MHz, $CDCl_3$): δ 170.3, 170.1, 170.0, 169.5 (4 x $COCH_3$) ,

163.3 (*C*O, C-a,), 141.3 (*C*-f), 134.33 (*C*-d), 128.7 (*C*-b), 125.8 (*C*-g), 123.4 (*C*-c), 100.8 (*C*-1), 70.8 (*C*-y), 70.5 (*C*-3), 70.1 (*C*-e), 68.4 (*C*-2), 67.43 (*C*-z), 66.8 (*C*-4), 61.1 (*C*-5), 50.1 (*C*-6), 20.6, 20.5, 20.5, 20.4 ppm (4 x CO*C*H$_3$). The data agrees with the reported literature values.[200]

4-Azidoethoxy-*O*-β-D-galactopyranosyloxy)-*tert*-butyl-(4-methyloxy)carbamate (47)

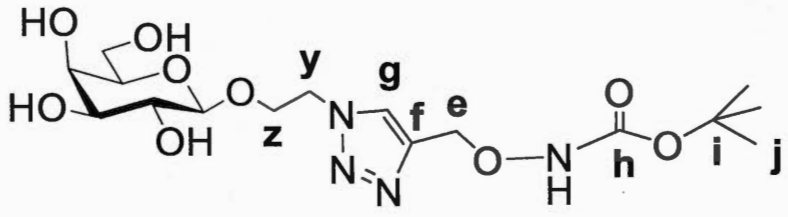

To a solution of 4-azidoethoxy-2-(2,3,4,6-tetra-*O*-acetyl-β-D-galactopyranosyloxy) *tert*-butyl(4-methyloxy)carbamate **27** (50 mg, 0.085 mmol, 1.0 equiv.) in MeOH (3mL), was added K_2CO_3 as catalytic amount, (5 mg, 0.036 mmol, 0.40 equiv.). The mixture was then stirred at room temperature overnight. The completion of the reaction judged by the complete deacetylation of the compound **27**. After completion of the reaction, the mixture filtered and evaporated under reduced pressure. The main product **(47)** was afforded as a white solid solvable in methanol (33 mg, 0.078 mmol, 92%) with (DCM/ MeOH (3:2); R_f = 0.3). ^{1}H NMR (300 MHz, MeOD): δ 8.12 (s, 1H), 4.76 (s, 2H), 4.66 (s, 2H), 4.25 (d, 2H, *J* = 11.8 Hz), 4.13 – 3.95 (m, 1H), 3.90 (s, 1H), 3.74 (d, 2H, *J* = 5.2 Hz), 3.50 (d, 3H, *J* = 7.0 Hz), 1.35 ppm (d, 9H, *J* = 12.5 Hz).

Diethyleneglycol-bis(p-toluenesulfonate) (44) (protocol 1)

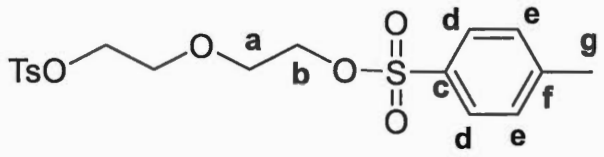

Diethylene glycol **43** (1.00 g, 9.42 mmol, 1.0 equiv.) in THF (10 mL) was treated by Et_3N (2.89 mL, 20.68 mmol, 2.2 equiv.) under nitrogen at room temperature and the 0.1M solution of TsCl in THF (3950 mg, 20.70 mmol, 2.2 equiv. dissolved in 207 mL THF) was added to the main solution and stirred under nitrogen overnight. Then the solvent was evaporated, and the residue dissolved in EtOAc. The organic phase was washed with water, dried over Na_2SO_4, filtered and evaporated. The main product **44** was afforded through silica gel column chromatography using the appropriate eluent system (Hexene/EtOAc (7:3); R_f = 0.25) as a white solid (3.00 g, 7.23 mmol, 77%). ^1H NMR (300 MHz, $CDCl_3$): δ 7.78 (d, 4H, J = 8.4 Hz, H-d), 7.35 (d, 4H, J = 8.0 Hz, H-e), 4.12 – 4.06 (m, 4H, H-b), 3.64 – 3.58 (m, 4H, H-a), 2.45 ppm (s, 6H, H-g).

Diethylene glycol bis (p-toluenesulfonate) (44) (protocol 2)

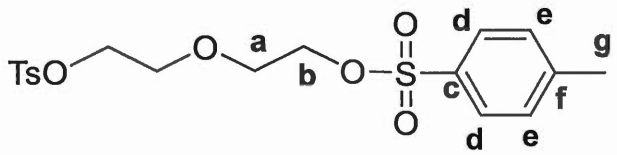

The compounds **44** was prepared according to the literature procedure.[204] Diethylene glycol **43** (2000 mg, 16.96 mmol, 1.0 equiv.) and TsCl (7.20 g, 37.77 mmol, 2.0 equiv.) dissolved in DCM (18 mL) were treated by KOH 85% (8440 mg, 150.42 mmol, 8.0 equiv.) portion wise under nitrogen at 0 °C. The reaction mixture was stirred at 0 °C for 3 hours and after completion of reaction water added to the mixture and the organic phase was extracted by DCM and dried over Na_2SO_4, filtered and in the next step the solvent was evaporated. The residue dissolved in minimum amount of MeOH and was kept in the fridge overnight, filtered and washed with cold MeOH to afford desired product (Hexene/EtOAc (7:3); R_f = 0.25) as a pure white crystal **44** (6.372 mg, 15.37 mmol, 91%). ^{1}H NMR (300 MHz, $CDCl_3$): δ 7.82- 7.75 (m, 4H, H-d), 7.35 (d, 4H, J = 8.0 Hz, H-e), 4.11 – 4.07 (m, 4H, H-b), 3.64 – 3.58 (m, 4H, H-a), 2.45 ppm (s, 6H, H-g). ^{13}C NMR (75 MHz, $CDCl_3$): δ 145.3 (*C*-c), 133.1 (*C*-f), 130.2 (*C*-e), 128.2 (*C*-d), 69.3 (*C*-a), 69.0 (*C*-b), 21.9 ppm (*C*-g). The data agrees with the reported literature values.[204]

Tripropargyl-pentaerythritol (39)

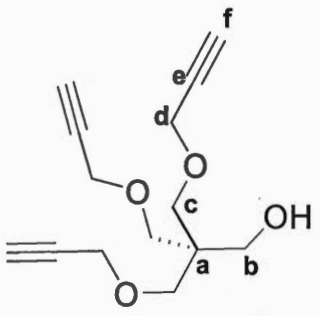

The compounds **39** was prepared according to the literature procedure.[205] Pentaerythritol **38** (2.00 g, 14.69 mmol, 1.0 equiv.) was dissolved in DMSO (15 mL), and a solution of NaOH 40% (4000 mg in 10 mL water) (10 mL) was added to it. After 30 minutes stirring at room temperature, a solution of propargyl bromide **25** (9.6 mL, 107.31 mmol, 7.3 equiv.) in toluene (80%) was added drop wise to the reaction mixture. The reaction was left stirring at room temperature overnight. Once the reaction was completed, water was added to the mixture, and extracted with diethyl ether. The organic layer was isolated, combined, washed with water, brine and dried over Na_2SO_4, then filtered and evaporated. The main product **39** was afforded through silica gel column chromatography using the appropriate eluent system (Hexene/EtOAc (3:2); $R_f = 0.43$) as a yellow oil (2.20 g, 8.78 mmol, 59%). ^{1}H NMR (300 MHz, $CDCl_3$): δ 4.11 (d, 6H, $J = 2.4$ Hz, H-d), 3.67 (s, 2H, H-b), 3.54 (s, 6H, H-c), 2.42 ppm (t, $J = 2.4$ Hz, 3H, H-f). ^{13}C NMR (75MHz, CDCl3) δ = 44.6, 58.7, 65.0, 70.1, 74.5, 79.6 ppm. The data agrees with the reported literature values.[205]

3-{2-[2-(2-Chloroethoxy)ethoxymethyl]-3-prop-2-ynyloxy-2-prop-2-ynyloxymethylpropoxy}-propyne (41)

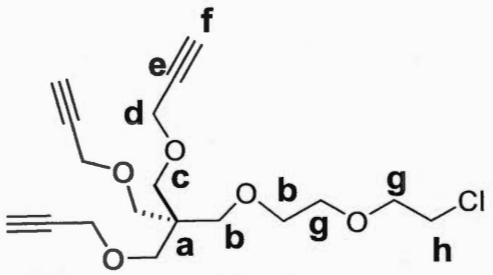

The compounds **44** was prepared according to the literature procedure.[205] To a solution of tripropargyl-pentaerythritol **39** (2.00 g, 8.00 mmol, 1equiv.) and Bu_4NHSO_4 (5.432 g, 16 mmol, 2 equiv.) in 2-chloroethyl ether **40** (6 mL, 50 mmol, 6 equiv.) was added aqueous NaOH (50%, 10 mL). The two-phase reaction mixture was vigorously stirred at room temperature for 48 hours. DCM and water were added to the mixture and the organic phase separated and successively washed with water, dried over Na_2SO_4 and evaporated. The desired compound **41** was afforded through the purification by column chromatography using the appropriate eluent system (Hexene/EtOAc (7:3); $R_f = 0.5$) as a colorless oil (2500 mg, 7.00 mmol, 85%). ^{1}H NMR (300 MHz, $CDCl_3$): δ 4.11 (d, 6H, J = 2.4 Hz, H-d), 3.77 (dd, 2H, J = 8.8, 3.2 Hz, H-h), 3.66 – 3.58 (m, 6H, H-g), 3.52 (s, 6H, H-c), 3.46 (s, 2H, H-b), 2.41 ppm (dt, 3H, J = 9.3, 2.3 Hz, H-f). ^{13}C NMR (75 MHz, $CDCl_3$): δ 80.4 (*C*-e), 74.4 (*C*-f), 71.7 (*C*-b), 71.4 (*C*-b), 70.8 (*C*-g), 70.2 (*C*-g), 69.4 (*C*-c), 59.0 (*C*-d), 45.3 (*C*-h), 43.2 ppm (*C*-a). The data agrees with the reported literature values.[205]

3-Mer glycocluster (31)

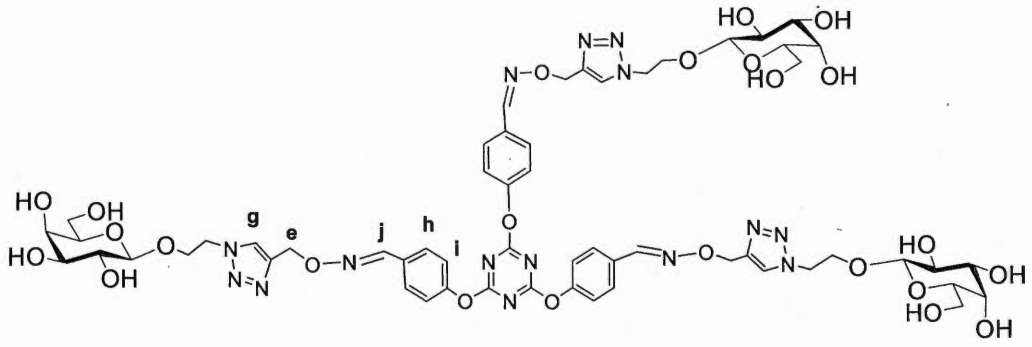

A solution of 2-azidoethyl-β-D-galactopyranoside carbamate **(27)** (100 mg, 0.170 mmol, 1.0 equiv.) in methanol (4 mL), was treated drop wise with acetyl chloride, AcCl 98% (400 µL, 5.61 mmol, 33.0 equiv.) in 0 °C for 7h. After completion of the reaction include Boc and acetyl deprotection 9, the solvent was removed under reduced pressure. The dissolved residue in MeOH/H_2O (4:1,v/v) was treated with tri-(4-formacylphenoxy)-1,3,3-triazine **11** (16.5 mg, 0.037 mmol, 0.22 equiv.) for overnight at room temperature. Subsequently the solvent was removed under reduced pressure and the product **31** with both *Z*/*E*-isomer obtained as a white solid after semi-preparative high-performance liquid chromatography (HPLC) by choosing appropriate eluent system (H_2O/ACN (8:2); R_f = 0.54) . HPLC purification was useful to separate the monomer from few partially substituted derivatives, we could not achieve 100% purified compound through this method. The ^1H NMR of the resulting fraction is shown in annex. The mass spectral analysis clearly established the nature of the compound **31** (ESI-MS-TOF: *m/z* calcd. For $C_{57}H_{69}N_{15}O_{24}$: 1347.46 found: 1348.8 [M+ H^+] and 1370.8 [M+ Na^+] as shown in annex.

6-Mer glycocluster (33)

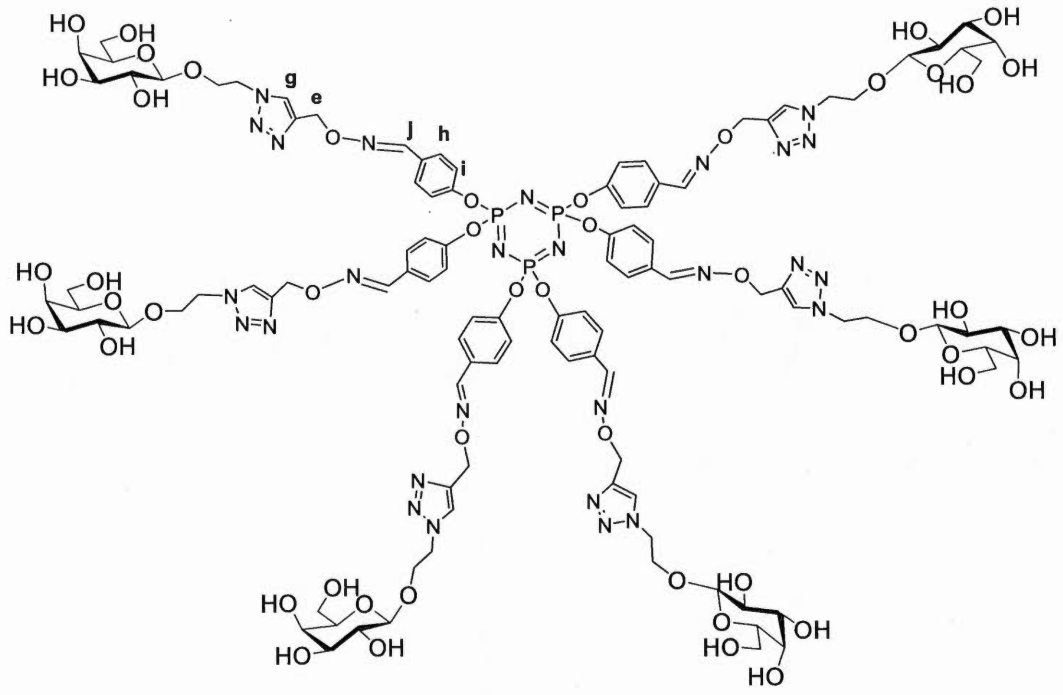

A solution of 2-azidoethyl -β-D-galactopyranoside carbamate **27** (200 mg, 0.34 mmol, 1.0 equiv.) in methanol (8 mL), was treated drop wise with acetyl chloride, AcCl 98% (800 µL, 11.22 mmol, 33.0 equiv.) in 0 °C for 7h. After completion of the reaction include BOC and acetyl deprotection **9,** the solvent was removed under reduced pressure. The dissolved residue in (MeOH/H_2O (6:2)) was treated with 6-Mer aldehyde core **14** (24.30 mg, 0.028 mmol, 0.083 equiv.) for overnight at room temperature. Subsequently the solvent was removed under reduced pressure and the main product **33** was afforded as a white solid after semi-preparative high-performance liquid chromatography (HPLC) by choosing appropriate eluent system (H_2O/ACN (60:40)). The mass spectral analysis clearly established the nature of the compound **33** (ESI-

MS-TOF: *m/z* calcd. For $C_{108}H_{138}N_{27}O_{48}P_3$: 2673.84 found: 2699.523 [M+ D^++ Na^+] as shown in **Figure 3.20**.

CONCLUSION

According to the all information discussed above, it is concluded that infections by pathogenic agents are frequently triggered by their adhesion on host surfaces. The early step in adhesion strategy involves initial recognition of host cell glycoconjugates by sugar-binding proteins (lectins) on, or released by the viruses or the bacteria that are specific for the targeted tissues. *Pseudomonas aeruginosa* is an opportunistic pathogen implicated in the development of lung infections in cystic fibrosis (CF) patients through these sugar–protein complementary interactions. *P. aeruginosa*'s mechanism of action is governed by the adhesion of their virulence lectins (PA-IL and PA-IIL) that bind to galactoside and fucoside subunits of glycoconjugates, respectively. Our project was to design potent anti-adhesion inhibitors against the galactoside-dependent PA-IL. To enhance the binding affinities of galactoside residues, nanometer size glycodendrimers have been designed and carried out.

Therefore, the synthesis of two multivalent glycoclusters in zero generation with 3 and 6 galactoside moieties was achieved by efficient and versatile "click chemistry" involving oxime ligation between aminooxylated galactosides and two suitably prepared poly-aldehyde scaffolds. The necessary aminooxylated galactopyranoside has been synthesized from the known 2-azidoethyl-β-D-galactopyranoside by condensing with a suitably *O*-propargylated hydroxylamino derivative.

Oxime ligation is an efficient reaction which offers several advantages such as mild reaction condition, short reaction time and reagent free coupling. It ensures the excellent reproducibility, yield and purity. The resulted compounds prepared through this strategy can be employed as anti-adhesive agents in biological phenomena.

The condensation of oxyamines with carbonyl functional groups leads to the formation of oxime compounds. Oximes are more stable compared to imines and these are more widely utilized in biological applications due to their stability in aqueous media.

ANNEXE A

SPECTRA OF SYNTHESIZED COMPOUNDS

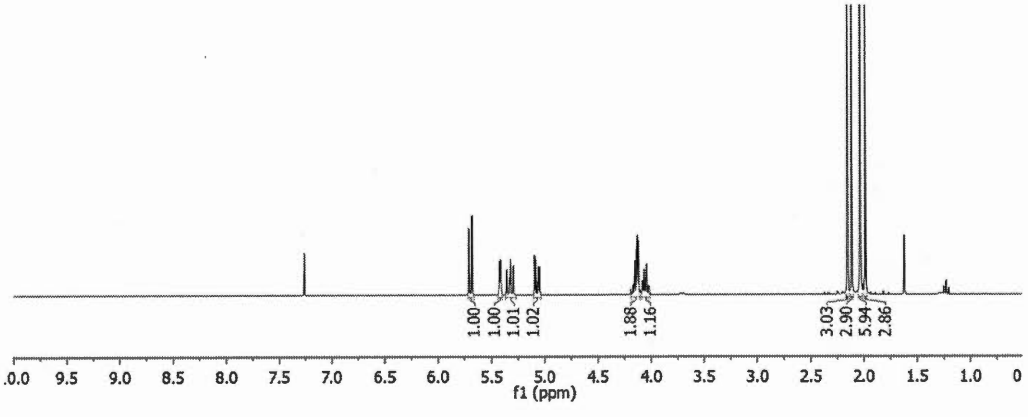

^{1}H NMR spectrum (300 MHz, $CDCl_3$) of compound **2**

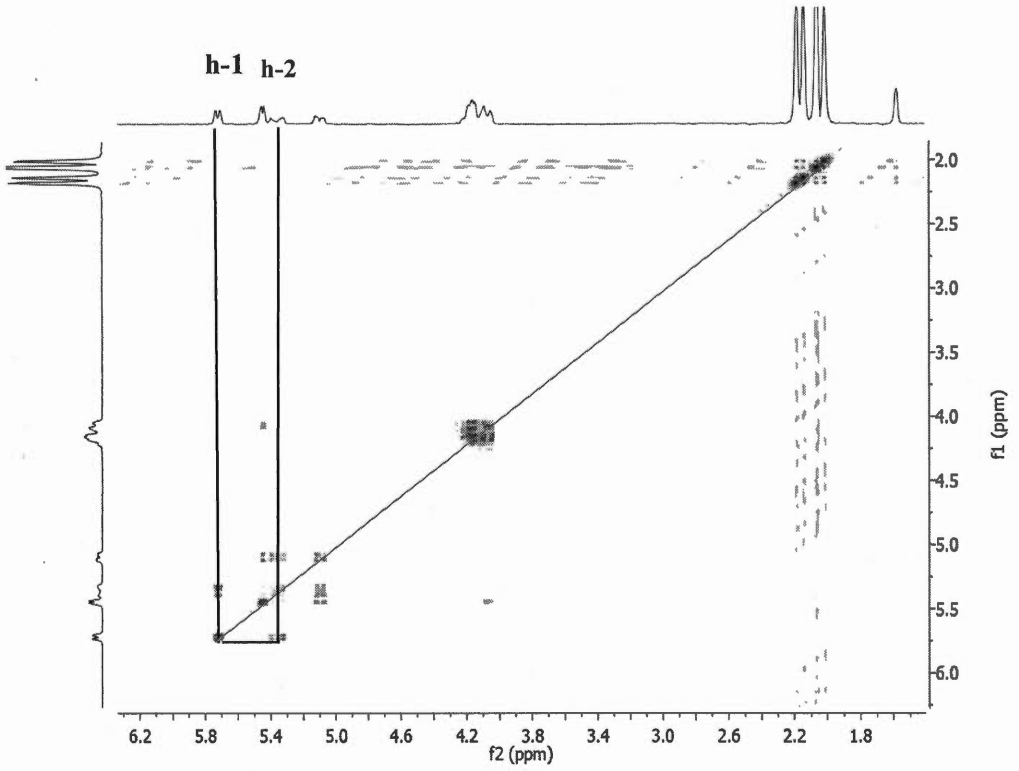

COSY NMR spectrum (300 MHz, $CDCl_3$) of compound **2**

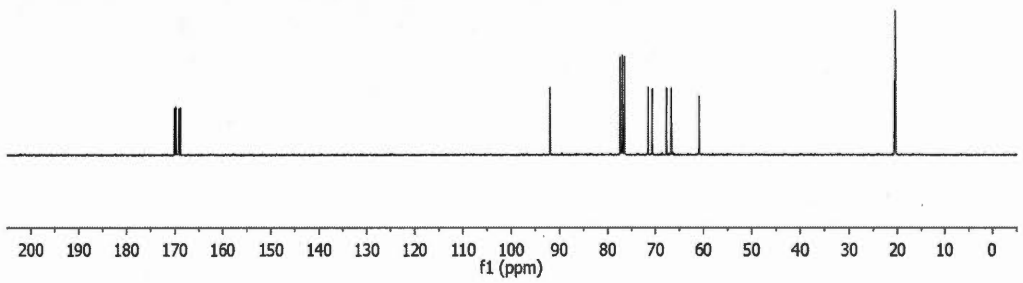

^{13}C NMR spectrum (300 MHz, $CDCl_3$) of compound **2**

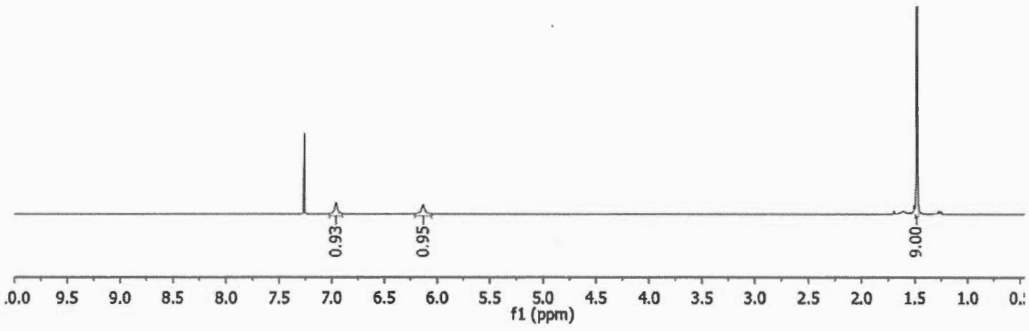

^{1}H NMR spectrum (300 MHz, $CDCl_3$) of compound **24**

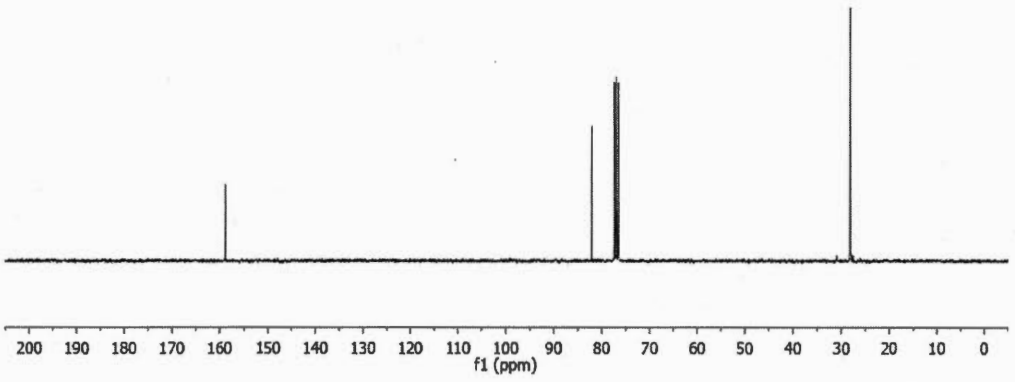

^{13}C NMR spectrum (300 MHz, $CDCl_3$) of compound **24**

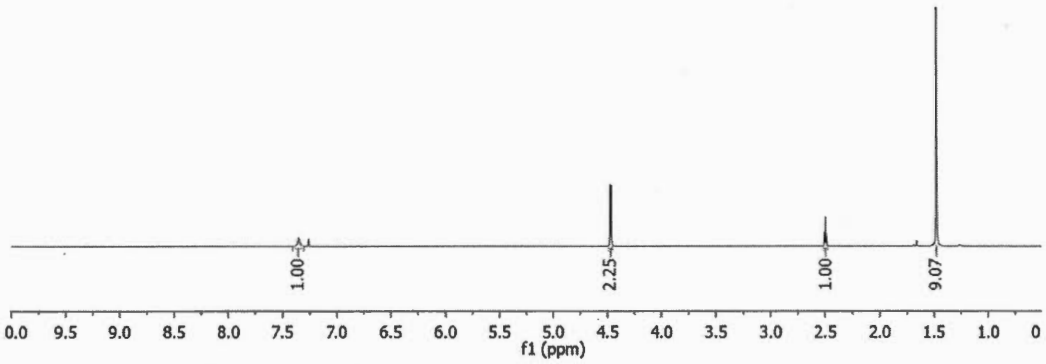

^{1}H NMR spectrum (300 MHz, $CDCl_3$) of compound **26**

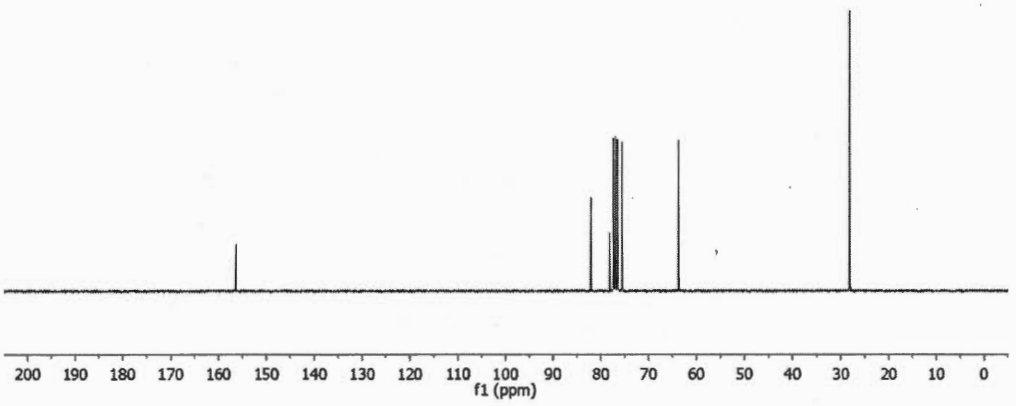

^{13}C NMR spectrum (300 MHz, $CDCl_3$) of compound **26**

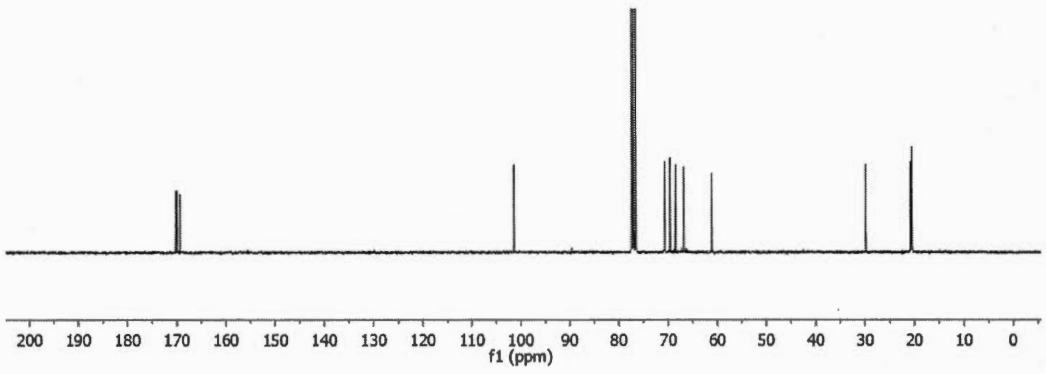

^{13}C NMR spectrum (300 MHz, $CDCl_3$) of compound **5**

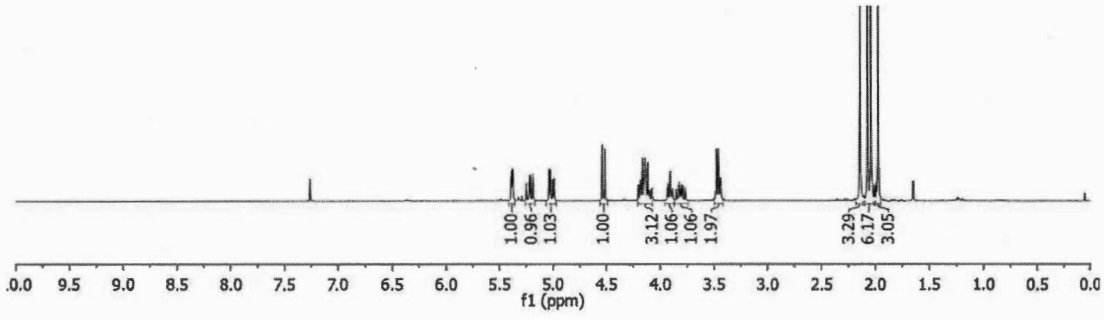

^{1}H NMR spectrum (300 MHz, $CDCl_3$) of compound **5**

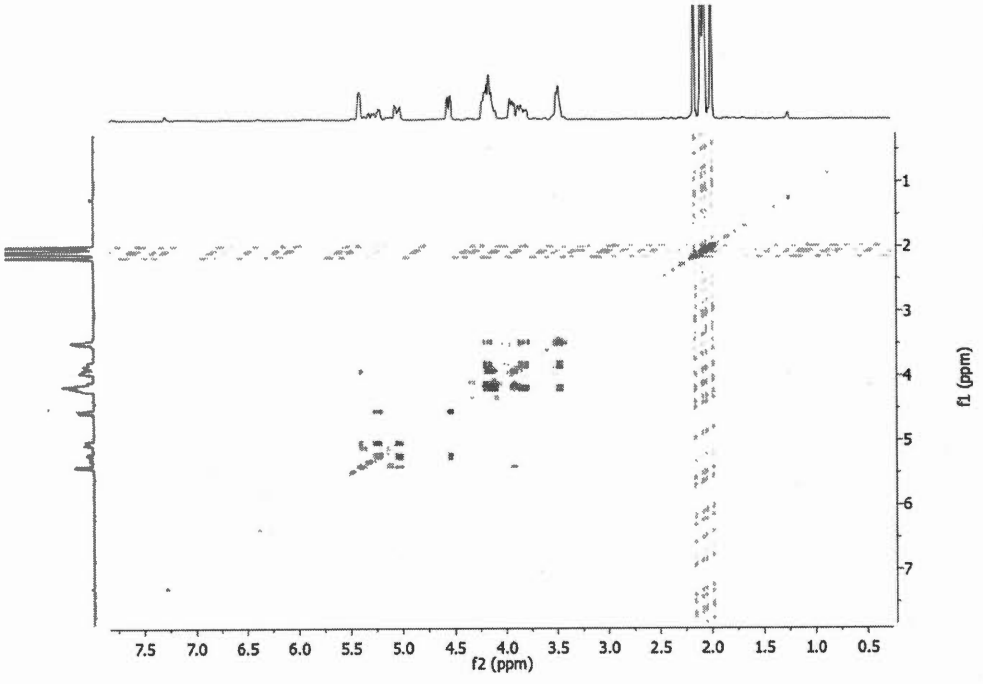

COSY NMR spectrum (300 MHz, $CDCl_3$) of compound **5**

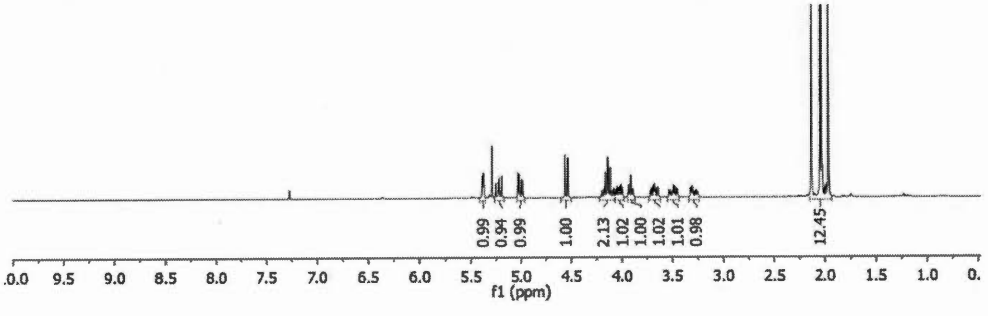

^1H NMR spectrum (300 MHz, $CDCl_3$) of compound **22**

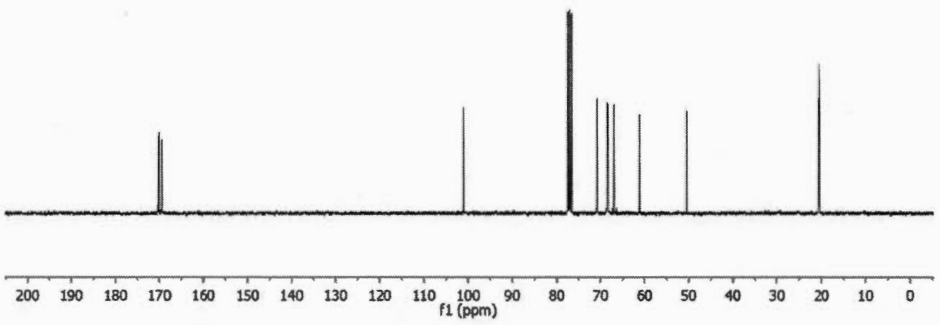

^{13}C NMR spectrum (300 MHz, $CDCl_3$) of compound **22**

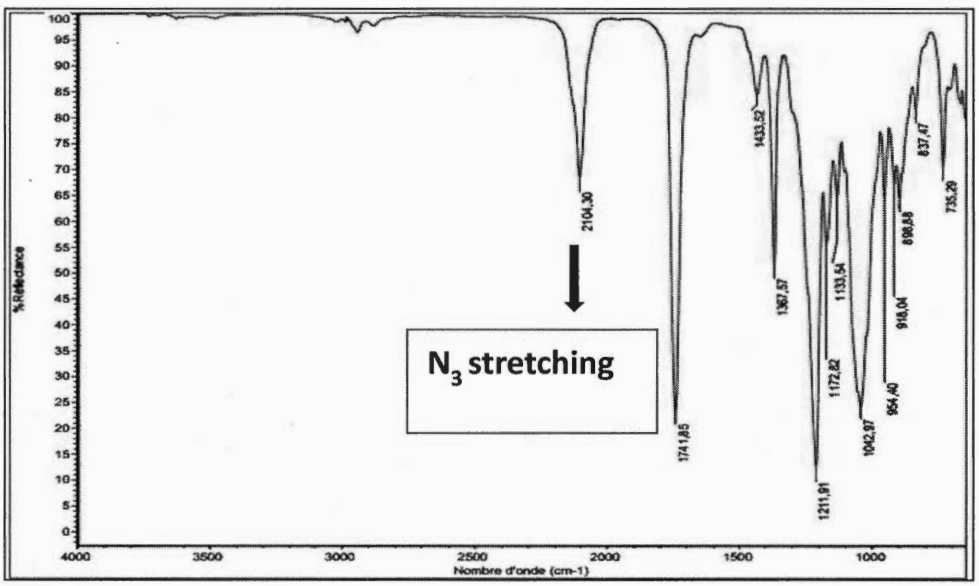

FT-IR spectrum of compound **22**

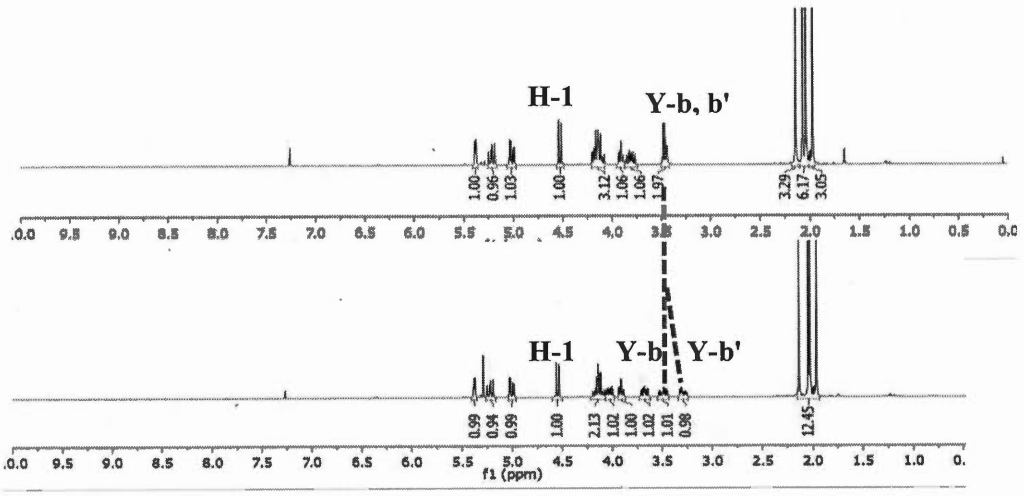

Chemical shift exchange of ^{1}H NMR spectrum (300 MHz, $CDCl_3$) between compound **5** & **22**

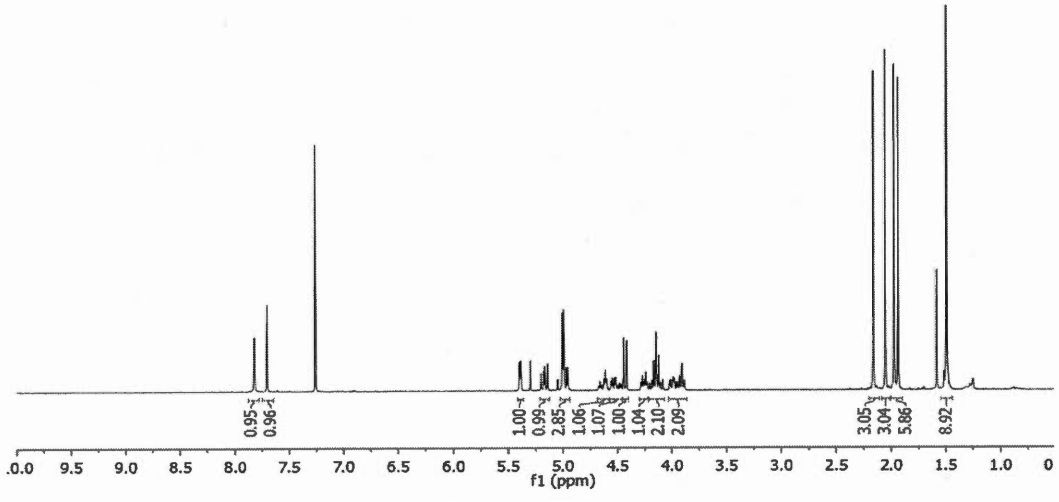

^{1}H NMR spectrum (300 MHz, $CDCl_3$) of compound **27**

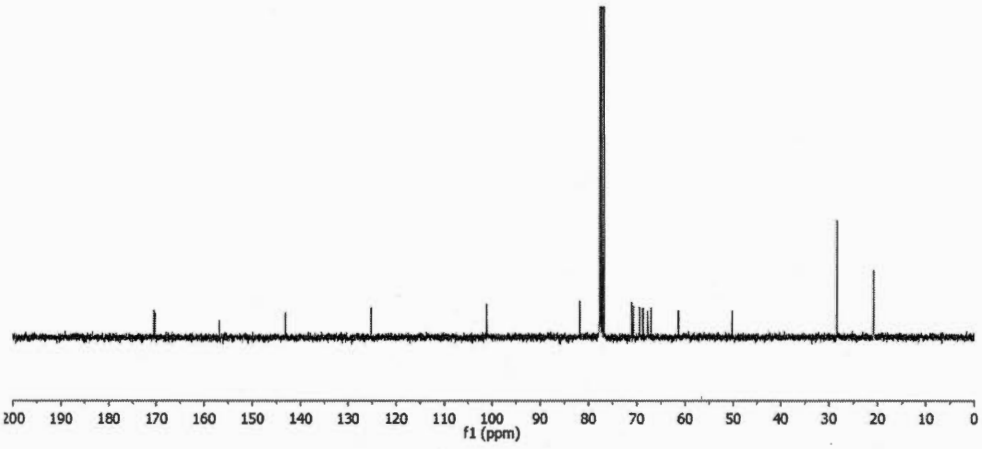

^{13}C NMR spectrum (300 MHz, $CDCl_3$) of compound **27**

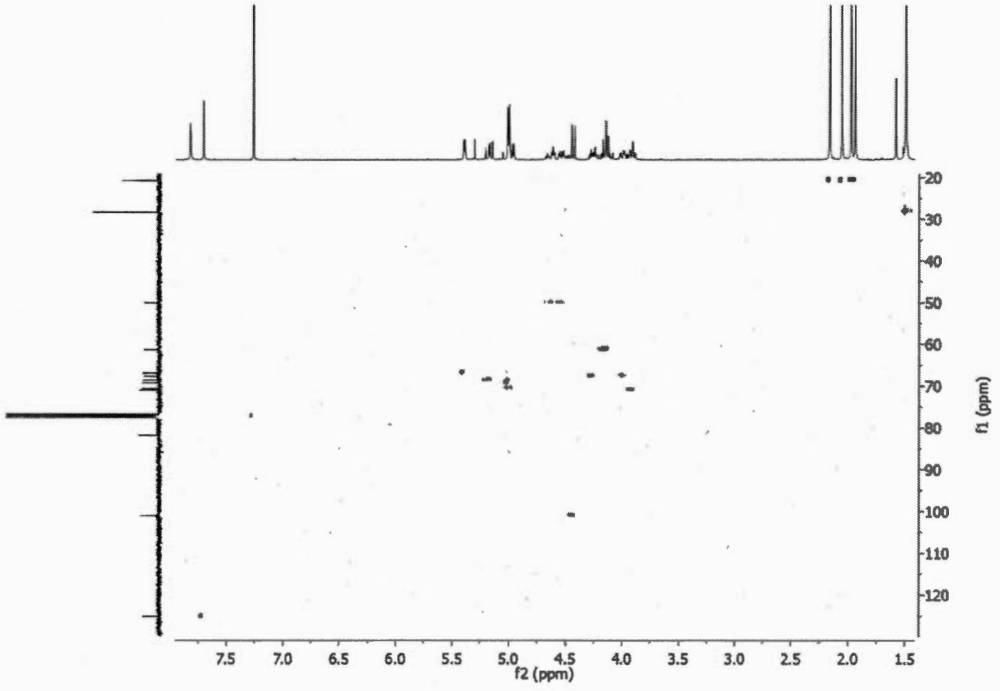

HSQC spectrum (300 MHz, $CDCl_3$) of compound **27**

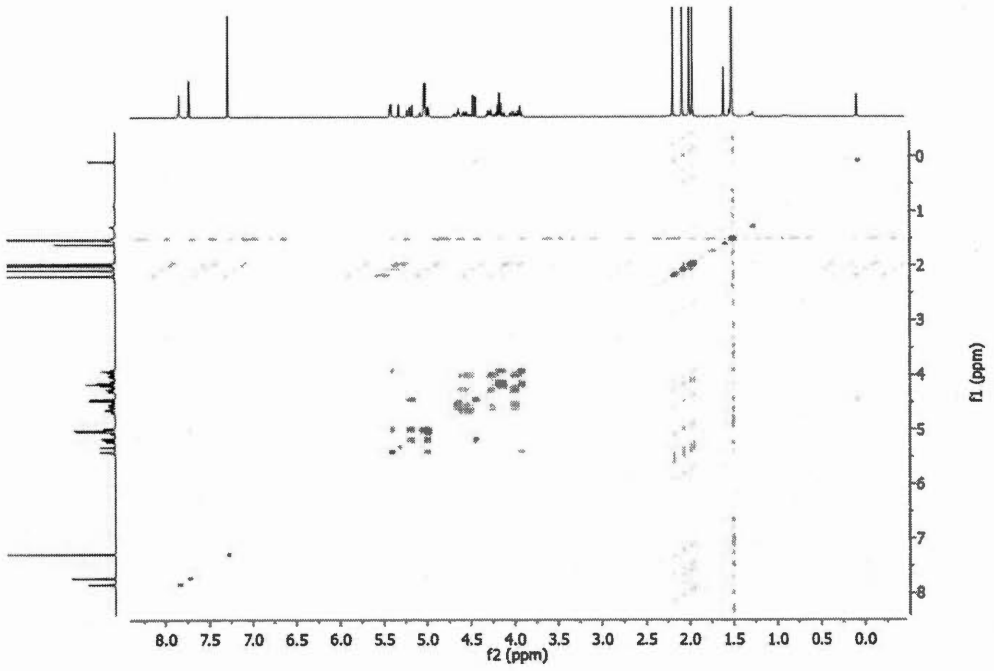

COSY spectrum (300 MHz, $CDCl_3$) of compound **27**

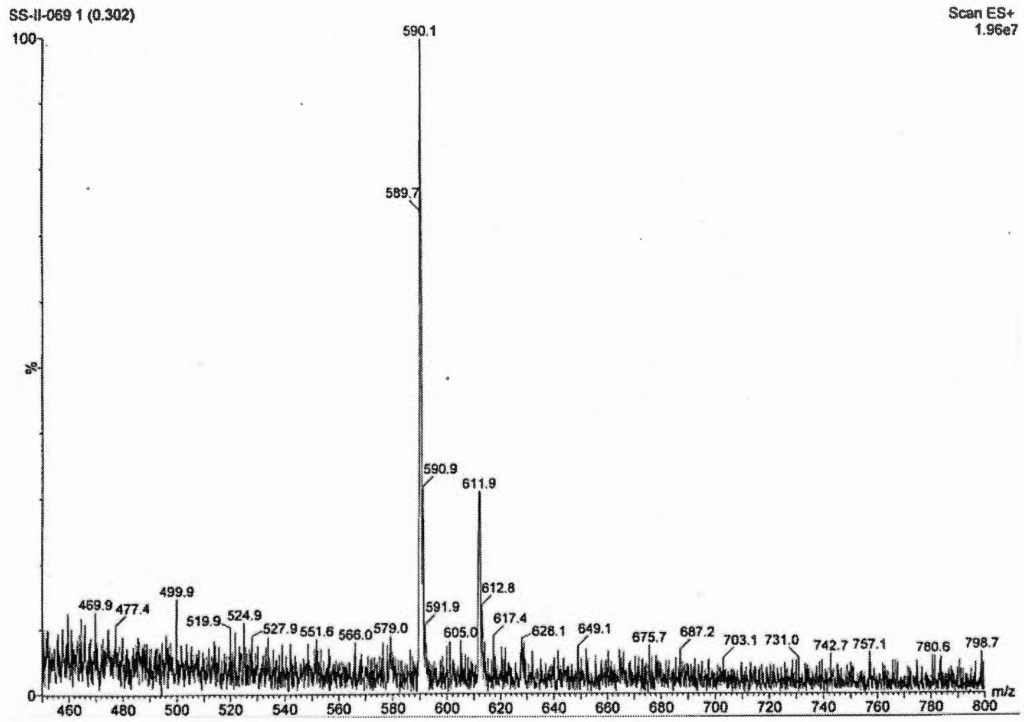

ESI$^+$-MS spectrum of compound **27**

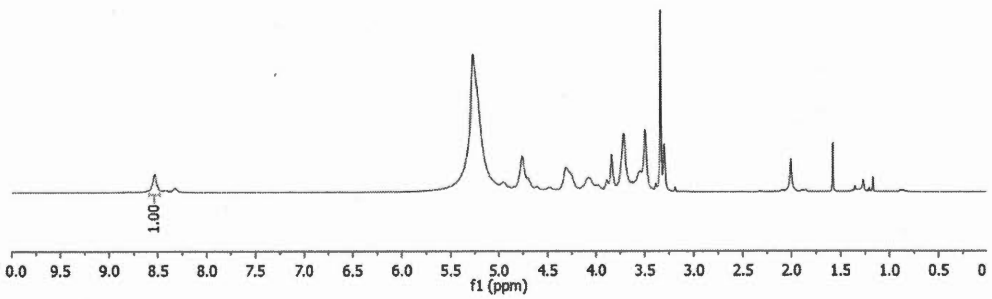

^{1}H NMR spectrum (300 MHz, $CDCl_3$) of compound **28**

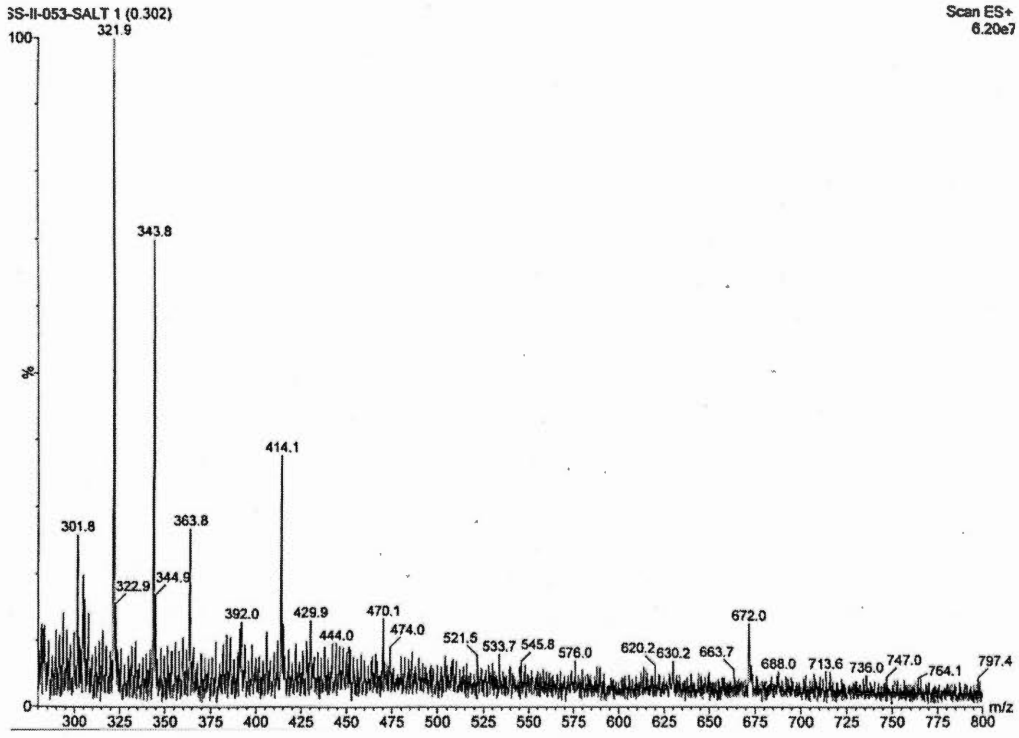

ESI^{+}-MS spectrum of compound **28**

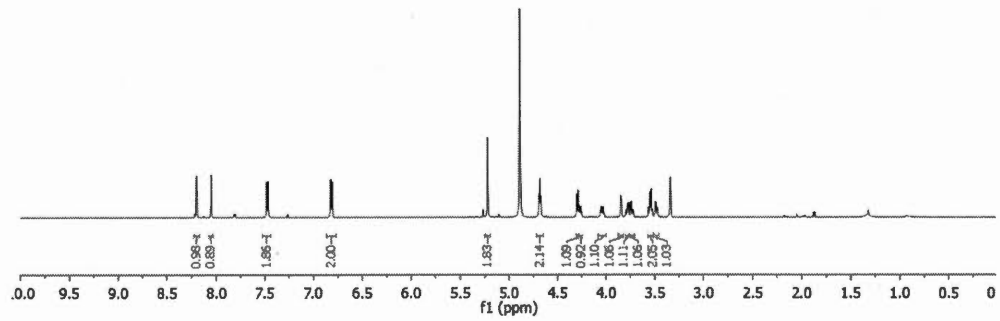

^{1}H NMR spectrum (600 MHz, MeOD) of compound **30**

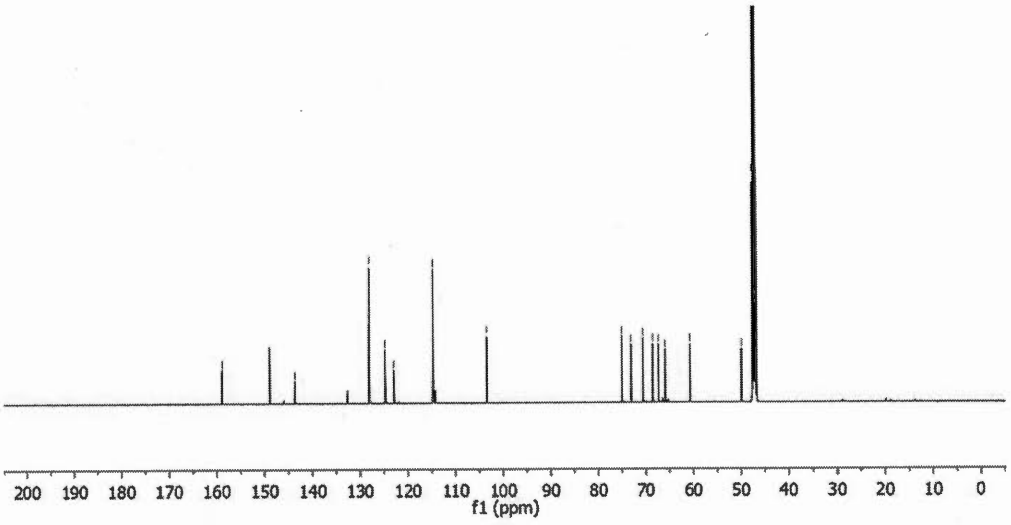

^{13}C NMR spectrum (600 MHz, MeOD) of compound **30**

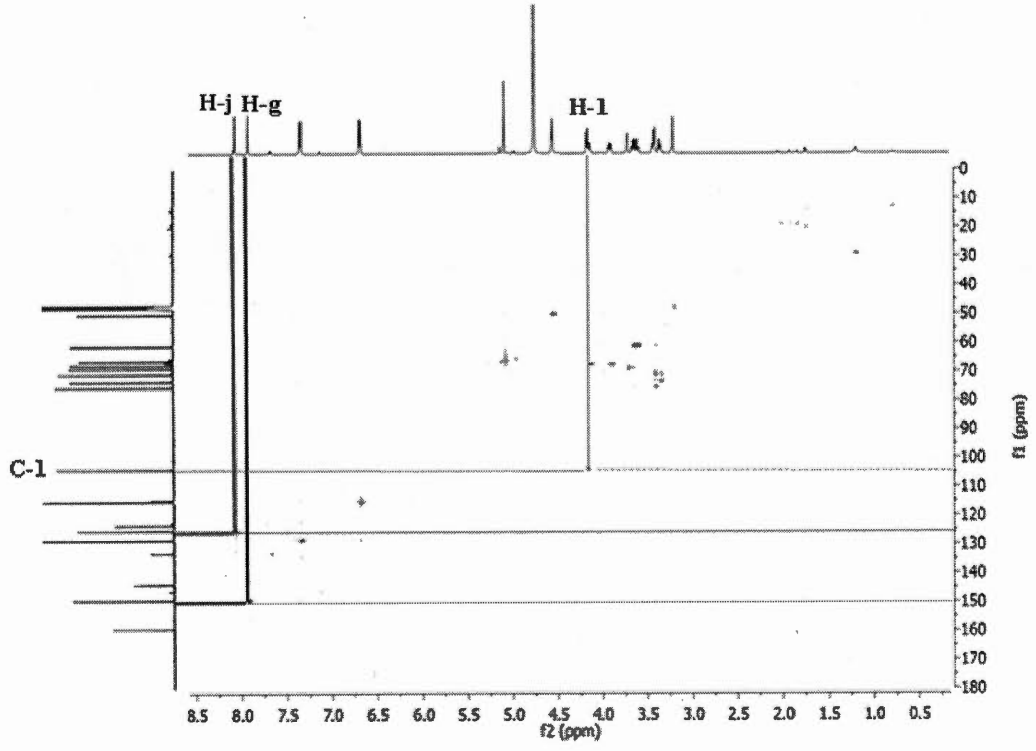

COSY spectrum (600 MHz, MeOD) of compound **30**

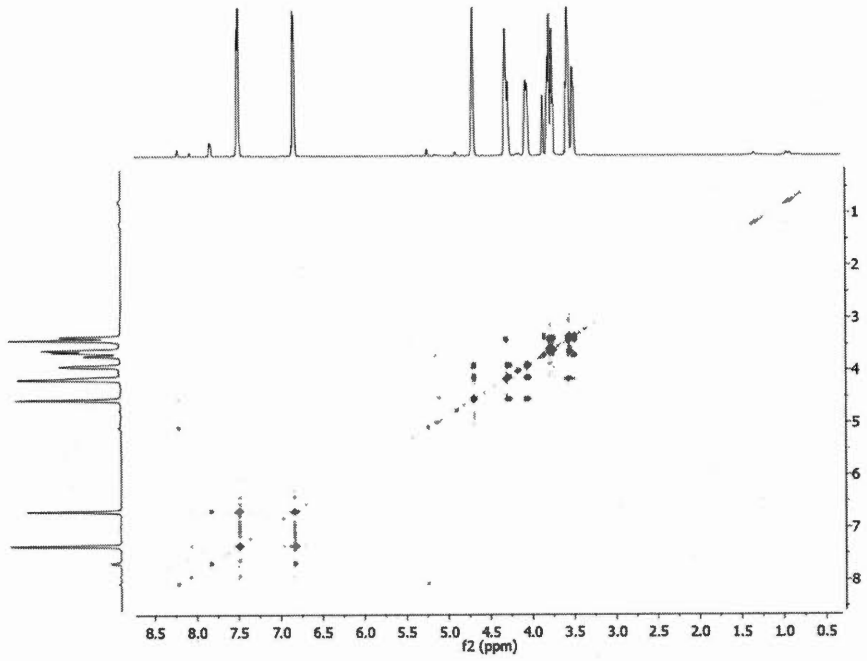

HSQC spectrum (600 MHz, MeOD) of compound **30**

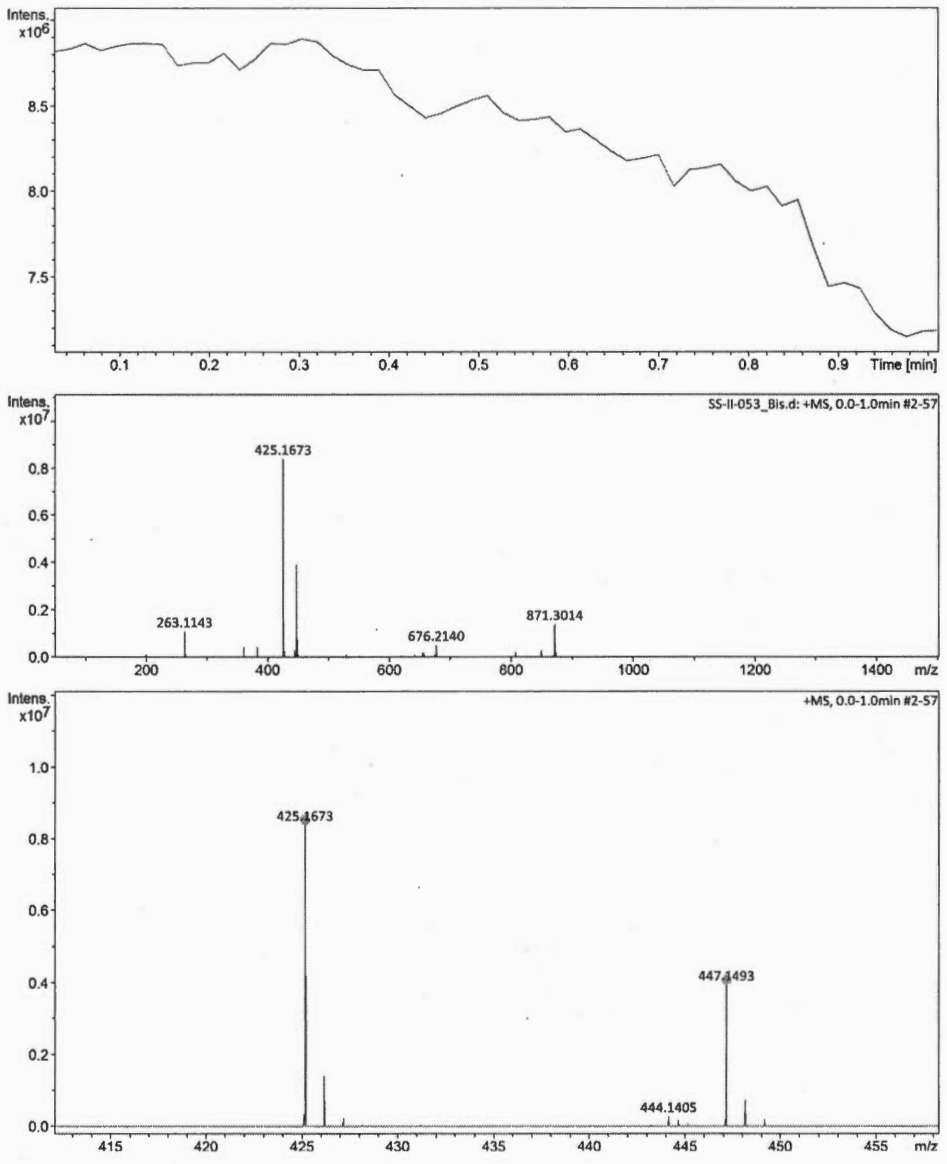

HRMS (ESI^+) spectrum of compound **30**

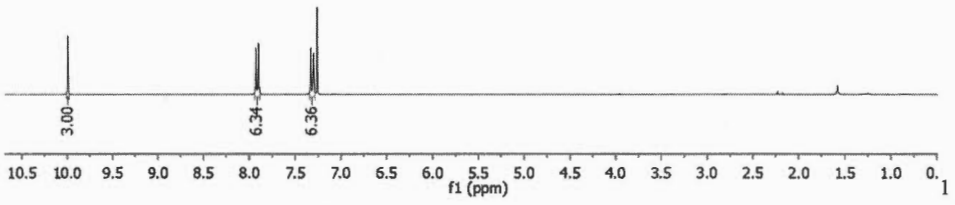

H NMR spectrum (300 MHz, $CDCl_3$) of compound **11**

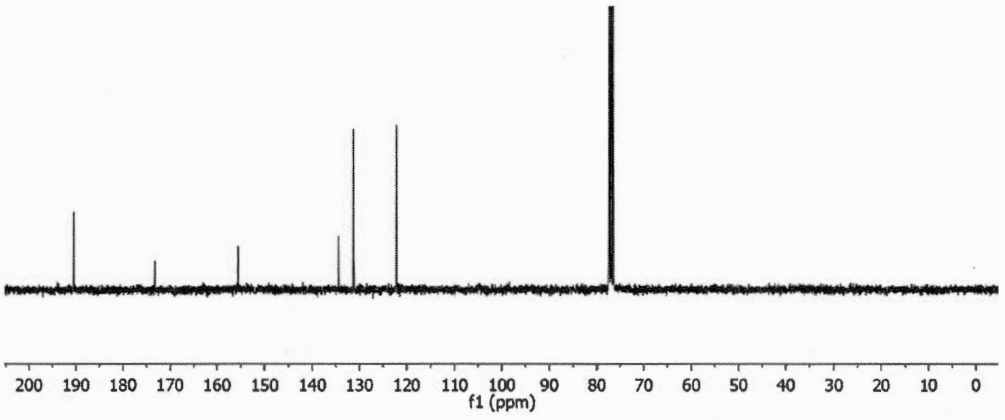

^{13}C NMR spectrum (300 MHz, $CDCl_3$) of compound **11**

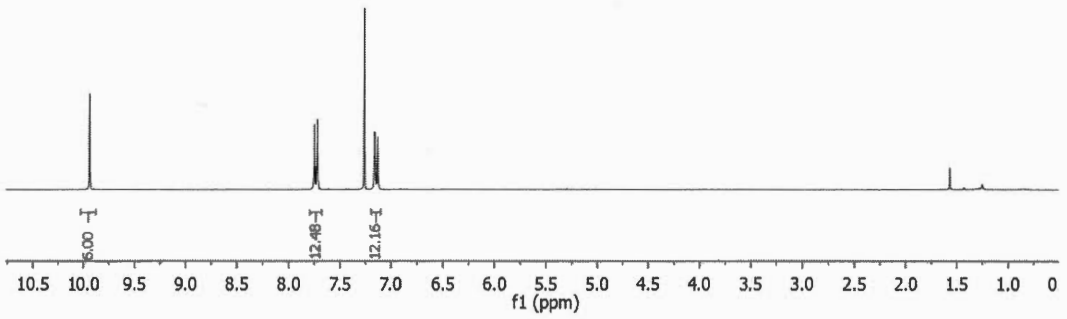

^{1}H NMR spectrum (300 MHz, $CDCl_3$) of compound **14**

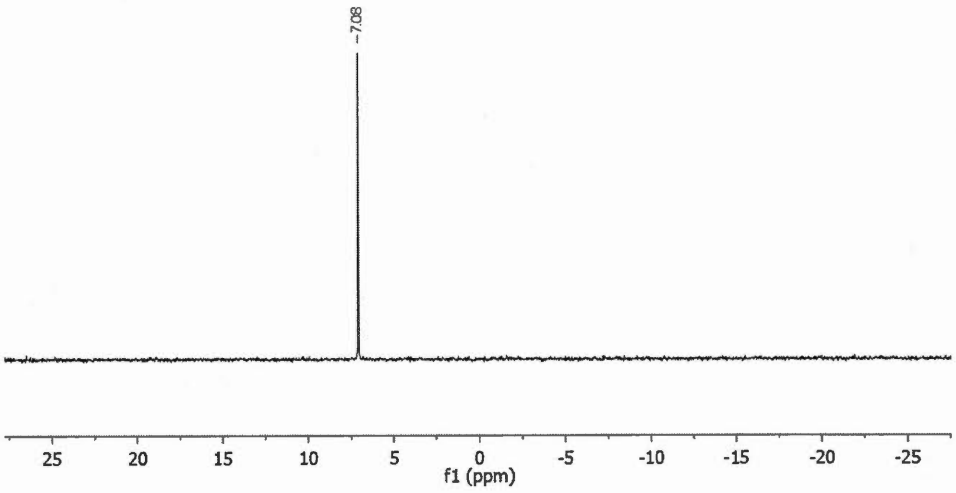

^{31}P NMR spectrum (300 MHz, $CDCl_3$) of compound **14**

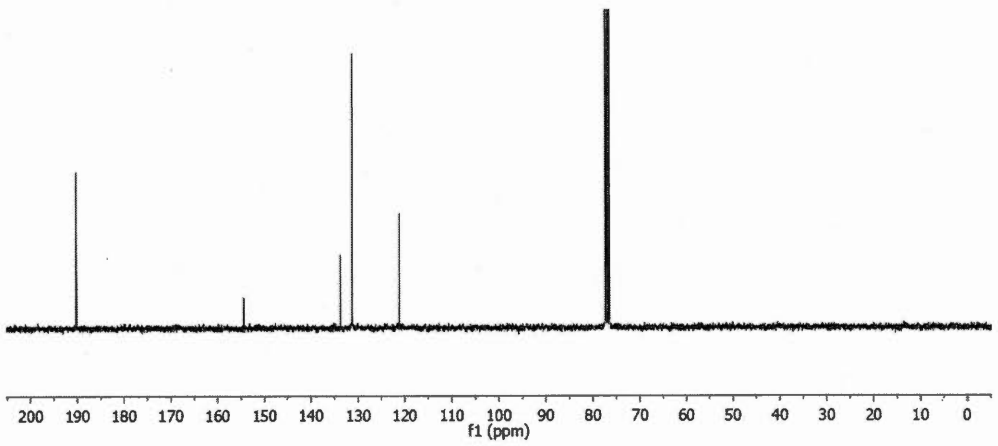

^{13}C NMR spectrum (300 MHz, $CDCl_3$) of compound **14**

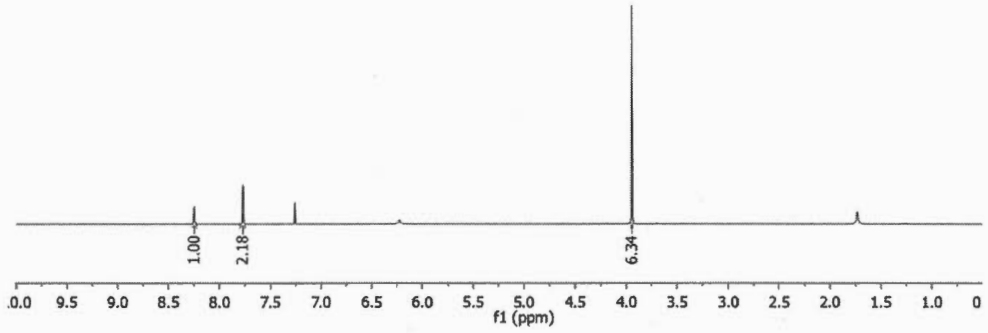

^{1}H NMR spectrum (300 MHz, $CDCl_3$) of compound **17**

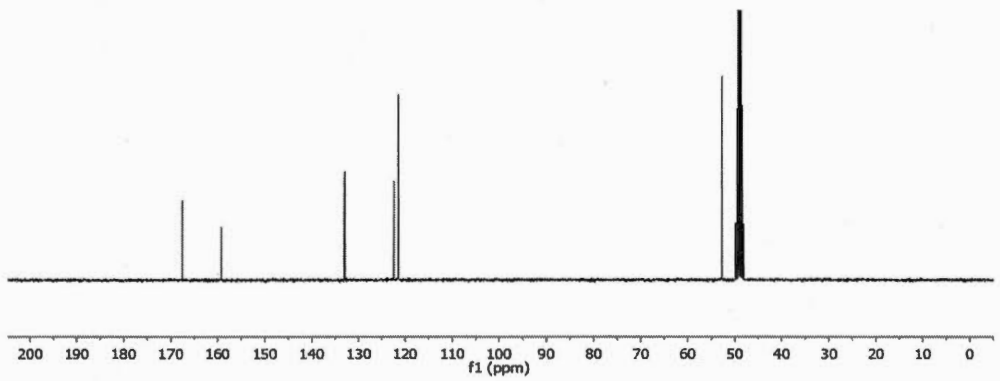

^{13}C NMR spectrum (300 MHz, $CDCl_3$) of compound **17**

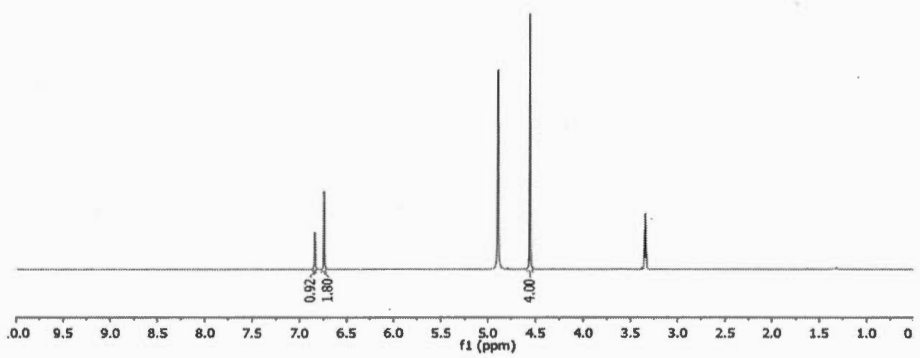

^{1}H NMR spectrum (300 MHz, MeOD) of compound **18**

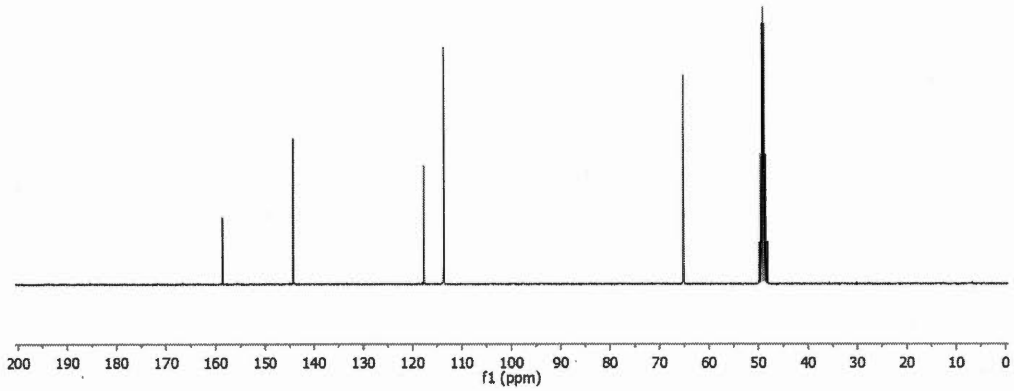

^{13}C NMR spectrum (75 MHz, MeOD) of compound **18**

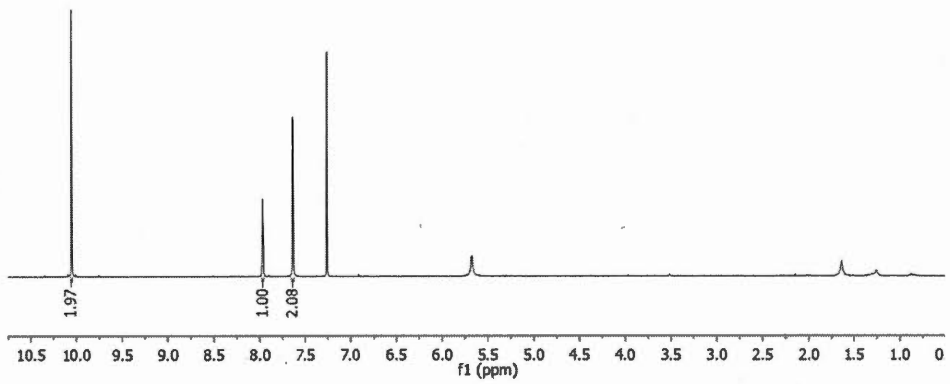

^{1}H NMR spectrum (300 MHz, $CDCl_3$) of compound **19**

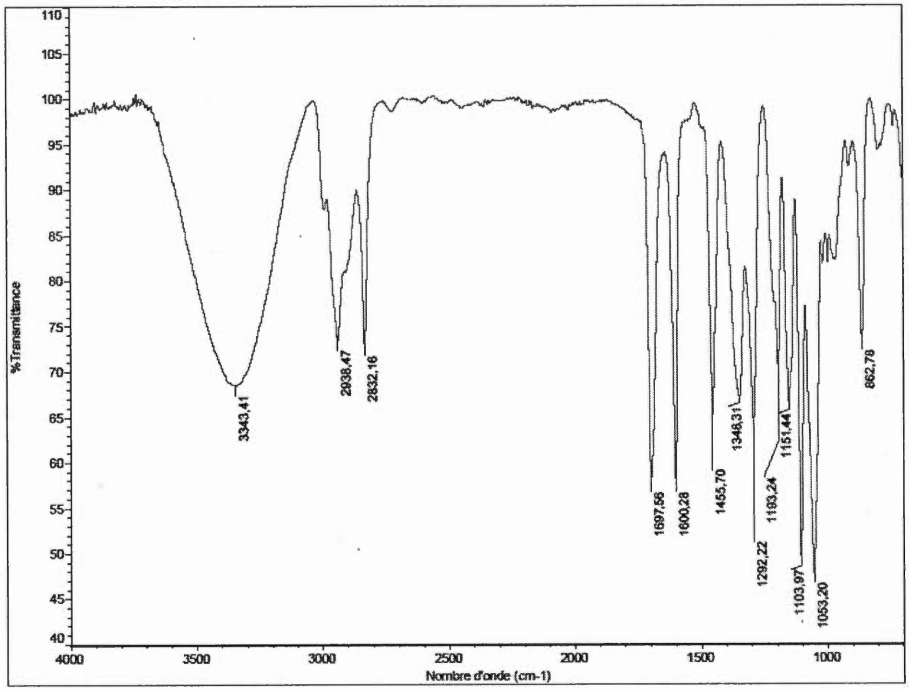

FT-IR spectrum of compound **19**

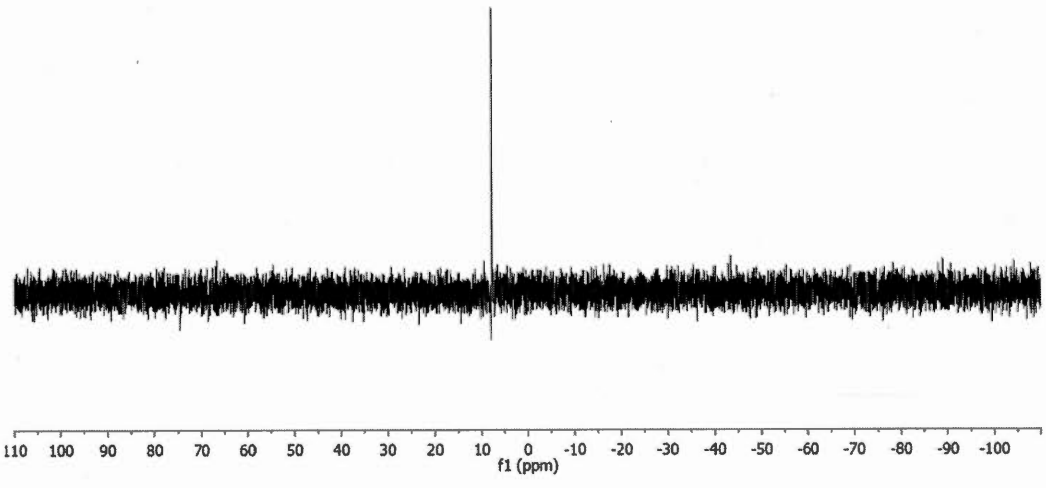

^{31}P NMR spectrum (122 MHz, DMSO, d_6) of compound **20**

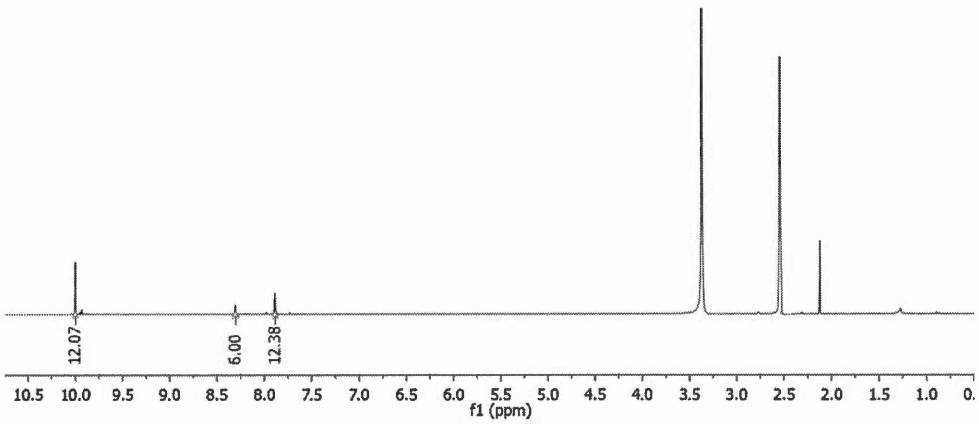

^{1}H NMR spectrum (300 MHz, DMSO, d_6) of compound **2**

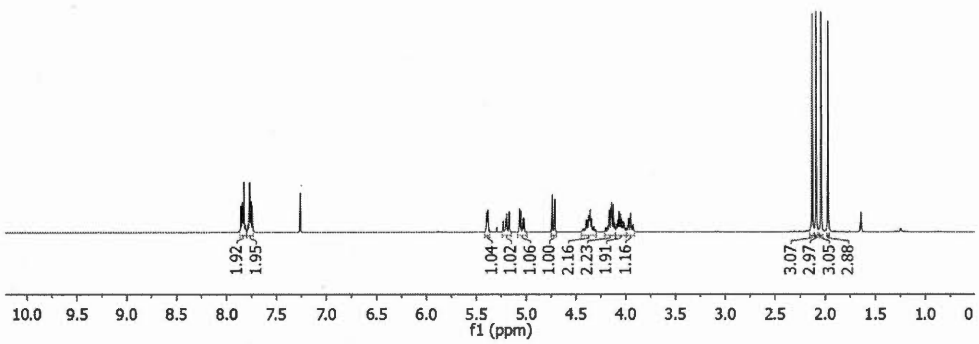

^{1}H NMR spectrum (300 MHz, $CDCl_3$) of compound **7**

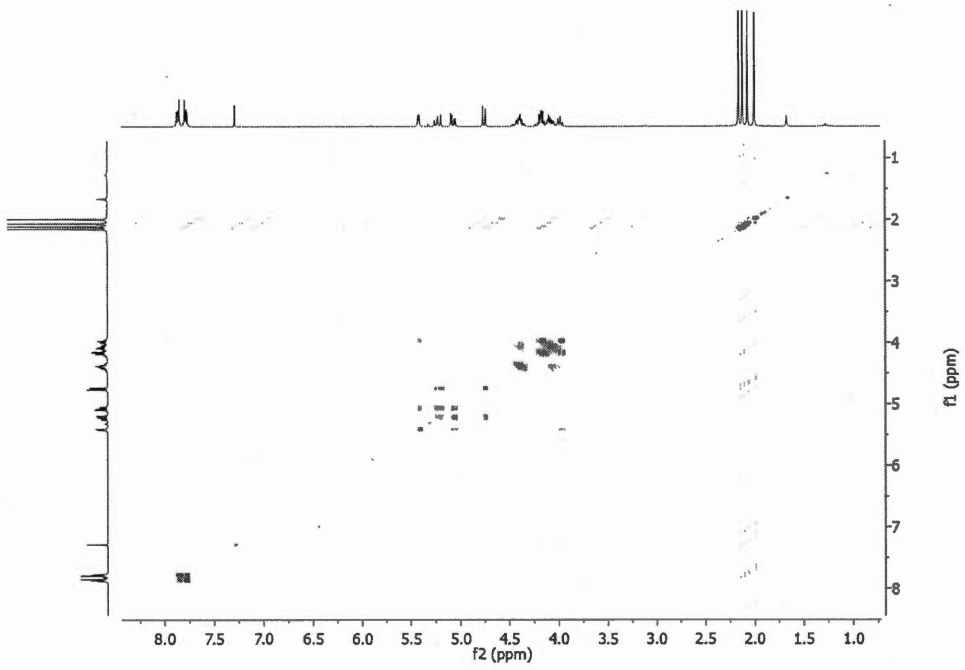

COSY spectrum (300 MHz, $CDCl_3$) of compound **7**

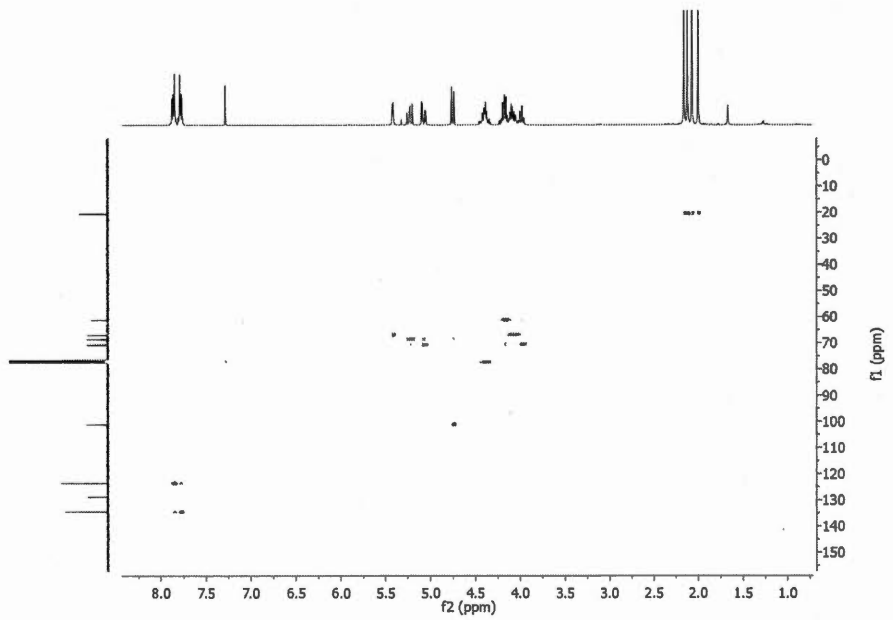

HSQC spectrum (300 MHz, $CDCl_3$) of compound **7**

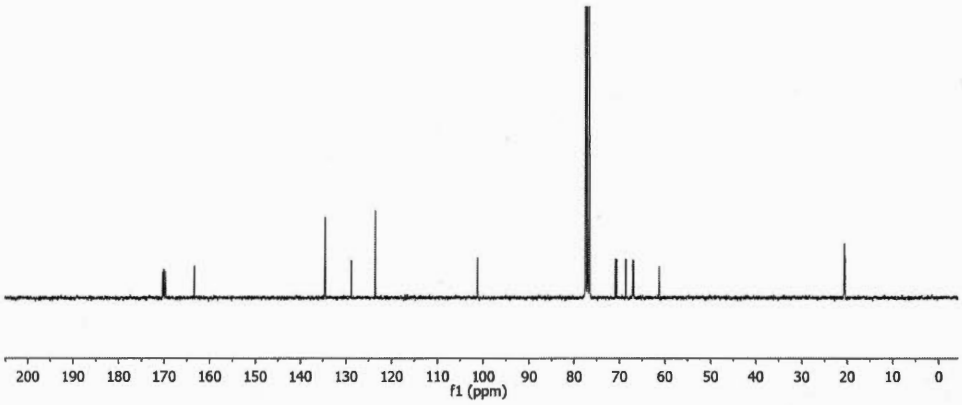

^{13}C NMR spectrum (75 MHz, $CDCl_3$) of compound **7**

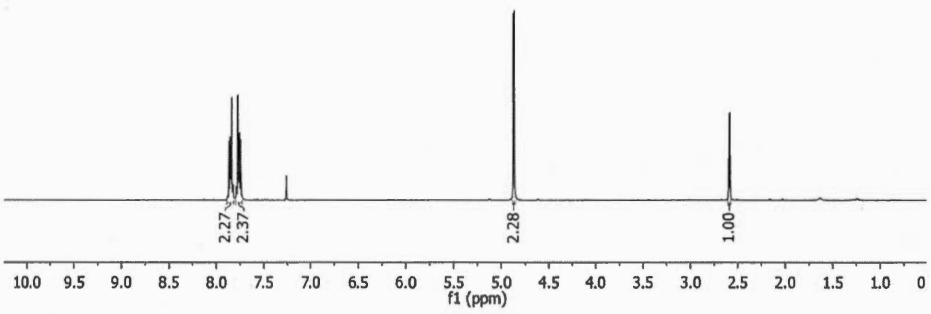

^{1}H NMR spectrum (300 MHz, $CDCl_3$) of compound **35**

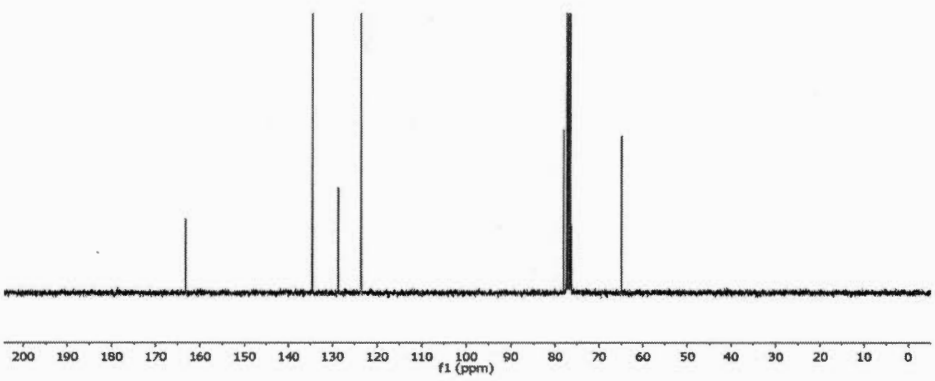

^{13}C NMR spectrum (75 MHz, $CDCl_3$) of compound **35**

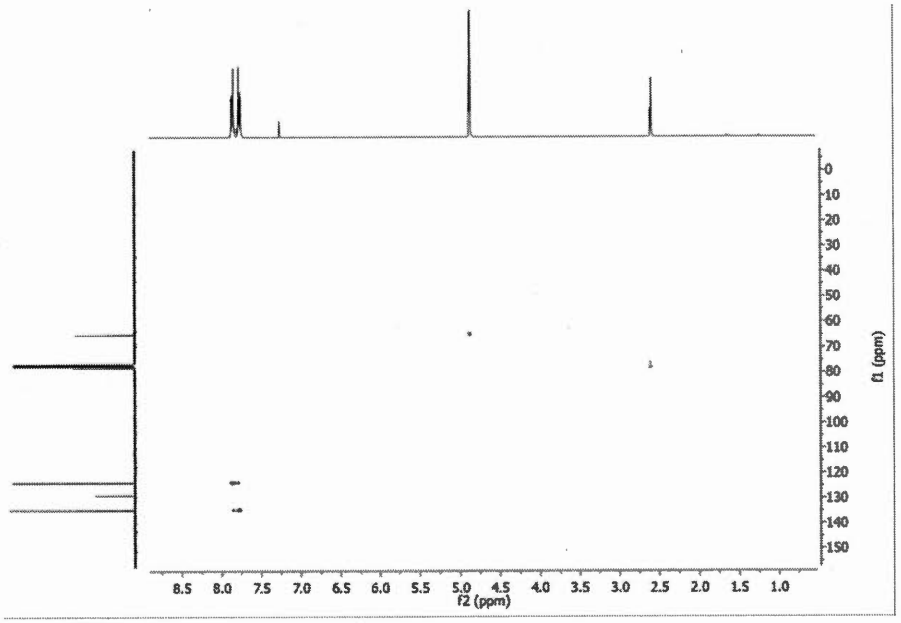

HSQC spectrum (300 MHz, $CDCl_3$) of compound **35**

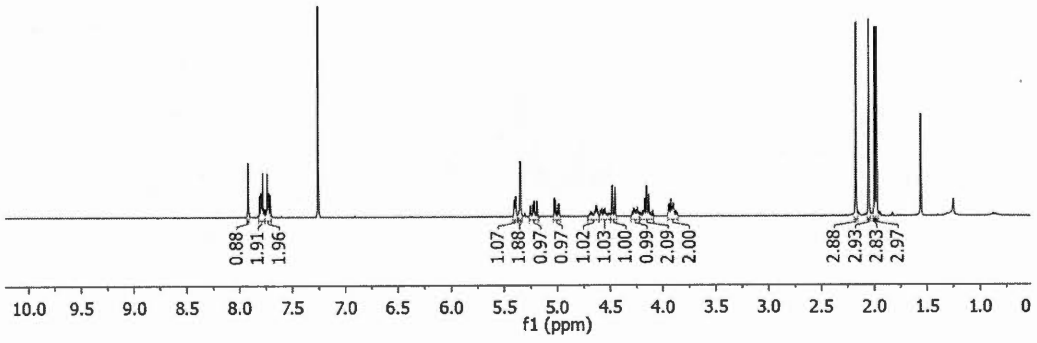

^1H NMR spectrum (300 MHz, $CDCl_3$) of compound **36**

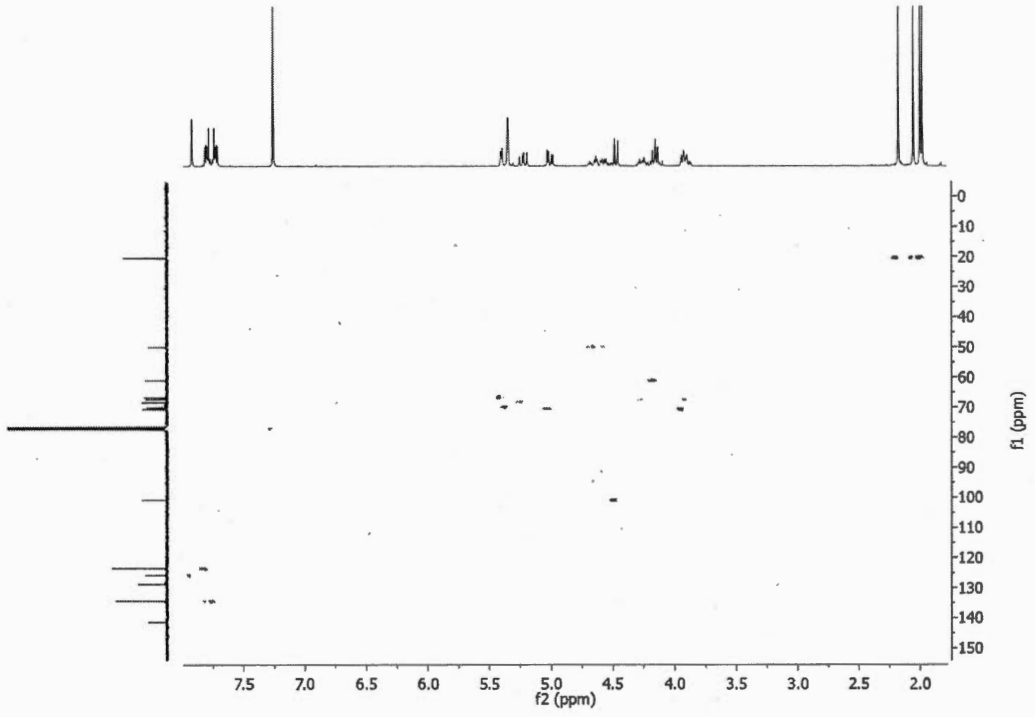

HSQC spectrum (300 MHz, $CDCl_3$) of compound **36**

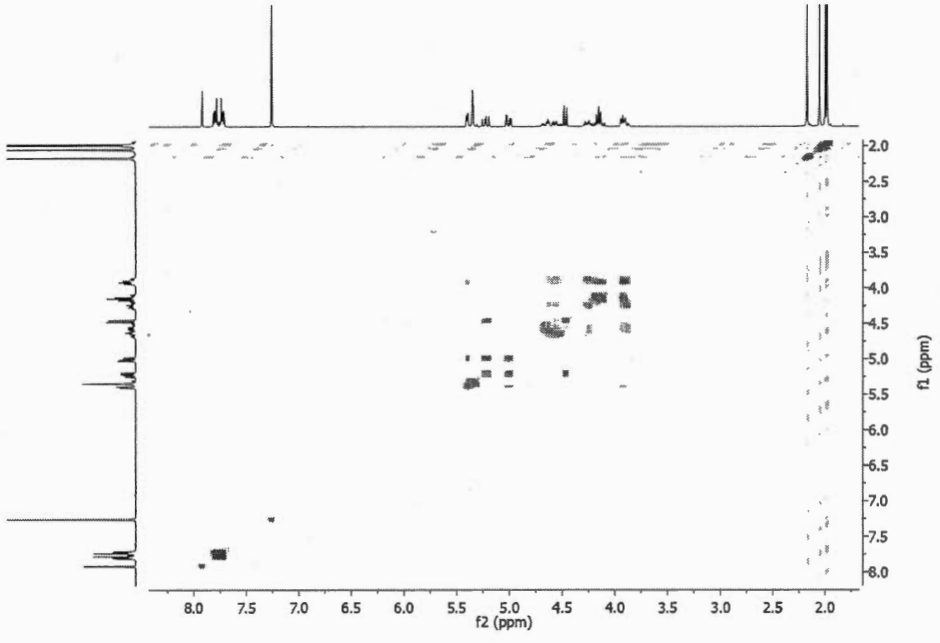

COSY spectrum (300 MHz, $CDCl_3$) of compound **36**

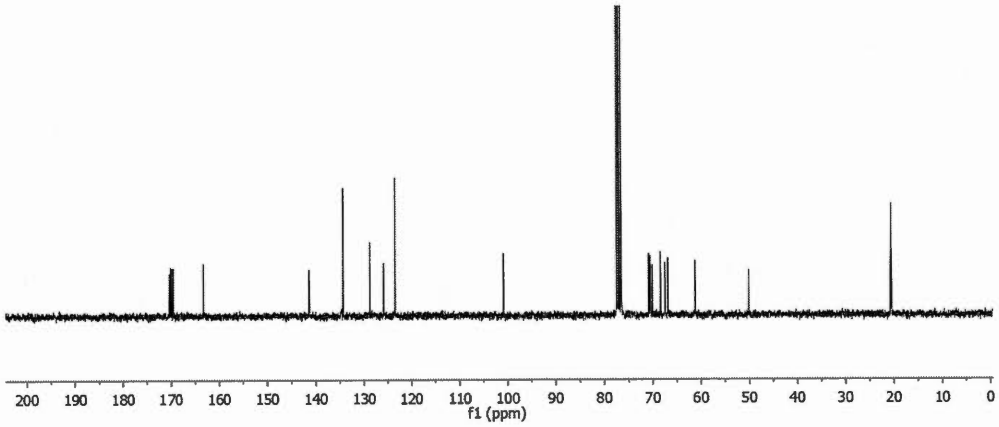

^{13}C NMR spectrum (75 MHz, $CDCl_3$) of compound **36**

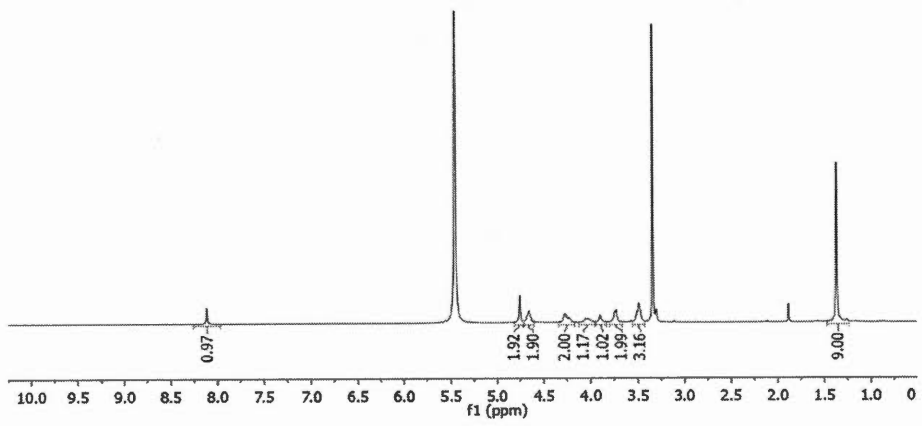

^{1}H NMR spectrum (300 MHz, $CDCl_3$) of compound **47**

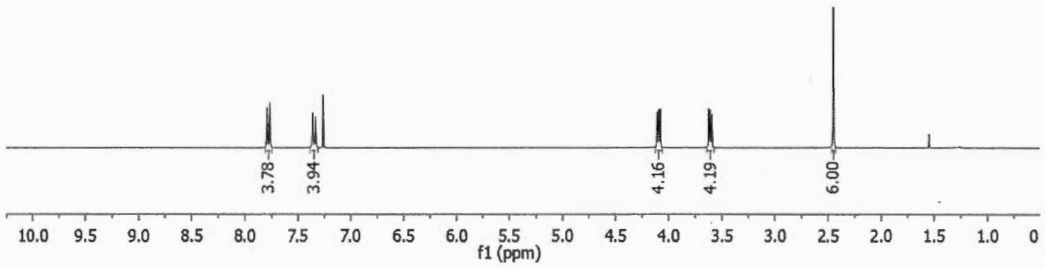

^{1}H NMR spectrum (300 MHz, $CDCl_3$) of compound **44**

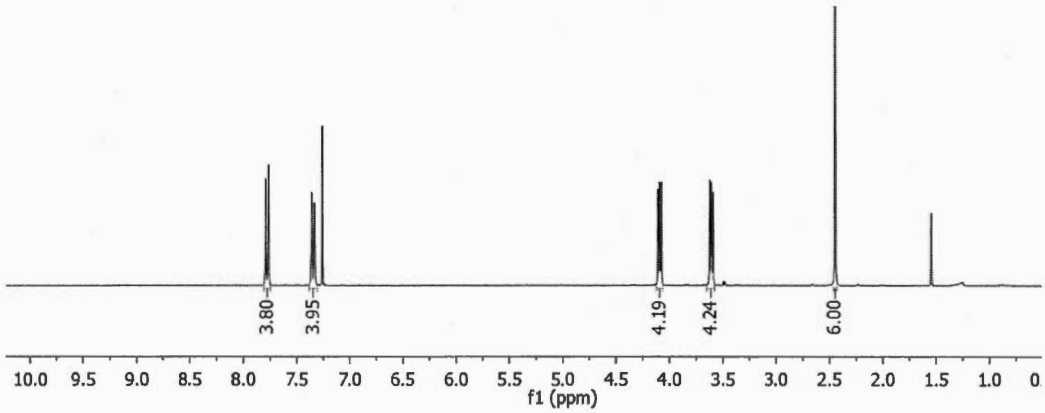

^{1}H NMR spectrum (300 MHz, $CDCl_3$) of compound **44**

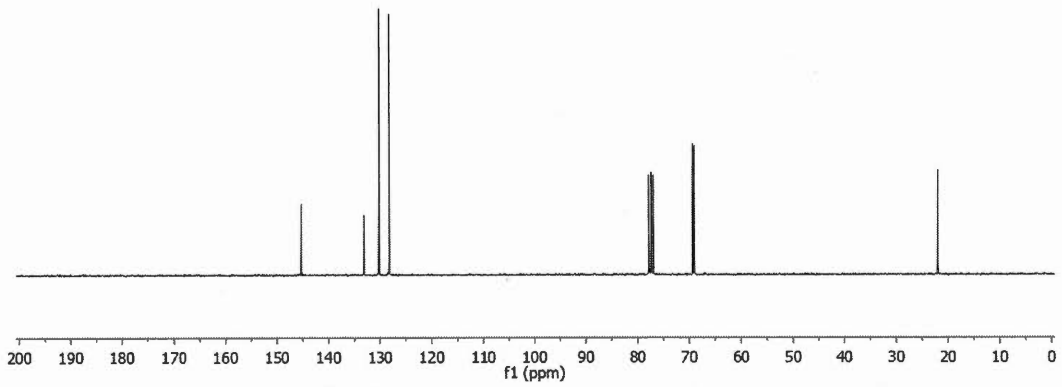

^{13}C NMR spectrum (75 MHz, $CDCl_3$) of compound **44**

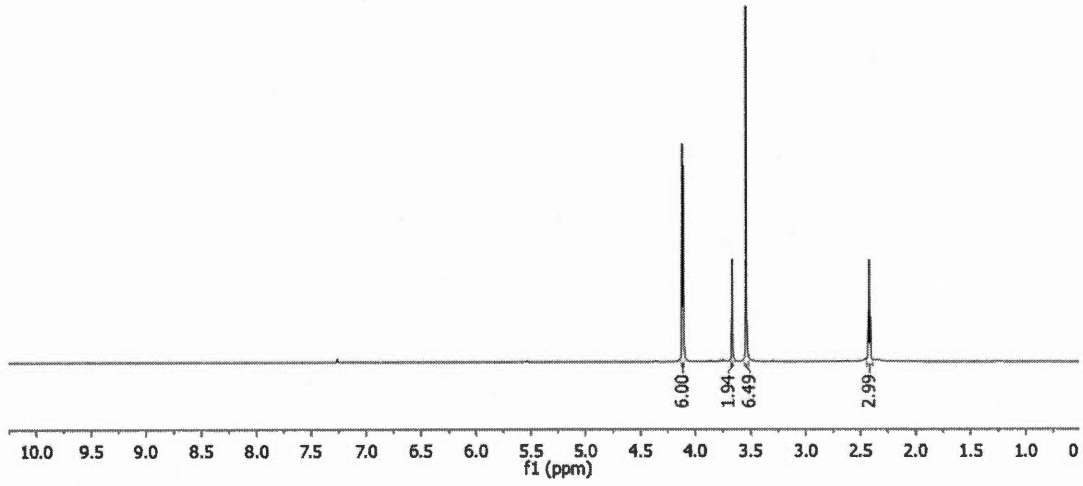

^{1}H NMR spectrum (300 MHz, $CDCl_3$) of compound **39**

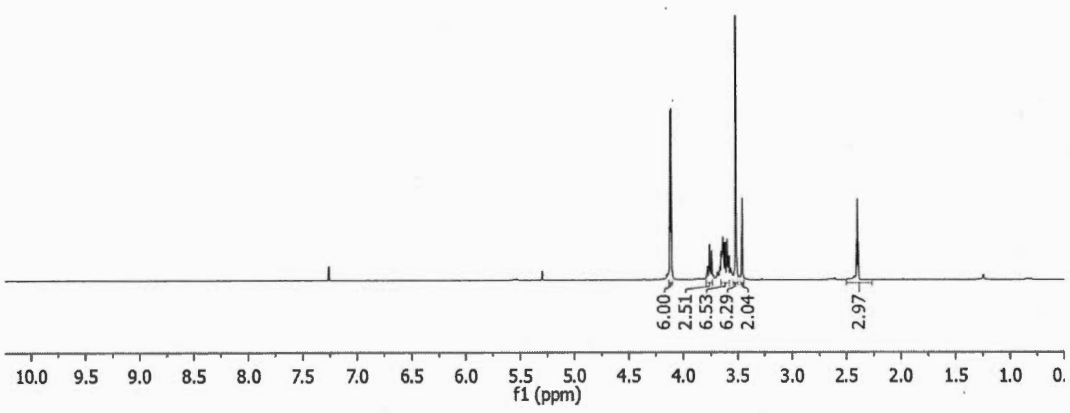

^{1}H NMR spectrum (300 MHz, $CDCl_3$) of compound **41**

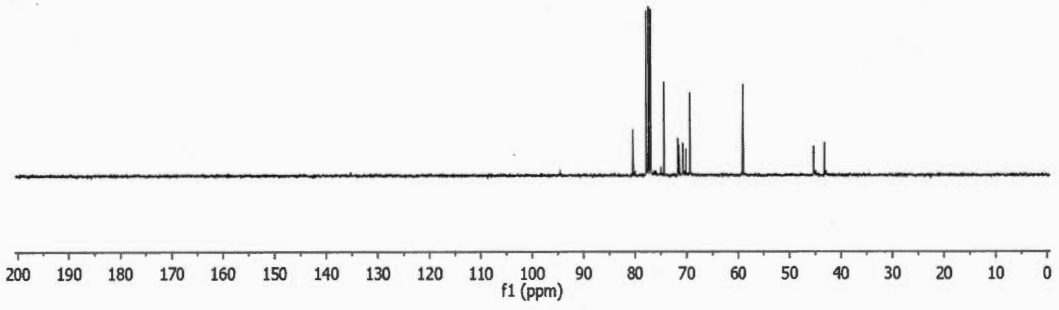

^{13}C NMR spectrum (75 MHz, $CDCl_3$) of compound **41**

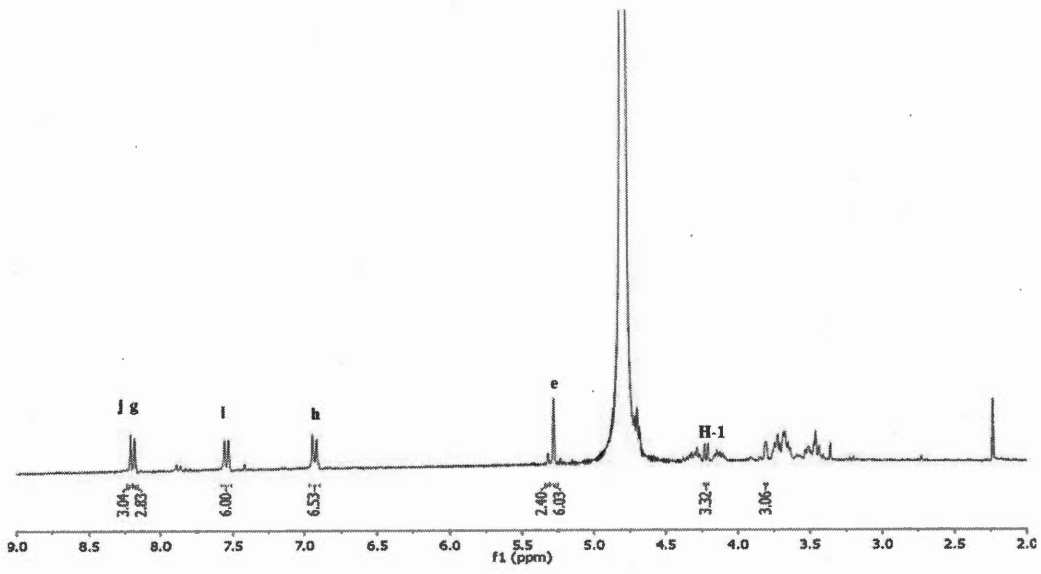

^{1}H NMR (600 MHz, D_2O) of fraction collected from HPLC for compound **31**

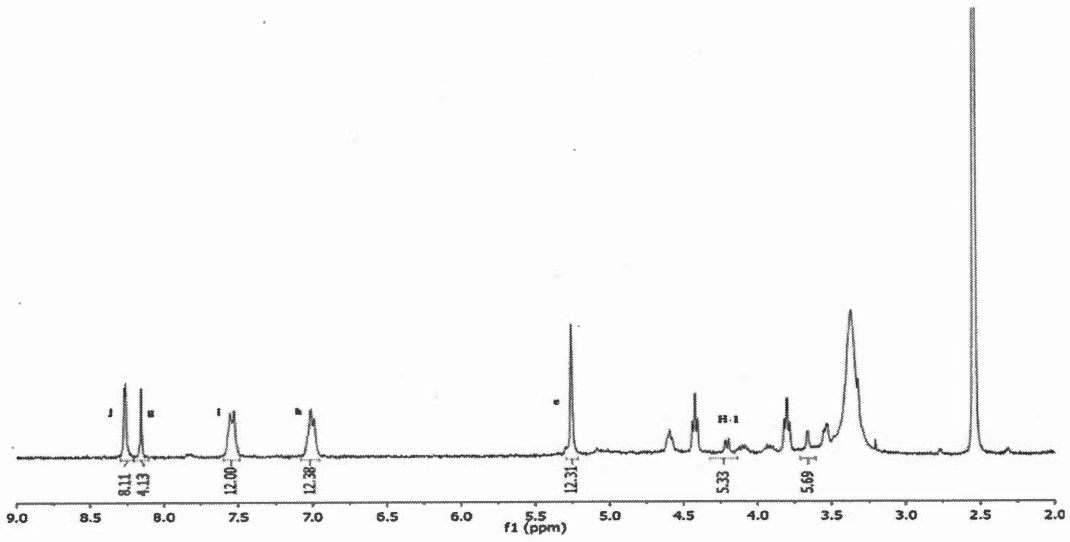

^{1}H NMR (300 MHz, DMSO) of remaining residue of compound **33** after dialysis

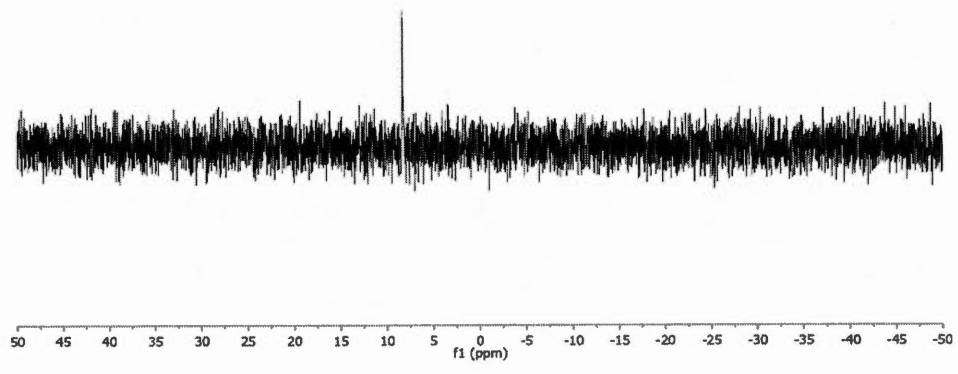

^{13}P NMR (300 MHz, DMSO) of remaining residue of compound **33** after dialysis.

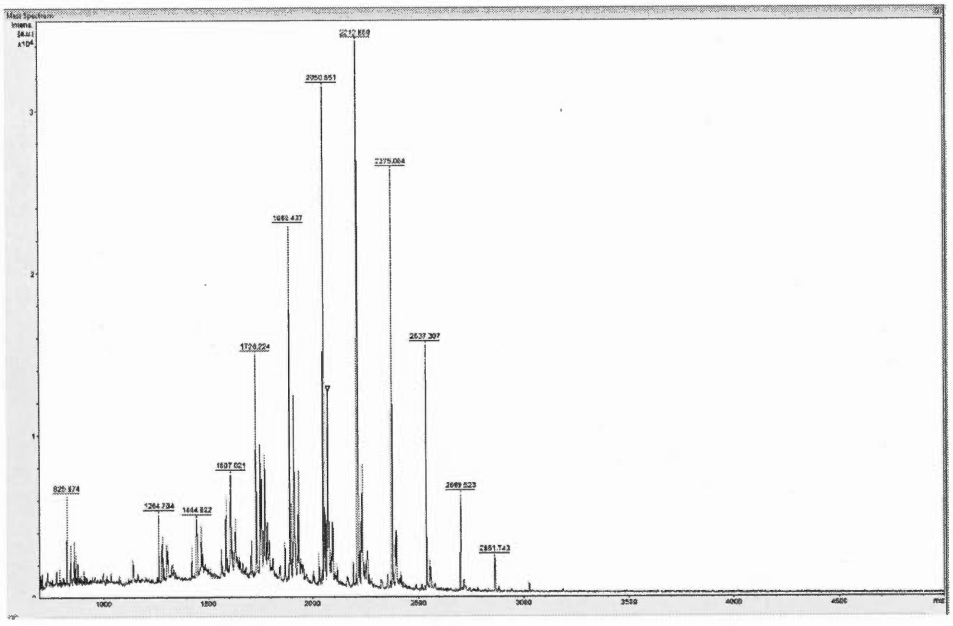

Mass spectroscopy (MOLDI-TOF MS) of compound **33**

REFERENCE

(1) Hourani, R.; Kakkar, A. Advances in the Elegance of Chemistry in Designing Dendrimers. *Macromol. Rapid Commun.* **2010**, *31* (11), 947–974.

(2) Svenson, S. Dendrimers as Versatile Platform in Drug Delivery Applications. *Eur. J. Pharm. Biopharm.* **2009**, *71* (3), 445–462.

(3) Caminade, A.-M.; Turrin, C.-O. Dendrimers for Drug Delivery. *J Mater Chem B.* **2014**, *2* (26), 4055–4066.

(4) L'Haridon, L.; Mallet, J.-M. Chapter 13. Carbohydrate-Based Dendrimers. In *Carbohydrate Chemistry*; Pilar Rauter, A., Lindhorst, T., Queneau, Y., Eds.; Royal Society of Chemistry: Cambridge, 2014; Vol. 40, pp 257–269.

(5) Sowinska, M.; Urbanczyk-Lipkowska, Z. Advances in the Chemistry of Dendrimers. *New J. Chem.* **2014**, *38* (6), 2168.

(6) Mintzer, M. A.; Grinstaff, M. W. Biomedical Applications of Dendrimers: A Tutorial. *Chem Soc Rev* **2011**, *40* (1), 173–190.

(7) Cheng, Y.; Zhao, L.; Li, Y.; Xu, T. Design of Biocompatible Dendrimers for Cancer Diagnosis and Therapy: Current Status and Future Perspectives. *Chem. Soc. Rev.* **2011**, *40* (5), 2673.

(8) Flory, P. J. Molecular Size Distribution in Three Dimensional Polymers. I. Gelation [1]. *J. Am. Chem. Soc.* **1941**, *63* (11), 3083–3090.

(9) Flory, P. J. Molecular Size Distribution in Three Dimensional Polymers. II. Trifunctional Branching Units. *J. Am. Chem. Soc.* **1941**, *63* (11), 3091–3096.

(10) Flory, P. J. Molecular Size Distribution in Three Dimensional Polymers. II. Trifunctional Branching Units. *J. Am. Chem. Soc.* **1941**, *63* (11), 3096-3100.

(11) de Brabander-van den Berg, E. M. M.; Meijer, E. W. Poly(Propylene Imine) Dendrimers: Large-Scale Synthesis by Hetereogeneously Catalyzed Hydrogenations. *Angew. Chem. Int. Ed. Engl.* **1993**, *32* (9), 1308–1311.

(12) Roy, R. Carbohydrates and glycoconjugates: Current Opinion in Structural Biology: Synthesis and some applications of chemically defined multivalent glycoconjugates. **1996,** *6,* 692-702.

(13) Tomali, D. A.; Baker, H.; Dewald, J. A New Class of Polymers: Starburst-Dendritic Macromolecules. *Polymer J.* **1985**, *17* (1), 117-132.

(14) Nanjwade, B. K.; Bechra, H. M.; Derkar, G. K.; Manvi, F. V.; Nanjwade, V. K. Dendrimers: Emerging Polymers for Drug-Delivery Systems. *Eur. J. Pharm. Sci.* **2009**, *38* (3), 185–196.

(15) CalderÃ³n, M.; Quadir, M. A.; Sharma, S. K.; Haag, R. Dendritic Polyglycerols for Biomedical Applications. *Adv. Mater.* **2010**, *22* (2), 190–218.

(16) Irfan, M.; Seiler, M. Encapsulation Using Hyperbranched Polymers: From Research and Technologies to Emerging Applications. *Ind. Eng. Chem. Res.* **2010**, *49* (3), 1169–1196.

(17) Khanna, K.; Varshney, S.; Kakkar, A. Miktoarm Star Polymers: Advances in Synthesis, Self-Assembly, and Applications. *Polym. Chem.* **2010**, *1* (8), 1171.

(18) Gillies, E.; Frechet, J. Dendrimers and Dendritic Polymers in Drug Delivery. *Drug Discov. Today* **2005**, *10* (1), 35–43.

(19) Lee, C. C.; MacKay, J. A.; Fréchet, J. M. J.; Szoka, F. C. Designing Dendrimers for Biological Applications. *Nat. Biotechnol.* **2005**, *23* (12), 1517–1526.

(20) Shcharbin, D.; Shakhbazau, A.; Bryszewska, M. Poly(Amidoamine) Dendrimer Complexes as a Platform for Gene Delivery. *Expert Opin. Drug Deliv.* **2013**, *10* (12), 1687–1698.

(21) Cloninger, M. J. Biological Applications of Dendrimers. **2002,** *6*, 742-748.

(22) Prasad, B. B.; Jauhari, D. A Dual-Template Biomimetic Molecularly Imprinted Dendrimer-Based Piezoelectric Sensor for Ultratrace Analysis of Organochlorine Pesticides. *Sens. Actuators B Chem.* **2015**, *207*, 542–551.

(23) Sorsak, E.; Volmajer, J. Application Of Pamam Dendrimer In Optical Sensing. *Royal Society Of Chem. J.* **2014,** *00*, 1-11.

(24) Bhattacharya, P.; Nasybulin, E. N.; Engelhard, M. H.; Kovarik, L.; Bowden, M. E.; Li, X. S.; Gaspar, D. J.; Xu, W.; Zhang, J.-G. Dendrimer-Encapsulated Ruthenium Oxide Nanoparticles as Catalysts in Lithium-Oxygen Batteries. *Adv. Funct. Mater.* **2014**, *24* (47), 7510–7519.

(25) Shellaiah, M.; Ramakrishnam Raju, M. V.; Singh, A.; Lin, H.-C.; Wei, K.-H.; Lin, H.-C. Synthesis of Novel Platinum Complex Core as a Selective Ag^{+} Sensor and Its H-Bonded Tetrads Self-Assembled with Triarylamine Dendrimers for Electron/Energy Transfers. *J Mater Chem A* **2014**, *2* (41), 17463–17476.

(26) Ornelas, C.; Pennell, R.; Liebes, L. F.; Weck, M. Construction of a Well-Defined Multifunctional Dendrimer for Theranostics. *Org. Lett.* **2011**, *13* (5), 976–979.

(27) Dalton, L. R.; Benight, S. J.; Johnson, L. E.; Knorr, D. B.; Kosilkin, I.; Eichinger, B. E.; Robinson, B. H.; Jen, A. K.-Y.; Overney, R. M. Systematic Nanoengineering of Soft Matter Organic Electro-Optic Materials †. *Chem. Mater.* **2011**, *23* (3), 430–445.

(28) Kadam, R. U.; Bergmann, M.; Hurley, M.; Garg, D.; Cacciarini, M.; Swiderska, M. A.; Nativi, C.; Sattler, M.; Smyth, A. R.; Williams, P.; et al. A Glycopeptide Dendrimer Inhibitor of the Galactose-Specific Lectin LecA and of Pseudomonas Aeruginosa Biofilms. *Angew. Chem. Int. Ed.* **2011**, *50* (45), 10631–10635.

(29) Shaw, P. E.; Chen, S. S. Y.; Wang, X.; Burn, P. L.; Meredith, P. High-Generation Dendrimers with Excimer-like Photoluminescence for the Detection of Explosives. *J. Phys. Chem. C* **2013**, *117* (10), 5328–5337.

(30) Neibert, K.; Gosein, V.; Sharma, A.; Khan, M.; Whitehead, M. A.; Maysinger, D.; Kakkar, A. "Click" Dendrimers as Anti-Inflammatory Agents: With Insights into Their Binding from Molecular Modeling Studies. *Mol. Pharm.* **2013**, *10* (6), 2502–2508.

(31) Lim, J.; Simanek, E. E. Triazine Dendrimers as Drug Delivery Systems: From Synthesis to Therapy. *Adv. Drug Deliv. Rev.* **2012**, *64* (9), 826–835.

(32) Soliman, G. M.; Sharma, A.; Maysinger, D.; Kakkar, A. Dendrimers and Miktoarm Polymers Based Multivalent Nanocarriers for Efficient and Targeted Drug Delivery. *Chem. Commun.* **2011**, *47* (34), 9572.

(33) Chabre, Y. M.; Roy, R. Multivalent Glycoconjugate Syntheses and Applications Using Aromatic Scaffolds. *Chem. Soc. Rev.* **2013**, *42* (11), 4657.

(34) Shubayev, V. I.; Pisanic, T. R.; Jin, S. Magnetic Nanoparticles for Theragnostics. *Adv. Drug Deliv. Rev.* **2009**, *61* (6), 467–477.

(35) Janib, S. M.; Moses, A. S.; MacKay, J. A. Imaging and Drug Delivery Using Theranostic Nanoparticles. *Adv. Drug Deliv. Rev.* **2010**, *62* (11), 1052–1063.

(36) Lee, J. H.; Nan, A. Combination Drug Delivery Approaches in Metastatic Breast Cancer. *J. Drug Deliv.* **2012**, *2012*, 1–17.

(37) Tomali, D. A.; Baker, H.; Dewald, J. A New Class of Polymers: Starburst-Dendritic Macromolecules. *Polymer J.* **1985**, *17* (1), 117-132.

(38) Tomali, D. A.; Baker, H.; Dewald, J. A New Class of Polymers: Starburst-Dendritic Macromolecules. *Polymer J.* **1985**, *17* (1), 117-132.

(39) Fischer, M.; Vögtle, F. Dendrimers: From Design to Application—A Progress Report. *Angew. Chem. Int. Ed.* **1999**, *38* (7), 884–905.

(40) Hawker, C. J.; Frechet, J. M. J. Preparation of Polymers with Controlled Molecular Architecture. A New Convergent Approach to Dendritic Macromolecules. *J. Am. Chem. Soc.* **1990**, *112* (21), 7638–7647.

(41) Mintzer, M. A.; Grinstaff, M. W. Biomedical Applications of Dendrimers: A Tutorial. *Chem Soc Rev.* **2011**, *40* (1), 173–190.

(42) Roy, R.; Shiao, T. C. Glyconanosynthons as Powerful Scaffolds and Building Blocks for the Rapid Construction of Multifaceted, Dense and Chiral Dendrimers. *Chem. Soc. Rev.* **2015**, *44* (12), 3924–3941.

(43) Kottari, N.; Chabre, Y. M.; Shiao, T. C.; Rej, R.; Roy, R. Efficient and Accelerated Growth of Multifunctional Dendrimers Using Orthogonal Thiol–Ene and SN2 Reactions. *Chem. Commun.* **2014**, *50* (16), 1983.

(44) Sharma, R.; Kottari, N.; Chabre, Y. M.; Abbassi, L.; Shiao, T. C.; Roy, R. A Highly Versatile Convergent/Divergent "Onion Peel" Synthetic Strategy toward Potent Multivalent Glycodendrimers. *Chem Commun* **2014**, *50* (87), 13300–13303.

(45) Sharma, R.; Naresh, K.; Chabre, Y. M.; Rej, R.; Saadeh, N. K.; Roy, R. "Onion Peel" Dendrimers: A Straightforward Synthetic Approach towards Highly Diversified Architectures. *Polym Chem* **2014**, *5* (14), 4321–4331.

(46) Santoyo-González, F.; Hernández-Mateo, F. Azide–Alkyne 1,3-Dipolar Cycloadditions: A Valuable Tool in Carbohydrate Chemistry. In *Heterocycles from Carbohydrate Precursors*; El Ashry, E. S. H., Ed.; Springer Berlin Heidelberg: Berlin, Heidelberg, 2007; Vol. 7, pp 133–177.

(47) Dondoni, A.; Marra, A. Recent Applications of Thiol–Ene Coupling as a Click Process for Glycoconjugation. *Chem Soc Rev* **2012**, *41* (2), 573–586.

(48) Antoni, P.; Nyström, D.; Hawker, C. J.; Hult, A.; Malkoch, M. A Chemoselective Approach for the Accelerated Synthesis of Well-Defined Dendritic Architectures. *Chem Commun* **2007**, No. 22, 2249–2251.

(49) Mulders, S. J. E.; Brouwer, A. J.; van der Meer, P. G. J.; Liskamp, R. M. J. Synthesis of a Novel Amino Acid Based Dendrimer. *Tetrahedron Lett.* **1997**, *38* (4), 631–634.

(50) Kolb, H. C.; Finn, M. G.; Sharpless, K. B. Click Chemistry: Diverse Chemical Function from a Few Good Reactions. *Angew. Chem. Int. Ed.* **2001**, *40* (11), 2004–2021.

(51) Huisgen, R. Kinetics and Reaction Mechanisms: Selected Examples from the Experience of Forty Years. *Pure Appl. Chem.* **1989**, *61* (4), 613–628.

(52) Rostovtsev, V. V.; Green, L. G.; Fokin, V. V.; Sharpless, K. B. A Stepwise Huisgen Cycloaddition Process: Copper(I)-Catalyzed Regioselective "Ligation" of Azides and Terminal Alkynes. *Angew. Chem. Int. Ed.* **2002**, *41* (14), 2596–2599.

(53) Tornøe, C. W.; Christensen, C.; Meldal, M. Peptidotriazoles on Solid Phase: [1,2,3]-Triazoles by Regiospecific Copper(I)-Catalyzed 1,3-Dipolar Cycloadditions of Terminal Alkynes to Azides. *J. Org. Chem.* **2002**, *67* (9), 3057–3064.

(54) Wu, P.; Feldman, A. K.; Nugent, A. K.; Hawker, C. J.; Scheel, A.; Voit, B.; Pyun, J.; Fréchet, J. M. J.; Sharpless, K. B.; Fokin, V. V. Efficiency and Fidelity in a Click-Chemistry Route to Triazole Dendrimers by the Copper(I)-Catalyzed Ligation of Azides and Alkynes. *Angew. Chem. Int. Ed.* **2004**, *43* (30), 3928–3932.

(55) Himo, F.; Lovell, T.; Hilgraf, R.; Rostovtsev, V. V.; Noodleman, L.; Sharpless, K. B.; Fokin, V. V. Copper(I)-Catalyzed Synthesis of Azoles. DFT Study Predicts Unprecedented Reactivity and Intermediates. *J. Am. Chem. Soc.* **2005**, *127* (1), 210–216.

(56) Worrell, B. T.; Malik, J. A.; Fokin, V. V. Direct Evidence of a Dinuclear Copper Intermediate in Cu(I)-Catalyzed Azide-Alkyne Cycloadditions. *Science* **2013**, *340* (6131), 457–460.

(57) Chabre, Y. M.; Roy, R. Design and Creativity in Synthesis of Multivalent Neoglycoconjugates. In *Advances in Carbohydrate Chemistry and Biochemistry*; Elsevier, 2010; Vol. 63, pp 165–393.

(58) Röckendorf, N.; Lindhorst, T. K. Glycodendrimers. In *Dendrimers IV*; Vögtle, F., Schalley, C. A., Eds.; de Meijere, A., Kessler, H., Ley, S. V., Thiem, J., Vögtle, F., Houk, K. N., Lehn, J.-M., Schreiber, S. L., Trost, B. M., Yamamoto, H., Series Eds.; Springer Berlin Heidelberg: Berlin, Heidelberg, 2001; Vol. 217, pp 201–238.

(59) Turnbull, W. B.; Stoddart, J. F. Design and Synthesis of Glycodendrimers. *Rev. Mol. Biotechnol.* **2002**, *90* (3–4), 231–255.

(60) Wittmann, V. Structural Investigation of Multivalent Carbohydrate–Protein Interactions Using Synthetic Biomolecules. *Curr. Opin. Chem. Biol.* **2013**, *17* (6), 982–989.

(61) Chabre, Y. M.; Roy, R. Multivalent Glycoconjugate Syntheses and Applications Using Aromatic Scaffolds. *Chem. Soc. Rev.* **2013**, *42* (11), 4657.

(62) Gingras, M.; Chabre, Y. M.; Roy, M.; Roy, R. How Do Multivalent Glycodendrimers Benefit from Sulfur Chemistry? *Chem. Soc. Rev.* **2013**, *42* (11), 4823.

(63) Mammen, M.; Choi, S.-K.; Whitesides, G. M. Polyvalent Interactions in Biological Systems: Implications for Design and Use of Multivalent Ligands and Inhibitors. *Angew. Chem. Int. Ed.* **1998**, *37* (20), 2754–2794.

(64) Lee, Y. C.; Lee, R. T. Carbohydrate-Protein Interactions: Basis of Glycobiology. *Acc. Chem. Res.* **1995**, *28* (8), 321–327.

(65) Lundquist, J. J.; Toone, E. J. The Cluster Glycoside Effect. *Chem. Rev.* **2002**, *102* (2), 555–578.

(66) Roy, R.; Shiao, T. C. Glyconanosynthons as Powerful Scaffolds and Building Blocks for the Rapid Construction of Multifaceted, Dense and Chiral Dendrimers. *Chem. Soc. Rev.* **2015**, *44* (12), 3924–3941.

(67) Lahmann, M. Architectures of Multivalent Glycomimetics for Probing Carbohydrate–Lectin Interactions. In *Glycoscience and Microbial Adhesion*; Lindhorst, T. K., Oscarson, S., Eds.; Springer Berlin Heidelberg: Berlin, Heidelberg, 2009; Vol. 288, pp 183–165.

(68) Jayaraman, N. Multivalent Ligand Presentation as a Central Concept to Study Intricate Carbohydrate–Protein Interactions. *Chem. Soc. Rev.* **2009**, *38* (12), 3463.

(69) Pieters, R. J. Maximising Multivalency Effects in Protein–Carbohydrate Interactions. *Org. Biomol. Chem.* **2009**, *7* (10), 2013.

(70) Dam, T. K.; Brewer, C. F. Multivalent Lectin—Carbohydrate Interactions. In *Advances in Carbohydrate Chemistry and Biochemistry*; Elsevier, 2010; Vol. 63, pp 139–164.

(71) Deniaud, D.; Julienne, K.; Gouin, S. G. Insights in the Rational Design of Synthetic Multivalent Glycoconjugates as Lectin Ligands. *Org Biomol Chem* **2011**, *9* (4), 966–979.

(72) Shiao, T. C.; Roy, R. Glycodendrimers as Functional Antigens and Antitumor Vaccines. *New J Chem* **2012**, *36* (2), 324–339.

(73) Wittmann, V.; Pieters, R. J. Bridging Lectin Binding Sites by Multivalent Carbohydrates. *Chem. Soc. Rev.* **2013**, *42* (10), 4492.

(74) Cecioni, S.; Imberty, A.; Vidal, S. Glycomimetics versus Multivalent Glycoconjugates for the Design of High Affinity Lectin Ligands. *Chem. Rev.* **2015**, *115* (1), 525–561.

(75) Roy, R.; Zanini, D.; Meunier, S. J.; Romanowska, A. Solid-Phase Synthesis of Dendritic Sialoside Inhibitors of Influenza A Virus Haemagglutinin. *J. Chem. Soc. Chem. Commun.* **1993**, No. 24, 1869.

(76) Gleria, M.; De Jaeger, R. Polyphosphazenes: A Review. In *New Aspects in Phosphorus Chemistry V*; Majoral, J.-P., Ed.; Springer Berlin Heidelberg: Berlin, Heidelberg, 2005; Vol. 250, pp 165–251.

(77) Allcock, H. R.; Pucher, S. R.; Scopelianos, A. G. Poly[(Amino Acid Ester)Phosphazenes]: Synthesis, Crystallinity, and Hydrolytic Sensitivity in Solution and the Solid State. *Macromolecules* **1994**, *27* (5), 1071–1075.

(78) Inoue, K.; Sakai, H.; Tanigaki, T. Preparation and Conformation of Hexaarmed Star Poly(β-benzyl-L-aspartates) Utilizing *Hexakis*(4-aminophenoxy)cyclotriphosphazene. *J. Am. Chem. Soc.* **1994,** *116* (23), 10783-10784.

(79) Inoue, K.; Miyahara, A.; Itaya, T. Enantioselective Permeation of Amino Acids across Membranes Prepared from 3α-Helix Bundle Polyglutamates with Oxyethylene Chains. *J. Am. Chem. Soc.* **1997,** *119* (26), 6191-6192.

(80) Rengan, K.; Engel, R. The Synthesis of Phosphonium Cascade Molecules. *J. Chem. Soc. Perkin 1* **1991**, No. 5, 987.

(81) Konar, V.; Yilmaz, Ö.; Öztürk, A. İ.; Kirbağ, S.; Arslan, M. Antimicrobial and Biological Effects of Bomphos and Phomphos on Bacterial and Yeast Cells. *Bioorganic Chem.* **2000**, *28* (4), 214–225.

(82) Yilmaz, Ö.; Aslan, F.; Öztürk, A. İ.; Vanli, N. S.; Kirbağ, S.; Arslan, M. Antimicrobial and Biological Effects of N-Diphenylphosphoryl-P-Triphenylmonophosphazene-II and Di(o-Tolyl) Phosphoryl-P-Tri(o-Tolyl)Monophosphazene-III on Bacterial and Yeast Cells. *Bioorganic Chem.* **2002**, *30* (5), 303–314.

(83) Yilmaz, okkes; Kirba?, S.; Arslan, M. Antimicrobial and Biological Effects of Ipemphos and Amphos on Bacterial and Yeast Strains. *Cell Biochem. Funct.* **2000**, *18* (2), 117–126.

(84) Roy, R. Carbohydrates and glycoconjugates: Current Opinion in Structural Biology: Synthesis and some applications of chemically defined multivalent glycoconjugates. **1996,** *6,* 692-702.

(85) Varki, A. Biological Roles of Oligosaccharides: All of the Theories Are Correct. *Glycobiology* **1993**, *3* (2), 97–130.

(86) Dwek, R. A. Glycobiology: Toward Understanding the Function of Sugars. *Chem. Rev.* **1996**, *96* (2), 683–720.

(87) Roy, R. Carbohydrates and glycoconjugates: Current Opinion in Structural Biology: Synthesis and some applications of chemically defined multivalent glycoconjugates. **1996,** *6,* 692-702.

(88) Toone, E. J. Structure and Energetics of Protein-Carbohydrate Complexes. *Curr. Opin. Struct. Biol.* **1994,** *4* (5), 719–728.

(89) Kiessling, L. L.; Pohl, N. L. Strength in Numbers: Non-Natural Polyvalent Carbohydrate Derivatives. *Chem. Biol.* **1996,** *3* (2), 71–77.

(90) Mintzer, M. A.; Dane, E. L.; O'Toole, G. A.; Grinstaff, M. W. Exploiting Dendrimer Multivalency To Combat Emerging and Re-Emerging Infectious Diseases. *Mol. Pharm.* **2012,** *9* (3), 342–354.

(91) J. Rojo; R. Delgado. Dendrimers and Dendritic Polymers as Anti-Infective Agents: New Antimicrobial Strategies for Therapeutic Drugs. *Anti-Infect. Agents Med. Chem.* **2007,** *6* (3), 151–174.

(92) Imberty, A.; Chabre, Y. M.; Roy, R. Glycomimetics and Glycodendrimers as High Affinity Microbial Anti-Adhesins. *Chem. - Eur. J.* **2008,** *14* (25), 7490–7499.

(93) 38 Mintzer Molecular Recognition and Polymers_ Control of Polymer Structure and Self ... - Google Books.Html.

(94) *Protein-Carbohydrate Interactions in Infectious Diseases*; Bewley, C. A., Ed.; Royal Society of Chemistry: Cambridge, 2006.

(95) Vyas, N. K. Atomic Features of, Protein-Carbohydrate interactions. Current Opinion in Structural Biology. **1991,** *1,* 732-740.

(96) Lee, Y. C.; Lee, R. T.; Rice, K.; Ichikawa, Y.; Wong, T.-C. Topography of Binding Sites of Animal Lectins: Ligands' View. *Pure Appl. Chem.* **1991,** *63* (4), 499–506.

(97) Lis, H.; Sharon, N. Lectins: Carbohydrate-Specific Proteins That Mediate Cellular Recognition †. *Chem. Rev.* **1998,** *98* (2), 637–674.

(98) Quiocho, F. A. Probing the Atomic Interactions between Proteins and Carbohydrates. *Biochem. Soc. Trans.* **1993,** *21* (2), 442–448.

(99) Sears, P.; Wong, C.-H. Carbohydrate Mimetics: A New Strategy for Tackling the Problem of Carbohydrate-Mediated Biological Recognition. *Angew. Chem. Int. Ed.* **1999,** *38* (16), 2300–2324.

(100) Imberty, A.; Gautier, C.; Lescar, J.; Pérez, S.; Wyns, L.; Loris, R. An Unusual Carbohydrate Binding Site Revealed by the Structures of Two *Maackia Amurensis* Lectins Complexed with Sialic Acid-Containing Oligosaccharides. *J. Biol. Chem.* **2000,** *275* (23), 17541–17548.

(101) Sharon, N.; Ofek, I. In Protein-Carbohydrate Interaction in Infection Disease. *The Royal Society of Chemistry.* **2006,** 49-72.

(102) Freeland, J.; Milani, T.; Perlstein, J. *J. Am. Chem. Soc.***2001,** *123* (1), 191-192.

(103) Steiner, T.; Desiraju, G. R. Distinction between the Weak Hydrogen Bond and the van Der Waals Interaction. *Chem. Commun.* **1998,** No. 8, 891–892.

(104) Sears, P.; Wong, C.-H. Carbohydrate Mimetics: A New Strategy for Tackling the Problem of Carbohydrate-Mediated Biological Recognition. *Angew. Chem. Int. Ed.* **1999**, *38* (16), 2300–2324.

(105) Bouckaert, J.; Berglund, J.; Schembri, M.; De Genst, E.; Cools, L.; Wuhrer, M.; Hung, C.-S.; Pinkner, J.; Slättegård, R.; Zavialov, A.; et al. Receptor Binding Studies Disclose a Novel Class of High-Affinity Inhibitors of the Escherichia Coli FimH Adhesin: A Novel Class of FimH High-Affinity Ligands. *Mol. Microbiol.* **2004**, *55* (2), 441–455.

(106) Meyer, E. A.; Castellano, R. K.; Diederich, F. Interactions with Aromatic Rings in Chemical and Biological Recognition. *Angew. Chem. Int. Ed.* **2003**, *42* (11), 1210–1250.

(107) Asensio, J. L.; Ardá, A.; Cañada, F. J.; Jiménez-Barbero, J. Carbohydrate–Aromatic Interactions. *Acc. Chem. Res.* **2013**, *46* (4), 946–954.

(108) Chabre, Y. M.; Giguère, D.; Blanchard, B.; Rodrigue, J.; Rocheleau, S.; Neault, M.; Rauthu, S.; Papadopoulos, A.; Arnold, A. A.; Imberty, A.; et al. Combining Glycomimetic and Multivalent Strategies toward Designing Potent Bacterial Lectin Inhibitors. *Chem. - Eur. J.* **2011**, *17* (23), 6545–6562.

(109) Gabius, H. J. The How and Why of Protien-carbohydrate Interaction: A Primer to the Theoritical Concept and a Guide to Application in Drug Design. *Pharmaceutical Research.* **1998,** *15* (1), 23-30.

(110) Cioci, G.; Mitchell, E. P.; Gautier, C.; Wimmerová, M.; Sudakevitz, D.; Pérez, S.; Gilboa-Garber, N.; Imberty, A. Structural Basis of Calcium and Galactose Recognition by the Lectin PA-IL of *Pseudomonas Aeruginosa*. *FEBS Lett.* **2003**, *555* (2), 297–301.

(111) Vavricka, C. J.; Muto, C.; Hasunuma, T.; Kimura, Y.; Araki, M.; Wu, Y.; Gao, G. F.; Ohrui, H.; Izumi, M.; Kiyota, H. Synthesis of Sulfo-Sialic Acid Analogues: Potent Neuraminidase Inhibitors in Regards to Anomeric Functionality. *Sci. Rep.* **2017**, *7* (1).

(112) Brown, R. D.; Brewer, C. F.; Koenig, S. H. Conformation States of Concanavalin A: Kinetics of Transitions Induced by Interaction with Mn2+ and Ca2+ Ions? 14.

(113) Garber, N.; Guempel, U.; Doyle, R. J. On the specificity of the D-galactose-binding lectin (PA-I) of *Pseudomonas aeruginosa* and its strong binding to hydrophilic derivatives of D-galactose and thiogalactose. *Biochemica et Biophysica Acta. J.***1992,** 331-333.

(114) Imberty, A.; Wimmerová, M.; Mitchell, E. P.; Gilboa-Garber, N. Structures of the Lectins from Pseudomonas Aeruginosa: Insights into the Molecular Basis for Host Glycan Recognition. *Microbes Infect.* **2004**, *6* (2), 221–228.

(115) Cioci, G.; Mitchell, E. P.; Gautier, C.; Wimmerová, M.; Sudakevitz, D.; Pérez, S.; Gilboa-Garber, N.; Imberty, A. Structural Basis of Calcium and Galactose Recognition by the Lectin PA-IL of *Pseudomonas Aeruginosa*. *FEBS Lett.* **2003**, *555* (2), 297–301.

(116) Hall, D. A. Regulation of Gene Expression by a Metabolic Enzyme. *Science* **2004**, *306* (5695), 482–484.

(117) Roussel, P.; Lamblin, G. The Glycosylation of Airway Mucins in Cystic Fibrosis and Its Relationship with Lung Infection by Pseudomonas Aeruginosa. In *Glycobiology and Medicine*; Axford, J. S., Ed.; Springer US: Boston, MA, 2003; Vol. 535, pp 17–32.

(118) Boukerb, A. M.; Rousset, A.; Galanos, N.; Méar, J.-B.; Thépaut, M.; Grandjean, T.; Gillon, E.; Cecioni, S.; Abderrahmen, C.; Faure, K.; et al. Antiadhesive Properties of Glycoclusters against *Pseudomonas Aeruginosa* Lung Infection. *J. Med. Chem.* **2014**, *57* (24), 10275–10289.

(119) Qian, L.; Sand, R. Z. Enhancement of biofilm formation on Pyrite by *Sulfobacillus thermosulfidooxidans* : Extracellular polymeric substances involved in adhesion and biofilm formation by *Sulfobacillus thermosulfidooxidans*. *Minerals*. **2016,** *6* (3),71-72.

(120) Schuster, M.; Lostroh, C. P.; Ogi, T.; Greenberg, E. P. Identification, Timing, and Signal Specificity of Pseudomonas Aeruginosa Quorum-Controlled Genes: A Transcriptome Analysis. *J. Bacteriol.* **2003**, *185* (7), 2066–2079.

(121) Winzer, K.; Falconer, C.; Garber, N. C.; Diggle, S. P.; Camara, M.; Williams, P. The Pseudomonas Aeruginosa Lectins PA-IL and PA-IIL Are Controlled by Quorum Sensing and by RpoS. *J. Bacteriol.* **2000**, *182* (22), 6401–6411.

(122) Tielker, D. Pseudomonas Aeruginosa Lectin LecB Is Located in the Outer Membrane and Is Involved in Biofilm Formation. *Microbiology* **2005**, *151* (5), 1313–1323.

(123) Wyss, D.; Choi, J.; Li, J.; Knoppers, M.; Willis, K.; Arulanandam, A.; Smolyar, A.; Reinherz, E.; Wagner, G. Conformation and Function of the N-Linked Glycan in the Adhesion Domain of Human CD2. *Science* **1995**, *269* (5228), 1273–1278.

(124) Gilboa-Garber, N.; Mizrahi, L.; Garber, N. Purification of the Galactose-Binding Hemagglutinin of *Pseudomonas Aeruginosa* by Affinity Column Chromatography Using Sepharose. *FEBS Lett.* **1972**, *28* (1), 93–95.

(125) Cecioni, S.; Lalor, R.; Blanchard, B.; Praly, J.-P.; Imberty, A.; Matthews, S.; Vidal, S. Achieving High Affinity towards a Bacterial Lectin through Multivalent Topological Isomers of Calix[4]Arene Glycoconjugates. *Chem. - Eur. J.* **2009**, *15* (47), 13232–13240.

(126) Cecioni, S.; Lalor, R.; Blanchard, B.; Praly, J.-P.; Imberty, A.; Matthews, S.; Vidal, S. Achieving High Affinity towards a Bacterial Lectin through Multivalent Topological Isomers of Calix[4]Arene Glycoconjugates. *Chem. - Eur. J.* **2009**, *15* (47), 13232–13240.

(127) Gour, N.; Verma, S. Synthesis and AFM Studies of Lectin–Carbohydrate Self-Assemblies. *Tetrahedron* **2008**, *64* (30–31), 7331–7337.

(128) Lameignere, E.; Shiao, T. C.; Roy, R.; Wimmerova, M.; Dubreuil, F.; Varrot, A.; Imberty, A. Structural Basis of the Affinity for Oligomannosides and

Analogs Displayed by BC2L-A, a Burkholderia Cenocepacia Soluble Lectin. *Glycobiology* **2010**, *20* (1), 87–98.

(129) Sicard, D.; Cecioni, S.; Iazykov, M.; Chevolot, Y.; Matthews, S. E.; Praly, J.-P.; Souteyrand, E.; Imberty, A.; Vidal, S.; Phaner-Goutorbe, M. AFM Investigation of Pseudomonas Aeruginosa Lectin LecA (PA-IL) Filaments Induced by Multivalent Glycoclusters. *Chem. Commun.* **2011**, *47* (33), 9483.

(130) Sicard, D.; Chevolot, Y.; Souteyrand, E.; Imberty, A.; Vidal, S.; Phaner-Goutorbe, M. Molecular Arrangement between Multivalent Glycocluster and *Pseudomonas Aeruginosa* LecA (PA-IL) by Atomic Force Microscopy: Influence of the Glycocluster Concentration: AFM STUDY OF GLYCOCLUSTER CONCENTRATION ON COMPLEXES WITH (PA-IL) LECTINS. *J. Mol. Recognit.* **2013**, *26* (12), 694–699.

(131) Bertozzi, C. R. Chemical Glycobiology. *Science* **2001**, *291* (5512), 2357–2364.

(132) Heldin, C.-H. Dimerization of Cell Surface Receptors in Signal Transduction. *Cell* **1995**, *80* (2), 213–223.

(133) Gestwicki, J. E.; Kiessling, L. L. Inter-Receptor Communication through Arrays of Bacterial Chemoreceptors. *Nature* **2002**, *415* (6867), 81–84.

(134) Gestwicki, J. E.; Strong, L. E.; Kiessling, L. L. Tuning Chemotactic Responses with Synthetic Multivalent Ligands. *Chem. Biol.* **2000**, *7* (8), 583–591.

(135) Kiessling, L. L.; Gestwicki, J. E.; Strong, L. E. Synthetic Multivalent Ligands as Probes of Signal Transduction. *Angew. Chem. Int. Ed.* **2006**, *45* (15), 2348–2368.

(136) Guiard, J.; Fiege, B.; Kitov, P. I.; Peters, T.; Bundle, D. R. "Double-Click" Protocol for Synthesis of Heterobifunctional Multivalent Ligands: Toward a Focused Library of Specific Norovirus Inhibitors. *Chem. - Eur. J.* **2011**, *17* (27), 7438–7441.

(137) Rademacher, C.; Guiard, J.; Kitov, P. I.; Fiege, B.; Dalton, K. P.; Parra, F.; Bundle, D. R.; Peters, T. Targeting Norovirus Infection-Multivalent Entry Inhibitor Design Based on NMR Experiments. *Chem. - Eur. J.* **2011**, *17* (27), 7442–7453.

(138) Dam, T. K.; Gerken, T. A.; Brewer, C. F. Thermodynamics of Multivalent Carbohydrate−Lectin Cross-Linking Interactions: Importance of Entropy in the Bind and Jump Mechanism. *Biochemistry* **2009**, *48* (18), 3822–3827.

(139) Bourne, Y.; Bolgiano, B.; Cambillau, C. Crosslinking of mammalian lectin (galectin-1) by complex biatennary saccharides. *Structural Biology J.* **1994**, *1* (12), 863-870.

(140) Sacchettini, J. C.; Baum, L. G.; Brewer, C. F. Multivalent Protein−Carbohydrate Interactions. A New Paradigm for Supermolecular Assembly and Signal Transduction. *Biochemistry* **2001**, *40* (10), 3009–3015.

(141) Olsen, L. R.; Dessen, A.; Gupta, D.; Sabesan, S.; Sacchettini, J. C.; Brewer, C. F. X-Ray Crystallographic Studies of Unique Cross-Linked Lattices

between Four Isomeric Biantennary Oligosaccharides and Soybean Agglutinin†,. 8.

(142) Dam, T. K.; Gerken, T. A.; Cavada, B. S.; Nascimento, K. S.; Moura, T. R.; Brewer, C. F. Binding Studies of α-GalNAc-Specific Lectins to the α-GalNAc (Tn-Antigen) Form of Porcine Submaxillary Mucin and Its Smaller Fragments. *J. Biol. Chem.* **2007**, *282* (38), 28256–28263.

(143) Chetcuti, M. J.; Devoille, A. M. J.; Othman, A. B.; Souane, R.; Thuéry, P.; Vicens, J. Synthesis of Mono-, Di- and Tetra-Alkyne Functionalized Calix[4]Arenes: Reactions of These Multipodal Ligands with Dicobalt Octacarbonyl to Give Complexes Which Contain up to Eight Cobalt Atoms. *Dalton Trans.* **2009**, No. 16, 2999.

(144) Dam, T. K.; Brewer, C. F. Thermodynamic Studies of Lectin–Carbohydrate Interactions by Isothermal Titration Calorimetry. *Chem. Rev.* **2002**, *102* (2), 387–430.

(145) Kulkarni, K. A.; Katiyar, S.; Surolia, A.; Vijayan, M.; Suguna, K. Structural Basis for the Carbohydrate-Specificity of Basic Winged-Bean Lectin and Its Differential Affinity for Gal and GalNAc. *Acta Crystallogr. D Biol. Crystallogr.* **2006**, *62* (11), 1319–1324.

(146) Garber, N.; Guempel, U.; Doyle, R. J. On the specificity of the D-galactose-binding lectin (PA-I) of *Pseudomonas aeruginosa* and its strong binding to hydrophilic derivatives of D-galactose and thiogalactose. *Biochemica et Biophysica Acta. J.***1992,** 331-333.

(147) Lanne, B.; Bergstrm, J.; Motas, C.; Karlsson, K.-A. Binding of the Galactose-SpecificPseudomonas Aeruginosa Lectin, PA-I, to Glycosphingolipids and Other Glycoconjugates. *Glycoconj. J.* **1994**, *11* (4), 292–298.

(148) Chen, C.-P.; Song, S.-C.; Gilboa-Garber, N.; Chang, K. S. S.; Wu, A. M. Studies on the Binding Site of the Galactose-Specific Agglutinin PA-IL from Pseudomonas Aeruginosa. *Glycobiology* **1998**, *8* (1), 7–16.

(149) Garber, N.; Doyle, R. J. Specificity on the fucose-binding lectin of *Pseudomonas aeruginosa. Federation of European Microbiological Societies.* **1987,** 331-334.

(150) Mitchell, E.; Houles, C.; Sudakevitz, D.; Wimmerova, M.; Gautier, C.; Pérez, S.; Wu, A. M.; Gilboa-Garber, N.; Imberty, A. Structural Basis for Oligosaccharide-Mediated Adhesion of Pseudomonas Aeruginosa in the Lungs of Cystic Fibrosis Patients. *Nat. Struct. Biol.* **2002**, *9* (12), 918–921.

(151) Blanchard, B.; Nurisso, A.; Hollville, E.; Tétaud, C.; Wiels, J.; Pokorná, M.; Wimmerová, M.; Varrot, A.; Imberty, A. Structural Basis of the Preferential Binding for Globo-Series Glycosphingolipids Displayed by Pseudomonas Aeruginosa Lectin I. *J. Mol. Biol.* **2008**, *383* (4), 837–853.

(152) Lanne, B.; Copraga, J.; Bergstrm, J.; Motas, C.; Karlsson, K.-A. Binding of the Galactose-SpecificPseudomonas Aeruginosa Lectin, PA-I, to Glycosphingolipids and Other Glycoconjugates. *Glycoconj. J.* **1994**, *11* (4), 292–298.

(153) Chemani, C.; Imberty, A.; de Bentzmann, S.; Pierre, M.; Wimmerova, M.; Guery, B. P.; Faure, K. Role of LecA and LecB Lectins in Pseudomonas Aeruginosa-Induced Lung Injury and Effect of Carbohydrate Ligands. *Infect. Immun.* **2009**, *77* (5), 2065–2075.

(154) Chemani, C.; Imberty, A.; de Bentzmann, S.; Pierre, M.; Wimmerova, M.; Guery, B. P.; Faure, K. Role of LecA and LecB Lectins in Pseudomonas Aeruginosa-Induced Lung Injury and Effect of Carbohydrate Ligands. *Infect. Immun.* **2009**, *77* (5), 2065–2075.

(155) Marotte, K.; Sabin, C.; Préville, C.; Moumé-Pymbock, M.; Wimmerová, M.; Mitchell, E. P.; Imberty, A.; Roy, R. X-Ray Structures and Thermodynamics of the Interaction of PA-IIL FromPseudomonas Aeruginosa with Disaccharide Derivatives. *ChemMedChem* **2007**, *2* (9), 1328–1338.

(156) Marotte, K.; Préville, C.; Sabin, C.; Moumé-Pymbock, M.; Imberty, A.; Roy, R. Synthesis and Binding Properties of Divalent and Trivalent Clusters of the Lewis a Disaccharide Moiety to Pseudomonas Aeruginosa Lectin PA-IIL. *Org. Biomol. Chem.* **2007**, *5* (18), 2953.

(157) Soomro, Z. H.; Cecioni, S.; Blanchard, H.; Praly, J.-P.; Imberty, A.; Vidal, S.; Matthews, S. E. CuAAC Synthesis of Resorcin[4]Arene-Based Glycoclusters as Multivalent Ligands of Lectins. *Org. Biomol. Chem.* **2011**, *9* (19), 6587.

(158) Kadam, R. U.; Bergmann, M.; Hurley, M.; Garg, D.; Cacciarini, M.; Swiderska, M. A.; Nativi, C.; Sattler, M.; Smyth, A. R.; Williams, P.; et al. A Glycopeptide Dendrimer Inhibitor of the Galactose-Specific Lectin LecA and of Pseudomonas Aeruginosa Biofilms. *Angew. Chem. Int. Ed.* **2011**, *50* (45), 10631–10635.

(159) Pertici, F.; Pieters, R. J. Potent Divalent Inhibitors with Rigid Glucose Click Spacers for Pseudomonas Aeruginosa Lectin LecA. *Chem. Commun.* **2012**, *48* (33), 4008.

(160) Reynolds, M.; Marradi, M.; Imberty, A.; Penadés, S.; Pérez, S. Multivalent Gold Glycoclusters: High Affinity Molecular Recognition by Bacterial Lectin PA-IL. *Chem. - Eur. J.* **2012**, *18* (14), 4264–4273.

(161) Roy, R. Carbohydrates and glycoconjugates: Current Opinion in Structural Biology: Synthesis and some applications of chemically defined multivalent glycoconjugates. **1996,** *6,* 692-702.

(162) Rodrigue, J.; Ganne, G.; Blanchard, B.; Saucier, C.; Giguère, D.; Shiao, T. C.; Varrot, A.; Imberty, A.; Roy, R. Aromatic Thioglycoside Inhibitors against the Virulence Factor LecA from Pseudomonas Aeruginosa. *Org. Biomol. Chem.* **2013**, *11* (40), 6906.

(163) Chabre, Y. M.; Giguère, D.; Blanchard, B.; Rodrigue, J.; Rocheleau, S.; Neault, M.; Rauthu, S.; Papadopoulos, A.; Arnold, A. A.; Imberty, A.; et al. Combining Glycomimetic and Multivalent Strategies toward Designing Potent Bacterial Lectin Inhibitors. *Chem. - Eur. J.* **2011**, *17* (23), 6545–6562.

(164) Marotte, K.; Sabin, C.; Préville, C.; Moumé-Pymbock, M.; Wimmerová, M.; Mitchell, E. P.; Imberty, A.; Roy, R. X-Ray Structures and Thermodynamics

of the Interaction of PA-IIL FromPseudomonas Aeruginosa with Disaccharide Derivatives. *ChemMedChem* **2007**, *2* (9), 1328–1338.

(165) Marotte, K.; Préville, C.; Sabin, C.; Moumé-Pymbock, M.; Imberty, A.; Roy, R. Synthesis and Binding Properties of Divalent and Trivalent Clusters of the Lewis a Disaccharide Moiety to Pseudomonas Aeruginosa Lectin PA-IIL. *Org. Biomol. Chem.* **2007**, *5* (18), 2953.

(166) Otsuka, I.; Blanchard, B.; Borsali, R.; Imberty, A.; Kakuchi, T. Enhancement of Plant and Bacterial Lectin Binding Affinities by Three-Dimensional Organized Cluster Glycosides Constructed on Helical Poly(Phenylacetylene) Backbones. *ChemBioChem* **2010**, *11* (17), 2399–2408.

(167) Soomro, Z. H.; Cecioni, S.; Blanchard, H.; Praly, J.-P.; Imberty, A.; Vidal, S.; Matthews, S. E. CuAAC Synthesis of Resorcin[4]Arene-Based Glycoclusters as Multivalent Ligands of Lectins. *Org. Biomol. Chem.* **2011**, *9* (19), 6587.

(168) Kadam, R. U.; Bergmann, M.; Hurley, M.; Garg, D.; Cacciarini, M.; Swiderska, M. A.; Nativi, C.; Sattler, M.; Smyth, A. R.; Williams, P.; et al. A Glycopeptide Dendrimer Inhibitor of the Galactose-Specific Lectin LecA and of Pseudomonas Aeruginosa Biofilms. *Angew. Chem. Int. Ed.* **2011**, *50* (45), 10631–10635.

(169) Pertici, F.; Pieters, R. J. Potent Divalent Inhibitors with Rigid Glucose Click Spacers for Pseudomonas Aeruginosa Lectin LecA. *Chem. Commun.* **2012**, *48* (33), 4008.

(170) Reynolds, M.; Marradi, M.; Imberty, A.; Penadés, S.; Pérez, S. Multivalent Gold Glycoclusters: High Affinity Molecular Recognition by Bacterial Lectin PA-IL. *Chem. - Eur. J.* **2012**, *18* (14), 4264–4273.

(171) Varki, A. Biological Roles of Oligosaccharides: All of the Theories Are Correct. *Glycobiology* **1993**, *3* (2), 97–130.

(172) Rudd, P. M. Glycosylation and the Immune System. *Science* **2001**, *291* (5512), 2370–2376.

(173) Jefferis, R. Glycosylation as a Strategy to Improve Antibody-Based Therapeutics. *Nat. Rev. Drug Discov.* **2009**, *8* (3), 226–234.

(174) Bertozzi, C. R. Chemical Glycobiology. *Science* **2001**, *291* (5512), 2357–2364.

(175) Pifferi, C.; Daskhan, G. C.; Fiore, M.; Shiao, T. C.; Roy, R.; Renaudet, O. Aminooxylated Carbohydrates: Synthesis and Applications. *Chem. Rev.* **2017**, *117* (15), 9839–9873.

(176) Pifferi, C.; Daskhan, G. C.; Fiore, M.; Shiao, T. C.; Roy, R.; Renaudet, O. Aminooxylated Carbohydrates: Synthesis and Applications. *Chem. Rev.* **2017**, *117* (15), 9839–9873.

(177) Kimmerlin, T.; Seebach, D. '100 Years of Peptide Synthesis': Ligation Methods for Peptide and Protein Synthesis with Applications to β-Peptide Assemblies*: 100 Years of Peptide Synthesis. *J. Pept. Res.* **2008**, *65* (2), 229–260.

(178) Rose, K. Facile Synthesis of Homogeneous Artificial Proteins. *J. Am. Chem. Soc.* **1994**, *116* (1), 30–33.
(179) Lee, M. D.; Dunne, T.; Borders, D. B. Calichemicins, a Novel Family of Antitumor Antibiotics. *J. Am. Chem. Soc.* **1987**, 109, 3466-3468.
(180) Walker, S.; Gupta, V.; Kahne, D.; Gange, D. Analysis of Hydroxylamine Glycosidic Linkages: Structural Consequences of the NO Bond in Calicheamicin. *J. Am. Chem. Soc.* **1994**, *116* (8), 3197–3206.
(181) Hang, H. C.; Bertozzi, C. R. Chemoselective Approaches to Glycoprotein Assembly. *Acc. Chem. Res.* **2001**, *34* (9), 727–736.
(182) Kiessling, L. L.; Splain, R. A. Chemical Approaches to Glycobiology. *Annu. Rev. Biochem.* **2010**, *79* (1), 619–653.
(183) Tiefenbrunn, T. K.; Dawson, P. E. Chemoselective Ligation Techniques: Modern Applications of Time-Honored Chemistry. *Biopolymers* **2010**, *94* (1), 95–106.
(184) Ulrich, S.; Boturyn, D.; Marra, A.; Renaudet, O.; Dumy, P. Oxime Ligation: A Chemoselective Click-Type Reaction for Accessing Multifunctional Biomolecular Constructs. *Chem. - Eur. J.* **2014**, *20* (1), 34–41.
(185) Johnson, R. W.; Stieglitz, J. The Velocity of Hydrolysis of Stereoisomeric Hydrazones and Oximes. *J. Am. Chem. Soc.* **1934**, *56* (9), 1904–1908.
(186) Canne, L. E.; Ferre- D'Amare, A. R.; Burley, S. K.; Kent, S. B. H. Total Chemical Synthesis of a Unique Transcription Factor-Related Protein: CMyc-Max. *J. Am. Chem. Soc.* **1995**, *117* (11), 2998–3007.
(187) Rose, K.; Zeng, W.; Regamey, P.-O.; Chernushevich, I. V.; Standing, K. G.; Gaertner, H. F. Natural Peptides as Building Blocks for the Synthesis of Large Protein-like Molecules with Hydrazone and Oxime Linkages. *Bioconjug. Chem.* **1996**, *7* (5), 552–556.
(188) Polyakov, V. A.; Nelen, M. I.; Nazarpack-Kandlousy, N.; Ryabov, A. D.; Eliseev, A. V. Imine Exchange InO-Aryl AndO-Alkyl Oximes as a Base Reaction for Aqueous 'Dynamic' Combinatorial Libraries. A Kinetic and Thermodynamic Study. *J. Phys. Org. Chem.* **1999**, *12* (5), 357–363.
(189) Kochendoerfer, G. G. Design and Chemical Synthesis of a Homogeneous Polymer-Modified Erythropoiesis Protein. *Science* **2003**, *299* (5608), 884–887.
(190) Kolonko, E. M.; Kiessling, L. L. A Polymeric Domain That Promotes Cellular Internalization. *J. Am. Chem. Soc.* **2008**, *130* (17), 5626–5627.
(191) Orbán, E.; Mező, G.; Schlage, P.; Csík, G.; Kulić, Ž.; Ansorge, P.; Fellinger, E.; Möller, H. M.; Manea, M. In Vitro Degradation and Antitumor Activity of Oxime Bond-Linked Daunorubicin–GnRH-III Bioconjugates and DNA-Binding Properties of Daunorubicin–Amino Acid Metabolites. *Amino Acids* **2011**, *41* (2), 469–483.
(192) Brunner, H.; Keck, C. Enantioselective Catalysis. 157 [1] Carbohydrate-Based, Water-Soluble Ligands for the Stereoselective Hydrogenation of Folic Acid. *Z. Für Anorg. Allg. Chem.* **2005**, *631* (13–14), 2555–2562.

(193) You, G.; Cheng, Z.; Peng, H.; He, H. The Synthesis and Characterization of a Novel Phosphorus-Nitrogen Containing Flame Retardant and Its Application in Epoxy Resins. *J. Appl. Polym. Sci.* **2014**, *131* (22).

(194) Chang, J. Y.; Ji, H. J.; Han, M. J.; Rhee, S. B.; Cheong, S.; Yoon, M. Preparation of Star-Branched Polymers with Cyclotriphosphazene Cores. *Macromolecules* **1994**, *27* (6), 1376–1380.

(195) Touaibia, M.; Roy, R. First Synthesis of "Majoral-Type" Glycodendrimers Bearing Covalently Bound α- D -Mannopyranoside Residues onto a Hexachlocyclotriphosphazene Core. *J. Org. Chem.* **2008**, *73* (23), 9292–9302.

(196) Servin, P.; Rebout, C.; Laurent, R.; Peruzzini, M.; Caminade, A.-M.; Majoral, J.-P. Reduced Number of Steps for the Synthesis of Dense and Highly Functionalized Dendrimers. *Tetrahedron Lett.* **2007**, *48* (4), 579–583.

(197) Lajiness, J. P.; Robertson, W. M.; Dunwiddie, I.; Broward, M. A.; Vielhauer, G. A.; Weir, S. J.; Boger, D. L. Design, Synthesis, and Evaluation of Duocarmycin *O* -Amino Phenol Prodrugs Subject to Tunable Reductive Activation. *J. Med. Chem.* **2010**, *53* (21), 7731–7738.

(198) Wei, S.; Shalhout, S.; Ahn, Y.-H.; Bhagwat, A. S. A Versatile New Tool to Quantify Abasic Sites in DNA and Inhibit Base Excision Repair. *DNA Repair* **2015**, *27*, 9–18.

(199) Bagul, R. S.; Hosseini, M. M.; Shiao, T. C.; Roy, R. "Onion Peel" Glycodendrimer Syntheses Using Mixed Triazine and Cyclotriphosphazene Scaffolds. *Can. J. Chem.* **2017**, *95* (9), 975–983.

(200) Sharma, R.; Kottari, N.; Chabre, Y. M.; Abbassi, L.; Shiao, T. C.; Roy, R. A Highly Versatile Convergent/Divergent "Onion Peel" Synthetic Strategy toward Potent Multivalent Glycodendrimers. *Chem Commun* **2014**, *50* (87), 13300–13303.

(201) Nudelman, A.; Bechor, Y.; Falb, E.; Fischer, B.; Wexler, B. A.; Nudelman, A. Acetyl Chloride-Methanol as a Convenient Reagent for: A) Quantitative Formation of Amine Hydrochlorides B) Carboxylate Ester Formation C) Mild Removal of N-t-Boc-Protective Group. *Synth. Commun.* **1998**, *28* (3), 471–474.

(202) Tejler, J.; Leffler, H.; Nilsson, U. J. Synthesis of O-Galactosyl Aldoximes as Potent LacNAc-Mimetic Galectin-3 Inhibitors. *Bioorg. Med. Chem. Lett.* **2005**, *15* (9), 2343–2345.

(203) Star, A.; Liu, Y.; Stoddart, J. F. Macromolecules supporting information: Noncovalant Side-Wall Functionalization of Single-Walled Carbon Nanotubes. *J. Am. Chem. Soc.***2002**.

(204) Loska, R.; Janiga, A.; Gryko, D. Design and Synthesis of Protoporphyrin IX/Vitamin B $_{12}$ Molecular Hybrids *via* CuAAC Reaction. *J. Porphyr. Phthalocyanines* **2013**, *17*, 104–117.

(205) Joosten, A.; Schneider, J. P.; Lepage, M. L.; Tarnus, C.; Bodlenner, A.; Compain, P. A Convergent Strategy for the Synthesis of Second-Generation Iminosugar Clusters Using "Clickable" Trivalent Dendrons: Synthesis of

Second-Generation Iminosugar Clusters. *Eur. J. Org. Chem.* **2014,** *2014* (9), 1866–1872.